MULTIPHASE FLOWS IN DEFORMABLE GEOMATERIALS

CHEMO-PHYSICAL MIXTURE COUPLING THEORY AND NON-EQUILIBRIUM THERMODYNAMICS

Xiaohui Chen and Manhui Wang

CRC Press
Taylor & Francis Group

Multiphase Flows in Deformable Geomaterials

Multiphase Flows in Deformable Geomaterials proposes that multiscale coupling of multiphase flow and multicomponents within a deformable porous medium is complex and interdisciplinary and lacks a unified theory. To address this gap, the book proposes chemo-physical Mixture-Coupling Theory and non-equilibrium thermodynamic processes to derive governing equations for multiphase transport and mechanical behavior. This addresses challenges in the existing multiscale coupling theory and brings together physics and chemistry within the realm of thermodynamics. The series of constitutive equations can be applied to any constitutive model in porous media, across many disciplines related to soils, concrete, and catalysis.

This book is particularly addressed to geotechnical and geoenvironmental engineering—bringing together multiphase flows of water and gas, chemicals, and within soils and rocks. Highlights include hydro-mechanical coupling, unsaturated hydro-mechanical-chemical coupling, thermo-hydro-mechanical coupling, and thermo-hydro-mechanical-chemical coupling, with consideration of chemo and thermo osmosis and microscopic swelling mechanisms. It is written for advanced students and researchers.

Prof. Dr. Xiaohui Chen is an Associate Professor in Geotechnical Engineering and a Chartered Environmentalist at the University of Leeds with a research focus in both geomechanics and geochemistry. He is a pioneer in the development of Mixture-Coupling Theory.

Dr. Manhui Wang is the Head of Research Platforms at the University of Liverpool's IT Services Department and an expert in computational chemistry and high-performance computing.

Multiphase Flows in Deformable Geomaterials

Chemo-Physical Mixture Coupling Theory and Non-Equilibrium Thermodynamics

Xiaohui Chen and Manhui Wang

CRC Press
Taylor & Francis Group
Boca Raton London New York

CRC Press is an imprint of the
Taylor & Francis Group, an **informa** business

First edition published 2026
by CRC Press
4 Park Square, Milton Park, Abingdon, Oxon, OX14 4RN

and by CRC Press
2385 NW Executive Center Drive, Suite 320, Boca Raton FL 33431

CRC Press is an imprint of Informa UK Limited

This research was supported by the Engineering and Physical Sciences Research Council [grant number EP/R511717/1]

British Library Cataloguing-in-Publication Data
A catalogue record for this book is available from the British Library

ISBN: 9780367343064 (hbk)
ISBN: 9781041017066 (pbk)
ISBN: 9780429324925 (ebk)

DOI: 10.1201/9780429324925

Typeset in Times
by codeMantra

Contents

Acknowledgments

The authors would like to extend their sincere gratitude to Professor Mike Hicks, Professor of Soil Mechanics and Head of Geo-Engineering at Delft University of Technology (Netherlands), for his invaluable feedback and significant contributions to the early drafts of this book, as well as to several related research endeavors.

The lead author also wishes to express deep appreciation to both current and former PhD stsudents. Dr. Yue Ma's assistance in reproducing numerical figures, Dr. Kai Wang's contributions to the Biot and Terzaghi theory sections, and the diligent efforts of Dr. Liyang Xu, Dr. Sulaiman Abdullah, Dr. Changyu Xu, Dr. Shangqi Ge, Dr. He Yang, and Mr. Liyang Mao in reviewing and refining the content have been indispensable.

The authors would also like to thank the Senior Editor from CRC Press & Routledge (imprints of Taylor & Francis), Mr. Tony Moore, for his excellent management of the publication process, ensuring the timely release of this book.

Additionally, the authors acknowledge the support of UK Research and Innovation (UKRI) for providing open access to this book. Their contributions have been crucial in making this work accessible to a broader audience.

This research was supported by the Engineering and Physical Sciences Research Council [grant number EP/R511717/1].

List of selected symbols

a_i	Molar activity of the ith chemical
$\mathbf{A}$	Affinity of a chemical reaction
$\boldsymbol{B}$	Material-dependent constant
B_q	Material-dependent constant with respect to temperature
c_α	Mass fraction of the αth phase, $c_\alpha = \rho_\alpha / \rho_f$
c_c	Mass fraction of the chemical, defined as $c_c = \rho_l^c / \rho_l^l = \rho_c / \rho_l$
c_w	Mass fraction of the water, defined as $c_w = \rho_l^w / \rho_l^l = \rho_w / \rho_l$
c_k	The kth species mass fraction, defined as $c_k = \dfrac{\rho_l^k}{\rho_l^l} = \dfrac{\rho_k}{\rho_l}$
C_α	Specific heat capacity of the α th phase
C_s	Specific heat capacity of the solid
C_w	Specific heat capacity of the water
C_v	Coefficient of consolidation
C_{v-f}	The compressibility of the water
C_s^p	Specific moisture content, which is defined in terms of pressure
$\mathbf{d}$	The total displacement vector, $\mathbf{d} = [d_i,\ d_j,\ d_k]$
d_i	The displacement in the i axis
$\dot{d}_i = \dfrac{\partial d_i}{\partial t}$	The time derivative of d_i.
D	Diffusion coefficient
e_0	Initial void ratio
e	Void ratio
$\mathbf{e}_i$	The unit vector in the ith direction
$\mathbf{E}$	Green strain
$\mathbf{f}_i$	ith driving force
$\mathbf{F}$	Deformation gradient
g	Gravity
G	Shear modulus of the geomaterial
H	The hydraulic head
H_0	The initial pore water pressure head

$i(k)$	Both used for the ith chemical or the kth chemical (subscript)
$\mathbf{I}_1$	Identity matrix
$\mathbf{I}$	Flux vector
$\mathbf{I}_c$	Chemical flux
$\mathbf{I}_k$	Flux of the kth chemical
$\mathbf{I}_q$	Heat flux
$\mathbf{I}_w$	Water flux
$\mathbf{I}_\alpha$	Flux of the αth phase
$\mathbf{j}_{\pi,ncon}$	Nonconvective flux into the region Ω
$\mathbf{j}_{\pi,con}$	Convective flux and non-convective flux into the region Ω
J	Jacobian of $\mathbf{F}$
J_{ch}	The rate of species change per unit volume
$\mathbf{J}_i$	ith diffusion flow (i = 1:n)
$\mathbf{J}_w$	Diffusion fluxes of the water
$\mathbf{J}_c$	Diffusion fluxes the chemical
k	Permeability; kth chemical (when used as subscript)
k_{rw}	Relative permeability with respect to water
k_{rl}	Relative permeability with respect to liquid (including chemicals)
K_H	Hydraulic conductivity
K	Bulk modulus of the geomaterial
K_s	Bulk modulus of the solid matrix of the geomaterial
K_v	The hydraulic conductivity in vertical direction
L_{ijkl}	Material-dependent constants
$L_{11}, L_{12}, L_{21}, L_{22}$	Phenomenological coefficients
m, M	van Genuchten parameters
M_{ij}	Material-dependent parameters
M_c	Molar mass of the chemical
M_w	Molar mass of the water
$\mathbf{n}$	Outward unit normal vector
n_k	The moles of the kth chemical

N_c	Total number of chemical species, corresponding to i or k
N_p	Total number of phases
p	System pressure (general)
p_{atm}	The atmospheric pressure
p_c	Capillary pressure
p_l	Pore liquid pressure of the mixture
p_{pore}	Pore pressure
p_g	Gas-phase pressure
p_w	Pore water pressure
$\dot{p}_w$	$\frac{\partial p_w}{\partial t}$, the time derivative of p_w
$\overline{p}$	Average pore pressure
q_α	Heat density of the αth phase
q_w	Heat density of water
q_s	Heat density of the solid
q_R	Heat generated by reaction
q	Local heat density
Q	Void compressibility
Q_1	Inflow rate at the lower surface of the element
Q_2	Outflow rate at the upper surface of the element
r	Reflection coefficient
r_c	Activity coefficient
r_π	Source term pertaining to the production of π
s_p	The elastic storativity of the pore space
S_w	Saturation of the water
S_l	Saturation of the liquid
S_g	Saturation of the gas
S_{ij}	Material coefficients with respect to swelling
S_{ij}^q	Material coefficients with respect to temperature
t	Time
T	Temperature
$\mathbf{u}$	Dacian velocity of a fluid
v	Dynamic viscosity of a fluid

$\mathbf{v}_s$	Velocity of a solid
$\mathbf{v}_l$	Barycentric motion of a liquid
$\mathbf{v}_f$	Barycentric motion of a fluid
$\mathbf{v}_\alpha$	Velocity of the flux, the water ($\alpha = w$) or chemical ($\alpha = c$)
V	Representative elementary volume
V_{pore}	Total pore volume
V_α	The volume of the αth phase
x_c	Mole fraction of a chemical
$\mathbf{x}_\alpha$	Material point for the αth phase in an arbitrary current configuration
x_i	Coordinates in current configuration
$\mathbf{X}_\alpha$	Material point for the αth phase in an arbitrary reference configuration
X_i	Coordinates in reference configuration
Z	Material coefficients with respect to swelling
Z_q	Material coefficients with respect to temperature

GREEK SYMBOLS

Π	Gibbs free energy
α	Multiphase (=1:*Np*, which represents multiphase: e.g., solid (s), gas (g), water (w)).
a_c	Activity of the solute
γ	Entropy production per unit volume
δ_{ij}	Kronecker delta (Section 1.5.2)
Γ	Boundary of the region Ω for a thermodynamically open system
θ	Poisson's ratio
ε	Internal energy density
ε_{ij}	Strain
ζ	Biot constant
η	Total entropy density, with η_w, η_c, η_q denoting entropy density for water, chemical, and thermo, respectively.
λ	Material thermal conductivity

μ	Chemical potential
μ_c	Chemical potential of the chemical
μ_i or μ_k	Chemical potential of the *i*th or *k*th chemical
μ_w	Chemical potential of water
μ_g	Chemical potential of the gas
υ	The porosity at any reference configuration
π	Bulk density of some extensive thermodynamic quantity
ρ_c	Mass density of the chemical with respect to the total volume
ρ_α	Density of the αth phase with respect to the total volume
ρ_s	Solid mass density with respect to the total volume
ρ_l	Mass density of the liquid with respect to the total volume
ρ_w	Mass density of the water with respect to the total volume
ρ_α^α	True density of the phase α
ρ_α^c	Partial density of the chemical in the phase α
ρ_l^l	True density of the liquid phase
ρ_l^w	Partial density or True density of the water in the liquid phase
$\rho_{w,ref}$	The mass density of water per unit reference volume
$\rho_{k,ref}$	The mass density of the *k*th chemical per unit reference volume
$\rho_{bound,ref}$	The reference mass density of the bound water
$\boldsymbol{\sigma}'$	Effective stress
$\boldsymbol{\sigma}$	Cauchy stress tensor
ξ	Extent of reaction at constant temperature and pressure
π	Bulk density of some extensive thermodynamic quantity
$\dot{\pi}$	Time derivative of π
$\frac{D\pi}{Dt}$	Material time derivative
ϕ	Porosity of the medium
ϕ_0	The initial porosity of a medium as a constant

ϕ_α	Volume fraction of the relevant αth fluid component: ϕ_s for solid, ϕ_f for fluid, and ϕ_l for liquid
ψ	Helmholtz free energy density
ψ_{pore}	Helmholtz free energy density of the pore fluid
χ	Internal frictional interaction force between the solid and fluid phases
Ψ	Reference configuration of ψ
ω	Swelling coefficient of a geomaterial
Ω	Region for a thermodynamically open system

OTHER SYMBOLS AND MATHEMATIC DESCRIPTIONS

$\because$	represents "because/since."
$\therefore$	represents "therefore."

$$\nabla = \frac{\partial}{\partial x_1}\mathbf{e}_1 + \frac{\partial}{\partial x_2}\mathbf{e}_2 + \frac{\partial}{\partial x_3}\mathbf{e}_3 = \frac{\partial}{\partial x_i}\mathbf{e}_i$$ ($\mathbf{e}_i$ is the unit vector).

Preface

The motivation behind writing this book arises from the growing need in contemporary engineering for highly interdisciplinary research to address complex global challenges, such as nuclear waste disposal, carbon capture and storage, and effective contaminated land restoration. In these areas, the gap between geomechanics and geochemistry has become a significant barrier to progress. To bridge this gap, the development of a unified theory is crucial, one that can form the foundation for constructing complex, coupled multiphysics and multiscale equations. Relying on borrowed equations from other disciplines has often led to stagnation and struggles in further development. Current approaches, which are heavily dependent on empirical experience, are inadequate for tackling the evolving challenges of modern engineering.

A theoretical framework is needed that enables the development of new, advanced equations capable of capturing new discoveries directly from fundamental principles, rather than relying on experiments for inspiration. This book aims to fill that gap by offering a new approach. While grounded in geotechnical engineering, the theory presented here transcends disciplinary boundaries. Non-equilibrium thermodynamics, the foundation of this theory, has been successfully applied across a wide range of engineering and scientific disciplines. It is hoped that this book will serve as a useful resource for researchers and practitioners in fields beyond geotechnical engineering, particularly those working with porous media.

Porous media serve as the scientific bedrock in various disciplines, including geotechnical and geoenvironmental engineering (e.g., soils/rocks), structural engineering (e.g., concrete), and chemical engineering (e.g., catalysts). The challenge of multiphysics coupling within deformable porous media—especially involving multiphase flow and multicomponents—represents one of the most complex topics in scientific and engineering research. This challenge arises from the need for interdisciplinary knowledge and the absence of a unified theory for multiphysics-multiscale coupling.

This book introduces a novel theoretical framework, known as "Mixture-Coupling Theory," based on fundamental non-equilibrium thermodynamics. By integrating energy and entropy states within the mixture, this theory establishes a robust mathematical structure. Mixture-Coupling Theory aims to address the challenges in theoretical

development by bridging physics and chemistry under the umbrella of thermodynamics and accounting for energy dissipation.

The primary application areas of Mixture-Coupling Theory lie in geotechnical and geoenvironmental engineering, specifically addressing multiphase flow (e.g., water, gas) and multicomponent systems (e.g., chemicals) within porous media (soils/rocks). This book delves into the development of Mixture-Coupling Theory, covering hydro-mechanical (HM) coupling, unsaturated hydro-mechanical-chemical (HMC) coupling, thermo-hydro-mechanical (THM) coupling, and thermo-hydro-mechanical-chemical (THMC) coupling. These models incorporate considerations of chemical and thermo osmosis and microscopic swelling mechanisms. All these models follow a consistent structure: (1) energy analysis of the mixture, (2) dissipative processes, (3) constitutive relationships, and (4) coupled field equations.

Mixture-Coupling Theory provides a foundational framework that allows for the development of tailored constitutive equations to meet the specific needs of various fields. By offering a unified theoretical approach, this framework is versatile enough to address a wide range of applications and scenarios in porous media.

1 Fundamentals of porous media

1.1 INTRODUCTION

Porous media encompass materials characterized by the presence of pores. This definition encompasses a wide array of both natural and engineered materials, including soils, rocks, cements, concretes, biological tissues (such as organs, cells, bones, and wood), sponges, and rubbers.

The passage of a fluid through the pores of a porous medium can induce deformation in the medium, through either fluid pressure or alterations in pore size resulting from chemical reactions. Moreover, the presence of multiphase fluids introduces additional complexity, as these fluids interact not only with each other but also with the porous medium itself, leading to intricate multiscale physical-chemical coupling phenomena. These couplings are influenced directly or indirectly by factors such as pore structure (solid phases), pore pressure (fluid phases), effective stress (interactions between solids and fluids), and chemical composition (both solid and fluid phases).

In the realm of geotechnical and geoenvironmental engineering, modeling multiphase flow in deformable geomaterials finds widespread application in various engineering contexts. These applications include but are not limited to addressing ground subsidence, ensuring foundation and slope stability, managing groundwater pollution and restoration efforts, implementing permeable reactive barriers, constructing embankments on soft or swelling ground, ensuring tunnelling and borehole stability, optimizing agricultural soil management, and managing oil, water, and gas reservoirs. Emerging applications also encompass areas such as radioactive waste disposal, carbon capture and storage, and shale gas exploration.

This chapter serves to lay the groundwork by introducing the fundamentals of geomaterials, with a specific focus on soils and rocks. It will cover basic physical laws governing fluid-solid interactions, provide an overview of the historical and current state of theoretical developments concerning multiphase couplings in geo-porous media, identify existing knowledge gaps, and present a conceptual model for the proposed Mixture-Coupling

DOI: 10.1201/9780429324925-1

Theory. Through this discussion, readers will gain insights into the intricate interplay between physical and chemical processes within porous media, setting the stage for further exploration in subsequent chapters.

1.2 UNDERSTANDING POROUS MEDIA: PROPERTIES AND PHYSICAL LAWS

1.2.1 Microscopic and macroscopic perspectives

Porous media present a dynamic interplay of various phases, constituents, and components, functioning across diverse scales. In the realm of thermodynamics, the notion of **phase** serves as a macroscopic concept, denoting substances that exhibit chemical and physical uniformity or homogeneity. These phases encompass familiar states such as solids, liquids, and gases, prevalent in soil/rock porous media. Additionally, they may encompass more intricate forms like crystalline, colloid, glassy, amorphous, and plasma phases, among others. Properties or variables associated with multiple phases are denoted using subscript $\alpha = 1 : N_p$, in which N_p is the total number of phases. Consequently, in a scenario with one solid, one liquid, and one gas, $N_p = 3$.

To differentiate between phases, solids are designated with subscript s, liquids with subscript l, and gases with subscript g. Solids typically constitute the structural framework of the porous medium, whereas liquids may comprise water or aqueous solutions, and gases may include air, for instance. For simplicity, liquids and gases are collectively referred to as fluids (denoted by subscript f). The solid matrix provides the framework housing pore spaces that accommodate fluids. Within these pore spaces, interactions among fluids occur, often resulting in the generation of pressure exerted on the solid structure. This interplay among phases within porous media underscores the complexity inherent in understanding their behavior and properties.

Components, on the other hand, refer to the constituents present within the mixture of a phase. In practical scenarios, the αth phase of a mixture, such as a fluid, may consist of multiple components (such as chemical species and colloidal or suspended particles) denoted as i *or* $k = 1 : N_c$. This representation enables a comprehensive understanding of the intricate composition of phases, particularly in complex mixtures.

The examination of porous media spans both microscopic and macroscopic scales. Microscopic analyses delve into intricate details like pore geometry and adsorption phenomena, offering valuable insights into the physical and chemical mechanisms operating at the pore

scale (Romm, 2004). However, these studies encounter notable limitations: (1) pore geometries observed at the micrometer scale may not seamlessly translate into practical applications in geotechnical and geoenvironmental engineering, where measurements typically range from centimeters to hundreds of meters (Gambolati and Verri, 1995). (2) Microscopic analyses often grapple with accurately distinguishing between voids and solid matrices. Most mathematical approaches necessitate considering volumes much larger than individual pores to accommodate the variability in material properties (Okabe and Blunt, 2005). (3) Current computational capabilities are constrained, capable of handling only a few thousand molecules of simple shapes for short durations (Parmigiani et al., 2011).

The **average method**, rooted in continuum mechanics, bridges discrete pore spaces into a continuous framework. It assumes that all quantities at any mathematical point can be defined by the mean of the appropriate quantity over the entire sample (Moyne et al., 2000). For example, macroscopic parameters, such as porosity and permeability, are obtained by regarding the porous medium as a whole instead of individual pores. Flow quantities (e.g., velocity and pressure) are variables of time and space, and are measured over areas or volumes that cross a large number of pores. Mixture-Coupling Theory uses the assumption of the average method that all phases are continuous.

At the core of average methods lies the **representative elementary volume** (REV), a microscopic domain within porous media with a significant enough volume to encapsulate all components, including solid, water, chemicals, and gas. A REV delineates an arbitrary microscopic domain Ω within a porous medium (Figure 1.1), with a sizeable enough total volume V to encapsulate all components, including solid, water, chemicals, and gas. Across its boundary Γ, multiple components, along with energy like heat, may traverse, facilitating a comprehensive understanding of porous media behavior.

1.2.2 Pore structure and density dynamics in porous media

This section delves into the intricate characteristics of pore space within porous media and its implications on fluid dynamics and density dynamics. Additionally, the section addresses the fundamental concepts of permeability and hydraulic conductivity, elucidating their roles in fluid flow through porous materials.

Porous media comprise two distinct types of pore space: effective and isolated. Effective pore space constitutes a continuous phase within the medium, facilitating fluid transport, while isolated pore space lacks

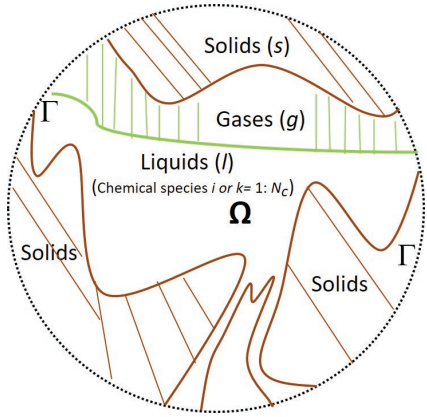

FIGURE 1.1 Conceptual model of a REV

connectivity and does not contribute to fluid flow (Chatzis and Dullien, 1983). In this book, the focus lies on understanding the interactions between fluids and solids, thus emphasizing effective pore space exclusively.

Porosity (ϕ) serves as a measure of the pore space (V_{pore}) relative to the total volume of the material, typically expressed as a percentage between 0% and 100%. It presents a kind of measurement of how much fluid the material can hold (Ehrenberg and Nadeau, 2005). The equation of porosity can be described as

$$\phi = \frac{V_{pore}}{V} \times 100\% \tag{1.1}$$

When the pore space is fully saturated with multiple fluids (volume V_f), including liquids (V_l) or gases (V_g), it results in

$$V_{pore} = V_f = V_l + V_g \tag{1.2}$$

Therefore, the porosity can be expressed as the volume fraction of the fluids

$$\phi_f = \frac{V_f}{V} = \frac{V_l + V_g}{V} \tag{1.3}$$

and the measurement of fluid volume fraction can determine the porosity. For example, in a water-saturated porous medium (e.g., sand), the porosity equals the volume fraction of water ϕ_w in a REV:

$$\phi = \phi_w = \frac{V_w}{V} \tag{1.4}$$

in which the relationship between the water volume V_w, solid volume V_s, and total volume V is

$$V = V_w + V_s \tag{1.5}$$

The mass density (ρ_α^i) of the $i$component within α phase is defined as its mass (m_α^i) divided by its corresponding phase volume V_α:

$$\rho_\alpha^i = \frac{m_\alpha^i}{V_\alpha} \tag{1.6}$$

Since this density is relative to the phase within which the ith component presents, it is termed as the partial density. When the phase is composed of one single component, the density becomes the true density used in science and engineering. For example, in a water (liquid)-saturated medium, the water density may be defined as

$$\rho_l^w = \frac{m_l^w}{V_l} \tag{1.7}$$

If there is salt (NaCl) dissolved in the water of a saturated porous medium (e.g., soil), the density of the salt in the pore liquid may be described as

$$\rho_l^{\mathrm{NaCl}} = \frac{m_l^{\mathrm{NaCl}}}{V_l} \tag{1.8}$$

However, the density of water may also be expressed relative to the total volume of the mixture (V) in a REV as

$$\rho_w = \frac{m_l^w}{V} \tag{1.9}$$

which is more convenient for analyzing the motion of the total mixture. Such an expression is termed the **mixture density**. The relationship between the two densities (ρ_l^w and ρ_w) can be obtained by dividing equation (1.7) by equation (1.9), leading to

$$\rho_w = \rho_l^w \frac{V_l}{V} = \phi_w \rho_l^w \tag{1.10}$$

The concepts of "water partial density" and "mixture density" are distinct yet intertwined, serving as vital descriptors for all phases and components present in the mixture. Further elucidation on these interconnected concepts will be provided in Sections 1.3.4 and 1.4.1.

Permeability (k) is a measure of the ability of a porous material to allow fluids to pass through it. Intrinsic permeability (also known as absolute permeability or specific permeability) denotes the permeability in a porous medium that is 100% saturated with a single-phase fluid (Nield and Bejan, 2006). Effective permeability is the ability to preferentially flow or transmit a particular fluid when other immiscible fluids are present (e.g., effective permeability of gas in a gas-water reservoir). The relative saturation of the fluids, as well as the nature of the medium, affects the effective permeability. In contrast, absolute permeability is a measure of the permeability when a single fluid or phase is present in the geomaterial (Civan, 2010). The concepts of permeability apply to laminar flows[1] that are nonreactive with respect to the material. However, for the fluid reacting with the solid matrix, such as water causing the clay to dissolve, a difference can be expected (Ibrahim et al., 2008).

Hydraulic conductivity (K_H) quantifies how easily a fluid flows through a soil or rock under a hydraulic gradient. Although the concepts of permeability and hydraulic conductivity are often used synonymously in geotechnical and geoenvironmental engineering, they differ significantly, because the intrinsic permeability (k) is a property of the porous medium and independent of the fluid, whereas hydraulic conductivity is not. The relationship between k and K_H can be described as

$$K_H = k\frac{\rho_l^w g}{\nu} \tag{1.11}$$

where ν is the dynamic viscosity of the fluid with density ρ_l^w (e.g., water density), and g is the acceleration due to gravity.

1.2.3 Darcy's law and mass flux

Darcy's law, pioneered by Henry Darcy in 1856, serves to elucidate unidirectional water flow within homogeneous and isotropic porous media (Darcy, 1856). It presents a proportionality between the Darcy velocity $\mathbf{u}$ and the water pressure gradient ∇p_w as

$$\mathbf{u} = -\frac{k}{\nu}\nabla p_w \left[\text{saturated}\right] \tag{1.12}$$

with an extension for unsaturated flow (Richards, 1931) as

$$\mathbf{u} = -k\frac{k_{rw}}{v}\nabla p_w \ \left[\text{unsaturated}\right] \tag{1.13}$$

where k_{rw} is the relative permeability for the unsaturated condition, which can also be denoted as k_{rl} for liquids (with chemical species in the water) and for chemical-related modeling in this book (e.g., Chapter 5), and ∇ is the gradient which can be expressed in three-dimensional space (x_1, x_2, x_3) as

$$\nabla = \frac{\partial}{\partial x_1}\mathbf{e}_1 + \frac{\partial}{\partial x_2}\mathbf{e}_2 + \frac{\partial}{\partial x_3}\mathbf{e}_3 = \frac{\partial}{\partial x_i}\mathbf{e}_i \tag{1.14}$$[2]

where $\mathbf{e}_i$ is the unit vector in the ith direction (i.e., $i = 1,\ 2,\ 3$). The fundamentals of scalars, vectors, and tensors can be found in Appendix 1.

The interstitial (pore) velocity of fluid (e.g., water), denoted as $\mathbf{v}_w$, correlates with Darcy velocity, solid velocity $\mathbf{v}_s$ (accounting for solid deformation), and porosity ϕ, as delineated by (Gersevanov, 1934)

$$(\mathbf{v}_w - \mathbf{v}_s) = \frac{\mathbf{u}}{\phi} \ \left[\text{saturated}\right]$$

or

$$(\mathbf{v}_w - \mathbf{v}_s) = \frac{\mathbf{u}}{S_w\phi}\left[\text{unsaturated}\right] \tag{1.15}$$

where S_w is the saturation ratio of water defined as $S_w = \dfrac{V_w}{V_{pore}}$.

A more comprehensive form of equation (1.15) for the αth phase of a multiphase flow may be described as

$$(\mathbf{v}_\alpha - \mathbf{v}_s) = \frac{\mathbf{u}_\alpha}{S_\alpha\phi} \tag{1.16}$$

where S_α is the saturation ratio of the αth phase, given by $S_\alpha = \dfrac{V_\alpha}{V_{pore}}$.

Equation (1.16) elucidates the connection between the microscopic interstitial (pore) velocity and macroscopic velocities like Darcy velocity. Utilizing the pore velocity and multiplying it by the density of the αth fluid phase (ρ_α) or kth species (ρ_k) in the phase, the **mass flux** of

the αth phase ($\mathbf{I}_\alpha$) or kth species ($\mathbf{I}_k$) in the porous medium can be obtained:

$$\mathbf{I}_\alpha = \rho_\alpha(\mathbf{v}_\alpha - \mathbf{v}_s)$$

or

$$\mathbf{I}_k = \rho_k(\mathbf{v}_k - \mathbf{v}_s) \tag{1.17}$$

where $\mathbf{v}_\alpha$ and $\mathbf{v}_k$ are the velocities of the αth phase and kth species, respectively.

For example, if the phase is water,

$$\mathbf{I}_w = \rho_w(\mathbf{v}_w - \mathbf{v}_s) \tag{1.18}$$

In a saturated solid-water porous medium, the water component mass density ρ_w is related to the unit volume of the solid-water mixture. Thus, it is related to the true mass density ρ_l^w (connected to the fluid volume in the unit) through equation (1.10):

$$\rho_w = \phi_w \rho_l^w$$

In an unsaturated solid-water coupled field, ρ_w is related to the true mass density ρ_l^wthrough

$$\rho_w \,/\, \underbrace{(\phi S_w)}_{\phi_w} = \rho_l^w \tag{1.19}$$

where ϕS_w equals the mass fraction of water ϕ_w.

By using the definition of Darcy velocity based on equation (1.16) as

$$\mathbf{u} = S_w \phi(\mathbf{v}_w - \mathbf{v}_s) \tag{1.20}$$

and using equations (1.18) and (1.19), the relationship between $\mathbf{I}_w$ and $\mathbf{u}$ can be obtained as

$$\mathbf{I}_w = \frac{\mathbf{u}\rho_w}{S_w \phi} = \mathbf{u}\rho_l^w \tag{1.21}$$

Note here: the $\mathbf{u}$ in equation (1.21) is for water transport. If there are k species in the water, the $\mathbf{u}$ represents the liquid transport, rather than the velocity for a single species.

Equation (1.21) can be expanded to a general αth fluid phase (e.g., gas or oil) in geomaterials, leading to

$$\mathbf{I}_\alpha = \frac{\mathbf{u}_\alpha \rho_\alpha}{S_\alpha \phi} = \mathbf{u}_\alpha \rho_\alpha^\alpha \tag{1.22}$$

This relationship between $\mathbf{I}_\alpha$ and $\mathbf{u}_\alpha$ is very useful for derivations in later chapters. If the αth phase is liquid, equation (1.22) may be written as

$$\mathbf{I}_l = \frac{\mathbf{u}\rho_l}{S_l \phi} = \mathbf{u}\rho_l^l \tag{1.23}$$

in which the liquid mass mixture density ρ_l and true density ρ_l^l can be described as a combination of all the species in the liquid by $\rho_l = \Sigma_k \rho_k$ and $\rho_l^l = \Sigma_k \rho_l^k$, respectively.

1.2.4 Fick's law and divergence of flux

Fick's law, established by Adolf Fick in 1855, provides a fundamental principle governing chemical diffusion (Fick, 1855). This law states that the transfer of the kth species in a fluid is proportional to its concentration gradient. At the molecular scale, the diffusion is the transport of compounds due to the random motion of the molecules (Bourg and Sposito, 2010). The diffusion mass flux, $\mathbf{J}_k$, is the rate of mass transferred across a plane perpendicular to the direction of the mass flow per unit time, per unit area. It is expressed as

$$\mathbf{J}_k = -\rho_l D \nabla c_k \tag{1.24}$$

where c_k is the species mass fraction that is defined as $c_k = \frac{\rho_l^k}{\rho_l^l} = \frac{\rho_k}{\rho_l}$, and D is the diffusion coefficient which varies with the temperature and molecular weight of the diffusing molecule.

For a moving liquid, the diffusion flux of the kth species ($\mathbf{J}_k$) within the liquid can be related to the liquid barycentric velocity $\mathbf{v}_l$ (Bedeaux et al., 2006), as illustrated

$$\mathbf{J}_k = \rho_k (\mathbf{v}_k - \mathbf{v}_l) \tag{1.25}$$

where $\mathbf{v}_l$ is described as

$$\mathbf{v}_l = \sum_k (\rho_k / \rho_l)\mathbf{v}_k \tag{1.26}$$

These fluxes $\mathbf{J}_k$ are not entirely independent; they must adhere to a constraint (equation (1.27)), resulting in one independent diffusion flux per species present.

$$\sum_k \mathbf{J}_k = 0 \tag{1.27}^3$$

For example, under the condition that a binary solution comprises a solute (e.g., NaCl) and a diluent (e.g., H_2O), there is one independent diffusion flux. Equation (1.27) leads to

$$\mathbf{J}_{\mathrm{NaCl}} + \mathbf{J}_{\mathrm{H_2O}} = 0$$

and then

$$\mathbf{J}_{\mathrm{NaCl}} = -\mathbf{J}_{\mathrm{H_2O}}$$

Therefore, it can be viewed as one independent diffusion flux. Similarly, if there are n species in the liquid, there should be $n - 1$ independent diffusion fluxes. Since the solute (NaCl, mass mixture density ρ_c) and water are a mixed liquid, the total liquid mass mixture density ρ_l can be defined as

$$\rho_l = \rho_w + \rho_c \tag{1.28}$$

In the mixed liquid, there is a difference between the velocities of the species ($\mathbf{v}_c$) and the water ($\mathbf{v}_w$). The liquid barycentric velocity may then be defined as the mass flux divided by the liquid mixture density, that is,

$$\mathbf{v}_l = (\rho_w / \rho_l)\mathbf{v}_w + (\rho_c / \rho_l)\mathbf{v}_c \tag{1.29}$$

Equation (1.29) establishes a crucial connection between the pore velocities of species within a moving fluid, such as a liquid. The diffusion flux is intricately influenced by both the mass flux and Darcy velocity, as introduced in Section 1.2.3. Therefore, it becomes imperative to establish the relationship between these variables.

Since the diffusion flux of the kth species relative to the barycentric motion (Herzig et al., 1970) can be written as equation (1.25), the relationship between $\mathbf{I}_k$ and $\mathbf{J}_k$ can be obtained as

$$\mathbf{J}_k = \mathbf{I}_k - \rho_k(\mathbf{v}_l - \mathbf{v}_s) \tag{1.30}^4$$

For example, in a binary solution, the diffusion flux is expressed as

$$\mathbf{J}_c = \mathbf{I}_c - \rho_c(\mathbf{v}_l - \mathbf{v}_s) \text{ and } \mathbf{J}_w = \mathbf{I}_w - \rho_w(\mathbf{v}_l - \mathbf{v}_s) \tag{1.31}$$

By considering the relationship between ρ_k and ρ_l^k, equation (1.30) can be written as

$$\mathbf{I}_k = \mathbf{J}_k + \rho_k(\mathbf{v}_l - \mathbf{v}_s) = \mathbf{J}_k + \rho_l^k \phi S_l(\mathbf{v}_l - \mathbf{v}_s) \tag{1.32}$$

Introducing the Darcy velocity for unsaturated flow, $\mathbf{u} = S_l\phi(\mathbf{v}_l - \mathbf{v}_s)$ (1.20), into equation (1.32) leads to the relationship between mass flux, diffusion flux, and Darcy velocity

$$\mathbf{I}_k = \mathbf{J}_k + \rho_l^k \mathbf{u}$$

or

$$\mathbf{J}_k = \mathbf{I}_k - \rho_l^k \mathbf{u} \tag{1.33}$$

This equation is particularly useful in later chapters for defining flux interactions.

Divergence of diffusion flux: The divergence conceptually represents the net flow in or out of the REV. In the absence of chemical reactions and solution advection, species mass remains conserved, meaning it cannot be created or destroyed. Any change in mass occurs solely due to inflow or outflow of $\mathbf{J}_k$ (see Figure 1.2). Consequently, alterations in species mass fraction within a liquid flow within a saturated porous medium are directly linked to the diffusion flux (Appelo and Postma, 2004):

$$(\phi\rho_l^l)\frac{\partial c_k}{\partial t} = -\nabla \cdot \mathbf{J}_k \tag{1.34}$$

where $\frac{\partial c_k}{\partial t}$ describes the partial derivative of c_k with respect to the time t. $\nabla \cdot \mathbf{J}_k$ is the divergence of $\mathbf{J}_k$, which can be expressed as

$$\begin{aligned} \nabla \cdot \mathbf{J}_k &= \left(\frac{\partial}{\partial x_1}\mathbf{e}_1 + \frac{\partial}{\partial x_2}\mathbf{e}_2 + \frac{\partial}{\partial x_3}\mathbf{e}_3\right) \cdot \left(J_{k(1)}\mathbf{e}_1 + J_{k(2)}\mathbf{e}_2 + J_{k(3)}\mathbf{e}_3\right) \\ &= \frac{\partial J_{k(1)}}{\partial x_1} + \frac{\partial J_{k(2)}}{\partial x_2} + \frac{\partial J_{k(3)}}{\partial x_3} \end{aligned} \tag{1.35}$$

where $\partial J_{k(1)}$, $\partial J_{k(2)}$, and $\partial J_{k(3)}$ are the components in the space directions (x_1, x_2, x_3) of the vector $\mathbf{J}_k$ and $\mathbf{e}_1$, $\mathbf{e}_2$, and $\mathbf{e}_3$ are the unit vectors in the directions of x_1, x_2, x_3, respectively. A positive divergence means a net outflow of the kth component, whereas a negative divergence means a net inflow.

In the context of chemical reactions (Appelo and Postma, 2004), equation (1.34) is extended to become

$$(\phi\rho_l^l)\frac{\partial c_k}{\partial t} = -\nabla\cdot\mathbf{J}_k + v_k J_{ch} \tag{1.36}$$

where J_{ch} is the rate of species change per unit volume, described as $J_{ch} = \dfrac{d\xi}{dt}$ (in which $d\xi$ is the extent of a chemical reaction[5]), and v_k is the stoichiometric coefficient for the kth component chemical reactions (Groot and Mazur, 1962). Equations (1.34) and (1.36) have not included the coupled influence of water flow. This will be discussed in Chapter 2 for a more general thermodynamic expression.

1.2.5 Fourier's law

Fourier's law (Fourier, 1878) describes the heat conduction flow rate through a material controlled by the negative gradient in the temperature (T). It is given by

$$\mathbf{I}_q' = -\lambda\nabla T \tag{1.37}$$

where $\mathbf{I}_q'$ is the heat conduction flux density and λ is the thermal conductivity of the material.

While Fourier's law provides a fundamental understanding of heat conduction in homogeneous materials, its application to porous media is limited. In porous media, heat transfer can also occur through multiphase flow processes, such as convection and advection. These additional mechanisms play a significant role in heat transport in porous media and are not fully captured by Fourier's law alone. Further details on multiphase heat transfer mechanisms in porous media will be discussed in Section 2.3.6.

1.3 SOLIDS-FLUIDS COUPLING: THEORY DEVELOPMENT AND CONSTITUTIVE MODELS

After establishing the fundamentals of single physics phenomena in porous media in Section 1.2, including water flow (Darcy's law), chemical diffusion (Fick's law), and thermal conduction (Fourier's law), this

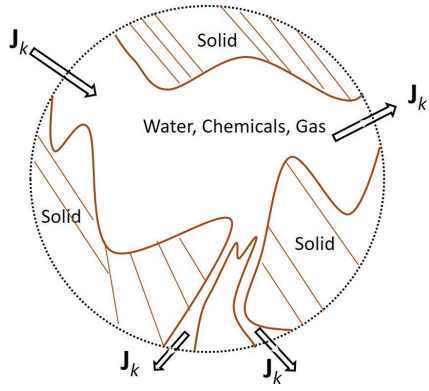

FIGURE 1.2 Inflow or outflow of a porous medium mixture

section investigates the interplay between two distinct physical phenomena: fluids and solids, particularly in the context of soils.

The strength of soils arises from the friction between soil particles. The total normal stress ($\boldsymbol{\sigma}$) is the force per unit area transmitted in a normal direction across a plane, assuming the soil to be a solid matrix and a single-phase material without any fluid (e.g., water). However, when pore water is present in the soil pores, the pore water pressure (p_w) tends to push the soil particles apart and reduces the friction between them.

1.3.1 Effective stress and pore water pressure

The concept of effective stress that controls the strength of the soil/rock solid matrix was developed by Terzaghi (1943), based on the assumption that the solid particles (but not the matrix) are incompressible. This principle, which applies to fully saturated soils, relates to three stresses. For example, in the vertical z-direction of the space coordinates x, y, z (equals to x_1, x_2, x_3 as introduced in previous sections), the relationship between the total vertical normal stress (σ_z), the pore water pressure (p_w), and the vertical effective normal stress (σ'_z) may be expressed as

$$\sigma'_z = \sigma_z - p_w \tag{1.38}$$

In the water-saturated condition, the water pressure (p_w) equals the pore pressure (p_{pore}). In a multiple phase flow (e.g., water, gas) condition, the pore pressure is the total pressure caused by the water pressure (p_w), gas pressure (p_g), and other immiscible phases (e.g., the oil pressure p_o in a porous oil reservoir).

The effective stress concept was extended to consider the compressibility of solid particles and fluids in three-dimensional space by Biot (1941). Hence, the general form of the effective stress concept may be defined as

$$\sigma'_{ij} = \sigma_{ij} - \zeta\, p_{pore}\delta_{ij} \tag{1.39}$$

where σ'_{ij} and σ_{ij} are the components of effective stress and total stress, respectively; ζ is Biot's coefficient, where, for soft soils, $\zeta \approx 1$; and δ_{ij} is the Kronecker delta, which equals to 1 if $i = j$ and to 0 if $i \neq j$ (Appendix 1). The total stress is carried partly by the water and partly by the solid constituent. In equation (1.39), the stress components can be expressed using tensors. For example, σ_{ij} can be expressed as a matrix $\boldsymbol{\sigma}$ (tensor), which is described as

$$\boldsymbol{\sigma} = [\sigma_{ij}] = \begin{bmatrix} \boldsymbol{\sigma}_1 \\ \boldsymbol{\sigma}_2 \\ \boldsymbol{\sigma}_3 \end{bmatrix} = \begin{bmatrix} \sigma_{11} & \sigma_{12} & \sigma_{13} \\ \sigma_{21} & \sigma_{22} & \sigma_{23} \\ \sigma_{31} & \sigma_{32} & \sigma_{33} \end{bmatrix} \quad (i, j = 1,\ 2,\ \text{and}\ 3) \tag{1.40}$$

The pore pressure may be interpreted as the average pressure $\overline{p}$ through (Lewis and Schrefler, 1982)

$$p_{pore} \approx \overline{p} = \sum_{\alpha=1}^{N_P} S_\alpha p_\alpha \tag{1.41}$$

where α (1, 2, … N_p) denotes the immiscible phase (e.g., water, gas, etc.), N_p is the total number of phases, and S_α is the saturation ratio of the corresponding phase (e.g., S_w and S_g are the water and gas saturation ratios, respectively), which can be expressed using the fraction of the volume of the α th phase V_α divided by the total pore volume V_{pore}, as

$$S_\alpha = \frac{V_\alpha}{V_{pore}} \tag{1.42}$$

The pressure differences of the multiple phases may influence the saturation ratio. For example, in unsaturated soils/rocks, p_c is the capillary pressure representing the pressure difference across the interface between air and water, which is defined as (Fredlund and Rahardjo, 1993)

$$p_c = p_{atm} - p_w \tag{1.43}$$

where p_{atm} is the atmospheric pressure. Since p_w for unsaturated soils/rocks is defined as negative, therefore p_c is positive. The degree of saturation and the pressure are characterized by the van Genuchten relationship (van Genuchten, 1980)[6]:

$$S_e = \left[(| p_c | / M)^{\frac{1}{(1-m)}} + 1 \right]^{-m} \tag{1.44}$$

where M [Pa or MPa] is proportional to the capillary entry pressure, m is a constant related to pore size distribution, and S_e is the effective saturation defined as

$$S_e = \frac{S_w - S_r}{1 - S_r} \tag{1.45}$$

where S_r is the irreducible water saturation after drainage.

Effective stress presents a link between the deformation of solids and the pore water pressure, although it does not sufficiently account for dynamic couplings between soils/fluids. Traditionally, two major average approaches have been developed to model water- and solid-phase coupling in deformable porous media, namely, the mechanics approach and the mixture theory approach. The mechanics approach is based on the classical geomechanics consolidation theories of Terzaghi and Biot (Biot, 1962, 1972; Terzaghi, 1943). Meanwhile, the mixture theory approach employs continuum mechanics to model individual components of the mixture (Bowen, 1976).

1.3.2 Terzaghi's one-dimensional consolidation theory

Terzaghi devised a straightforward one-dimensional vertical consolidation model to explore the dynamic interplay between soil deformation (specifically in the vertical z-direction) and water flow, expressed as the equation (Terzaghi, 1943)

$$\frac{\partial p_w}{\partial t} = C_v \frac{\partial^2 p_w}{\partial z^2} \tag{1.46}$$

Here, C_v represents the coefficient of consolidation, denoting the rate at which a saturated soil consolidates under an increase in pore water pressure.

This model operates under several key assumptions: (1) the soil is both homogeneous and isotropic; (2) individual particles within the soil are incompressible, though the soil skeleton is compressible; (3) any additional stress applied to the soil is evenly distributed horizontally, resulting in vertical compression and water seepage; (4) Darcy's law remains valid; (5) the hydraulic conductivity in vertical direction K_v remains constant; (6) external loading occurs suddenly and remains constant throughout the consolidation process; (7) soil deformation is solely due to the dissipation of pore water pressure.

The derivation process unfolds as follows: upon the application of a vertical external load to a fully saturated cohesive soil, the initial stress increase is borne by the water, initiating its escape and gradually transferring the load to the soil skeleton over time. Consequently, the soil undergoes compression, leading to alterations in its properties.

In constructing the model, the top surface is designated as the coordinate origin and is permeable, with the positive z-direction indicating downward movement. Assuming a soil layer resting atop an impervious base at depth b_1, an element (REV) situated at depth b within the saturated soil experiences an upward flow of porewater subsequent to the application of an external load on the surface (refer to Figure 1.3).

In accordance with *Darcy's law*, the inflow rate Q_1 (at the lower surface of the element) and the outflow rate Q_2 (at the upper surface) of this element are:

$$Q_1 = K_v(-\frac{\partial H}{\partial z})\, dxdy \tag{1.47}$$

$$Q_2 = Q_1 + \frac{\partial Q_1}{\partial z} dz = K_v(-\frac{\partial H}{\partial z} - \frac{\partial^2 H}{\partial z^2} dz)\, dxdy \tag{1.48}$$

where $\frac{\partial H}{\partial z}$ is the gradient of the hydraulic head in the z direction (H) and $dxdy$ is the cross-sectional area perpendicular to the water flow direction (z). The change in the volume of the flow rate can be derived as

$$Q_1 - Q_2 = K_v \frac{\partial^2 H}{\partial z^2} dzdxdy \tag{1.49}$$

Since the volume of this element changes due to the consolidation process, the time-dependent change in water volume within this element

can be calculated by considering the variation in the pore volume V_{pore} as follows:

$$Q_1 - Q_2 = \frac{\partial V_{pore}}{\partial t} \tag{1.50}$$

As $V_{pore} = \phi V$ in which ϕ is the porosity and V can be expressed as $dxdydz$, equation (1.50) becomes

$$Q_1 - Q_2 = \frac{\partial V_{pore}}{\partial t} = \frac{\partial \phi}{\partial t} dxdydz \tag{1.51}$$

Considering the relationship between ϕ and the void ration e as $\phi = \frac{e}{1+e_0}$, in which e_0 is the initial void ratio that is a constant depending on the properties of the soil, equation (1.51) can be rewritten as

$$Q_1 - Q_2 = \frac{\partial \phi}{\partial t} dxdydz = \frac{\partial \left(\frac{e}{1+e_0} \right)}{\partial t} dxdydz \tag{1.52}$$

Substitution of equation (1.49) into equation (1.50) leads to

$$K_v \frac{\partial^2 H}{\partial z^2} = \frac{1}{1+e_0} \frac{\partial e}{\partial t} \tag{1.53}$$

Equation (1.53) gives the relationship between the water pressure head H and the void ration e, and H is described as

$$H = H_0 + \frac{p_w}{\rho_l^w g} \tag{1.54}$$

where H_0 is the initial pore water pressure head before the external load is applied (the constant depends on the gravity potential datum point) and g is the gravity.

By substituting equation (1.54) into equation (1.53), the relationship between p_w and e can be obtained as

$$\frac{K_v}{\rho_l^w g} \frac{\partial^2 p_w}{\partial z^2} = \frac{1}{1+e_0} \frac{\partial e}{\partial t} \tag{1.55}$$

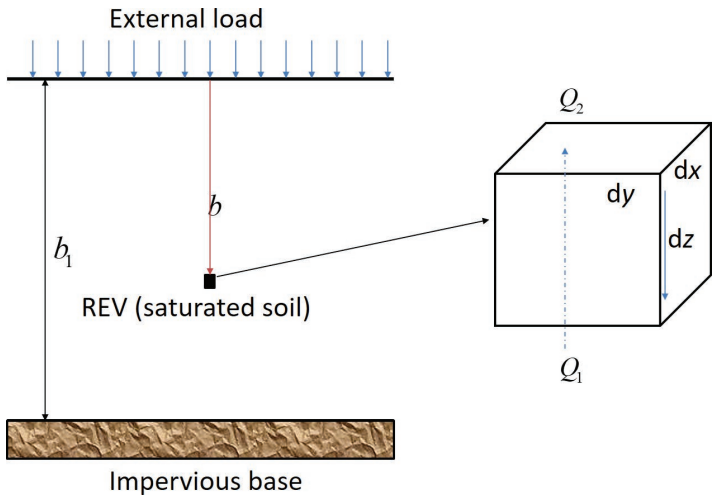

FIGURE 1.3 Conceptual model of Terzaghi's consolidation theory

Since the change in the void ratio $\frac{\partial e}{\partial t}$ is governed by soil deformation, the next step will focus on deriving the relationship between the void ratio and the effective stress (and eventually the water pressure p_w). This will allow equation (1.55) to be simplified further, containing only one variable, thereby making it solvable.

For the solid part of a saturated soil, the relationship between e and the effective stress σ' is expressed as

$$\frac{\partial e}{\partial t} = -Q_v \frac{\partial \sigma'}{\partial t} \tag{1.56}$$

where Q_v is the vertical compressibility of the soil. Substituting the effective stress equation (1.38) for saturated soils into equation (1.56) leads to

$$\frac{\partial e}{\partial t} = Q_v \frac{\partial p_w}{\partial t} - Q_v \frac{\partial \sigma}{\partial t} \tag{1.57}$$

Substituting equation (1.57) into equation (1.55) leads to

$$\frac{K_v}{\rho_l^w g} \frac{\partial^2 p_w}{\partial z^2} = \frac{Q_v}{1+e_0} \left(\frac{\partial p_w}{\partial t} - \frac{\partial \sigma}{\partial t} \right)$$

or simplified as

$$C_v \frac{\partial^2 p_w}{\partial z^2} = \frac{\partial p_w}{\partial t} - \frac{\partial \sigma}{\partial t} \tag{1.58}$$

where

$$C_v = \frac{K_v(1+e_0)}{Q_v \rho_l^w g} \tag{1.59}$$

is the coefficient of consolidation (vertical).

Assuming the total stress is constant $\left(\frac{\partial \sigma}{\partial t} = 0\right)$, equation (1.58) becomes identical to equation (1.46):

$$C_v \frac{\partial^2 p_w}{\partial z^2} = \frac{\partial p_w}{\partial t}$$

1.3.3 Biot's three-dimensional consolidation theory

In spite of Terzaghi's later development of a new differential equation for two- and three-dimensional consolidation, the assumption of constant total mechanical stress during consolidation lacks rigor (Cryer, 1963). Biot (1941) expanded Terzaghi's one-dimensional theory into a three-dimensional consolidation theory. The key difference between Biot's and Terzagh's theories lies in their treatment of mean total stress. While Terzaghi's theory assumes it to be constant, Biot's theory acknowledges its variability throughout consolidation (Sills, 1975).

Biot's elasticity, rooted in continuum mechanics, delineates the three-dimensional consolidation process in a porous saturated medium (i.e., containing water). In contrast to Terzaghi's theory, Biot's theory incorporates two fundamental coupled phenomena: (1) solid-to-fluid coupling, wherein stress variation leads to corresponding changes in fluid properties (e.g., fluid pressure and mass); (2) fluid-to-solid coupling, wherein changes in fluid properties induce variations in solid frame/skeleton properties (e.g., displacement or stress).

The equation governing solid deformation is

$$\left(K - \frac{2G}{3}\right)\frac{\partial^2 d_k}{\partial x_k \partial x_j} + G\left(\frac{\partial^2 d_i}{\partial x_j \partial x_j} + \frac{\partial^2 d_j}{\partial x_i \partial x_j}\right) - \zeta \frac{\partial p_w}{\partial x_j} = f_j \tag{1.60}$$

where G represents the shear modulus of the geomaterial, K denote the bulk modulus of the solid skeleton, and $\mathbf{d} = [d_i, d_j, d_k]$ (i, j, k = 1, 2, and 3) symbolizes the total displacement in which d_i is the displacement

in the i axis direction. $\zeta \dfrac{\partial p_w}{\partial x_j}$ is the fluid-to-structure coupling, in which ζ is the Biot constant that can be determined through experimental methods (Franquet and Abass, 1999).

The fluid flow is described as

$$\zeta \frac{\partial^2 d_i}{\partial x_i \partial t} + s_p \frac{\partial p_w}{\partial t} - \frac{k}{v} \frac{\partial^2 p_w}{\partial x_i^2} = 0 \tag{1.61}$$

where s_p represents the elastic storativity of the pore space, and the time derivative $\dfrac{\partial^2 d_i}{\partial x_i \partial t}$ signifies the structure-to-fluid coupling term.

Equations (1.60) and (1.61)) encapsulate poroelastic effects. Biot's theory relies on several assumptions (Biot, 1941): (1) isotropic material, (2) reversibility of stress-strain relations under final equilibrium conditions, (3) linearity of stress-strain relations, (4) small strains, and (5) adherence to Darcy's law for water flow through the porous skeleton.

The derivation process for Biot's equations unfolds as follows:

Part 1: Solid deformation: Consideration of a small cubic soil element (REV) in the subsurface reveals its sides to be parallel with the coordinate axes, sufficiently large to encompass both pores and solid parts, and treated as homogeneous. The equilibrium condition for the corresponding stress components of the element is

$$\frac{\partial \sigma_{ij}}{\partial x_j} + f_j = 0 \tag{1.62}$$

where f_j is the body force (e.g., gravity) and σ_{ij} is the three-dimensional Cauchy stress tensor.

Substituting equation (1.39) into equation (1.62) leads to

$$\frac{\partial \sigma'_{ij}}{\partial x_j} + \zeta \frac{\partial p_w}{\partial x_j} + f_j = 0 \tag{1.63}$$

The soil deformation is then characterized using strain ε_{ij} and displacement $\mathbf{d} = [d_i, d_j, d_k]$. Assuming the strain ε_{ij} is small, it can be defined in terms of displacement gradients $\left(d_{i,j} = \dfrac{\partial d_i}{\partial x_j} \right)$ as

$$\varepsilon_{ij} = \varepsilon_{ji} = \frac{1}{2}(d_{i,j} + d_{j,i}) = \frac{1}{2}\left(\frac{\partial d_i}{\partial x_j} + \frac{\partial d_j}{\partial x_i} \right) \tag{1.64}$$

and

$$\varepsilon_{kk} = d_{k,k} = \frac{\partial d_k}{\partial x_k} \tag{1.65}$$

As the effective stress σ'_{ij} determines the deformation and follows a linear elastic stress-strain relationship, σ'_{ij} can be described as

$$\sigma'_{ij} = -\left(K - \frac{2G}{3}\right)\varepsilon_{kk}\delta_{ij} - G\left(\frac{\partial d_i}{\partial x_j} + \frac{\partial d_j}{\partial x_i}\right) \tag{1.66}$$

Note: In equation (1.66), the minus sign is included to indicate that stresses are considered positive for compression. It's worth noting that, for Chapters 3–7, the convention is adopted where compression $\left(\sigma'_{ij} = \left(K - \frac{2G}{3}\right)\varepsilon_{kk}\delta_{ij} + G\left(\frac{\partial d_i}{\partial x_j} + \frac{\partial d_j}{\partial x_i}\right)\right)$ is represented by a negative sign. This convention aligns with the standard notations in engineering mechanics, as commonly observed in continuum mechanics literature (Haupt, 2013, Chaves, 2013). This approach facilitates the analysis of both swelling (positive) and consolidation (negative) phenomena within the framework of the book.

Substituting equation (1.66) into equation (1.63) leads to

$$\frac{\partial}{\partial x_j}\left(-\left(K - \frac{2G}{3}\right)\varepsilon_{kk}\delta_{ij} - G\left(\frac{\partial d_i}{\partial x_j} + \frac{\partial d_j}{\partial x_i}\right)\right) + \zeta\frac{\partial p_w}{\partial x_j} + f_j = 0 \tag{1.67}$$

Using $\varepsilon_{kk} = d_{k,k} = \frac{\partial d_k}{\partial x_k}$, equation (1.67) can be simplified as[7]

$$\left(K - \frac{2G}{3}\right)\frac{\partial^2 d_k}{\partial x_k \partial x_j} + G\left(\frac{\partial^2 d_i}{\partial x_j \partial x_j} + \frac{\partial^2 d_j}{\partial x_i \partial x_j}\right) - \zeta\frac{\partial p_w}{\partial x_j} = f_j \tag{1.68}$$

Part 2: Liquid transport (water): Considering the mass balance equation for water, the change in water volume can be calculated by accounting for the inflow and outflow of water from the soil element. This change in water volume is dependent on alterations in soil volume and water density, and can be expressed as

$$\frac{\partial(\phi\rho_l^w)}{\partial t} = -\nabla\cdot(\phi\rho_l^w\mathbf{v}_w) \tag{1.69}$$

If the porosity is not constant, equation (1.69) can be rewritten as

$$\frac{\rho_l^w \partial\phi}{\partial t} + \frac{\phi \partial \rho_l^w}{\partial t} + \nabla \cdot (\phi \rho_l^w \mathbf{v}_w) = 0 \tag{1.70}$$

The density equation can be linked to water pressure as

$$\frac{\partial \rho_l^w}{\partial t} = \rho_l^w C_{v-f} \frac{\partial p_w}{\partial t} \tag{1.71}$$

in which C_{v-f} is the compressibility of the water. Substituting equation (1.71) into equation (1.70) leads to

$$\frac{\rho_l^w \partial\phi}{\partial t} + \phi \rho_l^w C_{v-f} \frac{\partial p_w}{\partial t} + \nabla \cdot (\phi \rho_l^w \mathbf{v}_w) = 0 \tag{1.72}$$

To introduce the deformation of the solid into equation (1.72), it is necessary to consider the solid balance equation, which is

$$\frac{\partial\left[(1-\phi)\rho_s^s\right]}{\partial t} = -\nabla \cdot ((1-\phi)\rho_s^s \mathbf{v}_s) \tag{1.73}$$

where ρ_s^s is the true density of the solid (relative to the solid phase).

To simplify the tensor discussion and facilitate a comparison with Terzaghi's one-dimensional derivation, the initial derivation will be based on a one-dimensional (e.g., vertical) framework. Subsequently, it will be expanded to three dimensions. The change in solid density over time, which is linked to stress and pressure, can be expressed as:

$$\frac{\partial \rho_s^s}{\partial t} = \frac{\rho_s^s C_{v-s}}{1-\phi}\left(\frac{\partial \sigma}{\partial t} - \phi \frac{\partial p_w}{\partial t}\right) \tag{1.74}$$

Substituting equation (1.74) into equation (1.73) leads to

$$-\frac{\partial \phi}{\partial t} + C_{v-s}\left(\frac{\partial \sigma}{\partial t} - \phi \frac{\partial p_w}{\partial t}\right) + \nabla \cdot \mathbf{v}_s - \nabla \cdot \left(\phi \mathbf{v}_s\right) = 0 \tag{1.75}$$

By using both equations (1.75) and(1.72), and removing the term $\frac{\partial \phi}{\partial t}$, it leads to

$$\frac{\partial \varepsilon}{\partial t} + \phi(C_{v-f} - C_{v-s}) \frac{\partial p_w}{\partial t} + C_{v-s} \frac{\partial \sigma}{\partial t} = -\nabla \cdot \left(\phi(\mathbf{v}_w - \mathbf{v}_s)\right) \tag{1.76}^{8}$$

Since equation (1.39) can be rewritten in one-dimensional analysis as $\sigma = \sigma' + \zeta p_w$, and σ' may be described as $\sigma' = \dfrac{-\varepsilon}{C_m}$, in which C_m is the compressibility of the porous medium, which links with ζ and C_{v-s} through the relationship

$$\zeta = 1 - \frac{C_{v-s}}{C_m} \tag{1.77}$$

Equation (1.76) can be rewritten as

$$\zeta \frac{\partial \varepsilon}{\partial t} + s_p \frac{\partial p_w}{\partial t} = -\nabla \cdot \left(\phi(\mathbf{v}_w - \mathbf{v}_s)\right) = -\nabla \cdot (\mathbf{u}) \tag{1.78}^{9}$$

where s_p is the elastic storability of the pore space, defined as $s_p = \phi C_{v-f} + (\zeta - \phi) C_{v-s}$.

By using equation (1.12) for the Darcy velocity for the saturated condition, equation (1.78) can be reformed as

$$\frac{k}{v} \nabla^2 p_w = \zeta \frac{\partial \varepsilon}{\partial t} + s_p \dot{p}_w \tag{1.79}$$

where

$$\nabla^2 = \partial^2 / \partial x_i^2 + \partial^2 / \partial x_j^2 + \partial^2 / \partial x_k^2 \tag{1.80}$$

Equation (1.79) can be changed to three-dimension by using the relationship between strain and displacement (1.64), which leads to equation (1.61):

$$\zeta \frac{\partial \dot{d}_i}{\partial x_i} + s_p \dot{p}_w - \frac{k}{v} \frac{\partial^2 p_w}{\partial x_i^2} = 0$$

Note that equation (1.61) reduces to Terzaghi's equation under one-dimensional conditions when the time-dependent displacement is neglected, resulting in:

$$\frac{k}{s_p v} \frac{\partial^2 p_w}{\partial x_i^2} = \dot{p}_w \tag{1.81}$$

where $\dfrac{k}{s_p v} = C_v$ is the coefficient of consolidation. This leads to the conclusion that Terzaghi's equation for one-dimensional consolidation is a special case of Biot's three-dimensional consolidation model.

1.3.4 Mixture theory

Compared with Biot's theory, which emphasizes interactions between water and soils, mixture theory is developed for several overlapping continua based on continuum mechanics (Bowen, 1980). Mixture theory assumes that all phases are present at every material point, allowing for the use of momentum and mass balance equations. This section provides an overview of using mixture theory to analyze water-saturated porous mediums as a comparison with Biot's theory and Terzaghi's theory.

1.3.4.1 "Partial density," and "mixture density"

Two different but interlinked concepts of density are used in mixture theory (and Mixture-Coupling Theory), entitled "partial density" ρ_α^i (or true density ρ_α^α for a single-phase) and "mixture density" ρ_i (or ρ_α for a single-phase), respectively.

1.3.4.1.1 One fluid-saturated medium (liquid or gas)

The volume fraction of the solid ϕ_s and the fluid ϕ_f can be denoted as

$$\phi_s = \frac{V_s}{V},\ \phi_f = \frac{V_f}{V} = \phi \tag{1.82}$$

where V_s(or V_f) and V are the volumes of the solid (or fluid) phase and total mixture, respectively.

The relationship between the porosity ϕ and ϕ_s is

$$\phi_s = 1 - \phi_f \quad (\text{solid}) \tag{1.83}$$

The 'mixture density' of the solid-fluid mixture system is described as

$$\rho = \frac{\rho_s^s V_s + \rho_f^f V_f}{V} \tag{1.84}$$

where ρ_s^s and ρ_f^f are the "true density" of the solid and fluid phases, respectively.

By introducing equation (1.82) into equation (1.84), it leads to the relationship between the density (ρ) of the mixture, the solid and fluid "mixture density" (ρ_s and ρ_f), and their "partial density" (ρ_s^s and ρ_f^f), respectively:

$$\rho = \rho_s^s \phi_s + \rho_f^f \phi_f = \rho_s + \rho_f \tag{1.85}$$

If only water and solid particles are considered in the mixture (e.g., saturated soil), the partial density and mixture density of (1) the water are described as ρ_l^w and ρ_w, and of (2) the solid particles are described as ρ_s^s and ρ_s, respectively. These densities are also used for the derivation process of Mixture-Coupling Theory (more details are given in Section 1.4.1).

1.3.4.2 Constitutive equation development

The dynamic movement of solids and fluids adheres to the principles of mass balance and mechanical equilibrium. When considering only one solid phase and one fluid phase in the mixture, and employing continuum mechanics, the mass balance equations using mixture density in the absence of chemical reactions are derived as follows (Bowen, 1976; Araujo and McElwain, 2005):

$$\dot{\rho}_w + \nabla \cdot (\rho_w \mathbf{v}_w) = 0 \quad \text{and} \quad \dot{\rho}_s + \nabla \cdot (\rho_s \mathbf{v}_s) = 0 \tag{1.86}$$

which analogue to equations (1.69) and (1.72), respectively. The major difference between equation (1.86) and equation (1.69) is that the mixture density $\rho_w = \rho_l^w \phi$ is used in equation (1.86) to replace the porosity ϕ and simplify the derivation process.

The mass balance equation for the whole mixture is described as

$$\dot{\rho} + \nabla \cdot (\rho \mathbf{v}) = 0 \tag{1.87}$$

where $\mathbf{v}$ is the macroscopic medium velocity described as

$$\mathbf{v} = \frac{\rho_s}{\rho} \mathbf{v}_s + \frac{\rho_w}{\rho} \mathbf{v}_w \tag{1.88}$$

Using a similar derivation process to Section 1.3.3 (equations (1.68)–(1.74)) leads to the same function as equation (1.78)

$$\nabla \cdot (\mathbf{v}_s) + \phi(\mathbf{v}_w - \mathbf{v}_s) + \phi(C_{v\text{-}f} - C_{v\text{-}s}) \frac{\partial p_w}{\partial t} + C_{v\text{-}s} \frac{\partial \sigma}{\partial t} = 0$$

Conservation of momentum

$$\text{Fluid: } \frac{\partial(\rho_w \mathbf{v}_w)}{\partial t} + \nabla(\phi p_w) + \rho_w g + \boldsymbol{\chi} = 0 \tag{1.89}$$

$$\text{Solid particles: } \frac{\partial(\rho_s \mathbf{v}_s)}{\partial t} + \nabla(\boldsymbol{\sigma} - \phi p_w) + \rho_s g - \chi = 0 \tag{1.90}$$

where $\boldsymbol{\sigma}$ is the total stress tensor and χ is the internal frictional interaction force between the solid and fluid phases that can be described as

$$\chi = \frac{\phi^2 \nu}{k}(\mathbf{v}_w - \mathbf{v}_s) + p_w \nabla\phi \tag{1.91}$$

in which the term $\frac{\phi^2 \nu}{k}(\mathbf{v}_f - \mathbf{v}_s)$ denotes the friction between moving fluids and the solid particles system, and $p_w \nabla\phi$ defines the interaction caused by the change of the pore space resulting from water pressure.

Using equation (1.15) for saturated conditions, equation (1.91) can be reorganized as

$$\chi = \frac{\phi^2 v}{k}(\mathbf{v}_w - \mathbf{v}_s) + p_w \nabla\phi = \frac{\phi v \overbrace{\mathbf{u}}^{=\phi(\mathbf{v}_w - \mathbf{v}_s)}}{k} + p_w \nabla\phi \tag{1.92}$$

Substitution of equation (1.92) into (1.89) leads to

$$\frac{\partial(\rho_w \mathbf{v}_w)}{\partial t} + \nabla(\phi p_w) + \rho_w g + \frac{\phi v \mathbf{u}}{k} + p_w \nabla\phi = 0 \tag{1.93}$$

With the assumption of a quasi-static condition and ignoring the inertia terms, it leads to

$$\overbrace{\frac{\partial(\rho_w \mathbf{v}_w)}{\partial t}}^{=0} + \nabla(\phi p_w) + \rho_w g + \frac{\phi v \mathbf{u}}{k} + \overbrace{p_w \nabla\phi}^{=0} = 0 \tag{1.94}$$

which can be reformed as

$$\mathbf{u} = \frac{k\left(\nabla(p_w) + \rho_l^w g\right)}{v} \tag{1.95}[10]$$

Equation (1.95) is Darcy's law with the consideration of gravity.

Adding equations (1.89) and (1.90) leads to

$$\frac{\partial(\rho_w \mathbf{v}_w)}{\partial t} + \nabla(\phi p_w) + \rho_w g + \chi + \frac{\partial(\rho_s \mathbf{v}_s)}{\partial t} + \nabla(\boldsymbol{\sigma} - \phi p_w) + \rho_s g - \chi = 0 \tag{1.96}$$

By ignoring quasi-statics and the inertia term, equation (1.96) leads to

$$\nabla \cdot \boldsymbol{\sigma} + \rho g = 0 \qquad (1.97)^{11}$$

which is the same as equation (1.62). Following the rest of the derivation steps in Biot's consolidation, the same final equation of solid/fluid coupling can be obtained.

Mixture theory has found extensive applications across diverse fields, including civil engineering and biological sciences. In the realm of biological systems, it has been instrumental in developing constitutive equations for organs, tissues, and cells (Humphrey, 2003; Mow and Lai, 1979). For instance, it has been employed in modeling tumor growth and soft tissues (Byrne and Preziosi, 2003; Ambrosi and Preziosi, 2002; Preziosi and Tosin, 2009), arterial tissue (Klanchar and Tarbell, 1987; Jayaraman, 1983), lungs (Ford et al., 1990), and skin (Oomens et al., 1987).

In civil engineering, mixture theory has been applied to various areas such as soils, rocks, and concretes. For example, it has been utilized in modeling fluid injection into saturated geological porous media (Chen, 1996), analyzing mixtures of fluids and elastic solids interacting with electromagnetic fields (Eringen, 1998), developing one-dimensional sedimentation constitutive equations using the method of Lagrangian multipliers (Cvetković et al., 2011), and understanding heat conduction in laminated composites (Nayfeh, 1975). Moreover, mixture theory has been instrumental in studying reactive granular materials (Baer and Nunziato, 1986), exploring physical oceanography and meteorology (Kirwan, 1985), and investigating turbulent phenomena such as snow, air flows, and sedimentation (Decker, 1990).

1.3.5 Comparison of these theories

A comparison between the mechanics approach and the mixture theory approach has been elucidated by Chen and Hicks (2013). The mechanics approach offers the advantage of addressing hydromechanical coupled processes effectively, as it can establish a connection between water pressure and material stress through the concept of effective stress. However, to incorporate more intricate chemical processes into the coupling, the mechanics approach often necessitates borrowing chemical transport and reaction formulations from geochemistry due to the divide between geomechanics and geochemistry. Substantial research has been conducted in this domain, encompassing hydromechanical coupled models (Sanavia et al., 2002;

Meroi et al., 1995; Lewis and Schrefler, 1987, 1998), unsaturated soils (Thomas, 1985, 1988; Thomas and Rees, 1993), thermal coupling (Thomas and King, 1991; Thomas and Sansom, 1995; Thomas et al., 1998), and chemical coupling (Seetharam et al., 2007; Li et al., 2006; Huyghe and Janssen, 1999).

On the other hand, mixture theory preserves the individual characteristics of the solid and fluid phases (Truesdell and Toupin, 1960; Bowen, 1984), yet it can be challenging to obtain insights into the interaction between the phases and to address molecular couplings (Laloui et al., 2003). Nevertheless, mixture theory offers a deeper understanding of the mechanisms underlying solid and fluid interactions during the consolidation process (e.g., the consideration of χ and the velocity of the solid $\mathbf{v}_s$). Biot's equation and Terzaghi's equation thus become specific cases of mixture theory with simplifications (e.g., quasi-statics).

However, as the concept of friction (χ) derived from Newtonian mechanics primarily accounts for macroscale friction forces, a new theory, Mixture-Coupling Theory, is necessary to encompass molecule-scale frictions and other dissipative processes. Mixture-Coupling Theory is adept at handling both large and small deformations of fluid-filled porous media, necessitating the introduction of concepts such as large deformations and the Reynolds transport theorem.

1.3.6 Large deformation basics and Reynolds transport theorem

The preceding discussions concerning Terzaghi's theory, Biot's theory, and mixture theory in Sections 1.3.1–1.3.3 have primarily centered on the small deformation of porous media utilizing the Cauchy stress tensor (σ). However, it's important to acknowledge that geomaterials may undergo significant deformations, prompting the introduction of the fundamentals of large deformations.

1.3.6.1 Reference configuration vs current configuration

Configuration: The configuration of a solid is defined as the spatial arrangement occupied by the solid within a mixture. A reference configuration is typically chosen as a convenient reference point, often corresponding to the initial configuration prior to any deformation, represented by $\mathbf{X}(X_1, X_2, X_3)$ in Figure 1.4. The region now occupied by the solid following deformation is termed the current configuration, represented by $\mathbf{x}(x_1, x_2, x_3)$ in Figure 1.4. In mathematical terms, the

mapping between the current configuration and the reference configuration is assumed to be one-to-one and can be expressed as

$$\mathbf{x} = \mathbf{X}(\mathbf{X}_0, t) \tag{1.98}$$

where $\mathbf{X}_0$ is the position vector of the particle at the reference time when $t = t_0$.

The current configuration $\mathbf{x}$ may be described using the displacement $\mathbf{d}(\mathbf{X}, t)$ and reference configuration $\mathbf{X}$ as

$$\mathbf{x} = \mathbf{X} + \mathbf{d}(\mathbf{X}, t) \quad \text{or} \quad x_i = X_i + d_i(X_1, X_2, X_3, t) \,(\text{in index notation}) \tag{1.99}$$

The local velocity of the solid $\mathbf{v}_s(\mathbf{X}, t)$ (the average velocity of the solid particles) in the REV may be derived using the displacement as

$$\mathbf{v}_s(\mathbf{X}, t) = \frac{\partial \mathbf{x}}{\partial t} = \frac{\partial \mathbf{d}(\mathbf{X}, t)}{\partial t} \tag{1.100}$$

Utilizing displacement and velocity descriptions, the vectors of the current configuration can be expressed as functions of the positions of material particles before deformation, denoted as $\mathbf{X}$. This description is referred to as Lagrangian motion. Conceptually, the Lagrangian specification of motion can be likened to an observer moving along with a fixed point within the material (solid/fluid) through both space and time (Badin and Crisciani, 2018; Batchelor and Batchelor, 2000).

1.3.6.2 Deformation gradient and Euler's identity

Utilizing classical continuum mechanics to analyze large deformations as depicted in Figure 1.4, the deformation state of the soil/rock can be characterized. The deformation gradient for the solid, denoted as $\mathbf{F}$, is defined as (Bergstrom, 2015)

$$\mathbf{F}(\mathbf{X}, t) = \frac{\partial \mathbf{x}(\mathbf{X}, t)}{\partial \mathbf{X}} = \begin{bmatrix} \frac{\partial x_1}{\partial X_1} & \frac{\partial x_1}{\partial X_2} & \frac{\partial x_1}{\partial X_3} \\ \frac{\partial x_2}{\partial X_1} & \frac{\partial x_2}{\partial X_2} & \frac{\partial x_2}{\partial X_3} \\ \frac{\partial x_3}{\partial X_1} & \frac{\partial x_3}{\partial X_2} & \frac{\partial x_3}{\partial X_3} \end{bmatrix} \tag{1.101}$$

Here, both $\mathbf{X}$ and $\mathbf{x}$ are vectors: $\mathbf{X} = [X_1, X_2, X_3]$ and $\mathbf{x} = [x_1, x_2, x_3]$. The determinant of the deformation gradient ($\mathbf{F}$), which is a measure of the change of volume, is described as

$$\det(\mathbf{F}) = \frac{dV}{dV_0} = J \tag{1.102}$$

where dV is the volume element of the current configuration, while the corresponding volume element of the reference configuration is denoted as dV_0. The time derivative of J adheres to Euler's identity:

$$\frac{DJ}{Dt} = \dot{J} = J\nabla \cdot \mathbf{v}_s \tag{1.103}$$

Note: $J = \frac{dV_0}{dV_0} = 1$ remains constant at the reference configuration, while $\dot{J} = J\nabla \cdot \mathbf{v}_s$ can vary throughout the deformation process. If $J = \det(\mathbf{F}) = 1$ remains constant throughout the deformation process, the deformation is termed isochoric (Bergstrom, 2015).

By utilizing equations (1.102) and (1.103), the evolution pathway of the physical-chemical properties between the reference and current configurations can be determined. For instance, the relationship between the mixture mass density ρ_0 and the porosity υ of a REV at the reference configuration can be established using its density ρ and porosity ϕ at the current configuration, respectively, as

$$\rho_0 = J\rho \quad \text{and} \quad \upsilon = J\phi \tag{1.104}[12]$$

Note: In the following chapters, the mass $\rho_{ref}\left(\rho_0 = \frac{m}{V}\right)$ has been used to distinguish its density against current volume and reference volume, rather than using ρ_0.

1.3.6.3 Second Piola-Kirchhoff stress (PK2, T) and Green Strain (E)

The stress tensor at the current configuration is represented by the Cauchy stress tensor $\boldsymbol{\sigma}$, while for Mixture-Coupling Theory, the stress tensor at the reference configuration is the second Piola-Kirchhoff stress $\mathbf{T}$. This choice is motivated by the following reasons: (1) The second Piola-Kirchhoff stress can be derived from the derivative of the Helmholtz free energy with respect to the Green strain tensor $\mathbf{E}$ for a thermoelastic body (Mase et al., 2009), and the Helmholtz free energy is utilized in Mixture-Coupling Theory (see Section 2.2.3); (2) The second Piola-Kirchhoff stress is symmetric, which facilitates computational modeling.

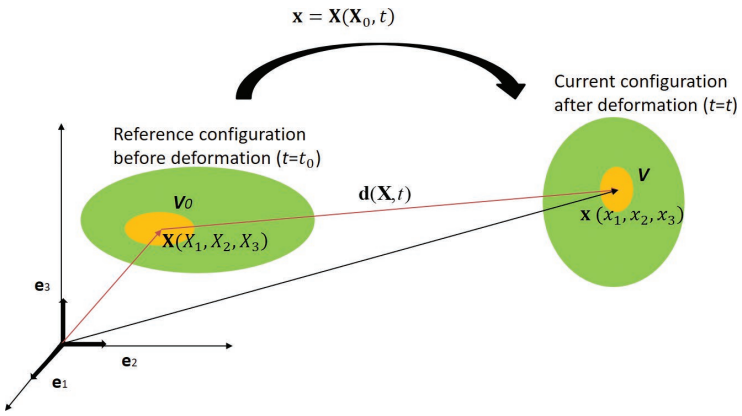

FIGURE 1.4 The concept of continuum mechanics (reference configuration vs current configuration), where eI represents the unit direction

The PK2 stress $\mathbf{T}$ and Green strain $\mathbf{E}$ are defined as

$$\mathbf{T} = J\mathbf{F}^{-1}\boldsymbol{\sigma}\mathbf{F}^{-\mathbf{T}} \quad \text{and} \quad \mathbf{E} = \frac{1}{2}(\mathbf{F}^{\mathbf{T}}\mathbf{F} - \mathbf{I}_1) \tag{1.105}$$

where $\mathbf{I}_1$ is the identity matrix that can be described by using the Kronecker delta as $\mathbf{I}_1 = [\delta_{ij}]$ (Appendix 1), with 1 along the main diagonal and 0 for the rest of the entries.

1.3.6.4 Reynolds transport theorem and the divergence theorem

To track changes in a quantity within a deforming volume (REV) that moves with the solid, the Reynolds transport theorem is employed. Let $\pi(x,t)$be a general quantity (scalar or vector) that varies with time and space, defined as the bulk density of an extensive thermodynamic property (e.g., mass density ρ). Utilizing Reynolds transport relations, the rate of change of $\pi(\mathbf{x},t)$ within the evolving REV volume ($V(t)$) of a deformed solid, excluding flux in/out and chemical reactions, can be expressed as

$$\frac{d}{dt}\int_{V(t)} \pi\, dV = \int_{V(t)} \left(\frac{\partial \pi}{\partial t}\right) dV + \int_{\Gamma(t)} (\mathbf{v}_s \cdot \mathbf{n})\pi\, d\Gamma \tag{1.106}$$

where dV and $d\Gamma$ are volume and surface elements, $\mathbf{n}$ is the outward unit normal vector on a changing surface $\Gamma(t)$, and $\mathbf{v}_s$ is the velocity of the solid (which equals the boundary velocity in continuum mechanics).

In equation (1.104), the surface integral term $\int_{\Gamma(t)} (\mathbf{v}_s \cdot \mathbf{n}) \pi \, d\Gamma$ can be converted into a volume integral term using the divergence theorem as

$$\int_{\Gamma} (\pi \mathbf{v}_s \cdot \mathbf{n}) d\Gamma = \int_{V} \nabla \cdot (\pi \mathbf{v}_s) dV \tag{1.107}$$

The divergence theorem (Pfeffer, 1986) states that the flux of the αth phase ($\mathbf{j}_\alpha$) through a closed surface $\Gamma(t)$ is mathematically described as the surface integral of the vector field over the closed surface $\int_{\Gamma} (\mathbf{j}_\alpha \cdot \mathbf{n}) d\Gamma$. This is equal to the volume integral of the divergence $(\nabla \cdot \mathbf{j}_\alpha)$ over the region Ω (with volume V) inside the surface, expressed as $\int_V (\nabla \cdot \mathbf{j}_\alpha) dV$. Generally, the divergence theorem can be written as

$$\int_{\Gamma} (\mathbf{j}_\alpha \cdot \mathbf{n}) d\Gamma = \int_{V} (\nabla \cdot \mathbf{j}_\alpha) dV \tag{1.108}$$

Using equation (1.108), equation (1.106) can be transformed to

$$\frac{d}{dt} \int_{V(t)} \pi \, dV = \int_{V(t)} \left(\frac{\partial \pi}{\partial t} \right) dV + \int_{\Gamma} (\mathbf{v}_s \cdot \mathbf{n}) \pi \, d\Gamma = \int_{V(t)} (\dot{\pi} + \pi \nabla \cdot \mathbf{v}_s) dV \tag{1.109}$$[13]

in which $\dot{\pi}$ is the material time derivative considering the change along with both the time (t) and velocity ($\mathbf{v}_s$), defined as

$$\dot{\pi} = \frac{D\pi}{Dt}\Big|_{\mathbf{X}} = \frac{\partial \pi}{\partial t}\Big|_{\mathbf{x}} + \mathbf{v}_s \cdot \nabla \pi \tag{1.110}$$

where $|_{\mathbf{X}}$ is with respect to the original configuration and $|_x$ is with respect to the current configuration.

To derive the Reynolds transport theorem in equation (1.109), equations (1.103) and (1.110) are employed. When considering the term $\frac{d}{dt} \int_{V(t)} \pi \, dV$, it's crucial to note that the time derivative cannot

be directly applied inside the integral $\int_{V(t)} \pi \, dV$, given that the volume $V(t)$ is time-dependent. In response, the integral is remapped back to V_0 which remains constant at the reference configuration:

$$\begin{aligned}\frac{d}{dt}\int_{V(t)} \pi \, dV = \frac{d}{dt}\int_{V_0} \pi J dV &= \int_{V_0}\left(J\frac{\partial \pi}{\partial t}\Big|_{\mathbf{X}} + \pi\frac{\partial J}{\partial t}\Big|_{\mathbf{X}}\right)dV = \int_{V_0}\left(J\frac{D\pi}{Dt} + \pi\frac{DJ}{Dt}\right)dV \\ &= \int_{V_0}\left(J\frac{D\pi}{Dt} + \pi J\nabla\cdot\mathbf{v}_s\right)dV = \int_{V_0}\left(\frac{D\pi}{Dt} + \pi\nabla\cdot\mathbf{v}_s\right)J\,dV \\ &= \int_{V}\left(\frac{D\pi}{Dt} + \pi\nabla\cdot\mathbf{v}_s\right)dV = \int_{V}\left(\dot{\pi} + \pi\nabla\cdot\mathbf{v}_s\right)dV \end{aligned} \tag{1.111}$$

1.4 MIXTURE-COUPLING THEORY INTRODUCTION

Figure 1.5(a) illustrates a conceptual model depicting multiscale-multiphase and multiphysics couplings within a mixture. Within the selected REV (Ω), various multiphase couplings can occur, involving solid phases (e.g., soils/rocks), liquid phases (e.g., water), or gaseous phases (e.g., air). These α phases interact with each other, such as when compression of solids expels liquid, as seen in geotechnical engineering's consolidation problems (Yong and Townsend, 1986).

Multiscale couplings are also prevalent, where phenomena at the microscale, such as water molecules in clay platelets causing swelling, influence macroscale deformation of porous mediums (Al-Rawas and Goosen, 2006). Chemical diffusion processes occurring at the molecular scale may lead to osmosis (Sections 1.4.4 and 1.4.5) at the mesoscale, subsequently affecting material deformation at the macroscale (Graf, 1982; Chen and Hicks, 2013).

Moreover, multiphysics couplings are observed, such as heat transport leading to geomaterial expansion (Vardon, 2015; Abu-Zreig et al., 2001) and affecting water transport through thermal osmosis (Zhou et al., 1998).

1.4.1 Mixture-Coupling Theory

Assumption: Mixture-Coupling Theory shares a foundational assumption with average methods, positing the presence of all phases at every

material point, facilitating the formulation of a mass balance equation for the multiphase.

Dissipation process of coupling: Diverging from mechanics approaches or the mixture theory approach, Mixture-Coupling Theory employs entropy production for dissipation processes occurring in porous media. Multiscale dissipative processes are propelled by relative entropy changes. Couplings between phases/species aim to minimize energy consumption (e.g., chemical potential) and maximize entropy (e.g., distribution of molecules) within the mixture to attain equilibrium. The concept of entropy will be introduced in Chapter 2.

Key advantages: Mixture-Coupling Theory excels in handling multiscale and multiphysics couplings. Unlike mixture theory and mechanics approaches, which utilize continuum mechanics as the foundational theory and study multiphase interactions employing Newton's classical mechanics for friction forces, Mixture-Coupling Theory is grounded in general nonequilibrium thermodynamics (e.g., free energy and entropy). This equips the theory to address irreversible processes of multiphase-multicomponent transport. Leveraging thermodynamics, widely employed in chemistry (e.g., chemical thermodynamics) and physics (e.g., thermomechanics), Mixture-Coupling Theory inherits the capability to address multiscale coupling (e.g., molecular-scale coupling) and multiphysics coupling (e.g., thermo, hydro, mechanical, chemo, bio, etc.).

For instance, in Figure 1.5(b), the illustration depicts liquid passing through a micropore, featuring a very narrow end (e.g., nano-channels) that facilitates the passage of small molecules (e.g., water) more readily than large molecules (e.g., sugar). While Newtonian mechanics (by mixture theory and mechanics approach) suffice for calculating liquid-solid surface interactions, molecular frictions between water and sugar fall beyond the scope of Newtonian mechanics. However, such frictions can be incorporated into entropy changes using nonequilibrium thermodynamics in Mixture-Coupling Theory.

The Mixture-Coupling Theory framework was initially proposed by Heidug and Wong for saturated rocks (Heidug and Wong, 1996) and subsequently extended to unsaturated and non-isothermal conditions by Chen and others (Chen et al., 2013, 2018; Chen and Hicks, 2013; Ma et al., 2020). Formerly referred to as "Modified Mixture Theory," it was renamed Mixture-Coupling Theory in 2016 (Chen et al., 2016) to better encapsulate its core principles and differentiate it from other forms of "Modified Mixture Theory" (Katsube and Carroll, 1987).

1.4.2 "Partial density" and "mixture density" for multiphase-multicomponent in unsaturated media

Mixture-Coupling Theory employs the concept of "mixture density" and "partial density" from mixture theory. The "partial density" of the kth species dissolved in the αth phase is its density relative to the phase volume V_α.

In Figure 1.6, the distinction between "partial density" and "mixture density" is illustrated. For instance, in a REV comprising three phases (solid, liquid, and gas), assuming k species present in the liquid occupying volume V_l, the mixture density of the k th species (with mass m_k) is defined as

$$\rho_k = \frac{m_k}{V_l + V_g + V_s} \tag{1.112}$$

and its "partial density" (in-liquid density) is defined as

$$\rho_l^k = \frac{m_k}{V_l} \tag{1.113}$$

The relationship between "partial density" and "mixture density," and volume fractions for the unsaturated condition, can be derived as follows:

The volume fraction of the αth phase ϕ_α can be denoted as

$$\phi_\alpha = \frac{V_\alpha}{V} \tag{1.114}$$

where V_α and V are the volumes of the α th phase and total mixture, respectively.

The relationship between the porosity ϕ and ϕ_α is

$$\phi_s = 1 - \phi\,(\text{solid}) \text{ and } \phi = \sum\nolimits_\alpha \phi_\alpha = \sum\nolimits_\alpha S_\alpha \phi\,(\alpha \neq s, \text{ fluids}) \tag{1.115}$$

where S_α is the saturation ratio of the αth fluid in the void. For example, S_i is the saturation ratio of liquid. If the liquid is water only, S_i may also be denoted as S_w.

Hence, using a similar derivation process as in equation (1.10), the relationship between $\rho_\alpha(\mathbf{x},t)$ and $\rho_\alpha^\alpha(\mathbf{x},t)$ is given by

$$\rho_\alpha(\mathbf{x},t) = \phi_\alpha \rho_\alpha^\alpha(\mathbf{x},t) = S_\alpha \phi \rho_\alpha^\alpha(\mathbf{x},t) \tag{1.116}$$[14]

If there are i or k species in the α phase (or liquid), equation (1.116) becomes

$$\rho_i / (\phi S_\alpha) = \rho_\alpha^i \text{ or } \rho_k / (\phi S_l) = \rho_l^k \quad (\text{in liquid phase}) \tag{1.117}$$

where

$$\rho_\alpha^i = \frac{m_i}{V_\alpha} \text{ or } \rho_l^k = \frac{m_k}{V_l} \text{ (mass/phase volume)} \tag{1.118}$$

Considering only one component in the α phase (e.g., water), the density is given as $\rho_l^w = \frac{m_w}{V_l}$ which is usually called true density; since $V_l = V_w$, it leads to $\rho_l^w = \frac{m_w}{V_w} = \frac{m_w}{S_w \phi V} = \frac{\rho_w}{S_w \phi}$, which is the same as equation (1.19).

The "true density" of a liquid (containing i species) can be described as

$$\rho_l^l = \sum_{i=1}^{N_c} \frac{m_i}{V_l}$$

or

$$\rho_l^l = \sum_{i=1}^{N_c} \frac{m_i}{V_l} = \sum_{i=1}^{N_c} \rho_l^i \quad (\text{liquid as an example}) \tag{1.119}$$

Note here: because ρ_l^i is the "partial density" according to the volume V_l, the volume fraction (e.g., ϕ_i) is not needed, compared with equation (1.116).

Further consideration of gas can be included as

$$\sum \phi_k = S_l \phi^{15}$$

or

$$\sum \phi_i + \sum \phi_k = S_g \phi + S_l \phi = \phi \, (\text{with gas}) \tag{1.120}$$

where ϕ_i is the volume fraction of the i th gas, ϕ_k denotes the volume fraction of the kth species in the liquid (not gas), S_g is the saturation ratio of the gas, and S_l denotes the saturation of the liquid (not gas).

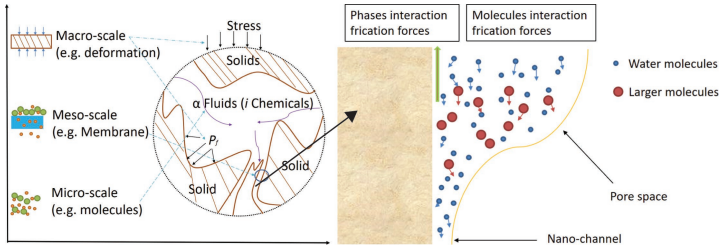

FIGURE 1.5 (a, left) Conceptual model of multiscale-multiphase coupling in a mixture; (b, right) Phases interactions and molecule interactions in fluids (e.g., liquid)

1.4.3 Multiscale coupling knowledge gap

Particles in a porous medium vary in diameter from 10^{-10} (1 Å) to 10^{-2}m, encompassing molecules, colloids, and suspended particles, as depicted in Figure 1.7. Geochemistry typically focuses on molecular-scale reactions (below or around 10^{-9} m = 1 nm (nanometers)) (Luther, 2016), while geomechanics concentrates on particles larger than 10^{-7} m = 100 nm (Soga et al., 2014). Consequently, there exists a knowledge gap of approximately 100 nm between these scales, with significant multiscale physical-chemical couplings:

Molecular-scale chemical processes can profoundly impact physical phenomena, such as membrane function at the molecular-nanoscale, resulting in osmosis flow that influences the deformation of soils and rocks at the macroscale. For instance, water molecules penetrating clay platelets can trigger physical swelling. Additionally, suspended particles and colloids, formed from chemical reactions (e.g., $CaCO_3/SiO_2$), may obstruct nanoscale pores and alter nanoscale porosity. Moreover, biological elements like viruses, bacteria, and algae, spanning from the molecular to macroscale can interact with biogeochemical reaction processes. All of these aspects pose significant challenges that remain largely unexplored in geotechnical engineering.

This book will introduce the utilization of Mixture-Coupling Theory to develop constitutive models for:

1. Molecular-macroscale coupling: Swelling induced by water molecules accumulated in clay platelets.
2. Molecular-mesoscale-macroscale coupling: Membrane function, including chemical osmosis and thermal osmosis.
3. Multiphase coupling: Hydro-mechanical-chemical and thermal interactions.

1.4.4 Swelling

Hydration swelling is a common phenomenon observed in water-sensitive materials like clays or clay-rich shales, such as montmorillonite (Al-Rawas and Goosen, 2006). This process gives rise to macroscale hydration forces due to the alignment of polar water molecules near hydrated surfaces (Figure 1.8). These forces are repulsive in nature and can cause the stacked silicate layers to separate, leading to swelling. Typically, about one to four layers of water molecules can intercalate between the clay platelets, resulting in an increase in spacing that determines the extent of swelling (Laird, 2006).

1.4.5 Chemical osmosis

An ideal semipermeable membrane permits only small molecules to pass through, whereas a permeable membrane in reality allows some larger molecules to permeate. Figure 1.9 illustrates a scenario separated by an ideal semipermeable membrane. Due to the selective nature of this membrane, sugar molecules are unable to traverse it, allowing only water molecules to pass through. Water moves from regions of lower sugar concentration to higher concentrations, eventually reaching equilibrium with a fluid pressure differential. This flow induced by chemical concentration differences is known as chemical osmosis. In this book, "positive" chemical osmosis refers to flow from lower to higher chemical concentration, while "negative" chemical osmosis denotes flow in the opposite direction, as theorized.

Osmosis frequently occurs in soil or rock with very low permeability, effectively acting as a permeable membrane that restricts solute molecule transport (e.g., when permeability is less than 10^{-10} m/s). Solute molecules may include salts or other chemicals relevant to geotechnical and geoenvironmental engineering applications (e.g., drilling fluids or landfill pollutants in case of leaks). Consequently, industrialists must consider the potential and implications of chemical osmosis. Previous studies (Chen and Hicks, 2013) have addressed chemical osmosis in radioactive waste disposal, and some research has extended Darcy's law to include chemical osmosis effects in low-permeability saturated shales (Schlemmer et al., 2003). However, chemical osmosis is complex, with osmotic efficiency generally contingent upon pore size and chemical composition of the porous medium.

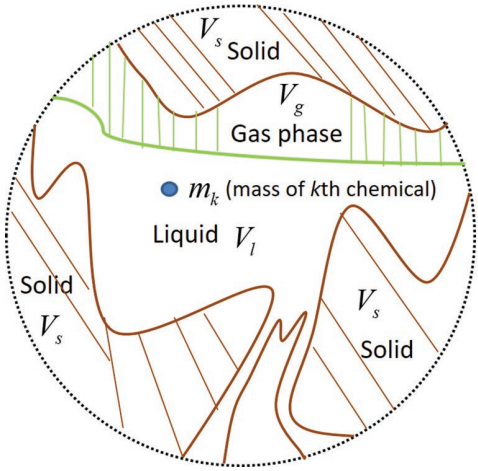

$$V_{\text{mixture}} = V_s + V_l + V_g$$

Mixture density

$$\rho_k = \frac{m_k}{V_{\text{mixture}}}$$

Partial density

$$\rho_l^k = \frac{m_k}{V_l}$$

FIGURE 1.6: Partial density vs mixture density

In biological tissues, which are porous in nature, osmotic effects can be significant (Gu et al., 1999). However, osmosis in rocks or clays may be more intricate due to numerous species and possible microorganism presence, making the osmotic capacity of different rocks or clays toward various species uncertain. Currently, most osmotic efficiency measurements have been conducted for common nonreactive chemical ions like Na^+ or Cl^- (Graf, 1982); further experimental research is necessary to evaluate osmotic capacity for radionuclide complexes, organic matter, and gases, especially concerning intermediate and low-level radioactive waste. While the influence of osmosis on geomaterials may be minimal for simple chemical ions like Na^+, it may be more pronounced for complex chemical compounds or organic matter, or in the presence of microbial activity.

1.4.6 Thermal osmosis

Thermo-osmosis refers to the phenomenon of fluid diffusion through a membrane driven by a temperature gradient (Denbigh and Raumann, 1952a). Experiments investigating thermal osmosis using a rubber membrane for CO_2 or H_2 individually revealed intriguing behaviors: CO_2 migrated from the colder side to the warmer side, while H_2 moved in the opposite direction, from the warmer side to the colder side (Figure 1.10) (Denbigh and Raumann, 1952b). A similar phenomenon was observed for liquids, such as helium II

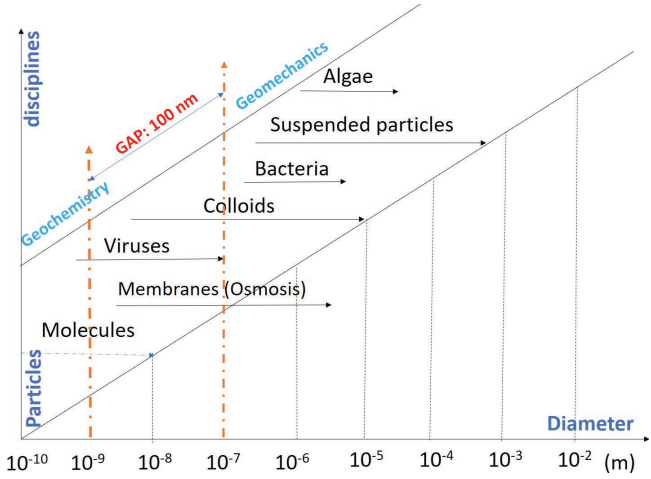

FIGURE 1.7 Highlighting the knowledge gap, based on the size of particles in a porous medium (Sharvelle et al., 2017)

Note: The figure includes viruses, bacteria, and algae which are not discussed in this book

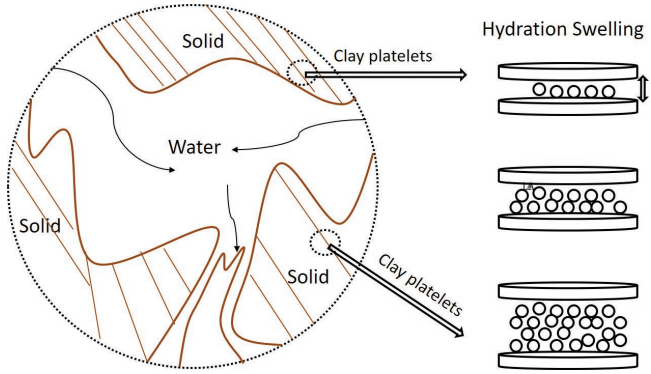

FIGURE 1.8 Concept of water-induced swelling

(Kapitza, 1941). Similar to the definition for chemical osmosis, the direction of flow from cooler to warmer is termed "positive" thermal osmosis, whereas flow from warmer to cooler is termed "negative" thermal osmosis.

Numerous studies on thermal osmosis have utilized cellophane and weakly charged cellulose acetate membranes (Fernández-Pineda

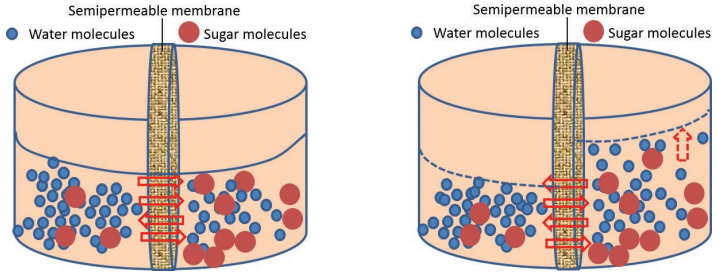

FIGURE 1.9 Chemical osmosis concept: (a) initial state (left); (b) equilibrium (right)

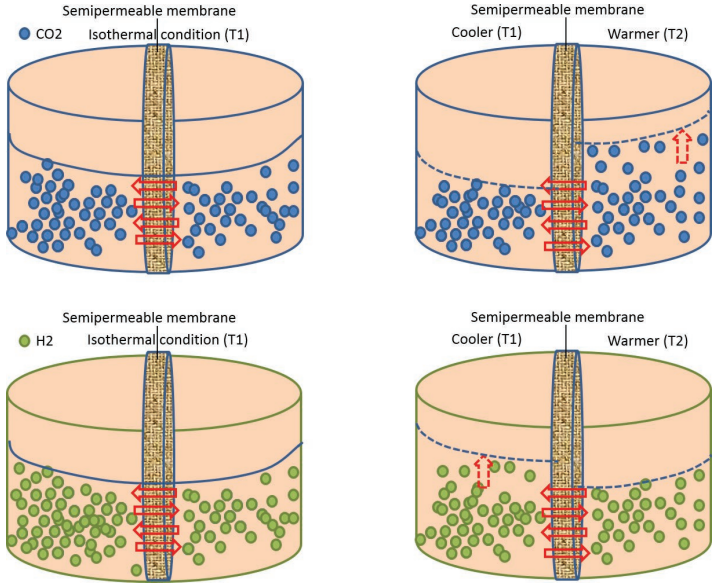

FIGURE 1.10 Thermal osmosis concept: (a) CO_2 state (upper); (b) H_2 state (lower)

and Vázquez-González, 1988; Mengual and Garcia-Lopez, 1988) or ion-exchange membranes like Nafion or Neosepta membranes (Tasaka et al., 1984, 1992). In geotechnical materials, thermo-osmosis in clay or shale with very low hydraulic conductivity (e.g., 10^{-10}–10^{-14} m) has garnered interest due to its potential significance compared to the direct effect of Darcian flow (Carnahan, 1983). A coupled thermoporoelastic model demonstrated the importance of thermodynamic coupling with thermo-osmosis (Zhou et al., 1998).

Nevertheless, understanding the detailed mechanism of thermo-osmosis in geomaterials or geomembranes remains challenging due to their complex physical structures, including various pore sizes and microstructures, as well as the presence of multiple species (e.g., reactive leachate transport).

1.5 CONCLUSION

This chapter has explored the foundational concepts and laws governing multiphase, multicomponent transport in porous media. Key topics discussed include effective stress, transport laws, classical theories for water-solid coupled models, and conservation principles. The chapter also touched on the influence of various couplings and introduced the conceptual framework of Mixture-Coupling Theory. The objective was to equip readers with a broad understanding of the fundamental mechanisms within porous media, an overview of current model development, and an awareness of existing knowledge gaps.

Through a comparison of different theories, a clear gap is identified, particularly in the areas of multiphase-multiscale interactions and physical-chemical couplings. Addressing this gap demands a shift toward more fundamental principles, with the development of rigorous mathematical models. Chapter 2 will introduce the core principles of nonequilibrium thermodynamics, providing the necessary foundation for the new Mixture-Coupling Theory outlined in this book.

NOTES

1 Laminar flow is characterized by high momentum diffusion and low momentum convection.

2 ∇y_α and $\nabla \cdot \mathbf{y}_\alpha$: Assuming y_α and $\mathbf{y}_\alpha$ are general scalar and vector/tensor variables of the α th phase, respectively; ∇y_α and $\nabla \cdot \mathbf{y}_\alpha$ denote the gradient and divergence, respectively. ∇y_α is a vector, whereas $\nabla \cdot \mathbf{y}_\alpha$ is a scalar.

3 Note: The symbol "$\because$" represents "because/since" and "$\therefore$" represents "therefore." This applies to all the footnote mathematical derivations in this book. The numbering scheme for equations in footnotes is defined as "fn" to distinguish from the numbering scheme in the main text of the book, in which "f" denotes the footnote and the subscript "n" denotes the equation number.
Mathematical proof of equation (1.27): $\because \mathbf{J}_k = \rho_k \left(\mathbf{v}_k - \mathbf{v}_l \right)$,

$\therefore \mathbf{J}_c = \rho_c(\mathbf{v}_c - \mathbf{v}_l)$ and $\mathbf{J}_w = \rho_w(\mathbf{v}_w - \mathbf{v}_l)$.

$\therefore \mathbf{J}_c + \mathbf{J}_w = \rho_c(\mathbf{v}_c - \mathbf{v}_l) + \rho_w(\mathbf{v}_w - \mathbf{v}_l)$ (f1).

$$\because \mathbf{v}_l = \sum\nolimits_k (\rho_k / \rho_l)\mathbf{v}_k, \therefore \mathbf{v}_l = \left(\frac{\rho_c}{\rho_l}\right)\mathbf{v}_c + \left(\frac{\rho_w}{\rho_l}\right)\mathbf{v}_w \text{ (f2)}$$

By substituting (equation (f2)) into (equation (f1)), it leads to

$$\begin{aligned}\mathbf{J}_c + \mathbf{J}_w &= \rho_c\left[\mathbf{v}_c - \left(\left(\frac{\rho_c}{\rho_l}\right)\mathbf{v}_c + \left(\frac{\rho_w}{\rho_l}\right)\mathbf{v}_w\right)\right] + \rho_w\left[\mathbf{v}_w - \left(\left(\frac{\rho_c}{\rho_l}\right)\mathbf{v}_c + \left(\frac{\rho_w}{\rho_l}\right)\mathbf{v}_w\right)\right] \\ &= \rho_c\mathbf{v}_c + \rho_w\mathbf{v}_w - \frac{\rho_c(\rho_c\mathbf{v}_c + \rho_w\mathbf{v}_w)}{\rho_l} + \frac{\rho_w(\rho_c\mathbf{v}_c + \rho_w\mathbf{v}_w)}{\rho_l} \\ &= \rho_c\mathbf{v}_c + \rho_w\mathbf{v}_w - \frac{(\rho_c + \rho_w)(\rho_c\mathbf{v}_c + \rho_w\mathbf{v}_w)}{\rho_l} = 0\end{aligned}$$

where $\rho_l = \rho_c + \rho_w$.

4 Equation (1.17) can be rewritten as $\mathbf{v}_k = \frac{\mathbf{I}_k}{\rho_k} + \mathbf{v}_s$. Substitution of this equation into equation (1.25) leads to $\mathbf{J}_k = \rho_k(\mathbf{v}_k - \mathbf{v}_l) =$ $\rho_k\left(\frac{\mathbf{I}_k}{\rho_k} + \mathbf{v}_s - \mathbf{v}_l\right) = \mathbf{I}_k - \rho_k(\mathbf{v}_l - \mathbf{v})$.

5 The extent of a reaction is defined as $d\zeta = \frac{dn_i}{v_i}$, which is a quantity measuring the extent to which the reaction proceeds. In other words, it defines the amount of substance that is being changed in an equilibrium reaction. In this equation, n_i denotes the amount of the i th reactant and v_i is the stoichiometric coefficient of the i th reactant.

6 van Genuchten relationship is only one of many published equations linking saturation and pressure.

7 $$\frac{\partial}{\partial x_j}\left(-(K - \frac{2G}{3})\varepsilon_{kk}\delta_{ij}\right) = -\left(K - \frac{2G}{3}\right)\frac{\partial}{\partial x_j}(\varepsilon_{kk}\delta_{ij}) = -\left(K - \frac{2G}{3}\right)\frac{\partial}{\partial x_j}$$
$$(d_{kk}) = -\left(K - \frac{2G}{3}\right)\frac{\partial}{\partial x_j}\left(\frac{\partial d_k}{\partial x_k}\right)$$

8 $$\rho_l^w\left[C_{v\text{-}s}\left(\frac{\partial\sigma}{\partial t} - \phi\frac{\partial p_w}{\partial t}\right) + \nabla\cdot\mathbf{v}_s - \nabla\cdot(\phi\mathbf{v}_s)\right] + \phi\rho_l^w C_{v-f}\frac{\partial p_w}{\partial t}$$
$$+\nabla\cdot(\phi\rho_l^w\mathbf{v}_w) = 0$$

$$C_{v-s}\rho_l^w\frac{\partial\sigma}{\partial t}-\rho_l^w\phi C_{v\text{-}s}\frac{\partial p_w}{\partial t}+\rho_l^w\nabla\cdot\mathbf{v}_s-\rho_l^w\cdot\left(\phi\mathbf{v}_s\right)+\phi\rho_l^wC_{v-f}\frac{\partial p_w}{\partial t}+\nabla\cdot\left(\phi\rho_l^w\mathbf{v}_w\right)=0$$

$$C_{v-s}\rho_l^w\frac{\partial\sigma}{\partial t}+\rho_l^w\phi\left(C_{v-f}-C_{v-s}\right)\frac{\partial p_w}{\partial t}+\rho_l^w\nabla\cdot\mathbf{v}_s=\rho_l^w\nabla\cdot\left(\phi\mathbf{v}_s\right)-\nabla\cdot\left(\phi\rho_l^w\mathbf{v}_w\right)$$

$$C_{v-s}\frac{\partial\sigma}{\partial t}+\phi\left(C_{v-f}-C_{v-s}\right)\frac{\partial p_w}{\partial t}+\underbrace{\nabla\cdot\mathbf{v}_s}_{\frac{\partial\varepsilon}{\partial t}}=-\nabla\cdot\left(\phi\mathbf{v}_w-\phi\mathbf{v}_s\right)$$

Note for $\nabla\cdot\mathbf{v}_s=\dfrac{\partial\varepsilon}{\partial t}$: Since $\mathbf{v}_s=\mathbf{d}$ (where $\mathbf{d}$ is the displacement vector), $\therefore\nabla\cdot\mathbf{v}_s=\nabla\cdot\mathbf{d}$. $\therefore\nabla\cdot\mathbf{d}=\varepsilon$, $\therefore\nabla\cdot\mathbf{d}=\dfrac{\partial\varepsilon}{\partial t}$, and therefore, $\nabla\cdot\mathbf{v}_s=\nabla\cdot\mathbf{d}=\dfrac{\partial\varepsilon}{\partial t}$ leads to equation (1.76).

9

$$\frac{\partial\varepsilon}{\partial t}+\phi\left(C_{v-f}-C_{v-s}\right)\frac{\partial p_w}{\partial t}+C_{v-s}\frac{\partial\sigma}{\partial t}=-\nabla\cdot\left(\phi\left(\mathbf{v}_w-\mathbf{v}_s\right)\right)$$

$$\frac{\partial\varepsilon}{\partial t}+\phi\left(C_{v-f}-C_{v-s}\right)\frac{\partial p_w}{\partial t}+C_{v-s}\frac{\partial\left[\sigma'+\zeta p_w\right]}{\partial t}=-\nabla\cdot\left(\phi\left(\mathbf{v}_w-\mathbf{v}_s\right)\right)$$

$$\frac{\partial\varepsilon}{\partial t}+\phi\left(C_{v-f}-C_{v-s}\right)\frac{\partial p_w}{\partial t}+C_{v-s}\frac{\partial\left[\dfrac{-\varepsilon}{C_m}+\zeta p_w\right]}{\partial t}=-\nabla\cdot\left(\phi\left(\mathbf{v}_w-\mathbf{v}_s\right)\right)$$

$$\frac{\partial\varepsilon}{\partial t}-\frac{C_{v-s}}{C_m}\frac{\partial\varepsilon}{\partial t}+\left[\phi\left(C_{v-f}-C_{v-s}\right)+\zeta C_{v-s}\right]\frac{\partial p_w}{\partial t}=-\nabla\cdot\left(\phi\left(\mathbf{v}_w-\mathbf{v}_s\right)\right)$$

$$\overbrace{\left[1-\frac{C_{v-s}}{C_m}\right]}^{\zeta}\frac{\partial\varepsilon}{\partial t}+\overbrace{\left[\phi C_{v-f}+\left(\zeta-\phi\right)C_{v-s}\right]}^{s_p}\frac{\partial p_w}{\partial t}=-\nabla\cdot\left(\phi\left(\mathbf{v}_w-\mathbf{v}_s\right)\right)$$

Substitution of Darcy velocity through equation (1.15) for the saturated condition leads to equation (1.78).

10

$$\frac{\phi v\mathbf{u}}{k}=-\left(\phi\nabla\left(p_w\right)+\rho_wg\right)$$

$$\mathbf{u}=-\frac{k\left(\phi\nabla\left(p_w\right)+\rho_wg\right)}{\phi v}=-\frac{k\left(\phi\nabla\left(p_w\right)+\rho_wg\right)}{\phi v}=-\frac{k\left(\nabla\left(p_w\right)+\rho_l^wg\right)}{v}$$

11 $$\frac{\partial(\rho_w \mathbf{v}_w)}{\partial t}+\nabla(\phi p_w)+\rho_w g+\boldsymbol{\chi}+\frac{\partial(\rho_s \mathbf{v}_s)}{\partial t}+\nabla(\boldsymbol{\sigma}-\phi p_w)+\rho_s g-\boldsymbol{\chi}=0$$

$$\frac{\partial(\rho_w \mathbf{v}_w)}{\partial t}+\nabla(\phi p_w)+\frac{\partial(\rho_s \mathbf{v}_s)}{\partial t}+\nabla(\boldsymbol{\sigma}-\phi p_w)+(\rho_s+\rho_w)g=0$$

$$\overbrace{\frac{\partial(\rho_w \mathbf{v}_w)}{\partial t}+\frac{\partial(\rho_s \mathbf{v}_s)}{\partial t}}^{=0}+\overbrace{\nabla(\phi p_w)-\nabla(\phi p_w)}^{=0}+\nabla\boldsymbol{\sigma}+(\rho_s-\rho_w)g=0$$

12 Assuming the mass of the mixture is m, since $\frac{\rho_0}{\rho}=\frac{\frac{m}{V_0}}{\frac{m}{V}}=\frac{V}{V_0}=\frac{V}{V_0}=J$, it leads to $\rho_0 = J\,\rho$. Considering a water-saturated soil, it leads to $\rho_{w(0)} = J\,\rho_{w(t)}$ in which $\rho_{w(0)}$ is at the reference configuration and $\rho_{w(t)}$ is at the current configuration. Using equation (1.102), ($\rho_{w(0)} = \upsilon\rho_l^w$; $\rho_{w(t)} = \phi\rho_l^w$) for both the reference configuration and current configuration (in which ρ_l^w is the partial mass density of water, which equals the true density of water), leads to $\upsilon = J\,\phi$.

13 $$\frac{d}{dt}\int_V \pi\, dV=\int_V\left(\frac{\partial\pi}{\partial t}\right)dV+\int_\Gamma(\pi\mathbf{v}_s\cdot\mathbf{n})\,d\Gamma=\int_V\left(\frac{\partial\pi}{\partial t}\right)dV+\int_V\nabla\cdot(\pi\mathbf{v}_s)\,dV$$

$$=\int_V\left(\frac{\partial\pi}{\partial t}\right)dV+\int_V\left(\pi\nabla\cdot\mathbf{v}_s+\mathrm{v}_s\cdot\pi\right)dV=\int_V\left(\frac{\partial\pi}{\partial t}+\mathbf{v}_s\nabla\cdot\pi+\pi\nabla\cdot\mathbf{v}_s\right)dV$$

$$=\int_V\left(\dot{\pi}+\pi\nabla\cdot\mathbf{v}_s\right)dV$$

14 Derivation note (1) for water-saturated soils/rocks: $\because\ \rho_w=\frac{m_w}{V}$ and $\rho_l^w=\frac{m_w}{V_1}\ \therefore,\ \frac{\rho_w}{\rho_l^w}=\frac{V_l}{V}=\phi,\ \ \rho_w=\rho_l^w\phi$; (2) for unsaturated: $\because\ \rho_w=\frac{m_w}{V}$ and $\rho_w=\frac{m_w}{V_l}$, $\because\ V_l=V\phi S_;\ \frac{\rho_w}{\rho_l^w}=\frac{V_l}{V}=\phi S_l$.

15 Considering k chemicals in a liquid, it leads to $\phi_k=\frac{V_k}{V}$ and $S_l=\frac{V_l}{V_{pore}}$. Since $\sum\phi_k=\sum\frac{V_k}{V}=\frac{1}{V}\sum V_k$ and, $\sum V_k=V_l$ thus, $\sum\phi_k=\frac{V_l}{V}=\frac{S_l V_{pore}}{V}=S_l\phi,$ where $\phi=\frac{V_{pore}}{V}$. Considering i chemicals in a gas, using a similar derivation process, it leads to $\sum\phi_l=S_g\phi$.

REFERENCES

Abu-Zreig, M. M., Al-Akhras, N. M. & Attom, M. F. (2001) Influence of heat treatment on the behavior of clayey soils. *Applied Clay Science* **20(3)**: 129–135.

Al-Rawas, A. A. & Goosen, M. F. (2006) *Expansive soils: recent advances in characterization and treatment*. London, Taylor & Francis.

Ambrosi, D. & Preziosi, L. (2002) On the closure of mass balance models for tumor growth. *Mathematical Models and Methods in Applied Sciences* **12(5)**: 737–754.

Appelo, C. A. J. & Postma, D. (2004) *Geochemistry, groundwater and pollution*. London, CRC Press.

Araujo, R. P. & McElwain, D. S. (2005) A mixture theory for the genesis of residual stresses in growing tissues I: a general formulation. *SIAM Journal on Applied Mathematics* **65(4)**: 1261–1284.

Badin, G. & Crisciani, F. (2018) *Variational formulation of fluid and geophysical fluid dynamics. Mechanics, symmetries and conservation laws*. Cham, Springer.

Baer, M. R. & Nunziato, J. W. (1986) A two-phase mixture theory for the deflagration-to-detonation transition (DDT) in reactive granular materials. *International Journal of Multiphase Flow* **12(6)**: 861–889.

Batchelor, C. K. & Batchelor, G. (2000) *An introduction to fluid dynamics.* Cambridge, MA, Cambridge University Press.

Bedeaux, D., Kjelstrup, S. & Öttinger, H. C. (2006) On a possible difference between the barycentric velocity and the velocity that gives translational momentum in fluids. *Physica A: Statistical Mechanics and its Applications* **371(2)**: 177–187.

Bergstrom, J. S. (2015) *Mechanics of solid polymers: theory and computational modeling*. Norwich, William Andrew.

Biot, M. A. (1941) General theory of three-dimensional consolidation. *Journal of Applied* Physics **12(2)**: 155–164.

Biot, M. A. (1962) Mechanics of deformation and acoustic propagation in porous media. *Journal of Applied Physics* **33**: 1482–1498.

Biot, M. A. (1972) Theory of finite deformations of porous solids. *Indiana University Mathematics Journal* **21**: 597–620.

Bourg, I. C. & Sposito, G. (2010) Connecting the molecular scale to the continuum scale for diffusion processes in smectite-rich porous media. *Environmental Science & Technology* **44(6)**: 2085–2091.

Bowen, R. M. (1976) Theory of mixtures. In *Continuum physics*. (Eringen, A. C. (ed)) New York, Academic Press, vol. 3, pp. 1–127.

Bowen, R. M. (1980) Incompressible porous media models by use of the theory of mixtures. *International Journal of Engineering* Science **18(9)**: 1129–1148.

Bowen, R. M. (1984) Diffusion models implied by the theory of mixtures. In *Rational thermodynamics*. (Truesdell, C. (ed)) New York, Springer-Verlag, pp. 237–263.

Byrne, H. & Preziosi, L. (2003) Modelling solid tumour growth using the theory of mixtures. *Mathematical Medicine and Biology: A Journal of the IMA* **20(4)**: 341–366.

Carnahan, C. L. (1983) Thermodynamic coupling of heat and matter flows in near-field regions of nuclear waste repositories. MRS Online Proceedings Library 26: 1023.

Chatzis, I. & Dullien, F. (1983) Dynamic immiscible displacement mechanisms in pore doublets: theory versus experiment. *Journal of Colloid and Interface Science* **91(1)**: 199–222.

Chaves, E. W. V. (2013) *Notes on continuum mechanics*. Dordrecht: Springer.

Chen, P. J. (1996) A coupled solid/fluids mixture theory that suffices for diffusion problems. *Journal of Elasticity* **45**: 117–134.

Chen, X. & Hicks, M. A. (2013) Unsaturated hydro-mechanical-chemo coupled constitutive model with consideration of osmotic flow. *Computers and Geotechnics* **54**: 94–103.

Chen, X., Pao, W. & Li, X. (2013) Coupled thermo-hydro-mechanical model with consideration of thermal-osmosis based on modified mixture theory. *International Journal of Engineering Science* **64**: 1–13.

Chen, X., Pao, W., Thornton, S. & Small, J. (2016) Unsaturated hydro-mechanical–chemical constitutive coupled model based on mixture coupling theory: hydration swelling and chemical osmosis. *International Journal of Engineering Science* **104**: 97–109.

Chen, X., Thornton, S. F. & Pao, W. (2018) Mathematical model of coupled dual chemical osmosis based on mixture-coupling theory. *International Journal of Engineering Science* **129**: 145–155.

Civan, F. (2010) Non-isothermal permeability impairment by fines migration and deposition in porous media including dispersive transport. *Transport in Porous Media* **85(1)**: 233–258.

Cryer, C. W. A. (1963) A comparison of the three-dimensional consolidation theories of Biot and Terzaghi. *The Quarterly Journal of Mechanics and Applied Mathematics* **16(4)**: 401–412.

Cvetković, B. P., Kuzmanović, D. S. & Cvetković, P. A. (2011) An application of continuum theory on the case of one-dimensional sedimentation. *FME Transactions* **39(2)**: 61–65.

Darcy, H. (1856) *Les Fontaines Publiques de la Ville de Dijon.* Paris, Victor Dalmont.

Decker, R. (1990) A continuum mixture theory with an application to turbulent snow, air flows and sedimentation. *Journal of Wind Engineering and Industrial Aerodynamics* **36**: 877–887.

Denbigh, K. & Raumann, G. (1952a) The thermo-osmosis of gases through a membrane. I. Theoretical. In Proceedings of the Royal Society of London A: Mathematical, Physical and Engineering Sciences. The Royal Society, vol. 210, pp. 377–387.

Denbigh, K. G. & Raumann, G. (1952b) The thermo-osmosis of gases through a membrane. II. Experimental. Proceedings of the Royal Society of London. Series A. Mathematical and Physical Sciences 210(1103): 518–533.

Ehrenberg, S. & Nadeau, P. (2005) Sandstone vs. carbonate petroleum reservoirs: a global perspective on porosity-depth and porosity-permeability relationships. AAPG Bulletin 89(4): 435–445.

Eringen, A. C. (1998) A mixture theory of electromagnetism and superconductivity. International Journal of Engineering Science 36(5–6): 525–543.

Fernández-Pineda, C. & Vázquez-González, M. I. (1988) Differential thermo-osmotic permeability in water–cellophane systems. Journal of the Chemical Society, Faraday Transactions 1: Physical Chemistry in Condensed Phases 84(2): 647–656.

Fick, A. (1855) Ueber diffusion. Annalen der Physik 170(1): 59–86.

Ford, T., Sachs, J., Grotberg, J. & Glucksberg, M. (1990) Mechanics of the perialveolar interstitium of the lung. In First World Congress of Biomechanics. La Jolla, vol. 1, p. 31.

Fourier, J. (1878) The analytical theory of heat. Cambridge,MA, The University Press.

Franquet, J. A. & Abass, H. H. (1999). Experimental evaluation of Biot's poroelastic parameter–Three different methods. In ARMA US Rock Mechanics/Geomechanics Symposium, ARMA, pp. ARMA-99-0349.

Fredlund, D. G. & Rahardjo, H. (1993) Soil mechanics for unsaturated soils. New York, John Wiley & Sons.

Gambolati, G. & Verri, G. (1995) Advanced methods for gr*oundwater pollution control.* Berlin, Springer-verlag.

Gersevanov, N. (1934) *Dynamika Gruntovii Mass*. Moscow, Gosstroizzdat.

Graf, D. L. (1982) Chemical osmosis, reverse chemical osmosis, and the origin of subsurface brines. *Geochimica et Cosmochimica Acta* **46(8)**: 1431–1448.

Groot, S. R. D. & Mazur, P. (1962) *Non-equilibrium thermodynamics.* New York, Interscience Publishers.

Gu, W., Lai, W. & Mow, V. (1999) Transport of multi-electrolytes in charged hydrated biological soft tissues. In: De Boer, R. (eds) *Porous* media: theory and experiments. Springer, pp. 143–157.

Haupt, P. (2013) *Continuum mechanics and theory of materials*. Berlin, Heidelberg: Springer Science & Business Media.

Heidug, W. K. & Wong, S. W. (1996) Hydration swelling of water-absorbing rocks: a constitutive model. *International Journal for Numerical and Analytical Methods in Geomechanics* **20(6)**: 403–430.

Herzig, J., Leclerc, D. & Goff, P. L. (1970) Flow of suspensions through porous media—application to deep filtration. *Industrial & Engineering Chemistry* **62(5)**: 8–35.

Humphrey, J. D. (2003) Continuum biomechanics of soft biological tissues. *Proceedings of the Royal Society of London. Series A: Mathematical, Physical and Engineering Sciences* **459(2029)**: 3–46.

Huyghe, J. M. & Janssen, J. D. (1999) Thermo-chemo-electro-mechanical formulation of saturated charged porous solids. *Transport in Porous Media* **34**: 129–141.

Ibrahim, F., Elaiw, A. & Bakr, A. (2008) Effect of the chemical reaction and radiation absorption on the unsteady MHD free convection flow past a semi infinite vertical permeable moving plate with heat source and suction. *Communications in Nonlinear Science and Numerical Simulation* **13(6)**: 1056–1066.

Jayaraman, G. (1983) Water transport in the arterial wall—a theoretical study. *Journal of Biomechanics* **16(10)**: 833–840.

Kapitza, P. (1941) The study of heat transfer in helium II. *Journal of Physics (Moscow)* **4**: 181.

Katsube, N. & Carroll, M. M. (1987) The modified mixture theory for fluid-filled porous materials: theory. *Journal of Applied Mechanics* **54(1)**: 35–40.

Kirwan Jr, A. D. (1985) A review of mixture theory with applications in physical oceanography and meteorology. *Journal of Geophysical Research: Oceans* **90(C2)**: 3265–3283.

Klanchar, M. & Tarbell, J. M. (1987) Modeling water flow through arterial tissue. *Bulletin of Mathematical Biology* **49(6)**: 651–669.

Laird, D. A. (2006) Influence of layer charge on swelling of smectites. *Applied Clay Science* **34(1–4)**: 74–87.

Laloui, L., Klubertanz, G. & Vulliet, L. (2003) Solid-liquid-air coupling in multiphase porous media. *International Journal for Numerical and Analytical Methods in Geomechanics* **27**: 183–206.

Lewis, R. W. & Schrefler, B. A. (1982) *A finite element simulation of the subsidence of gas reservoirs undergoing a waterdrivem in finite elements in fluids.* London, Wiley.

Lewis, R. W. & Schrefler, B. A. (1987) *The finite-element method in deformation and consolidation of porous media.* New York, Wiley.

Lewis, R. W. & Schrefler, B. A. (1998) *The finite element method in the static and dynamic deformation and consolidation of porous media*. 2nd edn. New York, John Wiley & Sons.

Li, X., Li, R. & Schrefler, B. A. (2006) A coupled chemo-thermo-hygro-mechanical model of concrete at high temperature and failure analysis. *International Journal for Numerical and Analytical Methods in Geomechanics* **30**: 635–681.

Luther III, G. W. (2016) *Inorganic chemistry for geochemistry and environmental sciences*: *fundamentals and applications.* Chichester, John Wiley & Sons.

Ma, Y., Chen, X. H., Yu, H. S. (2020) An extension of Biot's theory with molecular influence based on mixture coupling theory: mathematical model. *International Journal of Solids and Structures* **191**: 76–86.

Mase, G. T., Smelser, R. E. & Mase, G. E. (2009) *Continuum mechanics for engineers*. London, CRC press.

Mengual, J. & Garcia-Lopez, F. (1988) Thermoosmosis of water, methanol, and ethanol through cellulose acetate membranes. *Journal of Colloid and Interface Science* **125(2)**: 667–678.

Meroi, E. A., Schrefler, B. A. & Zienkiewicz, O. C. (1995) Large strain static and dynamic semisaturated soil behaviour. *International Journal for Numerical and Analytical Methods in Geomechanics* **19(2)**: 81–106.

Mow, V. C. & Lai, W. M. (1979) Mechanics of animal joints. *Annual Review of Fluid Mechanics* **11(1)**: 247–288.

Moyne, C., Didierjean, S., Souto, H. A. & Da Silveira, O. (2000) Thermal dispersion in porous media: one-equation model. *International Journal of Heat and Mass Transfer* **43(20)**: 3853–3867.

Nayfeh, A. H. (1975) A continuum mixture theory of heat conduction in laminated composites. *Journal of Applied Mechanics* **42(2)**: 399–404.

Nield, D. A. & Bejan, A. (2006) Convection in porous media. Berlin, Springer Science & Business Media.

Okabe, H. & Blunt, M. J. (2005) Pore space reconstruction using multiple-point statistics. *Journal of Petroleum Science and Engineering* **46(1–2)**: 121–137.

Oomens, C. W. J., Van Campen, D. H. & Grootenboer, H. J. (1987) A mixture approach to the mechanics of skin. *Journal of Biomechanics* **20(9)**: 877–885.

Parmigiani, A., Huber, C., Bachmann, O. & Chopard, B. (2011) Pore-scale mass and reactant transport in multiphase porous media flows. *Journal of Fluid Mechanics* **686**: 40–76.

Pfeffer, W. F. (1986) The divergence theorem[J]. *Transactions of the American Mathematical Society*, **295**(2): 665–685.

Preziosi, L. & Tosin, A. (2009) Multiphase and multiscale trends in cancer modelling. *Mathematical Modelling of Natural Phenomena* **4(3)**: 1–11.

Richards, L. A. (1931) Capillary conduction of liquids through porous mediums. *Physics* **1(5)**: 318–333.

Romm, F. (2004) *Microporous media: synthesis, properties, and modeling.* New York, Marcel Dekker, Inc.

Sanavia, L., Schrefle, B. A. & Steinmann, P. (2002) A formulation for an unsaturated porous medium undergoing large inelastic strains. *Computational Mechanics* **28(2)**: 137–151.

Schlemmer, R., Friedheim, J., Growcock, F., Bloys, J., Headley, J. & Polnaszek, S. (2003) Chemical osmosis, shale, and drilling fluids. *SPE Drilling & Completion* **18(4)**: 318–331.

Seetharam, S. C., Thomas, H. R. & Cleall, P. J. (2007) Coupled thermo/hydro/chemical/mechanical model for unsaturated soils-numerical algorithm. *International Journal for Numerical Methods in Engineering* **70(12)**: 1480–1511.

Sills, G. C. (1975) Some conditions under which Biot's equations of consolidation reduce to Terzaghi's equation. *Geotechnique* **25(1)**: 129–132.

Soga, K., Kumar, K., Biscontin, G. & Kuo, M. (2014) *Geomechanics from micro to macro*. London, CRC Press.

Tasaka, M., Hirai, T., Kiyono, R. & Aki, Y. (1992) Solvent transoport across cation-exchange membranes under a temperature difference and under an osmotic pressure difference. *Journal of Membrane Science* **71(1–2)**: 151–159.

Tasaka, M., Kishi, K. & Okita, M. (1984) Thermoosmosis of various electrolyte solutions through anion-exchange membranes. *Journal of Membrane Science* **17(2)**: 149–160.

Terzaghi, K. (1943) *Theoretical soil mechanics.* New York, John Wiley & Sons.

Thomas, H. (1985) Modelling two-dimensional heat and moisture transfer in unsaturated soils, including gravity effects. *International Journal for Numerical and Analytical Methods in Geomechanics* **9(6)**: 573–588.

Thomas, H. (1988) A nonlinear analysis of two-dimensional heat and moisture transfer in partly saturated soil. *International Journal for Numerical and Analytical Methods in Geomechanics* **12(1)**: 31–44.

Thomas, H., Rees, S. & Sloper, N. (1998) Three-dimensional heat, moisture and air transfer in unsaturated soils. *International Journal for Numerical and Analytical Methods in Geomechanics* **22(2)**: 75–95.

Thomas, H. R. & King, S. D. (1991) Coupled temperature/capillary potential variations in unsaturated soil. *Journal of Engineering Mechanics* **117(11)**: 2475–2491.

Thomas, H. R. & Rees, S. W. (1993) The numerical simulation of seasonal soil drying in an unsaturated clay soil. *International Journal for Numerical and Analytical Methods in Geomechanics* **17(2)**: 119–132.

Thomas, H. R. & Sansom, M. R. (1995) Fully coupled analysis of heat, moisture, and air transfer in unsaturated soil. *Journal of Engineering Mechanics* **121(3)**: 392–405.

Truesdell, C. & Toupin, R. (1960) The classical field theories. In *Handbuch der Physik*. (Flügge, S. (ed)) Berlin, Springer-Verlag, pp. 226–793.

Van Genuchten, M. T. (1980) A closed-form equation for predicting the hydraulic conductivity of unsaturated soils. *Soil Science Society of America Journal* **44(5)**: 892–898.

Vardon, P. J. (2015) Climatic influence on geotechnical infrastructure: a review. *Environmental* Geotechnics **2(3)**: 166–174.

Sharvelle, S., Ashbolt, N., Clerico, E., Holquist, R., Levernz, H. & Olivieri, A. (2017) Risk-based framework for the development of public health

guidance for decentralized non-potable water systems. In *WEFTEC 2017*. Water Environment Federation.

Yong, R. N. & Townsend, F. C. (1986) *Consolidation of soils: testing and evaluation: a symposium.* Baltimore, MD, ASTM International.

Zhou, Y., Rajapakse, R. & Graham, J. (1998) A coupled thermoporoelastic model with thermo-osmosis and thermal-filtration. *International Journal of Solids and Structures* **35(34–35)**: 4659–4683.

2 Nonequilibrium thermodynamics concepts for multiphase porous media

2.1 INTRODUCTION

Thermodynamics is a branch of physical science concerned with the relationships between different forms of energy (e.g., mechanical, chemical, heat) and the properties of matter. It finds applications across various fields such as mechanical engineering, chemical engineering, and physical chemistry. Unlike continuum mechanics, which is grounded in Newtonian mechanics, thermodynamics adopts an energy-based perspective. It encompasses two main directions: equilibrium thermodynamics and nonequilibrium thermodynamics, distinguished primarily by the time courses of physical processes, with the former neglecting while the latter emphasizing.

Nonequilibrium thermodynamics addresses physical systems that are not in thermodynamic equilibrium, building upon the second law of thermodynamics regarding entropy. In such systems, there is energy dissipation (e.g., due to friction) that cannot be harnessed for mechanical work. Nonequilibrium thermodynamics offers a robust framework for deriving the evolution equations of dissipative systems. By "unifying dissipative and nondissipative evolution," as articulated by (Ván, 2020), nonequilibrium thermodynamics serves as the foundation for innovations like Mixture-Coupling Theory, which seeks to integrate multiple dissipative and nondissipative processes within complex porous medium systems.

This chapter will primarily introduce key concepts of nonequilibrium thermodynamics relevant to Mixture-Coupling Theory, such as

DOI: 10.1201/9780429324925-2

free energy, entropy, and chemical potential. These concepts facilitate the analysis and transformation of energy into dynamics within mixtures of soils/rocks, water, gas, chemicals, and other constituents.

2.2 THERMODYNAMIC PROPERTIES OF MULTIPHASE/MULTICOMPONENT FLOW IN PORES AND THEIR RELATIONS

Traditionally, fluid mechanics has relied on pressure to propel flow, chemical concentration gradients to drive diffusion, and temperature disparities to induce chemical reactions. Yet, grappling with the intricate interplay of pressure, heat transfer, and chemical concentration changes has posed a challenge.

Enter the representative elementary volume (REV), a microcosm featuring multiphase flow encompassing solids, liquids (laden with chemical species), and gases (see Figure 2.1). Here, the nexus between non-useful work (e.g., entropy), total energy (e.g., enthalpy), and useful work (e.g., Helmholtz free energy) unfolds. Through this exploration, the internal energy of chemical constituents (e.g., chemical potential) is swayed by temperature and entropy, emanating from the fluid within the solution (e.g., fluids or gases). This connection forges a vital link between molecular-scale potential (i.e., chemical potential) and macroscopic thermodynamic attributes (e.g., temperature and pressure) ubiquitous in geotechnical and geoenvironmental engineering.

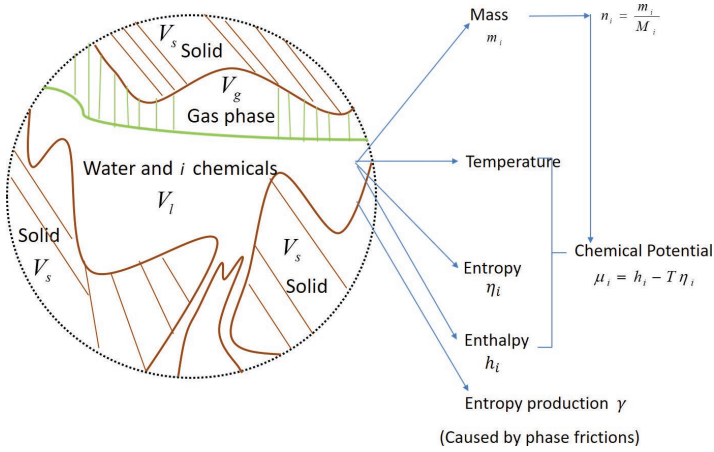

FIGURE 2.1 Overview of relationships between thermodynamical properties within a REV

Moreover, the concept of entropy production, the byproduct of dissipative processes (e.g., frictional forces), takes center stage in nonequilibrium thermodynamics for scrutinizing irreversible phenomena.

These foundational concepts pave the way for a unified analysis, seamlessly transitioning from the microscale (e.g., fluid chemical potential) to the macroscale (e.g., pressure). As a result, the knowledge chasm highlighted in Figure 1.7, spanning down to 100 nm, is bridged.

2.2.1 Entropy and enthalpy

In a geoporous medium, understanding entropy from a statistical mechanics perspective helps grasp its essence, wherein entropy characterizes the randomness or disorder of a system (Mishra, 2012). For instance, in a saturated soil comprising only soil and water, with no change in the solid phase (no deformation), when water transitions to ice, each water molecule's freedom decreases as it becomes bonded within the solid. This reduction in freedom reduces the system's randomness, primarily due to the water's evolution process, leading to a decrease in the system's entropy.

In thermodynamics, entropy (Θ) is defined as a measure of thermal energy per unit temperature (T) that is not available for doing useful work of a system. It may be more convenient to use entropy density (η) rather than the total entropy (Θ) for the REV system, with a description as

$$\eta = \frac{\Theta}{V} \tag{2.1}$$

If the heat density stored in the mixture of a REV is described as q, the entropy density may also be described as

$$\eta = \frac{q}{T} = \frac{\Theta}{V} \tag{2.2}$$

The heat at this temperature is to measure the freedom of the system (e.g., distances between molecules in equilibrium). If the ith component is considered, its entropy density is given by

$$\eta_i = \frac{q_i}{T} \tag{2.3}$$

Compared with entropy density, enthalpy density (h_i) for the ith component is not a state but an energy definition, measuring the energy of the

selected thermodynamic system. The total enthalpy density of the ith components (e.g., species) in the αth phase may be described as

$$\rho_\alpha^i h_i = \varepsilon_i + p_i \tag{2.4}$$[1]

where ε_i is the internal energy density required to create the system for the components, which can be described as a sum of terms that can be interpreted as kinetic energy (e.g., motion) and potential energy (e.g., chemical potential energy that is stored in chemical bonds of a substance).

In a REV, if the pore space (V_{pore}) is selected as the thermodynamics system, the enthalpy density of the water phase is a sum of the internal energy of the water (ε_w, contained within water molecules) and its water pressure, which is defined as

$$\rho_l^w h_w = \varepsilon_w + p_w$$

2.2.2 Chemical potential

The chemical potential, denoted as μ_i or μ_α, pertains to the ith component (e.g., species) in a solution (liquid, gas, or solid) or a pure α phase. It represents an energy that can be absorbed or released due to changes in pressure (p_i or p_α), temperature (T), or chemical reactions. This relationship among the chemical potential of the ith component/species (or the αth phase), entropy, and enthalpy can be expressed using general thermodynamics, as described (Haase, 1969)

$$\mu_i = h_i - T\eta_i \text{ or } \mu_\alpha = h_\alpha - T\eta_\alpha \tag{2.5}$$

In chemical thermodynamics, the chemical potential of the ith species in the a solution can be expressed as a function of its molar activity a_i, which measures the "effective concentration" of the solute in the mixture (Wolt, 1994). The relationship can be described as (Kondepudi and Prigogine, 2014)

$$\mu_i = g_i(p_i, T) + \left(\frac{RT}{M_i}\right)(\ln a_i) \tag{2.6}$$[2]

where R is the gas constant; M_i is the molar mass of the ith species, and $g_i(p_i, T)$ is a function that depends on pressure and temperature.

Under the ideal solution assumption, equation (2.6) simplifies to

$$\mu_{i(c)} = \left(\frac{RT}{M_i}\right)(\ln a_i) \tag{2.7}$$

where $\mu_{i(c)}$ is the term of chemical potential that only depends on molar activity of the ith species. a_i can be expressed as mole fraction x_i using the equation

$$a_i = r_i x_i \tag{2.8}$$

where r_i is the activity coefficient that accounts for the intermolecular interactions between the ith species with itself (between molecules) and other different species (e.g., the jth species, and $j \neq i$).

In a geoporous medium, if only two chemical components are present in a system, the solute (chemical potential μ_c) and diluent (water chemical potential μ_w), and assuming the solution is an ideal solution, the relationship between the activity a_c and the mole fraction x_c of chemical c is given by

$$a_c = r_c x_c \tag{2.9}$$

where r_c is the activity coefficient.

It is more convenient to use mass faction rather than mole fraction. Assuming the solution is ideal, which leads to $r_c = 1$, the solute activity a_c becomes equal to the solute mole fraction x_c $(a_c = x_c)$. The mole fraction x_c can be related to the solute mass fraction c_c through

$$c_c = x_c M_c / (x_c M_c + (1 - x_c) M_w) \tag{2.10}$$

where M_c and M_w are the molar mass of the chemical and water, respectively.

2.2.3 Helmholtz free energy

2.2.3.1 Helmholtz free energy of the mixture

To relate the system's freedom (entropy) with the energy available for useful work, Hermann von Helmholtz introduced the concept of Helmholtz free energy (F) in 1882. This thermodynamic potential quantifies the usable work obtainable from a thermodynamic system and is defined as the difference between internal energy (U) and entropy (Θ) (Tillner-Roth and Friend, 1998; Helmholtz, 1882):

$$F \equiv U - T\Theta \tag{2.11}$$

For a selected system (e.g., REV), the Helmholtz free energy density (ψ) can be described as

$$\psi = \frac{F}{V} = \frac{U}{V} - \frac{T\Theta}{V} = \varepsilon - T\eta \tag{2.12}$$

where $\varepsilon = \frac{U}{V}$ is the total internal energy density of the REV and $\eta = \frac{\Theta}{V}$ is the total entropy density.

In a geoporous medium, the useful work described by Helmholtz free energy may encompass soil/rock deformation and the transport of heat and fluids (e.g., liquid and gas). Entropy may be generated during fluid transport processes. For instance, in an isothermal saturated soil undergoing deformation (consolidation process), the internal energy of the REV system includes soil deformation energy (e.g., $\boldsymbol{\sigma}\mathbf{v}_s$) and water flow energy exchange (e.g., $\mathbf{I}_w h_w$). The entropy flux during this process mainly arises from water flow (e.g., $\mathbf{I}_w \eta_w$), with additional entropy generated by friction between the solid and fluid surfaces. Dissipative processes will be further discussed in Section 2.4.

2.2.3.2 Helmholtz free energy of the pore fluids

In a REV, fluids (e.g., water) in the pores are minimally influenced by intermolecular and surface forces due to the large pore dimensions relative to the distances over which these forces act (Israelachvili, 1991). Thus, thermodynamic relations are appropriate for bulk fluids.

Considering a saturated soil as the simplest case, using equation (2.4), the internal energy density may be described as

$$\varepsilon_{pore} = \rho_l^w h_w - p_w \tag{2.13}$$

in which $p_w = p_{pore}$ is the pore pressure.

Substitution of equation (2.13) into equation (2.12) yields

$$\psi_{pore} = \rho_l^w h_w - p_w - T\rho_l^w \eta_w = \rho_l^w (h_w - T\eta_w) - p_w \tag{2.14}$$

Using equation (2.5) for chemical potential, it follows:

$$\psi_{pore} = \rho_a^w \mu_w - p_w \tag{2.15}$$

Based on classical thermodynamics and a similar derivation process, the Helmholtz free energy density of a single phase (α) with multiple chemical species (total i species) is described as

$$\psi_{pore} = -p_{pore} + \sum_i \rho_\alpha^i \mu_i \tag{2.16}$$

where p_{pore} is the pore pressure.

For multiple immiscible phases ($\alpha > 2$), such as oil, air, and water, with multiple chemicals (e.g., i,k) in each phase, the equation can be extended to

$$\psi_{pore} = -p_{pore} + \sum_{\alpha=1}^{N_p-1} S_\alpha \left(\sum_{i=1}^{N_c} \rho_\alpha^i \mu_i \right) \tag{2.17}$$

where $S_\alpha = \dfrac{V_\alpha}{V_{pore}}$ is the saturation ratio of the αth fluid and $\sum_\alpha S_\alpha = 1$, N_p is the total number of phases, and N_c is the total number of chemicals in the α phase.

Using equation (2.17), the free energy density for a gas and liquid mixture in a pore can be written as

$$\psi_{pore} = -p_{pore} + S_l \sum_k \rho_l^k \mu_k + S_g \sum_i \rho_g^i \mu_i \tag{2.18}$$

where μ_k and μ_i are the chemical potential of the kth and ith chemical components in the liquid and gas, respectively; S_l and S_g are the saturation of the liquid and gas, respectively; and p_{pore} is the total pore pressure of the fluids in the pore that can be replaced using average pressure as

$$p_{pore} \approx \overline{p} = S_l p_l + S_g p_g \tag{2.19}$$

2.2.4 Gibbs-Duhem equation

Considering a multiphase-multiconponents mixture in a REV, the **Gibbs-Duhem equation** describes the relationship between the chemical potential of the ith components (e.g., species) and other macroscopic thermodynamical properties (e.g., pressure and temperature) for the αth fluid phase (containing i chemicals) as (Sacchetti, 2001; Darken, 1950)

$$\sum_{i=1}^{N_c} n_i d\mu_n^i = V_\alpha dp_\alpha - \Theta_\alpha dT \tag{2.20}$$

where n_i is the mole of the ith chemical, μ_n^i is the molar chemical potential of the ith species; Θ_α is the total entropy of the αth phase within the mixture, V_α is the volume of the α th phase (compare with the mixture volume V), and p_α is the pressure of the α th phase. For the convenience of linking with mass density (ρ_α^i) in this book, equation (2.20) can be organized as

$$\sum_{i=1}^{N_c} \rho_\alpha^i d\mu_i = dp_\alpha - \eta_\alpha^\alpha dT \tag{2.21}^3$$

where $\mu_i = \dfrac{\mu_n^i}{M_i}$ is the chemical potential of the i th chemical within the phase relative to the mass density ρ_α^i and M_i is its molar mass, and $\eta_\alpha^\alpha = \dfrac{\Theta_\alpha}{V_\alpha}$ is the true density of entropy of the αth phase (this definition applies throughout the book).

The derivative of equation (2.21) with respect to Eulerian space (dx, dy, dz) or time (dt) leads to the following discussions regarding various scenarios or assumptions:

- If $dT = 0$, which is the isothermal, then $\sum_{i=1}^{N_c} \rho_\alpha^i d\mu_i = dp_\alpha$. This gives the relationship between chemical potential and fluid pressure change with respect to space, as

$$\sum_i \rho_\alpha^i \nabla \mu_i = \nabla p_\alpha \tag{2.22}$$

  or with respect to time (with the assumption of constant density) as

$$\sum_i \rho_\alpha^i \dot{\mu}_i = \dot{p}_\alpha \tag{2.23}$$

- If $dp_\alpha = 0$ and $dT = 0$, then

$$\sum_{i=1}^{N_c} \rho_\alpha^i d\mu_i = 0 \tag{2.24}$$

which gives the relationship of chemical potential between k chemicals with in the αth phase under isothermal and equilibrium conditions.

For a liquid-and-gas mixture under unsaturated conditions, equation (2.22) can be applied to the liquid and gas separately, resulting in

$$\sum_k \rho_\alpha^k \nabla \mu_k = \nabla p_l \text{ or } \sum_i \rho_\alpha^i \nabla \mu_i = \nabla p_g \tag{2.25}$$

where p_l is the liquid pressure and p_g is the gas pressure, respectively. Considering the saturation ratio of gas (S_g) and liquid (e.g., water saturation as S_w), respectively, the equation (2.25) can be changed by multiplying S_l and S_g on both sides, leading to

$$S_l \sum_k \rho_\alpha^k \nabla \mu_k = S_l \nabla p_l \text{ or } S_g \sum_i \rho_\alpha^i \nabla \mu_i = S_g \nabla p_g \tag{2.26}$$

2.3 GENERAL BALANCE LAW FOR THERMODYNAMIC PROPERTIES: CURRENT AND REFERENCE CONFIGURATIONS

2.3.1 Current configuration

Considering a REV as a region volume V (boundary surface Γ) within a deformable porous medium, the mixture of fluids may move into and out of the region. Since the porous medium may deform, the solid part of the region has a velocity $\mathbf{v}_s$. The modified general balance laws of the thermodynamic open system (REV), coupled with the movement of the solid, can be described as (Truesdell and Toupin, 1960; Kondepudi, 2008; Sandler, 2017)

$$\frac{d}{dt}\left(\int_{V(t)} \pi(\mathbf{x},t)\, dV \right) = -\int_\Gamma \mathbf{j}_{\pi,ncon} \cdot \mathbf{n}\, d\Gamma - \int_\Gamma \mathbf{j}_{\pi,con} \cdot \mathbf{n}\, d\Gamma + \int_{V(t)} r_\pi\, dV \tag{2.27}$$

In this book, the integration domain denoted by the subscript V(t) can be abbreviated as V. Where π denotes the bulk density of some extensive thermodynamic quantity (e.g., mass density, energy, and so on); $\mathbf{j}_{\pi,con}$ (e.g., $\mathbf{I}_k$ for the kth species) and $\mathbf{j}_{\pi,ncon}$ (e.g., $\mathbf{I}'_q$ for heat conduction) are

the convective flux and nonconvective flux into the region Ω (volume $V(t)$ is time-dependent. In this book, the integration domain denoted by the subscript $V(t)$ can be abbreviated as V.), respectively; $\mathbf{n}$ is the outward unit normal vector on Γ; and r_π is a source term pertaining to the production of π.

By using similar decrivation process for $\frac{d}{dt}\left(\int_{V(t)} \pi(\mathbf{x},t)\,dV\right)$ in Section 1.3.6, and employing the divergence theorem (Pfeffer, 1986), the local version of equation (2.27) can be obtained as

$$\dot{\pi} + \pi \nabla \cdot \mathbf{v}_s = -\nabla \cdot \mathbf{j}_{\pi,ncon} - \nabla \cdot \mathbf{j}_{\pi,con} + r_\pi \tag{2.28}$$

where $\dot{\pi}(\mathbf{x},t)$ is the material time derivative following the motion of the solid defined as in equation (1.108):

$$\dot{\pi}(\mathbf{x},t) = \frac{\partial \pi(\mathbf{x},t)}{\partial t} + \nabla \pi(\mathbf{x},t) \cdot \mathbf{v}_s \tag{2.29}$$

The classic Reynold's transport theorem (Reynolds et al., 1903) can be derived from equation (2.28) as a special case for fluid transport. For example, in Mixture-Coupling Theory for the REV, the balance law for the mass density of the α th phase in the absence of chemical reactions is given by

$$\frac{d}{dt}\int_V \rho_\alpha \, dV = -\int_\Gamma \rho_\alpha (\mathbf{v}_\alpha - \mathbf{v}_s) \cdot \mathbf{n} \, d\Gamma \tag{2.30}$$

where $\mathbf{v}_\alpha$ is the velocity of the αth phase. Using the divergence theorem (Pfeffer, 1986) leads to the local version of equation (2.30):

$$\dot{\rho}_\alpha + \rho_\alpha \nabla \cdot \mathbf{v}_s + \nabla \cdot \mathbf{I}_\alpha = 0 \tag{2.31}$$

Equation (2.31) presents the balance equation of the α th phase at the current configuration.

2.3.2 Reference configuration

Since Mixture-Coupling Theory includes a deformation pathway for reference configuration, multiplying J on both sides of equation (2.31) leads to

$$J\dot{\rho}_\alpha + J\rho_\alpha \nabla \cdot \mathbf{v}_s + J\nabla \cdot \mathbf{I}_\alpha = 0 \tag{2.32}$$

Using the Euler identity as $\dot{J} = J\nabla \cdot \mathbf{v}_s$ leads to

$$(J\rho_\alpha)^{\cdot} + J\nabla \cdot \mathbf{I}_\alpha = 0 \tag{2.33}$$

Substituting the relationship between ρ_α and ρ_α^α in equation (1.114) and the porosity evolution relationship in equation (1.102), respectively, as

$$\rho_\alpha(\mathbf{x},t) = \phi_\alpha \rho_\alpha^\alpha(\mathbf{x},t) = S_\alpha \phi \rho_\alpha^\alpha(\mathbf{x},t) \text{ and } \upsilon = J\phi$$

into equation (2.33) leads to

$$(S_\alpha \upsilon \rho_\alpha^\alpha)^{\cdot} + J\nabla \cdot \mathbf{I}_\alpha = 0 \tag{2.34}$$

Invoking equation (1.22), equation (2.34) can be written as

$$(S_\alpha \upsilon \rho_\alpha^\alpha)^{\cdot} + J\nabla \cdot (\mathbf{u}_\alpha \rho_\alpha^\alpha) = 0 \tag{2.35}$$

Equation (2.35) includes the porosity (υ) evolution, representing the balance equation at the reference configuration.

2.3.3 Balance equation for solid mass

The balance equation for the solid mass, considering no solid mass crosses the boundary Γ and the motion of the solid, is

$$\frac{d}{dt}\int_V \rho_s \, dV = -\int_\Gamma \rho_s(\mathbf{v}_s - \mathbf{v}_s)\cdot \mathbf{n} \, d\Gamma = 0 \tag{2.36}$$

and the local version of the equation can be derived as

$$\dot{\rho}_s + \rho_s \nabla \cdot \mathbf{v}_s = 0 \tag{2.37}$$

2.3.4 Balance equation for water mass

The balance equation for the water mass is

$$\frac{d}{dt}\int_V \rho_w \, dV = -\int_\Gamma \rho_w(\mathbf{v}_w - \mathbf{v}_s)\cdot \mathbf{n} \, d\Gamma \tag{2.38}$$

Using the divergence theorem (Pfeffer, 1986) leads to

$$-\int_{\Gamma} \rho_w(\mathbf{v}_w - \mathbf{v}_s)\cdot\mathbf{n}\, d\Gamma = -\int_V \nabla\cdot\mathbf{I}_w\, dV \tag{2.39}$$

Hence,

$$\frac{d}{dt}\int_V \rho_w\, dV = -\int_V \nabla\cdot\mathbf{I}_w\, dV \tag{2.40}$$

and the local version of the equation can be derived as

$$\dot{\rho}_w + \rho_w \nabla\cdot\mathbf{v}_s + \nabla\cdot\mathbf{I}_w = 0 \tag{2.41}$$

Note: Derivation of the balance equation for the solid and water mass at the reference configuration can be obtained by following the same process as in equations (2.31) to (2.35). The details can be found in Chapters 3 and 4, and are not reiterated here.

2.3.5 Balance equation for chemicals

2.3.5.1 Current configuration

The balance equation for the *k*th chemical in a liquid (in the absence of chemical reaction) is

$$\frac{d}{dt}\left(\int_V \rho_k\, dV\right) = -\int_{\Gamma} \mathbf{I}_k\cdot\mathbf{n}\, d\Gamma \tag{2.42}$$

and the local version of the equation can be derived using the divergence theorem as

$$\dot{\rho}_k + \rho_k \nabla\cdot\mathbf{v}_s + \nabla\cdot\mathbf{I}_k = 0 \tag{2.43}^4$$

Substitution of the relationship $\rho_k / (\phi S_l) = \rho_l^k$ into equation (2.43) leads to the equation of partial mass density:

$$(\rho_l^k \phi S_l)^{\cdot} + \rho_l^k \phi S_l \nabla\cdot\mathbf{v}_s + \nabla\cdot\mathbf{I}_k = 0 \tag{2.44}$$

By transferring $\mathbf{I}_k$ to $\mathbf{J}_k$ and using equation (1.33), this leads to

$$(\rho_l^k \phi S_l)^{\cdot} + \rho_l^k \phi S_l \nabla\cdot\mathbf{v}_s + \nabla\cdot(\mathbf{J}_k + \rho_l^k \mathbf{u}) = 0 \tag{2.45}$$

2.3.5.2 Reference configuration

By multiplying both sides of equation (2.45) with J, this leads to

$$J(\rho_l^k \phi S_l)^{\cdot} + \rho_l^k \phi S_l J \nabla \cdot \mathbf{v}_s + J\nabla \cdot (\mathbf{J}_k + \rho_l^k \mathbf{u}) = 0 \tag{2.46}$$

Since $\dot{J} = J\nabla \cdot \mathbf{v}_s$, equation (2.46) can be rewritten as

$$(\upsilon \rho_l^k S_l)^{\cdot} + J\nabla \cdot (\rho_l^k \mathbf{u}) + J\nabla \cdot \mathbf{J}_k = 0 \tag{2.47}$$

Introducing the mass fraction $c_k = \rho_l^k \,/\, \rho_l^l$ leads to

$$(S_l \upsilon \rho_l^l c_k)^{\cdot} + J\nabla \cdot (\rho_l^l c_k \mathbf{u}) + J\nabla \cdot \mathbf{J}_k = 0 \tag{2.48}$$

Because $\Sigma_k c_k = 1$ and $\Sigma_k \mathbf{J}_k = 0$, summing over all the liquid components leads to the relationship for the fluid (e.g., liquid) transport[5]:

$$(\upsilon S_l \rho_l^l)^{\cdot} + J\nabla \cdot (\rho_l^l \mathbf{u}) = 0 \tag{2.49}$$

By invoking equation (2.49), equation (2.48) can be transformed to

$$(\upsilon S_l \rho_l^l)\dot{c}_k + J\rho_l^l \mathbf{u} \cdot \nabla c_k + J\nabla \cdot \mathbf{J}_k = 0 \tag{2.50}$$

which is a general equation for chemical transport in the absence of chemical reaction.

2.3.6 Balance equation for heat

2.3.6.1 Current configuration

In a REV, heat (q) can be stored in the solids/fluids according to the relationship

$$q_\alpha = \rho_\alpha C_\alpha T \tag{2.51}$$

where q_α, C_α, and ρ_α are the heat density, specific heat capacity, and mass density of the αth phase, respectively. For example, the heat density of a solid can be defined as

$$q_s = \rho_s C_s T \tag{2.52}$$

where C_s is the specific heat capacity of the solid and ρ_s is the density of the solid. The heat density of water can be defined as

$$q_w = \rho_w C_w T \tag{2.53}$$

where C_w denotes the specific heat capacities of water and ρ_w is the density of the water.

The total heat flow $\mathbf{I}_q$ across the boundary Γ of the REV (which may alter the total heat q) can be separated into two parts:

1. The heat flow contained in the fluids (or thermal convection) expressed as

$$h_\alpha \mathbf{I}_\alpha \tag{2.54}$$

in which h_α denotes the enthalpy of the α phase, defined as $h_\alpha = C_\alpha T$, with T representing temperature. For example, h_w for the enthalpy of water is defined as $h_w = C_w T$, where C_w is the specific heat capacity of the water.

2. The reduced heat flow $\mathbf{I}'_q$ (thermal conduction or diffusive heat flow) is defined as

$$\mathbf{I}'_q = \mathbf{I}_q - \sum_{\alpha=1}^{N_p-1} h_\alpha \mathbf{I}_\alpha \tag{2.55}$$

where $N_p - 1$ means the solid is excluded.

To establish the relationship between the total heat within the REV and the heat flow crossing the boundary of the REV, using the fundamental balance equation for thermodynamically open systems (equation (2.27)), the thermo balance equation of the REV is obtained:

$$\frac{d}{dt}\int_V \left(q_s + \sum_{\alpha=1}^{N_p-1} q_\alpha \right) dV = -\int_\Gamma \mathbf{I}_q \cdot \mathbf{n}\, d\Gamma \tag{2.56}$$

where $\sum_{\alpha=1}^{N_p-1} q_\alpha$ is the total heat density of α fluid phase. The local version of the balance equation can be derived as

$$\left(q_s+\sum_{\alpha=1}^{N_p-1}q_\alpha\right)+\left(q_s+\sum_{\alpha=1}^{N_p-1}q_\alpha\right)\nabla\cdot\mathbf{v}_s+\nabla\cdot\mathbf{I}_q=0 \tag{2.57}$$

2.3.6.2 Reference configuration

Multiplying both sides of equation (2.57) by J and utilizing the Euler identity $\dot{J}=J\nabla\cdot\mathbf{v}_s$ leads to

$$(Jq_s+J\sum_{\alpha=1}^{N_p-1}q_\alpha)^{\cdot}+J\nabla\cdot\mathbf{I}_q=0 \tag{2.58}$$

Since q_s and q_α are related with the mass densities ρ_s and ρ_α, expressed relative to the unit volume of the liquid and solid mixture, the thermo density relative to the "true density" can be defined as q_s^s and q_α^α. The relationships between q_s, q_s^s and q_α, q_α^α can be defined as

$$q_s^s=q_s/\phi_s \text{ and } q_\alpha^\alpha=q_\alpha/S_\alpha\phi \tag{2.59}$$

Substituting equation (2.59) into (2.58) and using the relationship $\upsilon=J\phi$ leads to

$$\left(q_s^s(J-\upsilon)+\upsilon\sum_{\alpha=1}^{N_p-1}q_\alpha^\alpha S_\alpha\right)^{\cdot}+J\nabla\cdot\mathbf{I}_q=0 \tag{2.60}$$

If there are a total of N_c chemicals (i for an individual chemical) in the αth phase, and each chemical has a different heat capacity (q_α^i), equation (2.60) may be further extended as

$$\left(q_s^s(J-\upsilon)+\upsilon\sum_{\alpha=1}^{N_p-1}S_\alpha\left(\sum_{i}^{Nc}q_\alpha^i\right)\right)^{\cdot}+J\nabla\cdot\mathbf{I}_q=0 \tag{2.61}$$

where $q_\alpha^\alpha=\sum_{i}^{Nc}q_\alpha^i$. Note: In this book, the thermo transport in multiple chemicals within the α states are not extensively considered in equation (2.61), as chemicals are mixed in the state of matter at molecular scales. If only one liquid is considered, equation (2.60) can be simplified using equation (1.23) as

$$(q_s^s(J-\upsilon)+\upsilon q_l^l S_l)^{\cdot}+J\nabla\cdot\mathbf{I}_q=0$$

or

$$(q_s^s(J-\upsilon)+\upsilon q_l^l S_l)^{\cdot}+J\nabla\cdot\left(\mathbf{I}'_q+\sum_{\alpha=1}^{N_p-1}h_\alpha\mathbf{I}_\alpha\right)=0 \tag{2.62}$$

2.3.7 Balance equation for entropy

2.3.7.1 Current configuration

This section provides entropy density flow ($\mathbf{I}_\eta$) for analysis in Chapter 6 of non-isothermal conditions. From classical thermodynamics, the entropy flow equation is described as

$$\mathbf{I}_\eta=\frac{\mathbf{I}_q-\sum_{i=1}^{N_c}\mu_i\mathbf{I}_i}{T} \tag{2.63}$$

Since the chemical potential can be interpreted as $\mu_i=h_i-T\eta_i$ in equation (2.5), the relationship between $\mathbf{I}_\eta$ and $\mathbf{I}'_q$ can be reorganized as

$$\mathbf{I}_\eta=\frac{\mathbf{I}_q-\sum_{i=1}^{N_c}(\mathbf{I}_i\mu_i)}{T}=\frac{\mathbf{I}_q-\sum_{i=1}^{N_c}(\mathbf{I}_i(h_i-T\eta_i))}{T}=\frac{\mathbf{I}_q-\sum_{i=1}^{N_c}(\mathbf{I}_ih_i-\mathbf{I}_iT\eta_i)}{T}$$

$$=\frac{\mathbf{I}'_q+\sum_{i=1}^{N_c}(\mathbf{I}_iT\eta_i)}{T} \tag{2.64}$$

This relationship is useful for Section 2.5.1 and Chapter 6 for entropy production analysis.

The balance equation of entropy density flow can be written as

$$\frac{d}{dt}\int_V\left(\eta_s+\sum_\alpha\eta_\alpha\right)dV=-\int_\Gamma\mathbf{I}_\eta\cdot\mathbf{n}\,d\Gamma \tag{2.65}$$

where η_s is the entropy density of the solid related to the unit volume of the solid-fluid mixture and η_α is the entropy density of the fluid. In equation (2.65), if there is only a liquid (e.g., water and chemicals) and a solid (e.g., geomaterials) in the mixture, equation (2.65) can be simplified as

$$\frac{d}{dt}\int_V (\eta_s + \eta_l)\, dV = -\int_\Gamma \mathbf{I}_\eta \cdot \mathbf{n}\, d\Gamma \tag{2.66}$$

where η_l is the entropy density of the liquid related to the unit volume of the solid-fluid mixture. The local balance version of equation (2.66) can be derived as

$$(\eta_s + \eta_l)^{\cdot} + (\eta_s + \eta_l)\nabla \cdot \mathbf{v}_s = -\nabla \cdot \mathbf{I}_\eta \tag{2.67}$$

2.3.7.2 Reference configuration

Multiplying by J on both sides of equation (2.67) gives

$$J(\eta_s + \eta_l)^{\cdot} + (\eta_s + \eta_l)J\nabla \cdot \mathbf{v}_s = -J\nabla \cdot \mathbf{I}_\eta \tag{2.68}$$

and using the Euler identity $\dot{J} = J\nabla \cdot \mathbf{v}_s$ leads to

$$(J\eta_s + J\eta_l)^{\cdot} = -J\nabla \cdot \mathbf{I}_\eta \tag{2.69}$$

Substituting the relationship between entropy density related to the unit volume of the solid-fluid mixture (e.g., η_s and η_l) and the "state entropy density" (e.g., η_s^s and η_l^l) as

$$\eta_l / (\phi S_l) = \eta_l^l \text{ and } \eta_s / \phi_s = \eta_s^s \tag{2.70}$$

and $\upsilon = J\phi$, equation (2.69) then becomes

$$((J - \upsilon)\eta_s^s + S_l \upsilon \eta_l^l)^{\cdot} = -J\nabla \cdot \mathbf{I}_\eta \tag{2.71}^6$$

2.4 HELMHOLTZ FREE ENERGY FOR THE MIXTURE SYSTEM AND PORE FLUIDS

The Helmholtz free energy density (ψ) offers a means of integrating mechanical energy, fluid energy, and thermal energy of the mixture system. To derive the balance equation of ψ, which is related to the internal energy density (ε) and entropy density (η) as per equation (2.12), it is imperative to establish the balance equations of ε and η.

2.4.1 Flux and creation of internal energy and entropy

The creation of internal energy and entropy within a deformable multiphase porous media refers to the processes by which internal energy

and entropy are generated or altered within the medium. In a deformable porous media, such as soils or rocks containing multiple fluid phases, several mechanisms contribute to the creation of internal energy and entropy:

1. **Mechanical deformation**: Deformation of the porous medium due to mechanical forces results in the creation of internal energy. As the medium deforms, mechanical work is done on the material, leading to changes in its internal energy. This deformation can occur due to external loads or stresses applied to the medium.
2. **Heat conduction**: Heat conduction through the porous medium generates internal energy and entropy. When there is a temperature gradient within the medium, heat flows from regions of higher temperature to lower temperature, resulting in the creation of internal energy and entropy along the path of heat transfer.
3. **Chemical reactions**: Chemical reactions taking place within the porous medium can generate or consume internal energy and entropy. Exothermic reactions release heat energy, increasing the internal energy of the system, while endothermic reactions absorb heat energy. Chemical reactions can also lead to changes in entropy, depending on the nature of the reaction and the accompanying changes in molecular order.
4. **Fluid flow**: Fluid flow within the porous medium can also contribute to the creation of internal energy and entropy. Frictional forces associated with fluid flow result in the generation of heat, increasing the internal energy of the system. Additionally, fluid mixing and transport processes can lead to changes in entropy, particularly in multiphase flow systems where mixing of fluids with different properties occurs.

2.4.1.1 Nonconvective flux of internal energy and entropy

The nonconvective flux of internal energy ($\mathbf{j}_{\varepsilon,ncon}$) and entropy ($\mathbf{j}_{\eta,ncon}$) within a porous medium encompasses various mechanisms contributing to energy and entropy transfer that do not involve bulk fluid movement. In the context of deformable multiphase porous media, the nonconvective flux of internal energy is primarily driven by mechanical deformation and heat conduction. Mechanical deformation, characterized by changes in the material's shape or volume due to applied forces, leads to the generation of internal energy through the Cauchy stress tensor ($\boldsymbol{\sigma}$) acting on the boundary surfaces of the medium (Γ). Simultaneously,

heat conduction ($\mathbf{I}'_q$) across the boundaries of the medium contributes to the nonconvective flux of internal energy, wherein temperature gradients induce heat flow, altering the internal energy distribution within the system. The nonconvective flux of entropy ($\mathbf{j}_{\eta,ncon}$), on the other hand, arises predominantly from heat conduction processes, as the movement of heat within the porous medium leads to changes in entropy without the concurrent displacement of material. This flux is particularly relevant in analyzing thermal processes and their associated entropy generation within the porous medium.

(i) The nonconvective flux of internal energy $\mathbf{j}_{\varepsilon,ncon}$ composes the mechanical deformation energy and heat flow energy:
- The integral form of the mechanical deformation energy of the boundary of Ω can be described as

$$\int_{\Gamma} \boldsymbol{\sigma}\mathbf{v}_s \cdot \mathbf{n} d\Gamma \tag{2.72}$$

where $\boldsymbol{\sigma}$ is Cauchy stress tensor and $d\Gamma$ is the per unit contact surface of the fluid and solid. The term $\int_{\Gamma} (\boldsymbol{\sigma}\mathbf{v}_s) \cdot \mathbf{n}\, d\Gamma$ represents the rate of deformation energy caused by the traction $\boldsymbol{\sigma}$ on deforming the element area of the boundary with a velocity of $\mathbf{v}_s$. Note that equation (2.72) neglects the impact of body forces for simplification.
- The heat conduction energy across the boundary Γ is given by:

$$\int_{\Gamma} (-\mathbf{I}'_q) \cdot \mathbf{n}\, d\Gamma \tag{2.73}$$

(Note: The heat energy along with fluids transport is included in convective flux.)

By combining equations (2.72) and (2.73), it leads to

$$\mathbf{j}_{\varepsilon,ncon} = \boldsymbol{\sigma}\mathbf{v}_{\mathbf{s}} - \mathbf{I}'_q \tag{2.74}$$

(ii) The nonconvective entropy $\mathbf{j}_{\eta,ncon}$

In the absence of entropy flux related to elastic deformation, the nonconvective flux of entropy arises solely from heat conduction and can be represented as

$$\mathbf{j}_{\eta,ncon} = \frac{-\mathbf{I}'_q}{T} \tag{2.75}$$

(Note: Plastic deformation in soils involves processes that rearrange soil particles, leading to entropy generation which needs to be accounted for in the nonconvective entropy.)

2.4.1.2 Convective flux of internal energy $\mathbf{j}_{\varepsilon,con}$ and entropy $\mathbf{j}_{\eta,con}$

The convective flux of internal energy ($\mathbf{j}_{\varepsilon,con}$) and entropy ($\mathbf{j}_{\eta,con}$) within a deformable multiphase porous medium accounts for the transport of energy and entropy due to bulk fluid flow. In saturated media, such as water-saturated soils, the convective flux of internal energy is primarily governed by the movement of the water phases ($\mathbf{I}_w$), with energy (h_w) being carried along as the water flow through the porous medium. Similarly, the convective flux of entropy accompanies fluid flow and is influenced by changes in fluid composition, temperature gradients, and other factors. In multiphase systems involving multiple species (e.g., $\mathbf{I}_i$), the convective fluxes of internal energy (h_i) and entropy (η_i) become more complex, reflecting the interactions between different fluid phases and their respective energy and entropy contributions. Understanding and quantifying these convective fluxes are essential for analyzing heat and mass transfer phenomena within deformable porous media and elucidating their broader thermodynamic behavior.

i. For single-phase flow, saturated media such as water-saturated soils, the internal energy and its associated entropy flux are defined as

$$\mathbf{j}_{\varepsilon,con} = -h_w \mathbf{I}_w \text{ and } \mathbf{j}_{\eta,con} = -\eta_w \mathbf{I}_w \tag{2.76}$$

ii. In the case of multiphase flow systems with multiple species,

$$\mathbf{j}_{\varepsilon,con} = -\sum h_i \mathbf{I}_i \text{ and } \mathbf{j}_{\eta,con} = -\sum \eta_i \mathbf{I}_i \tag{2.77}$$

2.4.1.3 Source term of energy production and entropy within the system

The source term of energy production and entropy within a deformable multiphase porous medium encapsulates the mechanisms by

which energy is generated or consumed within the system. This term encompasses various processes such as frictional heating, chemical reactions, and other energy-producing phenomena occurring within the porous medium. Frictional heating, for example, arises from mechanical deformation and the associated energy dissipation due to frictional forces between solid particles or between the solid and fluid phases. Chemical reactions occurring within the medium may also release or absorb heat, contributing to the overall energy balance. Similarly, entropy production within the system reflects the irreversible processes that lead to an increase in entropy, often associated with dissipatio of energy and irreversible transformations.

The entropy produced within V is described as

$$\int_V \gamma \, dV \tag{2.78}$$

where γ is the entropy production per unit volume. The entropy production links with the dissipative process.

The heat generated due to chemical reaction may be described as

$$\int_V q_R \, dV \tag{2.79}$$

In this book, q_R is assumed to be zero to simplify the discussion. For chemical reactions that involve significant heat transfer, this term should be considered.

2.4.2 Balance equation of Helmholtz free energy density for the mixture system

The balance equation of Helmholtz free energy density (ψ) for the mixture system delineates the evolution of this fundamental thermodynamic quantity within the porous medium. As articulated in equation (2.12) $\psi = \varepsilon - T\eta$, the relationship between free energy density, internal energy density (ε), and entropy (η) underscores the interconnected nature of these variables. Thus, obtaining the balance equation for internal energy and entropy is a prerequisite for elucidating the dynamics of Helmholtz free energy density within the system.

Recall equation (2.27), the balance equation of internal energy is

$$\frac{d}{dt}\int_{V(t)} \varepsilon \, dV = \int_\Gamma (\boldsymbol{\sigma}\mathbf{v}_\mathbf{s} - \mathbf{I}_q)\cdot \mathbf{n}\, d\Gamma - \int_\Gamma \left(\sum h_i \mathbf{I}_i\right)\cdot \mathbf{n}\, d\Gamma \tag{2.80}$$

and the balance equation of entropy is

$$\frac{d}{dt}\int_{V(t)} \eta\, dV = -\int_{\Gamma}\left(\frac{\mathbf{I}_q}{T}\right)\cdot \mathbf{n}\, d\Gamma - \int_{\Gamma}\left(\sum \eta_i \mathbf{I}_i\right)\cdot \mathbf{n} d\Gamma + \int_V \gamma dV \qquad (2.81)$$

By considering isothermal condition, and multiplying temperature T on both sides of equation (2.81), it leads to

$$\frac{d}{dt}\int_{V(t)} T\eta\, dV = -\int_{\Gamma} \mathbf{I}_q \cdot \mathbf{n}\, d\Gamma - \int_{\Gamma} T\left(\sum \eta_i \mathbf{I}_i\right)\cdot \mathbf{n} d\Gamma + \int_V T\gamma dV \quad (2.82)$$

Substitution of equation (2.12) into equation (2.82) leads to

$$\frac{d}{dt}\int_{V(t)} (\varepsilon - T\eta)\, dV = \int_{\Gamma} (\boldsymbol{\sigma}\mathbf{v}_{\mathbf{s}})\cdot \mathbf{n}\, d\Gamma - \int_{\Gamma}\left(\sum (h_i - T\eta_i)\mathbf{I}_i\right)\cdot \mathbf{n} d\Gamma - \int_V T\gamma dV \qquad (2.83)^7$$

By considering the relationship between entropy, enthalpy, and chemical potential in equation (2.5), $\mu_i = h_i - T\eta_i$, it leads to

$$\frac{d}{dt}\int_V \psi\, dV = \int_{\Gamma} \boldsymbol{\sigma}\mathbf{v}_{\mathbf{s}} \cdot \mathbf{n} d\Gamma - \int_{\Gamma} \sum \mu_i \mathbf{I}_i \cdot \mathbf{n} d\Gamma - \int_V T\gamma\, dV \qquad (2.84)$$

By using the divergence theorem for equation (2.84) to transfer surface integral to volume integral, it leads to

$$\frac{d}{dt}\int_V \psi\, dV = \int_V \nabla\cdot(\boldsymbol{\sigma}\mathbf{v}_{\mathbf{s}}) dV - \int_V \nabla\cdot\left(\sum \mu_i \mathbf{I}_i\right) dV - \int_V T\gamma\, dV \qquad (2.85)$$

and its local balance equation becomes (see Chapters 3–5 for detailed derivations of various coupling scenarios) (Chen and Hicks, 2013; Heidug and Wong, 1996)

$$\dot{\psi} + \psi\cdot\nabla\mathbf{v}_s - \nabla\cdot(\boldsymbol{\sigma}\mathbf{v}_s) + \nabla\cdot\left(\sum \mu_i \mathbf{I}_i\right) = -\mathrm{T}\gamma \qquad (2.86)$$

This equation serves as a cornerstone for comprehending the thermodynamic characteristics of multiphase, multicomponent systems, playing a pivotal role in the development of comprehensive models for transport

and thermodynamic phenomena in porous media in isothermal conditions. However, in non-isothermal conditions where chemical reactions are absent, deviations from the Helmholtz free energy density balance equation may arise, as detailed in Chapter 6.

2.5 DISSIPATIVE PROCESSES AND ENTROPY PRODUCTION

Dissipative processes within multiphase multiscale porous media systems are fundamental mechanisms driving irreversible energy transformations and entropy production. Four major processes leading to dissipation, as illustrated in Figure 2.2, include (1) friction at the boundaries between solids and fluids; (2) friction at fluid interfaces, such as between gas and water phases; (3) dissipation resulting from chemical reactions; and (4) dissipation through thermal transport. These processes contribute to the generation of entropy, reflecting the system's tendency toward increased disorder and randomness. It is essential to note that while these four processes represent significant contributors to entropy production, additional factors such as nuclear radiation or biogeochemical reactions involving bacteria may introduce further dissipation mechanisms. However, this book primarily focuses on the aforementioned processes, with future research potentially exploring additional fields within the framework of Mixture-Coupling Theory. Understanding entropy production is crucial for distinguishing between traditional thermodynamics and nonequilibrium thermodynamics,

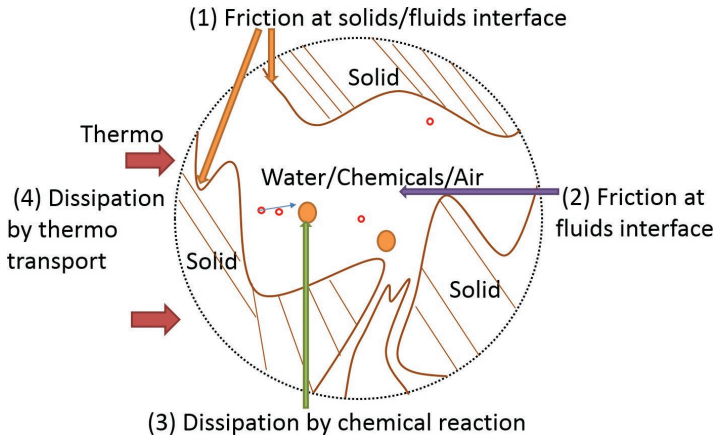

FIGURE 2.2 Entropy density production

highlighting the importance of incorporating dissipative processes into modeling porous media systems accurately.

2.5.1 Entropy production density generated by the dissipative process

Dissipative processes within the porous media system are quantified by entropy production, denoted as entropy production density γ in this book. This term represents the amount of entropy generated during any irreversible processes occurring within the system (Groot and Mazur, 1962). It's important to note that the entropy production density is defined as η to distinguish it from the general definition of entropy density introduced in Section 2.2.1. This distinction enables a clear differentiation between the concepts of entropy production and entropy within the context of the thermodynamic analysis presented in this work.

2.5.1.1 Isotherm and non-reaction

In the context of isothermal conditions without chemical reactions, the local entropy production density function for a single fluid (e.g., liquid) with multiple chemicals transported within porous media is described by:

$$0 \leq \gamma = \sum_{i=1}^{N_c} \frac{\mathbf{I}_i}{T} \cdot \nabla(-\mu_i) \tag{2.87}$$

This equation presents a combination of flows $(\mathbf{I}_i)$ and their respective driving forces $\left(\frac{\nabla(-\mu_i)}{T}\right)$. Under isothermal conditions, the temperature remains constant. The equation illustrates the entropy density generated by frictional resistance between the solid and fluid interfaces (e.g., soils and water) and the interactions among multiple chemicals (e.g., molecular interactions). This formulation provides insight into the entropy production arising from mechanical and chemical processes within the porous media system.

2.5.1.2 Non-isotherm and non-reaction

If the temperature T is not constant and a temperature gradient is applied to the system, it generates a heat flow $\mathbf{I}_q$, which consequently affects the chemical potential μ_i. The entropy density production function, encompassing both frictional and thermal dissipative processes, can be described in two different forms:

(i) Total heat flow (i.e., $\mathbf{I}_q$) or entropy density flow (i.e., $\mathbf{I}_\eta$) and chemical potential (i.e., μ)

$$0 \le \gamma = \mathbf{I}_q \cdot \nabla\left(\frac{1}{T}\right) + \sum_{i=1}^{N_c} \mathbf{I}_i \cdot \nabla\left(\frac{-\mu_i}{T}\right) \tag{2.88}$$

where $\mathbf{I}_q \cdot \nabla\left(\frac{1}{T}\right)$ is the entropy density generated by the heat dissipative process, which is the product of total flow of heat $\mathbf{I}_q$ and its driving force $\nabla\left(\frac{1}{T}\right)$. Following the ordinary differentiation rule, the $\nabla\left(\frac{1}{T}\right)$ can be expressed as

$$\nabla\left(\frac{1}{T}\right) = -\frac{1}{T^2}\nabla T \tag{2.89}$$

Therefore, $\nabla\left(\frac{-\mu_i}{T}\right)$ can be described as

$$\nabla\left(\frac{-\mu_i}{T}\right) = \frac{-1}{T}\nabla\mu_i + \frac{\mu_i}{T^2}\nabla T \tag{2.90}$$

Introducing equations (2.89) and (2.90) into equation (2.88) leads to

$$0 \le \gamma = \frac{\mathbf{I}_q - \sum_{i=1}^{N_c} \mu_i \mathbf{I}_i}{T^2} \cdot \nabla(-T) + \sum_{i=1}^{N_c} \frac{\mathbf{I}_i}{T} \cdot \nabla(-\mu_i) \tag{2.91}$$[8]

Introducing the entropy density flow function (2.63), $\mathbf{I}_\eta = \frac{\mathbf{I}_q - \sum_{i=1}^{N_c} \mu_i \mathbf{I}_i}{T}$ into equation (2.91) leads to a simplified version:

$$0 \le \gamma = \frac{\mathbf{I}_\eta}{T} \cdot \nabla(-T) + \sum_{i=1}^{N_c} \frac{\mathbf{I}_i}{T} \cdot \nabla(-\mu_i) \tag{2.92}$$

which provides a different form of the entropy equation (2.88) with flows $\mathbf{I}_\eta$ and $\mathbf{I}_i$, and their and driving force as $\frac{\nabla(-T)}{T}$ and $\frac{\nabla(-\mu_i)}{T}$, correspondingly.

(ii) Reduced heat flow ($\mathbf{I}'$) and concentration-dependent part of the chemical potential ($\mu_{i(c)}$)

In equation (2.88), the driving force for $\mathbf{I}_q$ is $\nabla(\frac{1}{T})$ which is not convenient for equation derivation, whereas, in equation (2.92), the driving force $\frac{\nabla(-T)}{T}$ has a corresponding flow as $\mathbf{I}_\eta$, which is not used in geotechnical and geoenvironmental engineering. It is therefore necessary to derive other forms. Since from equation (2.90), the $\nabla(\frac{-\mu_i}{T})$ can be expressed as

$$\nabla\left(\frac{-\mu_i}{T}\right) = \frac{-1}{T}\nabla\mu_i + \frac{-\mu_i}{T^2}\nabla T$$

in which $\nabla\mu_i$ can be expressed using a function of temperature gradient (∇T), pressure gradient (∇p_i), and the gradient of the concentration-dependent part of the chemical potential ($\nabla\mu_{i(c)}$) as (Mandl, 1988)

$$\nabla\mu_i = -\eta_i\nabla T + V_i\nabla p_i + \nabla\mu_{i(c)} \tag{2.93}$$

where $\mu_{i(c)}$ represents the concentration-dependent part of the chemical potential.

If the system is at the mechanical equilibrium condition that leads to $\nabla p_i = 0$, equation (2.93) can be simplified as

$$\nabla\mu_i = -\eta_i\nabla T + \nabla\mu_{i(c)} \tag{2.94}$$

Substituting the equation (2.94) into equation (2.90) and using the relation from equation (2.5), $h_i = T\eta_i + \mu_i$, Equation (2.90) can be rewritten as

$$\nabla\left(\frac{-\mu_i}{T}\right) = -h_i\nabla\left(\frac{1}{T}\right) + \frac{1}{T}\nabla\left(-\mu_{i(c)}\right) \tag{2.95}$$

By introducing equation (2.95) into equation (2.88), it leads to

$$\gamma = \left(\mathbf{I}_q - \sum_{i=1}^{N_c} h_i\mathbf{I}_i\right)\cdot\nabla\left(\frac{1}{T}\right) + \sum_{i=1}^{N_c}\mathbf{I}_i\cdot\nabla\left(\frac{-\mu_{i(c)}}{T}\right) \tag{2.96}$$

Using the reducing heat flow $\mathbf{I}'_q = \mathbf{I}_q - \sum_{i=1}^{N_c} h_i \mathbf{I}_i$, the equation can be reformed as

$$0 \le \gamma = \frac{\mathbf{I}'_q}{T^2} \cdot \nabla(-T) + \sum_{i=1}^{N_c} \frac{\mathbf{I}_i}{T} \cdot \nabla(-\mu_{i(c)}) \tag{2.97}$$

in which the flux has been changed to $\mathbf{I}'_q$, $\mathbf{I}_i$, and the driving force to $\frac{\nabla(-T)}{T^2}$, $\frac{\nabla(-\mu_{i(c)})}{T}$, respectively. Equation (2.97) will be used for Chapter 6, whereas, equation (2.87) will be used for Chapters 3–5. The detailed derivation between equations (2.97) and (2.92) can be found in Note[9].

2.5.1.3 Non-isotherm and reaction

If a chemical reaction is included, equation (2.92) or (2.97) can be extended as

$$0 \le \gamma = \frac{\mathbf{I}_\eta}{T} \cdot \nabla(-T) + \sum_{i=1}^{N_c} \frac{\mathbf{I}_i}{T} \cdot \nabla(-\mu_i) + I_{ch} \frac{A}{T} \tag{2.98}$$

or

$$0 \le \gamma = \frac{\mathbf{I}'_q}{T^2} \cdot \nabla(-T) + \sum_{i=1}^{N_c} \frac{\mathbf{I}_i}{T} \cdot \nabla(-\mu_i^c) + I_{ch} \frac{A}{T} \tag{2.99}$$

where $I_{ch} \frac{A}{T}$ is the entropy generated by chemical reactions. The affinity A is the negative partial derivative of Gibbs free energy Π with respect to the extent of the reaction ξ[10] at constant pressure and temperature

$$A = -\left(\frac{\partial \Pi}{\partial \xi} \right)_{P,T}$$

and can be further simplified as $A = -\Sigma N_i^s \mu_i$ (Katachalsky and Curran, 1965), in which N_i^s is stoichiometric coefficient for the ith component.

Note here: The entropy production of solid matrix including fracture and plasticity can be included for further extension of the theory to deal with complicated geoengineering applications.

2.5.2 Dissipation production

By using equations (2.98) and (2.99), the dissipation function for non-isothermal chemical reactions can be presented as the sum of the products of flows with their conjugated forces (Katachalsky and Curran, 1965):

$$0 \le T\gamma = \frac{\mathbf{I}'_q}{T} \cdot \nabla(-T) + \sum_{i=1}^{N_c} \mathbf{I}_i \cdot \nabla(-\mu_{i(c)}) + I_{ch} A \tag{2.100}$$

or

$$0 \le T\gamma = \mathbf{I}_\eta \cdot \nabla(-T) + \sum_{i=1}^{N_c} \mathbf{I}_i \cdot \nabla(-\mu_i) + I_{ch} A \tag{2.101}$$

These functions provide a thermodynamical description of the dissipative process, and they are an extension of Lord Rayleigh's dissipation function for studying the effects of velocity-proportional frictional forces (Goldstein, 1980).

If it is assumed that only a single dissipation (namely the friction) is generated at the solid/fluid boundary when the fluid moves through the porous skeleton, a macroscopic expression for isothermal fluid (including i chemicals) transport and dissipation process can be obtained by using standard nonequilibrium thermodynamics. This expression (known as Rayleigh's dissipation function), is given by

$$0 \le T\gamma = -\sum_i \mathbf{I}_i \cdot \nabla \mu_i \tag{2.102}$$

The chemical potential μ_i in equation (2.102) is described as the driving force for the corresponding flux $\mathbf{I}_i$. To link the μ_i with fluid pressure that is normally used as the driving force of fluids and to establish the links of the entropy of fluids, the Gibbs-Duhem equation is employed. Equation (2.102) gives the relationship between the flux $\mathbf{I}_i$ (relative to the solid velocity $\mathbf{v}_s$) and its driving force μ_i. It is necessary to obtain the driving force for the diffusion flux $\mathbf{J}_i$ (relative to the barycentric velocity of the fluid, e.g., $\mathbf{v}_l$ for liquid) and Darcy velocity $\mathbf{u}$. For example, in a liquid phase, by connecting $\mathbf{I}_k$ with $\mathbf{J}_k$ in Section 1.2.4, it leads to

$$\mathbf{J}_k = \mathbf{I}_k - \rho_k(\mathbf{v}_l - \mathbf{v}_s) \tag{2.103}$$

By using equations (2.22) and (2.103), equation (2.102) for saturated conditions (and unsaturated condition) can be rewritten as

$$0 \le T\gamma = -\mathbf{u} \cdot \nabla p_\alpha - \sum_k \mathbf{J}_k \cdot \nabla \mu_k \qquad (2.104)^{11}$$

where p_α denotes the pore pressure of the fluid.

2.6 PHENOMENOLOGICAL EQUATIONS

Equation (2.104) establishes the overall dissipation link between the flows (e.g., $\mathbf{u}$ and $\mathbf{J}_k$) and the corresponding driving forces (∇p_α and $\nabla \mu_k$). The relationship between these flows and driving forces will be developed by using phenomenological equations as (McMullin, 1968; Davidson and Tinkham, 1976; Tyrrell and Harris, 2013)

$$\begin{aligned}
\mathbf{J}_1 &= L_{11}\mathbf{f}_1 + L_{12}\mathbf{f}_2 + L_{13}\mathbf{f}_3 + \cdots + L_{1n}\mathbf{f}_n \\
\mathbf{J}_2 &= L_{21}\mathbf{f}_1 + L_{22}\mathbf{f}_2 + L_{23}\mathbf{f}_3 + \cdots + L_{2n}\mathbf{f}_n \\
&\cdots\cdots \\
\mathbf{J}_n &= L_{n1}\mathbf{f}_1 + L_{n2}\mathbf{f}_2 + L_{n3}\mathbf{f}_3 + \cdots + L_{nn}\mathbf{f}_n
\end{aligned} \qquad (2.105)$$

$$\text{or} \quad \mathbf{J}_i = \sum_{k=1}^{n} L_{ik}\mathbf{f}_k \quad (i = 1,2,3,\ldots n) \qquad (2.106)$$

Equations (2.105) and (2.106) are a set of functions to express the linear dependence of the flows ($\mathbf{J}_1 \ldots \mathbf{J}_n$) on the corresponding forces ($\mathbf{f}_1 \ldots \mathbf{f}_n$) (Onsager, 1931). Each flow ($\mathbf{J}_i$) is linearly proportional to its conjugated and nonconjugated forces, and the coefficient for the main driving force is L_{ii}, and for the side driving force is $L_{ik}\,(i \ne k)$.

For example, the linear relationships between the liquid flow $\rho_l^l \mathbf{u}$ and one chemical diffusion flux $\mathbf{J}_c$ and their corresponding driving forces ∇p_l and ∇c can be derived with phenomenological equations as (Chen and Hicks, 2013)

$$\rho_l^l \mathbf{u} = -(L_{11} / \rho_l^l)\nabla p_l - L_{12}\nabla c \qquad (2.107)$$

$$\mathbf{J}_c = -(L_{21} / \rho_l^l)\nabla p_l - L_{22}\nabla c$$

In equation (2.107), Darcy's law for water transport and the diffusion law for chemical transport have been extended to include additional driving forces from their couplings (e.g., water flux driven by chemical diffusion process $L_{12}\nabla c$).

TABLE 2.1
Fluids and thermal coupling

	Gradient		
Flow	**Hydro *(H)***	**Thermo *(T)***	**Chemo *(C)***
Fluid	**Darcy's law** (hydraulic flow)	Thermo osmosis	Chemo osmosis
Heat	Heat convection	**Fourier's law** (thermal conduction)	Dufour effect
Chemical (ion)	Ionic current (streaming current)	Soret effect	**Fick's law** (diffusion)

Modified from Keijzer (2000).

The phenomenon of interactions between multiple fluids/fluxes presented in equation (2.105) in a porous medium system is summarized in Table 2.1 (Keijzer, 2000), excluding the electric flow (Keijzer and Loch, 2001). Chemical osmosis and thermo osmosis have been introduced in Chapter 1. The Soret effect describes a chemical flux generated by a temperature gradient (Soret, 1880). For example, if a temperature gradient is applied to two ends of a tube containing a salt solution, the concentration (of salt) does not remain uniform, but becomes higher near the cold end than near the hot end. In contrast, the Dufour effect is the reciprocal phenomenon to the Soret effect, representing the energy flux caused by a chemical concentration gradient (Dufour, 1873). Ionic current (also named as streaming current) is a phenomenon that a chemical flow is driven by the gradient of hydrostatic pressure, which is the reciprocal phenomenon of chemical osmosis (Cheryan, 1986).

2.7 CONCLUSION

This chapter has introduced and extended key concepts of nonequilibrium thermodynamics for application within Mixture-Coupling Theory. Nonequilibrium thermodynamics offers a powerful framework to bridge the gap between geomechanics and geochemistry, particularly through the concepts of free energy and entropy. The Gibbs-Duhem equation plays a crucial role by integrating the microscopic chemical potential with macroscopic properties, such as pressure, thereby providing strong support for multiscale modeling processes. Furthermore,

phenomenological equations are employed to establish relationships between multiphase flows, which form the foundation for analyzing complex physical-chemical coupled processes within porous media.

As the subsequent chapters (Chapters 3–7) unfold, they will demonstrate how the Mixture-Coupling Theory framework can be established, starting from simple hydro-mechanical (HM) coupled models and progressing to more complex thermo-hydro-mechanical-chemical (THMC) models. This book addresses the long-standing challenges in capturing molecular-scale coupling (e.g., swelling induced by water molecules) and nanoscale phenomena (e.g., osmosis), which have proven difficult for traditional mechanical and mixture theory approaches. By solving these challenges, the book offers a novel and comprehensive approach to modeling coupled processes in geotechnical and geoenvironmental engineering.

NOTES

1 In equation (2.4), $p_i V$ is the amount of energy required to make room for the system by displacing its environment and establishing its volume (V) and pressure p_i. The energy density of $p_i V$ can be obtained as $\frac{p_i V}{V} = p_i$.

2 Note: Molar chemical potential is described as $\mu_n^i = g_i\left(p_\alpha, T\right) + RT\left(\ln a_i\right)$.

To link with mass density, the total chemical potential in V_α of a REV may be described as

$$\frac{n_i \mu_n^i}{V_\alpha} = \frac{\overbrace{n_i M_i \mu_n^i}^{m_i}}{M_i V_\alpha} = \frac{\overbrace{m_i \mu_n^i}^{\because \rho_\alpha^i = m_i / V_\alpha}}{M_i V_\alpha} = \frac{\rho_\alpha^i \mu_n^i}{M_i} = \rho_\alpha^i \frac{\overbrace{\mu_n^i}^{\text{simplified as } \mu_i}}{M_i} = \rho_\alpha^i \mu_i$$

It is more convenient to use $\mu_i = \frac{\mu_n^i}{M_i}$. ($\mu_{i(c)}$ accordingly) in this book corresponding with mass densites (e.g. ρ_ε^i), rather than using μ_n^i.

3

$$\sum_{i=1}^{N_c} d\frac{n_i \mu_n^i}{V_\alpha} = \sum_{i=1}^{N_c} d\frac{\overbrace{n_i M_i \mu_n^i}^{m_i}}{M_i V_\alpha} = \sum_{i=1}^{N_c} d\frac{\overbrace{m_i \mu_n^i}^{\because \rho_\alpha^i = m_i / V_\alpha}}{M_i V_\alpha} = \sum_{i=1}^{N_c} d\frac{\rho_\alpha^i \mu_n^i}{M_i} = \sum_{i=1}^{N_c} \rho_\alpha^i d$$

$$\left(\frac{\overbrace{\mu_n^i}^{\text{simplified as } \mu_i}}{M_i}\right) = dp_\alpha - \frac{\eta_\alpha}{V_\alpha} dT$$

4 The divergence theorem applied for the *k*th chemical leads to: .

$$\int_\Gamma \rho_k (\mathbf{v}_k - \mathbf{v}_s)\cdot \mathbf{n}\, \mathrm{d}\Gamma = \int_\Gamma \mathbf{I}_k \cdot \mathbf{n}\, d\Gamma = \int_V \nabla \cdot \mathbf{I}_k \, dV$$

5 Summing over all the liquid components for equation (2.48) leads to

$$(\upsilon \mathrm{S}_i \rho_l^l \sum_k c_k) + \mathbf{J}\nabla\cdot(\rho_l^l \sum_k c_k \mathbf{u}) + \mathbf{J}\nabla\cdot\sum_k \mathbf{J}_k = 0$$

and introducing equation $\sum_k c_k = 1$ and $\sum_k \mathbf{J}_k = 0$ results in equation (2.49).

$$(J\eta_s + J\eta_l)^{\cdot} + J\nabla\cdot\mathbf{I}_\eta = 0$$

$$(J\phi_s\eta_s^s + J\phi S_l\eta_l^l)^{\cdot} + J\nabla\cdot\mathbf{I}_\eta = 0$$

6

$$(J\overbrace{(1-\phi)}^{\because\ \phi_s=1-\phi}\eta_s^s + \overbrace{\upsilon}^{\because\ \upsilon=J\varphi} S_l\eta_l^l)^{\cdot} + J\nabla\cdot\mathbf{I}_\eta = 0$$

$$(J-\upsilon)\eta_s^s + \upsilon S_l\eta_l^l)^{\cdot} = -J\nabla\cdot\mathbf{I}_\eta$$

$$\begin{aligned}
&\frac{d}{dt}\int_{V(t)} (\varepsilon - T\eta)\, dV \\
7\quad &= \int_\Gamma (\boldsymbol{\sigma}\mathbf{v_s} - \mathbf{I}_q)\cdot\mathbf{n}\, d\Gamma - \int_\Gamma \left(\sum h_i\mathbf{I}_i\right)\cdot\mathbf{n}\, d\Gamma + \int_\Gamma \mathbf{I}_q\cdot\mathbf{n}\, d\Gamma \\
&+ \int_\Gamma T\left(\sum \eta_i\mathbf{I}_i\right)\cdot\mathbf{n} d\Gamma - \int_V T\gamma dV \\
&= \int_\Gamma (\boldsymbol{\sigma}\mathbf{v_s})\cdot\mathbf{n} d\Gamma - \int_\Gamma \left(\sum (h_i - T\eta_i)\mathbf{I}_i\right)\cdot\mathbf{n} d\Gamma - \int_V T\gamma dV
\end{aligned}$$

$$\begin{aligned}
8\quad \gamma &= \mathbf{I}_q\cdot\nabla\left(\frac{1}{T}\right) + \sum_{i=1}^{N_c}\mathbf{I}_i\cdot\nabla\left(\frac{-\mu_i}{T}\right) = \mathbf{I}_q\cdot\left(-\frac{1}{T^2}\nabla T\right) + \sum_{i=1}^{N_c}\mathbf{I}_i\cdot \\
&\quad \left(\frac{-1}{T}\nabla\mu_i + \frac{\mu_i}{T^2}\nabla T\right) \\
&= \mathbf{I}_q\cdot\left(-\frac{1}{T^2}\nabla T\right) + \sum_{i=1}^{N_c}\mathbf{I}_i\cdot\left(\frac{\mu_i}{T^2}\nabla T\right) + \sum_{i=1}^{N_c}\mathbf{I}_i\cdot\left(\frac{-1}{T}\nabla\mu_i\right) \\
&= \mathbf{I}_q\cdot\left(\frac{1}{T^2}\nabla(-T)\right) - \sum_{i=1}^{N_c}\mathbf{I}_i\cdot\left(\frac{\mu_i}{T^2}\nabla(-T)\right) + \sum_{i=1}^{N_c}\mathbf{I}_i\cdot\left(\frac{1}{T}\nabla(-\mu_i)\right) \\
&= \frac{\mathbf{I}_q - \sum_{i=1}^{N_c}\mu_i\mathbf{I}_i}{T^2}\cdot\nabla(-\mathrm{T}) + \sum_{i=1}^{N_c}\frac{\mathbf{I}_i}{T}\cdot\nabla(-\mu_i)
\end{aligned}$$

9 $$0 \le \gamma = \frac{\mathbf{I}'_q}{T^2} \cdot \nabla(-T) + \sum_{i=1}^{N_c} \frac{\mathbf{I}_i}{T} \cdot \nabla(-\mu_{i(c)}) = \frac{\mathbf{I}'_q}{T^2} \cdot \nabla(-T) - \sum_{i=1}^{N_c} \frac{\mathbf{I}_i}{T} \cdot \left(\nabla(\mu_i) + \eta_i \nabla(T)\right)$$

$$= \frac{\mathbf{I}'_q}{T^2} \cdot \nabla(-T) - \sum_{i=1}^{N_c} \frac{\mathbf{I}_i}{T} \cdot (\eta_i \nabla(T)) - \sum_{i=1}^{N_c} \frac{\mathbf{I}_i}{T} \cdot \left(\nabla(\mu_i)\right) = -\frac{\mathbf{I}'_q + \sum_{i=1}^{N_c} \cdot (\mathbf{I}_i T \eta_i)}{T^2} \nabla(T) - \sum_{i=1}^{N_c} \frac{\mathbf{I}_i}{T} \cdot \left(\nabla(\mu_i)\right)$$

Since, from equation (2.64), $\frac{\mathbf{I}'_q + \sum_{i=1}^{N_c} \cdot (\mathbf{I}_i T \eta_i)}{T^2} = \frac{\mathbf{I}_q - \sum_{i=1}^{N_c} \cdot \left(\mathbf{I}_i(\mu_i)\right)}{T^2} = \frac{\mathbf{I}_\eta}{T}$, it leads to $0 \le \gamma = \frac{\mathbf{I}_q - \sum_{i=1}^{N_c} \mu_i \mathbf{I}_i}{T^2} \cdot \nabla(-T) + \sum_{i=1}^{N_c} \frac{\mathbf{I}_i}{T} \cdot \nabla(-T) + \sum_{i=1}^{N_c} \frac{\mathbf{I}_i}{T} \cdot \nabla(-\mu_i)$

10 The change of the extent of reaction of the *i*th chemical can be defined as $d\xi_i = \frac{dn_i}{N_i^s}$, in which dn_i is the change of the moles of the *i*th reactant (dn_i), and N_i^s is the Stoichiometric coefficient of the *i*th chemical.

11 Mathematical proof for equation (2.102) = equation (2.104): substituting equation (1.16) $\left(\mathbf{u} = S_l \phi (\mathbf{v}_l - \mathbf{v}_s)\right)$ and equation (2.25) $\left(\sum_k \rho_l^k \nabla \mu_k = \nabla p_\alpha\right)$ into equation (2.104) leads to

$$0 \le T\gamma = -S_l \phi (\mathbf{v}_l - \mathbf{v}_s) \cdot \sum_k \rho_l^k \nabla \mu_k - \sum_k \mathbf{J}_k \cdot \nabla \mu_k$$

$$\because S_l \phi \rho_l^k = \rho_k \therefore 0 \le T\gamma = -(\mathbf{v}_l - \mathbf{v}_s) \cdot \sum_k \rho_k \nabla \mu_k - \sum_k \mathbf{J}_k \cdot \nabla \mu_k$$

$$\because \mathbf{J}_k = \mathbf{I}_k - \rho_k (\mathbf{v}_l - \mathbf{v}_s), \quad \therefore 0 \le T\gamma = -\sum_k \mathbf{I}_k \cdot \nabla \mu_k \tag{2.102}$$

REFERENCES

Chen, X. & Hicks, M. A. (2013) Unsaturated hydro-mechanical-chemo coupled constitutive model with consideration of osmotic flow. *Computers and Geotechnics* **54**: 94–103.

Cheryan, M. (1986) Ultrafiltration handbook. Lancaster, Pennsylvania, Technomic Publishing Co. Inc.

Darken, L. (1950) Application of the Gibbs-Duhem equation to ternary and multicomponent systems. *Journal of the American Chemical Society* **72(7)**: 2909–2914.

Davidson, A. & Tinkham, M. (1976) Phenomenological equations for the electrical conductivity of microscopically inhomogeneous materials. *Physical Review B* **13(8)**: 3261.

Dufour, L. (1873) Ueber die Diffusion der Gase durch poröse Wände und die sie begleitenden Temperaturveränderungen. *Annalen der Physik* **224(3)**: 490–492.

Goldstein, H. (1980) Classical mechanics. New York, Addison-Wesley Publishing Company.

Groot, S. R. D. & Mazur, P. (1962) Non-equilibrium thermodynamics. New York, Interscience Publishers.

Haase, R. (1969) *Thermodynamics of irreversible processes.* Reading, MA, Addison-Wesley.

Heidug, W. K. & Wong, S. W. (1996) Hydration swelling of water-absorbing rocks: a constitutive model. *International Journal for Numerical and Analytical Methods in Geomechanics* **20**: 403–430.

Helmholtz, H. (1882) On the thermodynamics of chemical processes. *Physical Memoirs Selected and Translated from Foreign Sources* **1**: 43–97.

Israelachvili, J. N. (1991) *Intermolecular and surface forces.* London, Academic Press.

Katachalsky, A. & Curran, P. F. (1965) Nonequilibrium thermodynamics in biophysics. Cambridge, MA, Harvard University Press.

Keijzer, T. J. & Loch, J. (2001) Chemical osmosis in compacted dredging sludge. *Soil Science Society of America Journal* **65(4)**: 1045–1055.

Keijzer, T. J. S. (2000) *Chemical osmosis in natural clayey materials.* Doctoral dissertation, Utrecht University.

Kondepudi, D. (2008) *Introduction to modern thermodynamics.* Chichester, England, Wiley.

Kondepudi, D. & Prigogine, I. (2014) *Modern thermodynamics: from heat engines to dissipative structures.* Chichester, West Sussex, John Wiley & Sons.

Mandl, F. (1988) *Statistical physics.* 2nd edn. New York, Wiley.

Mcmullin, E. (1968) What do physical models tell us? In *Studies in logic and the foundations of mathematics.* (Beklemishev, L. (eds)). Amsterdam, Elsevier, vol. 52, pp. 385–396.

Mishra, D. (2012) *Engineering Thermodynamics.* Delhi, Cengage Learning India Private Limited.

Onsager, L. (1931) Reciprocal relations in irreversible processes. I. Physical Review **37(4)**: 405–426.

Pfeffer, W. (1986) The divergence theorem. *Transactions of the American Mathematical Society 2***95(2)**: 665–685.

Reynolds, O., Brightmore, A. W. & Moorby, W. H. (1903) The sub-mechanics of the universe. Cambridge, University Press.

Sacchetti, M. (2001) The general form of the Gibbs-Duhem equation for multiphase/multicomponent systems and its application to solid-state activity measurements. *Journal of Chemical Education* **78(2)**: 260–263.

Sandler, S. I. (2017) *Chemical, biochemical, and engineering thermodynamics.* Hoboken, New Jersey, John Wiley & Sons.

Soret, C. (1880) *Sur l'etat d'équilibre que prend au point de vue de sa concentration une dissolution saline primitivement homogène dont deux parties sont portées a des températures différentes: Deuxieme note. C. R. Arch. Sci. Phys. Natur., Genève,* 2: 48–61.

Tillner-Roth, R. & Friend, D. G. (1998) A Helmholtz free energy formulation of the thermodynamic properties of the mixture {water+ ammonia}. *Journal of Physical and Chemical Reference Data* **27(1)**: 63–96.

Truesdell, C. & Toupin, R. (1960) The classical field theories. In Handbuch der Physik. (Flügge, S. (ed)) Berlin, Springer-Verlag, pp. 226–793.

Tyrrell, H. J. V. & Harris, K. (2013) *Diffusion in liquids: a theoretical and experimental study.* Kent, Butterworth-Heinemann.

Ván, P. (2020) *Nonequilibrium thermodynamics: emergent and fundamental*. *Philosophical Transactions of the Royal Society A*, 378(2170), 20200066.

Wolt, J. D. (1994) *Soil solution chemistry: applications to environmental science and agriculture.* New York, John Wiley and Sons.

3 Hydro-mechanical coupled model for molecule-induced swelling geomaterials

3.1 INTRODUCTION AND ENGINEERING BACKGROUND

Swelling in geomaterials, particularly in soils and rocks, is a significant challenge in geotechnical engineering. This phenomenon occurs when water molecules interact with soil or rock particles, causing them to expand. Swelling is often induced by molecular forces and is especially prevalent in materials such as clays or clay-rich shales, including montmorillonite. The swelling of soils and rocks can have serious implications for infrastructure, affecting the stability and performance of structures such as tunnels, foundations, and highways. For example, in rail and highway tunnels, swelling can lead to changes in volume and pressure, creating substantial risks for the stability of these structures.

Despite its importance, swelling in geomaterials remains difficult to model, as traditional geomechanics approaches typically do not account for molecule-induced forces. This is because classical consolidation theories focus primarily on macroscale physical processes, such as soil and rock deformation, without addressing the underlying molecular interactions. As a result, there is a significant gap in accurately modeling the swelling behavior of materials under different environmental conditions.

This chapter aims to provide a comprehensive approach to developing a constitutive model for swelling in geomaterials, incorporating molecular forces through Mixture-Coupling Theory. By including these molecular-level interactions, the chapter presents a more complete framework for understanding and predicting swelling behavior in soils and rocks. Additionally, it demonstrates how Biot's consolidation

DOI: 10.1201/9780429324925-3

model (Biot, 1941), which addresses hydro-mechanical coupling, can be viewed as a simplified case within this broader theoretical framework (Chen and Hicks, 2010).

3.2 ENERGY IN THE MIXTURE

Swelling in geomatrials is influenced not only by macroscopic forces but also by molecular interactions that contribute to the deformation. These molecular forces lead to volume changes that are critical for understanding the behavior of geotechnical materials. To analyze this behavior, it is essential to study the material at a local scale, which can be represented by a representative elementary volume (REV).

In a REV, the boundary (Γ) is attached to the solid phase, meaning that the solid phase does not move across the domain boundary; only the fluid phase moves. In the case of a constant temperature field, and in the absence of chemical reactions, it is useful to consider the Helmholtz free energy density, which is defined as $\psi = \varepsilon - T\eta$, where ε is the internal energy density, T is the temperature, η is the entropy density, which is defined in equation (2.1).

Thus, the balance equation for the Helmholtz free energy density, based on the principles outlined in equation (2.84), can be expressed as follows:

$$\frac{d}{dt}\int_V \psi \, dV = \int_\Gamma \boldsymbol{\sigma}\mathbf{v}_\mathbf{s} \cdot \mathbf{n} d\Gamma - \int_\Gamma \mu_w \mathbf{I}_w \cdot \mathbf{n} \, d\Gamma - T\int_V \gamma \, dV \tag{3.1}$$

where $\int_\Gamma \mu_w \mathbf{I}_w \cdot \mathbf{n} \, d\Gamma$ is the water energy flowing in or out, in which the chemical potential of water μ_w is defined as $\mu_w = h_w - T\eta_w$; $\int_\Gamma \boldsymbol{\sigma}\mathbf{v}_s \cdot \mathbf{n} \, d\Gamma$ is the deformation energy; and $T\int_V \gamma \, dV$ is the energy consumed by the dissipative process within the REV.

The derivative version of the balance equation for free energy density can be expressed as

$$\dot{\psi} + \psi\nabla \cdot \mathbf{v}_s - \nabla \cdot (\boldsymbol{\sigma}\mathbf{v}_s) + \nabla \cdot (\mu_w \mathbf{I}_w) = -T\gamma \leq 0 \tag{3.2}$$

3.3 DISSIPATIVE PROCESS

In a porous medium, water moving through the solid matrix generates dissipation, which leads to a reduction in the flow rate. This dissipation arises from various mechanisms that resist the movement of

water, particularly friction between the fluid and the solid skeleton. To model this dissipation, the primary mechanism is assumed to be friction generated at the solid-water boundary as the fluid moves through the porous matrix. This assumption allows for the derivation of a macroscopic expression for the dissipation caused by the frictional resistance at the interface.

By applying the principles of nonequilibrium thermodynamics, as discussed in equation (2.102) (Groot and Mazur, 1962), the dissipation generated by the frictional resistance can be represented by

$$0 \le T\gamma = -\mathbf{I}_w \cdot \nabla \mu_w \tag{3.3}$$

In this equation, $\mathbf{I}_w$ is the water flux, and the driving force is the gradient of the chemical potential of water. However, in the context of hydrogeology or geomechanics, the primary driving force for water flow is the pressure gradient. Therefore, it is essential to establish the relationship between the chemical potential and the pressure gradient.

By using the Gibbs-Duhem equation for a fluid at constant temperature as stated in equation (2.22), the relationship between the water pressure and the chemical potential is derived:

$$\nabla p_w = \rho_l^w \nabla \mu_w \tag{3.4}$$

where p_w is the pore water pressure. Also, the Darcy velocity may be defined by

$$\mathbf{u} = \phi_w (\mathbf{v}_w - \mathbf{v}_s) \tag{3.5}$$

Hence, by using equations (1.18), (3.4) and (3.5), the dissipation function of (3.3) can be rewritten as:

$$0 \le T\gamma = -\mathbf{u} \cdot \nabla p_w \tag{3.6}^{1}$$

The relationship between the flow $\rho_l^w \mathbf{u}$ and the driving force ∇p_w is obtained using phenomenological equations (Katachalsky and Curran, 1965) which express the linear dependence of flow on the corresponding force. This leads to

$$\begin{aligned} \rho_l^w \mathbf{u} &= -(L_{11} / \rho_l^w) \nabla p_w \\ \text{or} \quad \mathbf{u} &= -(L_{11} / (\rho_l^w)^2) \nabla p_w \end{aligned} \tag{3.7}$$

where L_{11} denotes a phenomenological coefficient. The coefficient $(L_{11}/(\rho_l^w)^2)$ can be determined through the experimental study. As Darcy's law is defined as

$$\mathbf{u} = -\frac{k}{v}\nabla p_w \tag{3.8}$$

where v is the fluid viscosity and k is the permeability. Substituting equation (3.8) into equation (3.7). This leads to $(L_{11}/(\rho_l^w)^2) = \frac{k}{v}$.

3.4 CONSTITUTIVE RELATIONS

The formulation of constitutive equations for stress and strain response in porous materials is a critical aspect of modeling their mechanical behavior under various conditions. These relations are derived by considering the principles of nonequilibrium thermodynamics, which govern energy dissipation and the flow of fluids within the material. In particular, the evolution of free energy density within the mixture plays a central role in these equations, linking the material's mechanical properties, fluid flow, and thermodynamic state.

3.4.1 Free energy density evolution path of the mixture

This section explores the evolution of free energy density within a mixture, focusing on the changes that occur as the material deforms and the phases interact. The concept of free energy density is central to understanding the thermodynamic behavior of porous materials, especially in the context of coupled mechanical and fluid processes. To model these changes, two key configurations are considered: the current configuration and the reference configuration.

The current configuration refers to the state of the mixture after it has undergone deformation, where the material and fluid phases are in their present spatial arrangement. The reference configuration, on the other hand, is the initial, undeformed state of the material, typically used as a baseline for measuring changes in stress, strain, and energy.

The path of free energy density evolution is analyzed by relating the free energy density in the current configuration to its counterpart in the reference configuration. This transition is crucial for understanding how energy is stored, dissipated, and transferred within the material system during deformation, fluid flow, and phase changes. The following equations (3.9)–(3.76) outline this process, beginning with

the assumptions for mechanical equilibrium and moving through the mathematical derivations for both configurations.

3.4.1.1 Current configuration

To model this scenario, it is assumed that the geomaterial maintains **mechanical equilibrium**, meaning that the material is in a stable state where all forces are balanced. Under the assumption of **no volume forces** acting on the system (such as gravitational or electromagnetic forces), the material is considered to be in equilibrium, which leads to the following expression:

$$\nabla \cdot \boldsymbol{\sigma} + \mathbf{b} = 0 \text{ or } \nabla \cdot \boldsymbol{\sigma} = \mathbf{0} \left(\frac{\partial \sigma_{ij}}{\partial x_j} = 0 \right) \tag{3.9}$$

where $\mathbf{b}$ is the body force. For simplicity in this discussion, the body force is ignored ($\mathbf{b} = 0$), as its inclusion complicates the analysis. However, readers are encouraged to consider the impact of body forces in their own work and derive the corresponding equations if needed.

Since $\nabla \cdot (\boldsymbol{\sigma} \mathbf{v}_s)$ in equation (3.2) for balance of free energy can be derived using tensor product rules as (Mase et al., 2009)

$$\nabla \cdot (\boldsymbol{\sigma} \mathbf{v}_s) = \text{tr}(\boldsymbol{\sigma}^{\mathrm{T}} \nabla \mathbf{v}_s) + \mathbf{v}_s \cdot (\nabla \cdot \boldsymbol{\sigma}) \tag{3.10}$$

where tr() represents the trace of the matrix; by using $\nabla \cdot \boldsymbol{\sigma} = 0$ for mechanical equilibrium assumption from equation (3.9), it leads to

$$\nabla \cdot (\boldsymbol{\sigma} \mathbf{v}_s) = \text{tr}(\boldsymbol{\sigma}^{\mathrm{T}} \nabla \mathbf{v}_s) \text{ (Appendix 1)} \tag{3.11}$$

By substituting equation (3.11) into equation (3.2) and using equation (3.3) for entropy production, the resulting balance equation for ψ is derived as

$$\dot{\psi} + \psi \nabla \cdot \mathbf{v}_s - \text{tr}(\boldsymbol{\sigma}^{\mathrm{T}} \nabla \mathbf{v}_s) + \mu_w \nabla \cdot \mathbf{I}_w = 0 \tag{3.12}^2$$

Equation (3.12) describes how the Helmholtz free energy density evolves within the current configuration of the material system, taking into account both mechanical deformation and fluid flow. This equation forms the foundation for the thermodynamic modeling of coupled processes in the material.

Next, the free energy density at the reference configuration—the initial, undeformed state of the material—can be determined by

applying classical continuum mechanics. The free energy at this initial configuration can be derived from the established expressions in equation (1.103), and subsequent mathematical transformations provide the necessary framework to compare the changes in free energy from the reference state to the current configuration.

3.4.1.2 Reference configuration

In the **reference configuration**, the material is in its undeformed state, serving as the baseline for evaluating the changes in energy and strain during deformation. To derive the balance equation for the Helmholtz free energy density in the reference configuration, equation (3.12) is multiplied by the **determinant of the deformation gradients**, denoted as J. This step accounts for the geometric changes in the material as it deforms. The equation then becomes

$$J\dot{\psi} + J\psi\nabla\cdot\mathbf{v}_s - J\mathrm{tr}(\boldsymbol{\sigma}^{\mathrm{T}}\nabla\mathbf{v}_s) + J\mu_w\nabla\cdot\mathbf{I}_w = 0 \tag{3.13}$$

This multiplication transforms the equation to reflect the volumetric changes from the current configuration to the reference configuration.

Next, to account for the evolution of the system in time, equation (1.103), $J\nabla\cdot\mathbf{v}_s = \dot{J}$, which relates to the time derivative of a quantity in the reference configuration, is introduced into equation (3.13). This provides the time derivative of the free energy density for the reference configuration:

$$\dot{\Psi} = (J\psi)^{\cdot} = J\dot{\psi} + J\psi\nabla\cdot\mathbf{v}_s \tag{3.14}$$

This step bridges the temporal changes in the system from the current configuration back to the reference configuration, ensuring the energy is evaluated with respect to the original, undeformed state of the material.

From classical continuum mechanics theory (Haupt, 2013), the current configuration's deformation is related to stress and strain through the second Piola-Kirchhoff stress ($\mathbf{T}$) and the Green strain ($\mathbf{E}$). The second Piola-Kirchhoff stress tensor is commonly used to express the stress in a reference configuration, while the Green strain tensor describes the strain based on the current configuration. Therefore, the term $J\mathrm{tr}(\boldsymbol{\sigma}^{\mathrm{T}}\nabla\mathbf{v}_s)$ in equation (3.13) can be linked with the second Piola-Kirchhoff stress ($\mathbf{T}$) and the Green strain ($\mathbf{E}$) through

$$J\mathrm{tr}(\boldsymbol{\sigma}^{\mathrm{T}}\nabla\mathbf{v}_s) = tr(\mathbf{T}\dot{\mathbf{E}}) \tag{3.15}$$

Using equations (3.13), (3.14), and (3.15), the balance of the Helmholtz free energy density at the reference configuration is derived. This final equation captures the evolution of free energy from the undeformed (reference) state, taking into account the energy dissipation due to deformation and the flow of materials:

$$\dot{\Psi} = tr(\mathbf{T}\dot{\mathbf{E}}) + \mu_w \dot{\rho}_{w,ref} \tag{3.16}^3$$

where

$$\Psi = J\psi,\ \rho_{w,ref} = J\rho_w = J\phi\rho_l^w \tag{3.17}$$

where $\rho_{w,ref}$ represents the mass of water per unit reference volume, a term necessary for accurately quantifying the energy contributions from the water phase in the system. These equations form the foundation for understanding how energy is conserved and transformed in the system as it deforms and evolves over time.

3.4.2 Helmholtz free energy density of the pore water and wetted solid matrix

In saturated water-absorbing geomaterials, particularly those rich in clay content, fluid resides within the spaces between individual clay platelets (around 1 Å or 0.1 nm) or within the broader pore space. Water within these pores does not experience the direct influence of intermolecular forces due to the relatively large dimensions of the pore spaces compared to the distances over which such forces typically operate (Madsen and Muller-von Moos, 1989). Therefore, thermodynamic relations can be applied to treat the water in the pores as a bulk fluid. This treatment allows the application of classical thermodynamics to model the behavior of the water phase within these materials.

3.4.2.1 Current configuration

The Helmholtz free energy density for the pore water under saturated conditions, based on classical thermodynamics, can be expressed as

$$\psi_{pore} = -p_w + \mu_w \rho_l^{pore} \tag{3.18}$$

where ρ_l^{pore} is the mass partial density of the fluid in the pore. Since some of the pore water is absorbed into the clay platelets, it leads to $\rho_l^{pore} < \rho_l^w$. The time derivative of equation (3.18) leads to

$$\dot{\psi}_{pore} = -\dot{p}_w + \dot{\mu}_w \rho_l^{pore} + \mu_w \dot{\rho}_l^{pore} \tag{3.19}$$

Also, according to the Gibbs-Duhem equation,

$$\dot{p}_w = \rho_l^{pore} \dot{\mu}_w \tag{3.20}$$

Hence, introducing equation (3.20) into equation (3.19) leads to

$$\dot{\psi}_{pore} = \mu_w \dot{\rho}_l^{pore} \tag{3.21}$$

3.4.2.2 Reference configuration

The free energy density of the wetted solid matrix (i.e, matrix with absorbed water but excluding pore water) in the reference configuration is expressed as $\Psi - J\phi\psi_{pore}$, and its time derivative can be defined, by using equations (3.16), (3.18) and (3.20), as

$$(\Psi - J\phi\psi_{pore})^{\cdot} = tr(\mathbf{T}\dot{\mathbf{E}}) + \mu_w \dot{\rho}_{bound,ref} + p_w \dot{\upsilon} \tag{3.22}[4]$$

where $\upsilon = J\phi$ is the pore volume per unit reference volume and $\rho_{bound,ref} = \rho_{w,ref} - J\phi\rho_l^{pore}$ is the reference mass density of the bound water.

Equation (3.22) establishes a time-dependent relationship between the Helmholtz free energy density in the reference configuration, the strain ($\dot{\mathbf{E}}$), the mass density of bound molecular water ($\dot{\rho}_{bound,ref}$), and the porosity of the material ($\dot{\upsilon}$). This relationship is fundamental for building constitutive models in geotechnical engineering, as it couples the mechanical response (through strain) with the chemical and physical behavior of the pore water.

However, measuring the mass density of bound molecular water is a challenging task in experiments or engineering applications. Therefore, rather than directly using equation (3.22), it is often more practical to incorporate the **solid matrix deformation energy** (such as elastic energy) into the model. This approach simplifies the modeling process, making it more accessible for practical applications.

3.4.3 Constitutive structure

To derive the constitutive relations for the solid phase in porous media, the solid matrix deformation potential density, W, is essential. This potential is often referred to as the *dual potential* (Heidug and Wong, 1996). W represents the free energy density of the solid

phase, encapsulating the energy contributions from all phases in the porous media. The form of W is influenced by the coupling mechanisms present within the system. Specifically, this chapter focuses on the coupling between the pore fluid and the bounded fluid within the solid phase.

In the context of saturated swelling geomaterials, the solid matrix deformation potential W is obtained by considering the energy contributions from various components. It can be expressed as the energy density of the wetted solid matrix, from which the energy density of the water molecules in the clay platelets and the energy resulting from the pore water pressure (which, in a saturated condition, equals the pore pressure) applied to the surface of the solid matrix are subtracted. This formulation is described in the work of Chen and Hicks (2010).

$$W = (\Psi - J\phi\psi_{pore}) - p_w \upsilon - \mu_w \rho_{bound,ref} \tag{3.23}$$

The term "dual potential" refers to the fact that W accounts for both the mechanical (elastic) energy stored in the solid matrix and the energy contributions from the pore and bounded fluids. This dual nature of the potential is critical in establishing a comprehensive constitutive model, as it allows for the incorporation of interactions between the solid matrix and the fluids, such as swelling, compaction, and pressure-driven deformations.

By including the energy contributions from the pore fluids, bounded fluids, and solid matrix, the solid deformation potential W captures the full range of energy changes and dissipative processes that occur in porous media. This enables the development of more accurate and robust constitutive models that can predict the behavior of geomaterials under a variety of loading and environmental conditions.

Substituting equation (3.22) into the time derivative of equation (3.23) results in the deformation power density function (that is the rate at which potential energy density is transferred), as

$$\dot{W} = tr(\mathbf{T}\dot{\mathbf{E}}) - \dot{p}_w \upsilon - \dot{\mu}_w \rho_{bound,ref} \tag{3.24}$$

which indicates W is a function of $\mathbf{E}$, p_w, and μ_w, described as $\dot{W}(\mathbf{E}, p_w, \mu_w)$. Equation (3.24) establishes a time-dependent relationship between the dual potential (W), the Green strain ($\mathbf{E}$), the pore pressure ($p_w = p_{pore}$ under the saturated condition) and the chemical potential of water (μ_w).

From equation (3.22) to (3.24), the variables υ and $\rho_{bound,ref}$ are replaced by p_w and μ_w, respectively. This substitution is based on the Legendre transformation,[5] which is an involution transformation commonly used in classical mechanics and thermodynamics (Arnol'd, 2013). In the context of porous media and coupled fluid-solid systems, this transformation enables a shift from the description of the system in terms of variables like volume and chemical mass density to a description in terms of pressure and chemical potential. This shift allows for the formulation of more practical models that describe the behaviors of the system under pressure-driven processes, such as fluid flow and deformation in porous materials, thereby providing a more convenient mathematical framework for solving the system's equations.

If the tensors **T** and **E** are written in a Cartesian coordinate system as T_{ij} / T_{kl} and E_{ij} / E_{kl} ($i,j=1,2,3$; $k,l=1,2,3$), using the total derivative and chain rule of partial differentiation, equation (3.24) must have

$$T_{ij}=\left(\frac{\partial W}{\partial E_{ij}}\right)_{p_w,\mu_w},\ \upsilon=-\left(\frac{\partial W}{\partial p_w}\right)_{E_{ij},\mu_w},\ \rho_{bound,ref}=-\left(\frac{\partial W}{\partial \mu_w}\right)_{E_{ij},p_w} \quad (3.25)^{6}$$

Equation (3.25) may be differentiated with respect to time to give

$$\dot{T}_{ij}=\frac{\partial T_{ij}}{\partial t}=\frac{\partial}{\partial t}\left(\frac{\partial W}{\partial E_{ij}}\right)_{p_w,\mu_w}=\left(\frac{\partial}{\partial E_{ij}}\left(\frac{\partial W}{\partial t}\right)\right)_{p_w,\mu_w}=\left(\frac{\partial \dot{W}}{\partial E_{ij}}\right)_{p_w,\mu_w}$$

$$\dot{\upsilon}=\frac{\partial \upsilon}{\partial t}=-\frac{\partial}{\partial t}\left(\frac{\partial W}{\partial p_w}\right)_{E_{ij},\mu_w}=-\left(\frac{\partial}{\partial p_w}\left(\frac{\partial W}{\partial t}\right)\right)_{E_{ij},\mu_w}=-\left(\frac{\partial \dot{W}}{\partial p_w}\right)_{E_{ij},\mu_w} \quad (3.26)$$

$$\dot{\rho}_{bound,ref}=\frac{\partial \rho_{bound,ref}}{\partial t}=-\frac{\partial}{\partial t}\left(\frac{\partial W}{\partial \mu_w}\right)_{E_{ij},p_w}=-\left(\frac{\partial}{\partial \mu_w}\left(\frac{\partial W}{\partial t}\right)\right)_{E_{ij},p_w}$$
$$=-\left(\frac{\partial \dot{W}}{\partial \mu_w}\right)_{E_{ij},p_w}$$

Since equation (3.24) for $\dot{W}(\mathbf{E},p_w,\mu_w)$ can be rewritten using tensor components T_{ij} and E_{ij} as

$$\dot{W}(\mathbf{E},p_w,\mu_w)=T_{ij}\dot{E}_{ij}-\upsilon\dot{p}_w-\rho_{bound,ref}\dot{\mu}_w \quad (3.27)$$

and by substituting equation (3.27) for $\dot{W}$ into the equation group (3.26), the fundamental constitutive equations for the evolution of stress, pore

volume fraction, and mass density of the bound water can be expressed as the group equations:

$$\frac{\partial T_{ij}}{\partial t}=\left(\frac{\partial \dot{W}}{\partial E_{ij}}\right)_{p_w,\mu_w}=\left(\frac{\partial T_{ij}}{\partial E_{kl}}\right)_{p_w,\mu_w}\dot{E}_{kl}-\left(\frac{\partial \upsilon}{\partial E_{ij}}\right)_{p_w,\mu_w}\dot{p}_w-\left(\frac{\partial \rho_{bound,ref}}{\partial E_{ij}}\right)_{p_w,\mu_w}\dot{\mu}_w \tag{3.28}^{7}$$

$$\frac{\partial \upsilon}{\partial t}=-\left(\frac{\partial \dot{W}}{\partial p_w}\right)_{E_{ij},\mu_w}=-\left(\frac{\partial T_{ij}}{\partial p_w}\right)_{E_{ij},\mu_w}\dot{E}_{ij}+\left(\frac{\partial \upsilon}{\partial p_w}\right)_{E_{ij},\mu_w}\dot{p}_w+\left(\frac{\partial \rho_{bound,ref}}{\partial p_w}\right)_{E_{ij},\mu_w}\dot{\mu}_w \tag{3.29}$$

$$\frac{\partial \rho_{bound,ref}}{\partial t}=-\left(\frac{\partial \dot{W}}{\partial \mu_w}\right)_{E_{ij},p_w}=-\left(\frac{\partial T_{ij}}{\partial \mu_w}\right)_{E_{ij},p_w}\dot{E}_{kl}+\left(\frac{\partial \upsilon}{\partial \mu_w}\right)_{E_{ij},p_w}\dot{p}_w+\left(\frac{\partial \rho_{bound,ref}}{\partial \mu_w}\right)_{E_{ij},p_w}\dot{\mu}_w \tag{3.30}$$

For convenience, equation (3.30) may be written in matrix form as follows:

$$\begin{bmatrix}\dot{T}_{ij}\\ \dot{\upsilon}\\ \dot{\rho}_{bound,ref}\end{bmatrix}=\begin{bmatrix}\overbrace{\left(\frac{\partial T_{kl}}{\partial E_{ij}}\right)_{p_w,\mu_w}}^{(1)} & \overbrace{-\left(\frac{\partial \upsilon}{\partial E_{ij}}\right)_{p_w,\mu_w}}^{(2)} & \overbrace{-\left(\frac{\partial \rho_{bound,ref}}{\partial E_{ij}}\right)_{p_w,\mu_w}}^{(3)}\\ \overbrace{-\left(\frac{\partial T_{ij}}{\partial p_w}\right)_{E_{ij},\mu_w}}^{(4)} & \overbrace{\left(\frac{\partial \upsilon}{\partial p_w}\right)_{E_{ij},\mu_w}}^{(5)} & \overbrace{\left(\frac{\partial \rho_{bound,ref}}{\partial p_w}\right)_{E_{ij},\mu_w}}^{(6)}\\ \overbrace{-\left(\frac{\partial T_{ij}}{\partial \mu_w}\right)_{E_{ij},p_w}}^{(7)} & \overbrace{\left(\frac{\partial \upsilon}{\partial \mu_w}\right)_{E_{ij},p_w}}^{(8)} & \overbrace{\left(\frac{\partial \rho_{bound,ref}}{\partial \mu_w}\right)_{E_{ij},p_w}}^{(9)}\end{bmatrix}\begin{bmatrix}\dot{E}_{ij}\\ \dot{p}_w\\ \dot{\mu}_w\end{bmatrix} \tag{3.31}^{8}$$

The matrix function of equation (3.31) describes the relationship between variables $\dot{T}_{ij},\dot{\upsilon},\dot{\rho}_{bound,ref}$, and $\dot{E}_{ij},\dot{p}_w,\dot{\mu}_w$. The matrix that links these two groups of variables is called the *coupling matrix* for the open thermodynamic system.

There are nine coefficients in this matrix (with numbers allocated at the top of each coefficient), and the next step is to discuss these coefficients (from 1 to 9). Substituting equation (3.25) into the coupling matrix

1. As $T_{ij} = \left(\frac{\partial W}{\partial E_{ij}}\right)_{p_w,\mu_w}$, it leads to

$$\left(\frac{\partial T_{ij}}{\partial E_{kl}}\right)_{p_w,\mu_w} = \left(\frac{\partial}{\partial E_{kl}}\left(\left(\frac{\partial W}{\partial E_{ij}}\right)_{p_w,\mu_w}\right)\right)_{p_w,\mu_w} = \left(\frac{\partial^2 W}{\partial E_{kl}\,\partial E_{ij}}\right)_{p_w,\mu_w} = \left(\frac{\partial T_{kl}}{\partial E_{ij}}\right)_{p_w,\mu_w} = L_{ijkl} \tag{3.32}$$

where L_{ijkl} is a stiffness tensor (fourth-order tensor represented by a matrix of $3 \times 3 \times 3 \times 3 = 81$ numbers). As a property of the material, it depends on physical state variables such as microstructure temperature, pressure etc.

2. As $\upsilon = -\left(\frac{\partial W}{\partial p_w}\right)_{E_{ij},\mu_w}$, it leads to

$$-\left(\frac{\partial \upsilon}{\partial E_{ij}}\right)_{p,\mu} = \left(\frac{\partial}{\partial E_{ij}}\left(\frac{\partial W}{\partial p_w}\right)_{E_{ij},\mu_w}\right)_{p_w,\mu_w} = \left(\frac{\partial}{\partial E_{ij}}\left(\frac{\partial W}{\partial p_w}\right)_{E_{ij},\mu_w}\right)_{p_w,\mu_w} = \left(\frac{\partial^2 W}{\partial p_w\,\partial E_{ij}}\right)_{\mu_w} = -M_{ij} \tag{3.33}$$

where M_{ij} describes the couplings between solid and fluids. It is an analogue of Biot's coefficient and is extended as a second-order tensor, depending on the solid material. To align with the effective stress concept in geomechanics, and to compare with Biot's theory, a minus sign "–" is added before M_{ij}.

3. As $\rho_{bound,ref} = -\left(\frac{\partial W}{\partial \mu_w}\right)_{E_{ij},p_w}$, it leads to

$$-\left(\frac{\partial \rho_{bound,ref}}{\partial E_{ij}}\right)_{p_w,\mu_w} = -\left(\frac{\partial}{\partial E_{ij}}\left(-\left(\frac{\partial W}{\partial \mu_w}\right)_{E_{ij},p_w}\right)\right)_{p_w,\mu_w} = \left(\frac{\partial^2 W}{\partial E_{ij}\,\partial \mu_w}\right)_{p_w} = S_{ij} \tag{3.34}$$

where S_{ij} describes the coupling between the chemical potential of water molecules within the clay platelets and their influence on the deformation.

4. As $T_{ij} = \left(\frac{\partial W}{\partial E_{ij}}\right)_{p_w,\mu_w}$, it leads to

$$-\left(\frac{\partial T_{ij}}{\partial p_w}\right)_{E_{ij},\mu_w} = -\left(\frac{\partial}{\partial p_w}\left(\frac{\partial W}{\partial E_{ij}}\right)_{p_w,\mu_w}\right)_{E_{ij},\mu_w} = -\left(\frac{\partial^2 W}{\partial p_w \partial E_{ij}}\right)_{\mu_w} = M_{ij} \tag{3.35}$$

5. As $\upsilon = -\left(\frac{\partial W}{\partial p_w}\right)_{E_{ij},\mu_w}$, it leads to

$$\left(\frac{\partial \upsilon}{\partial p_w}\right)_{E_{ij},\mu_w} = \left(\frac{\partial}{\partial p_w}\left(-\left(\frac{\partial W}{\partial p_w}\right)_{E_{ij},\mu_w}\right)\right)_{E_{ij},\mu_w} = -\left(\frac{\partial^2 W}{\partial p_w^2}\right)_{E_{ij},\mu_w} = Q \tag{3.36}$$

where Q is a coefficient for the coupling between the pore water pressure and the porosity.

6. As $\rho_{bound,ref} = -\left(\frac{\partial W}{\partial \mu_w}\right)_{E_{ij},p_w}$, it leads to

$$\left(\frac{\partial \rho_{bound,ref}}{\partial p_w}\right)_{E_{ij},\mu_w} = \left(\frac{\partial}{\partial p_w}\left(-\left(\frac{\partial W}{\partial \mu_w}\right)_{E_{ij},p_w}\right)\right)_{E_{ij},\mu_w} = -\left(\frac{\partial^2 W}{\partial p_w \partial \mu_w}\right)_{E_{ij}} = B \tag{3.37}$$

7. As $T_{ij} = \left(\frac{\partial W}{\partial E_{ij}}\right)_{p_w,\mu_w}$, it leads to

$$-\left(\frac{\partial T_{kl}}{\partial \mu_w}\right)_{E_{ij},p_w} = -\left(\frac{\partial}{\partial \mu_w}\left(\left(\frac{\partial W}{\partial E_{ij}}\right)_{p_w,\mu}\right)\right)_{E_{ij},p_w} = -\left(\frac{\partial^2 W}{\partial \mu_w \partial E_{ij}}\right)_{p_w} = -S_{ij} \tag{3.38}$$

8. As $\upsilon = -\left(\frac{\partial W}{\partial p_w}\right)_{E_{ij},\mu_w}$, it leads to

$$\left(\frac{\partial \upsilon}{\partial \mu_w}\right)_{E_{ij},p_w} = \left(\frac{\partial}{\partial \mu_w}\left(-\left(\frac{\partial W}{\partial p}\right)_{E_{ij},\mu_w}\right)\right)_{E_{ij},p_w} = -\left(\frac{\partial^2 W}{\partial \mu_w \partial p_w}\right)_{E_{ij}} = B \tag{3.39}$$

where B is a coefficient to describe the coupling between the porosity and the water chemical potential.

9. As $\rho_{bound,ref} = -\left(\frac{\partial W}{\partial \mu_w}\right)_{E_{ij},p_w}$, it leads to

$$\left(\frac{\partial \rho_{bound,ref}}{\partial \mu_w}\right)_{E_{ij},p_w} = \left(\frac{\partial}{\partial \mu_w}\left(-\left(\frac{\partial W}{\partial \mu_w}\right)_{E_{ij},p_w}\right)\right)_{E_{ij},p_w} = -\left(\frac{\partial^2 W}{\partial \mu_w^2}\right)_{E_{ij},p_w} = Z \tag{3.40}$$

where Z describes the chemical potential of water influence on the mass density of water molecules in the clay platelets.

Equations (3.32)–(3.40) demonstrates the interrelationship between the coefficients and also concludes that some of these coefficients are equal in value. Incorporating equations (3.32)–(3.40) in equation (3.31), and using simple symbols to replace the complex coefficients, leads to

$$\dot{T}_{ij} = L_{ijkl}\dot{E}_{kl} - M_{ij}\dot{p}_w + S_{ij}\dot{\mu}_w \tag{3.41}$$

$$\dot{\upsilon} = M_{ij}\dot{E}_{ij} + Q\dot{p}_w + B\dot{\mu}_w \tag{3.42}$$

$$\dot{\rho}_{bound,ref} = -S_{ij}\dot{E}_{ij} + B\dot{p}_w + Z\dot{\mu}_w \tag{3.43}$$

Equations (3.41) and (3.43) may be written in matrix format as

$$\begin{bmatrix} \dot{T}_{ij} \\ \dot{\upsilon} \\ \dot{\rho}_{bound,ref} \end{bmatrix} = \begin{bmatrix} L_{klij} & -M_{ij} & S_{ij} \\ M_{ij} & Q & B \\ -S_{ij} & B & Z \end{bmatrix} \begin{bmatrix} \dot{E}_{ij} \\ \dot{p}_w \\ \dot{\mu}_w \end{bmatrix} \tag{3.44}$$

where the parameters L_{ijkl}, M_{ij}, S_{ij}, Z, B, and Q are material-dependent constants that can be expressed as the equations (3.32)–(3.40). Note that (1) $\dot{E}_{kl}$ has been replaced as $\dot{E}_{ij}$ (as well as L_{klij} accordingly) for convenience of the matrix format.

The matrix reduces nearly half of the number of coefficients that need to be determined, thus partially addressing the challenge posed by the large number of coefficients in coupled analyses. The diagonal coefficients of the matrix represent the primary couplings within the system. For example, if the coupling between water and swelling is not considered, the equation $\dot{T}_{ij} = L_{ijkl}\dot{E}_{kl} - M_{ij}\dot{p}_w + S_{ij}\dot{\mu}_w$ simplifies to $\dot{T}_{ij} = L_{ijkl}\dot{E}_{kl}$ (or $\dot{T}_{ij} = L_{klij}\dot{E}_{ij}$), which describes the relationship between stress and strain without the influence of these additional couplings.

3.5 COUPLED FIELD EQUATIONS

Several assumptions are now made to simplify equations (3.41)–(3.43) by physical and geometrical linearization (Chen & Hicks, 2013). (Note that this simplification will be used throughout the remaining chapters to allow this book to focus on physical-chemical coupling.)

1. It is assumed that L_{ijkl}, M_{ij}, S_{ij}, Z, B, Q are material-dependent constants.
2. The strains are assumed to be small, so that the Green strain tensor E_{ij} and Piola-Kirchhoff stress T_{ij} can be replaced by the strain tensor ε_{ij} and Cauchy stress σ_{ij}:

$$E_{ij} = \varepsilon_{ij}, T_{ij} = \sigma_{ij} \tag{3.45}$$

3. Material symmetry is assumed, so that isotropic relationships are incorporated into the constitutive laws. For isotropic materials, the tensors M_{ij} and S_{ij} are diagonal, i.e., they can be written in the form of scalars ζ and ω:

$$M_{ij} = \zeta\delta_{ij}, S_{ij} = \omega\delta_{ij} \tag{3.46}$$

4. The elastic stiffness L_{ijkl} can be expressed as a fourth-order isotropic tensor (which has 81 components for three-dimensional analysis) by applying the analogue of Hooke's law for continuous porous media. This relationship represents a linear mapping between second-order tensors as σ and ε, and is given by

$$L_{ijkl} = G(\delta_{ik}\delta_{jl} + \delta_{il}\delta_{jk}) + \left(K - \frac{2G}{3}\right)\delta_{ij}\delta_{kl} \tag{3.47}$$

where G is the shear modulus of the geomaterial and K is the bulk modulus. Due to inherent symmetries, the 81 components of L_{ijkl} can be reduced to 21 independent elastic coefficients (note: k, l = 1, 2, 3).

3.5.1 Solid phase and porosity

3.5.1.1 Small strain constitutive equations

Substitution of equations (3.47) and (3.46) into equation (3.41) leads to

$$\dot{\sigma}_{ij} = \left(G(\delta_{ik}\delta_{jl} + \delta_{il}\delta_{jk}) + \left(K - \frac{2G}{3} \right) \delta_{ij}\delta_{kl} \right) \dot{\varepsilon}_{kl} - \zeta \dot{p}_w \delta_{ij} + \omega \dot{\mu}_w \delta_{ij} \quad (3.48)$$

in which the bracketed term can be expanded to give

$$\left(G(\delta_{ik}\delta_{jl} + \delta_{il}\delta_{jk}) + \left(K - \frac{2G}{3} \right) \delta_{ij}\delta_{kl} \right) \dot{\varepsilon}_{kl} = G\delta_{ik}\delta_{jl}\dot{\varepsilon}_{kl} + G\delta_{il}\delta_{jk}\dot{\varepsilon}_{kl} + \left(K - \frac{2G}{3} \right) \delta_{ij}\delta_{kl}\dot{\varepsilon}_{kl} \quad (3.49)$$

Since $G\delta_{il}\delta_{jk}\dot{\varepsilon}_{kl} = G\delta_{ii}\delta_{jj}\dot{\varepsilon}_{ji}$ and $\left(K - \frac{2G}{3} \right) \delta_{ij}\delta_{kl}\dot{\varepsilon}_{kl} = \left(K - \frac{2G}{3} \right) \delta_{ij}\delta_{kk}\dot{\varepsilon}_{kk}$,[9] equation (3.49) can be changed to

$$G\delta_{ik}\delta_{jl}\dot{\varepsilon}_{kl} + G\delta_{il}\delta_{jk}\dot{\varepsilon}_{kl} + \left(K - \frac{2G}{3} \right) \delta_{ij}\delta_{kl}\dot{\varepsilon}_{kl} = \left(K - \frac{2G}{3} \right) \dot{\varepsilon}_{kk}\delta_{ij} + 2G\dot{\varepsilon}_{ij} \quad (3.50)$$

and equation (3.48) can be reformed as

$$\dot{\sigma}_{ij} = \left(K - \frac{2G}{3} \right) \dot{\varepsilon}_{kk}\delta_{ij} + 2G\dot{\varepsilon}_{ij} - \zeta \dot{p}_w \delta_{ij} + \omega \dot{\mu}_w \delta_{ij} \quad (3.51)$$

The influences of water molecules in the clay platelets and the pore water pressure have been incorporated in equation (3.51).

By substituting equations (3.45) and (3.46) into equation (3.42), the pore fraction equation can be written as

$$\dot{\upsilon} = \zeta \dot{\varepsilon}_{ii} + Q\dot{p}_w + B\dot{\mu}_w \quad (3.52)$$

3.5.1.2 Parameter discussion

Based on the general assumption from equation (3.45) to equation (3.47), the parameters in equations (3.51) and (3.52) can be characterized through the assumption of linear elasticity of fluid-filled

geomaterials in response to mechanical and chemical loading (Nur and Byerlee, 1971, Rice and Cleary, 1976). This leads to the following relationships: the incremental relationship between the stress and the pore fluid pressure

$$\dot{\sigma}_{ij} = -\dot{p}_w \delta_{ij} \tag{3.53}$$

whereas the strain rate is related to the pore fluid pressure by

$$\dot{\varepsilon}_{ij} = -\frac{\dot{p}_w}{3K_s}\delta_{ij} \tag{3.54}$$

and the volume change is related to the pore fluid pressure by

$$\dot{\upsilon} = -\phi_0 \frac{\dot{p}_w}{K_s} \tag{3.55}$$

where K_s is the bulk modulus of the solid particles and ϕ_0 is the initial porosity as a constant. Please note that υ is the porosity at any reference configuration, and it is a variable representing the porosity evolution pathway.

The parameters can be obtained through the following steps:

3.5.1.2.1 The quantity ζ

Substituting equations (3.53) and (3.54) into equation (3.51), and neglecting the swelling term ($\omega = 0$), leads to

$$-\dot{p}_w \delta_{ij} = \left(K - \frac{2G}{3}\right)\left(-\frac{\dot{p}_w}{K_s}\right)\delta_{ij} + 2G\left(-\frac{\dot{p}_w}{3K_s}\delta_{ij}\right) - \zeta \dot{p}_w \delta_{ij} \tag{3.56}$$

Then, by eliminating the term $\dot{p}_w \delta_{ij}$ from both sides of the above equation, this leads to

$$-1 = \left(K - \frac{2G}{3}\right)\left(-\frac{1}{K_s}\right) + 2G\left(-\frac{1}{3K_s}\right) - \zeta \tag{3.57}$$

Hence, the quantity ζ is related to the bulk moduli, K (of the solid skelton of a porous medium), and K_s (of the solid particles forming the solid skelton) in a poroelastic manner:

$$\zeta = 1 - (K / K_s) \tag{3.58}$$

where ζ is also Biot's constant, which is also expressed using compresiblity (inverse of bulk modulus) as $\zeta = 1 - \frac{C_{v-s}}{C_m}$ (equation (1.77)). If the soil/rock particles are assumed to be incompressible, $K_s \approx \infty$ and $\zeta = 1$.

3.5.1.2.2 The void compressibility Q

By substituting equations (3.54) and (3.55) into a simplified form of equation (3.52) (where the influence of chemical potential is ignored, i.e., $\dot{\upsilon} = \zeta \dot{\varepsilon}_{ii} + Q\dot{p}_w$), and considering the relationship

$$\dot{\varepsilon}_{ii} = -\frac{\dot{p}_w}{3K_s}\delta_{ii} = -\frac{\dot{p}_w}{3K_s}3 = -\frac{\dot{p}_w}{K_s}$$

the resulting expression for $-\phi\frac{\dot{p}_w}{K_s} = \zeta(-\frac{\dot{p}_w}{K_s}) + Q\dot{p}_w$ can be obtained, which results in

$$-\frac{\phi_0}{K_s} = \zeta(-\frac{1}{K_s}) + Q$$

and leads to

$$Q = (1/K_s)(\zeta - \phi_0) \tag{3.59}$$

If the soil/rock particles are assumed to be incompressible, then $K_s \approx \infty$, so that $Q = 0$.

3.5.1.2.3 The coefficient B

At the equilibrium condition, when

$$\dot{p}_w = 0 \text{ and } \dot{\sigma}_{ij} = 0$$

equation (3.51) can be simplified as

$$\left(K - \frac{2G}{3}\right)\dot{\varepsilon}_{kk}\delta_{ij} + 2G\dot{\varepsilon}_{ij} + \omega\dot{\mu}_w\delta_{ij} = 0 \tag{3.60}$$

where ω is the swelling coefficient.

Since $\omega\ \dot{\mu}_w\delta_{ij}$ must exist ($i = j$), equation (3.60) can be written as

$$\left(K - \frac{2G}{3}\right)\dot{\varepsilon}_{kk}\delta_{ii} + 2G\dot{\varepsilon}_{ii} + \delta_{ii}\omega\dot{\mu}_w = 0 \tag{3.61}$$

Since $\delta_{ii} = 3$, it leads to

$$3\left(K - \frac{2G}{3}\right)\dot{\varepsilon}_{kk} + 2G\dot{\varepsilon}_{ii} + 3\omega\dot{\mu}_w = 0 \tag{3.62}$$

Because $\dot{\varepsilon}_{kk} = \dot{\varepsilon}_{ii}$,

$$\dot{\varepsilon}_{ii} = -\frac{1}{K}\omega\ \dot{\mu}_w \tag{3.63}$$

From equation (3.52), when there is no mechanical loading and $\dot{p}_w = 0$, and by substituting (3.63) into (3.52), this leads to

$$\dot{\upsilon} = -\frac{\zeta}{K}\omega\ \dot{\mu}_w + B\ \dot{\mu}_w \tag{3.64}$$

Because $\dot{\varepsilon}_{ii} = \dot{\upsilon}$ (when $\dot{p} = 0, \dot{\sigma}_{ij} = 0$ in equation (3.52) and assume $\zeta \approx 1$),

$$-\frac{1}{K}\omega\ \dot{\mu}_w = -\frac{\zeta}{K}\omega\ \dot{\mu}_w\ + B\ \dot{\mu}_w \tag{3.65}$$

By eliminating $\dot{\mu}_w$ from the above equation, this leads to the relationship

$$-\frac{1}{K}\omega = -\frac{\zeta}{K}\omega + B$$

and finally to

$$B = (1/K)(\zeta - 1)\omega \tag{3.66}$$

The coefficient B is related to K, ζ, and ω. It can be assumed to be zero if K is very big (e.g., for rocks). However, for soft geomaterials with a high potential for swelling (e.g., bentonite clay (Komine and Ogata, 1994)), the coefficient cannot be ignored. Further experimental and theoretical studies are needed to understand the influence of the coefficient B.

3.5.1.3 Simplified constitutive equation for solid phases and porosity

Substituting equation (3.20) that results in

$$\dot{\mu}_w = \left(\frac{1}{\rho_l^w}\right)\dot{p}_w \text{ (assuming } \rho_l^w = \rho_l^{pore})$$

into stress equation (3.51) and volume fraction equation (3.52) leads to

$$\dot{\sigma}_{ij} = \underbrace{\left(K - \frac{2G}{3}\right)\dot{\varepsilon}_{kk}\delta_{ij} + 2G\dot{\varepsilon}_{ij}}_{1} - \underbrace{\left(\zeta - \frac{\omega}{\rho_l^w}\right)\dot{p}_w\delta_{ij}}_{2} \tag{3.67}$$

$$\dot{\upsilon} = \zeta\dot{\varepsilon}_{ii} + \underbrace{\left(Q + \frac{B}{\rho_l^w}\right)\dot{p}_w}_{3} \tag{3.68}$$

where $\varepsilon_{ij} = \frac{1}{2}(d_{i,j} + d_{j,i})$ and $d_i\,(i = 1,2,3)$ is the displacement component.

Note: The numbers below equations (3.67) and (3.68) are used for discussing the physical meanings of the corresponding equation terms. This applies to the whole book. The physical meaning of terms in equations (3.67) and (3.68) may be summarized as follows:

- 1: Elastic deformation of the solids.
- 2: The coupling term, describing the influence of the water pressure on the deformation of the solids. The novelty of this equation is the swelling term $\frac{\omega}{\rho_l^w}$.
- 3: The coupling pressure term associated with the porosity, describing the influence of water pressure on the porosity change. The novelty of this equation is the swelling-related term $\frac{B}{\rho_l^w}$.

3.5.2 Fluid phase

Since the balance equation (refer to Section 2.3) for water is

$$\dot{\rho}_w + \rho_w \nabla \cdot \mathbf{v}_s + \nabla \cdot \mathbf{I}_w = 0 \tag{3.69}$$

using the relationship between ρ_w and ρ_l^w leads to

$$(\rho_l^w \phi)^{\cdot} + \rho_l^w \phi \nabla \cdot \mathbf{v}_s + \nabla \cdot \left(\rho_l^w \mathbf{u}\right) = 0 \tag{3.70}$$

Multiplying both sides of equation (3.70) with J, and using the Euler identity as $\dot{J} = J\nabla \cdot \mathbf{v}_s$ and $\upsilon = J\phi$, leads to

$$(\upsilon\rho_l^w)^{\cdot} + J\nabla \cdot (\rho_l^w \mathbf{u}) = 0^{10}$$

or

$$\rho_l^w \dot{\upsilon} + \upsilon \dot{\rho}_l^w + J\nabla \cdot (\rho_l^w \mathbf{u}) = 0 \tag{3.71}$$

If the reference configuration is selected at any given instant, it leads to $J = 1$, whereas $\dot{J} = J \cdot \nabla \mathbf{v}_s$ remains nonzero. By substituting equation (3.8) for the Darcy velocity and equation (3.68) into equation (3.71), and using equation (3.19),

$$\underbrace{\zeta \dot{\varepsilon}_{ii}}_{4} + \underbrace{\left(Q + \frac{B}{\rho_l^w} \right) \dot{p}_w + \upsilon \frac{\dot{\rho}_l^w}{\rho_l^w} + \nabla \cdot \left[-\frac{k}{v} \frac{\partial^2 p_w}{\partial x_i^2} \right]}_{5} = 0 \tag{3.72}$$

Physical meanings of terms and novelties in equation (3.72) are:

- 4: This coupling term in the water transport equation describes the influence of solid deformation on the water transport process.
- 5: This term describes the water transport with consideration of volume change.
- Key novelties: The swelling-related term $\left(Q + \frac{B}{\rho_l^w} \right) \dot{p}_w$ and the volume change-related term $\upsilon \dot{\rho}_l^w$.

3.6 NUMERICAL SIMULATION

The numerical simulations presented in this book are primarily for demonstration purposes, illustrating the differences between the new constitutive model and classic approaches (e.g., the Biot coupled model) or established laws (e.g., Darcy's law). The commercial software COMSOL, which has been validated for such applications, will be used to perform the finite element analysis and provide the results.

3.6.1 Mathematical equation

Mechanical (M): If the mechanical equilibrium condition, $\partial \sigma_{ij} / \partial x_j = 0$ (3.9), is introduced into equation (3.67), the final equation is (Chen and Hicks, 2010)

$$\left(K - \frac{2G}{3} \right) \frac{\partial^2 \dot{d}_k}{\partial x_k \partial x_i} + G \left(\frac{\partial^2 \dot{d}_i}{\partial x_j \partial x_j} + \frac{\partial^2 \dot{d}_j}{\partial x_i \partial x_j} \right) - \left(\zeta - \underbrace{\frac{\omega}{\rho_l^w}}_{\text{Swelling}} \right) \frac{\partial \dot{p}_w}{\partial x_i} = 0 \tag{3.73}$$

The porosity is assumed to be constant, so that equation (3.68) can be ignored to simplify the discussion for the numerical simulation.

Hydro (H): Considering the compressibility of water $\dot{\rho}_l^w$ in equation (3.72) as

$$\dot{\rho}_l^w = \rho_l^w \left(\frac{1}{\rho_l^w} \frac{\partial \rho_l^w}{\partial p} \right) \frac{\partial p_w}{\partial t} = \rho_l^w \frac{1}{K_w} \dot{p}_w \tag{3.74}$$

where K_w is the bulk modulus of water.

By substituting equation (3.74) into equation (3.71) and eliminating ρ_l^w from both sides, it leads to

$$\dot{\upsilon} + \upsilon \frac{1}{K_w} \dot{p}_w + \nabla \cdot \mathbf{u} = 0 \tag{3.75}$$

Therefore, the governing equation for the fluid phase can be written as

$$\zeta \frac{\partial \dot{d}_i}{\partial x_i} + (Q + \phi / K_w + B / \rho_l^w) \dot{p}_w - \frac{k}{v} \frac{\partial^2 p_w}{\partial x_i^2} = 0 \tag{3.76}$$

3.6.2 Discussion and comparison

Equations (3.73) and (3.76) govern the coupled hydro-mechanical process for swelling geomaterials in porous media. The difference between equations (3.73) and (3.76), and the classical Biot's consolidation equations are the terms $-\omega / \rho_l^w$ and B / ρ_l^w, which are related to the chemical potential of water. If the term $-\omega / \rho_l^w$ in equation (3.73) and B / ρ_l^w in equation (3.76) are ignored, the equations revert to Biot's equations. The influence of the term $\zeta - \omega / \rho_l^w$ in equation (3.73) can be shown by using finite elements. ζ is known as Biot's coefficient and ω is the swelling parameter introduced in the new formulation.

3.6.3 Conceptual model

By using the classic finite element method (Lewis and Schrefler, 1987; Smith and Griffiths, 2004), the governing equations are solved to analyze the mechanical and hydraulic behavior of a swelling geomaterial sample. To simplify the terms $(Q + \phi / K_w + B / \rho_l^w)$ and $B = (1 / K)(\zeta - 1)\omega$ in equation (3.76), it is assumed that Biot's constant is 1, leading to $B = 0$. Meanwhile, the term $\omega / \rho_l^w = sw$ in equation (3.73) is defined as the swelling parameter (note that *sw* is the swelling coefficient rather than the water saturation S_w), and its value has been

selected as 0.2. The swelling coefficient can be obtained by experiments (Madsen and Muller-von Moos, 1989; Komine and Ogata, 1994; Karnland et al., 2005), which is not discussed in this book as the attention is on the theoretical model.

A saturated geomaterial (plane stain) sample (0.1 m × 0.1 m) is constrained between two stiff and frictionless boundaries (Figure 3.1), which allow movement only in the horizontal direction (i.e., the x-direction). The adopted material parameters for the numerical simulation are listed in Table 3.1. Other details of the analysis are as follows:

Boundary conditions: Boundary B is fixed (displacement = 0), whereas boundary A is free to move. Both boundaries A and B are permeable, allowing free flow of water in and out of the sample.

Initial conditions: An equilibrium state is assumed at $t = 0$, with an external pressure (5 MPa) at boundary A to maintain equilibrium. At $t = 0$, the initial effective stress in the sample is zero and the water pressure is $p_w = 5$ MPa.

Start of the simulation: The water pressure at free boundary A is increased from 5 to 10 MPa and maintained at that value for the remainder of the analysis ($t > 0$); the water pressure at fixed boundary B is maintained at 5 MPa.

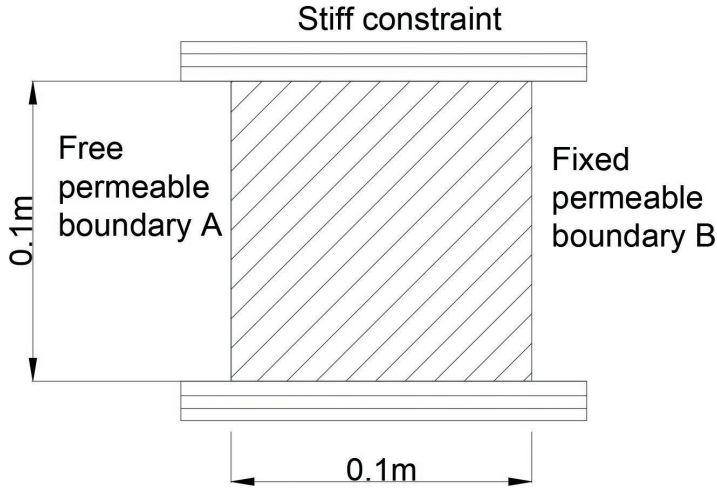

FIGURE 3.1 Geometry and boundary conditions

TABLE 3.1
Material parameters for swelling shale

Parameter	Physical meaning	Value and units
k	Absolute permeability	2.75E−21 m^2
v	Dynamic viscosity	8.54E−4 Pa·s ①
G	Shear modulus	239.08 MPa (SUGITA et al., 2004)②
E	Young's modulus	645.52 MPa③
θ	Poisson's ratio	0.35 (Rutqvist and Tsang, 2004)
ϕ	Porosity	0.41
ζ	Biot's coefficient	1 (assumed)
K_s	Bulk modulus of solid	∞ (assumed)
K_w	Bulk modulus of water	2E3 MPa
S_w	Swelling parameter	0.2 (assumed)

Zheng and Samper (2008), Zheng et al. (2010, 2011).

*Table notes:*①: calculated with $T = 300$ K; ②: calculated with density = 2,780 and saturation = 1; ③: calculated from the relationship: $E = 2G(1+\theta)$.

3.6.4 Numerical simulation results

Figure 3.2 presents a comparison of the evolution of pore water pressure under two different conditions: swelling and non-swelling. In the swelling case, the swelling coefficient is denoted as "Swelling" in the figure, while the non-swelling condition is represented by Biot's consolidation equation (Biot, 1941), denoted as "Biot (1941)" in the figure. The comparison is made at various time intervals to illustrate the impact of swelling on pore water pressure evolution.

As shown in the figure, the pore water pressure increases over time across the entire domain. This increase is driven by the pressure gradient, which provides the necessary force for water to flow through the material. However, a noticeable difference arises between the swelling and non-swelling conditions. Under swelling conditions, the pore water pressures are consistently lower than those under non-swelling conditions. This discrepancy can be attributed to the swelling effect, which acts to reduce the rate at which the pore water pressure increases.

The swelling of the material, particularly in clay-rich soils or rocks, causes the soil matrix to expand as water is absorbed, resulting in a reduction in the rate of pressure buildup. In contrast, under non-swelling conditions, where the solid matrix remains unchanged, the pore water pressure increases more rapidly, as there is no counteracting volumetric

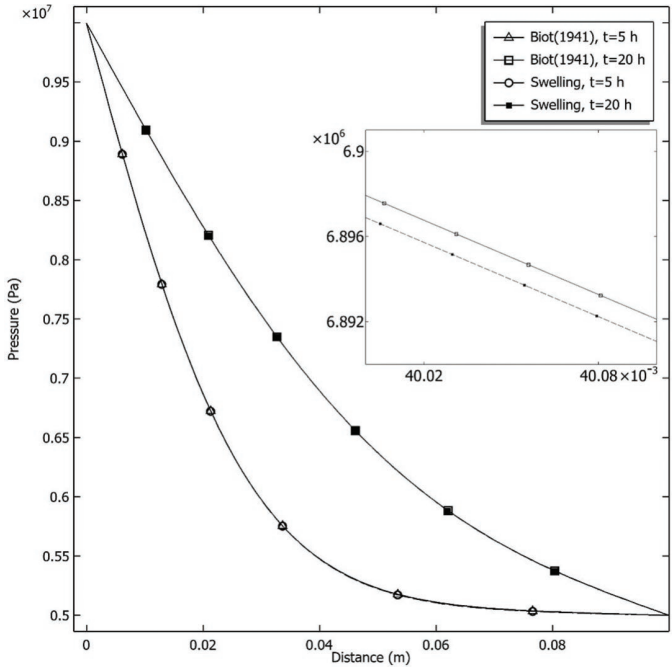

FIGURE 3.2 Evolution of pore water pressure with time

expansion. This behavior highlights the significant role that swelling plays in modifying the hydraulic response of the material, with implications for understanding and managing subsurface processes, such as those involved in land subsidence, foundation stability, and groundwater flow.

Figures 3.3 and 3.4 illustrate the evolution of effective stress and horizontal displacement, respectively, under different boundary conditions. In the simulation, the water pressure at boundary A is increased at the beginning of the analysis, while the pressure at boundary B remains constant. This pressure differential causes a sudden increase in effective stress at boundary B, which then stabilizes, while the effective stress at boundary A remains constant at zero. This behavior reflects a consolidation process, where the material adjusts due to the pressure gradient, leading to changes in the internal stress distribution.

The change in effective stress (shown in Figure 3.3) is notably smaller for the swelling geomaterial compared to the non-swelling geomaterial. This is because the swelling effect in the material reduces the

pressure's influence on the solid skeleton. When the material swells, the solid matrix expands due to the absorbed water, which limits the pressure buildup and, in turn, the increase in effective stress. In contrast, the non-swelling geomaterial does not undergo this expansion, so the applied water pressure results in a larger increase in effective stress.

This difference in effective stress leads to corresponding changes in horizontal displacement, as shown in Figure 3.4. The non-swelling geomaterial experiences a larger horizontal displacement than the swelling geomaterial. This is due to the fact that in the absence of swelling, the solid matrix is more responsive to changes in water pressure, leading to greater deformation. On the other hand, the swelling material, which already undergoes expansion due to water absorption, resists further displacement under the same pressure conditions. This analysis highlights the important role that swelling plays in modulating both the stress response and the deformation behavior of geomaterials, which is critical for understanding and predicting the performance of soils and rocks in engineering applications.

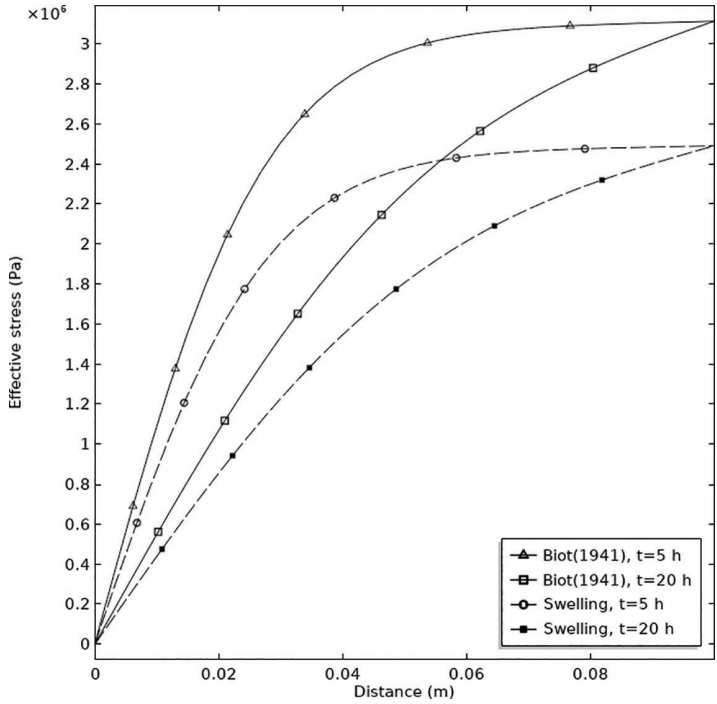

FIGURE 3.3 Evolution of effective stress with time

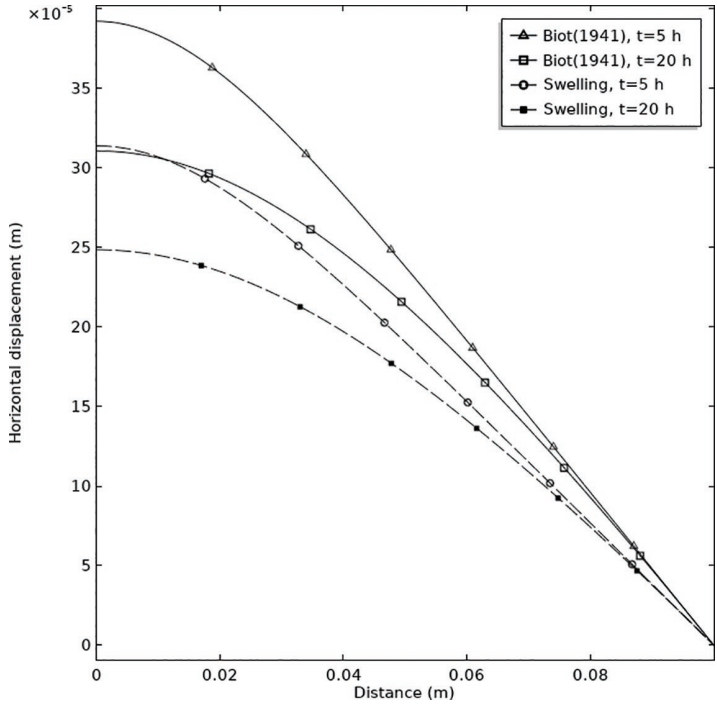

FIGURE 3.4 Evolution of horizontal displacement with time

3.7 CONCLUSION

This chapter introduces a novel constitutive equation for hydro-mechanical coupled analysis of swelling rocks and soils based on the Mixture-Coupling Theory. Biot's three-dimensional consolidation model is demonstrated as a specific case within the framework presented in this chapter.

The key innovation of this theory lies in the integration of entropy and dissipative processes, offering a significant advantage over traditional mechanical approaches. By incorporating entropy production as an energy variable within the balance equation for Helmholtz free energy, this theory captures the interactions between multiple coupled processes driven by various gradients. This unified approach enables the consideration of multiscale coupling effects, such as molecular-scale phenomena, by analyzing the Helmholtz free energy difference between the pore water and the wetted matrix.

Although the derivation process involves numerous equations, the overall structure of the theory remains clear and straightforward. It consists of three main components: (1) energy in the mixture, (2) dissipative processes, and (3) constitutive relations. This formulation not only addresses the complexities of swelling and deformation but also provides a solid foundation for extending the theory to other coupled processes in porous media.

Looking ahead, Chapter 4 will focus on the development of an unsaturated model based on the Mixture-Coupling Theory, further expanding the scope of coupled models for complex geotechnical systems.

NOTES

1 $$T\gamma = -\mathbf{I}_w \cdot \nabla\mu_w = -\overbrace{\rho_w(\mathbf{v}_w - \mathbf{v}_s)}^{\mathbf{I}_w} \cdot \frac{\overbrace{\nabla p_w}^{\nabla\mu_w}}{\rho_l^w} = -\frac{\rho_w}{\rho_l^w}(\mathbf{v}_w - \mathbf{v}_s)\cdot\nabla p_w$$
$$= -\phi(\mathbf{v}_w - \mathbf{v}_s)\cdot\nabla p_w = -\mathbf{u}\cdot\nabla p_w$$

2 Substituting equation (3.3) $T\gamma = -\mathbf{I}_w \cdot \nabla\mu_w$ into equation (3.2) $\dot{\psi} + \psi\nabla\cdot\mathbf{v}_s - \nabla\cdot(\boldsymbol{\sigma}\mathbf{v}_s) + \nabla\cdot(\mu\mathbf{I}_w) = -T\gamma \le 0$ leads to

$$\dot{\psi} + \psi\nabla\cdot\mathbf{v}_s - \nabla\cdot(\boldsymbol{\sigma}\mathbf{v}_s) + \nabla\cdot(\mu_w\mathbf{I}_w) = \mathbf{I}_w\cdot\nabla\mu_w$$
$$\dot{\psi} + \psi\nabla\cdot\mathbf{v}_s - \nabla\cdot(\boldsymbol{\sigma}\mathbf{v}_s) + \mu_w\nabla\cdot\mathbf{I}_w + \mathbf{I}_w\nabla\cdot\mu_w = \mathbf{I}_w\cdot\nabla\mu_w$$
$$\dot{\psi} + \psi\nabla\cdot\mathbf{v}_s - \nabla\cdot(\boldsymbol{\sigma}\mathbf{v}_s) + \mu_w\nabla\cdot\mathbf{I}_w = 0$$

Finally, substituting equation (3.11), $\nabla\cdot(\boldsymbol{\sigma}\mathbf{v}_s) = \mathrm{tr}(\boldsymbol{\sigma}^T\nabla\mathbf{v}_s) = (\boldsymbol{\sigma}\cdot\nabla\mathbf{v}_s)$ leads to equation (3.12).

3 $\mu_w\dot{\rho}_{w,ref} = \mu_w(J\rho_w)^{\cdot} = \mu_w\rho_w\dot{J} + \mu_w J\dot{\rho}_w$, using equation (2.31) and $\dot{J} = J\nabla\cdot\mathbf{v}_s$, therefore, $\mu_w\dot{\rho}_{w,ref} = \mu_w(J\rho_w)^{\cdot} = \mu_w\rho_w J\nabla\cdot\mathbf{v}_s + \mu_w J\dot{\rho}_w$.
$$= \mu_w J(\dot{\rho}_w + \rho_w\nabla\cdot\mathbf{v}_s) = -\mu_w J\nabla\cdot\mathbf{I}_w$$

4 $$(\Psi - \overbrace{J\phi}^{=\upsilon}\psi_{pore})^{\cdot} = \dot{\Psi} - \upsilon\dot{\psi}_{pore} - \dot{\upsilon}\psi_{pore}$$
$$= \left[tr(\mathbf{T}\dot{\mathbf{E}}) + \mu_w\dot{\rho}_{w,ref}\right] - \upsilon\overbrace{\mu_w\dot{\rho}_l^{pore}}^{\dot{\psi}_{pore}} - \dot{\upsilon}\left[\overbrace{-p_w + \mu_w\rho_l^{pore}}^{\psi_{pore}}\right]$$
$$= tr(\mathbf{T}\dot{\mathbf{E}}) + \mu_w\dot{\rho}_{w,ref} - \upsilon\mu_w\dot{\rho}_l^{pore} - \mu_w\rho_l^{pore}\dot{\upsilon} + p_w\dot{\upsilon}$$
$$= tr(\mathbf{T}\dot{\mathbf{E}}) + \mu_w\dot{\rho}_{w,ref} - \mu_w(\upsilon\rho_l^{pore})^{\cdot} + p_w\dot{\upsilon}$$
$$= tr(\mathbf{T}\dot{\mathbf{E}}) + \mu_w(\dot{\rho}_{w,ref} - (\upsilon\rho_l^{pore})^{\cdot}) + p_w\dot{\upsilon}$$
$$= tr(\mathbf{T}\dot{\mathbf{E}}) + \mu_w(\rho_{w,ref} - (J\phi\rho_l^{pore})^{\cdot}) + p_w\dot{\upsilon}$$
$$= tr(\mathbf{T}\dot{\mathbf{E}}) + \mu_w\dot{\rho}_{bound,ref} + p_w\dot{\upsilon}$$

5 The Legendre transformation is a mathematical procedure that allows for the transformation of a thermodynamic potential from one set of

variables to another, often to facilitate easier manipulation or to switch between different forms of energy representations.

6 Equation (3.24) can be rewritten as

$$\frac{dW}{dt} = tr\left(\mathbf{T}\frac{\partial \mathbf{E}}{\partial t}\right) - \frac{\partial p_w}{\partial t}\upsilon - \frac{\partial \mu_w}{\partial t}\rho_{bound,ref} \tag{f1}$$

As $W = W\left(\mathbf{E}, p_w, \mu_w\right)$, using the total derivative and chain rule of partial differentiation leads to $\frac{dW}{dt} = \frac{\partial W}{\partial E_{ij}}\frac{\partial E_{ij}}{\partial t} + \frac{\partial W}{\partial p_w}\frac{\partial p_w}{\partial t} + \frac{\partial W}{\partial \mu_w}\frac{\partial \mu_w}{\partial t}$. By comparing with equation (f1), it leads to (3.25). By using equation (3.25), the expression for $\dot{W}\left(\mathbf{E}, p_w, \mu_w\right)$ can be obtained as

$$\dot{W}\left(\mathbf{E}, p_w, \mu_w\right) = \left(\frac{\partial W}{\partial E_{ij}}\right)_{pw,\mu_w}\dot{E}_{ij} + \left(\frac{\partial W}{\partial p_w}\right)_{E_{ij},\mu_w}\dot{p}_w + \left(\frac{\partial W}{\partial \mu_w}\right)_{E_{ij},p_w}\dot{\mu}_w \tag{f2}$$

7 E_{ij} is the second-order strain tensor, which can be expressed as E_{kl}; T_{ij} is the second-order strain tensor, which can be expressed as T_{kl}. The reason of using *kl (*rather than *ij* for the derivation) is that the fourth-order tensor (e.g., L_{ijkl}) is to relate the two second-order tensors (e.g., T_{ij} and E_{kl}) (Bower, 2009).

8 $\left(\frac{\partial T_{ij}}{\partial E_{kl}}\right)_{p_w,\mu_w}$ in equation (3.28) is replaced as $\left(\frac{\partial T_{kl}}{\partial E_{ij}}\right)_{p_w,\mu_w}$ for the convenience of using the $\dot{E}_{ij}$ (rather than changing all to $\dot{E}_{kl}$) for the matrix form in equation (3.31). The relationship of these two forms can be found in equation (3.32).

9 Using the *Kronecker delta* δ_{ii} (Appendix 1) that is defined as $\delta_{ij} = \left\{\begin{array}{l} 1\left(i=j\right) \\ 0\left(i\neq j\right) \end{array}\right\}$, it leads to $\delta_{il} = 1$ $\left(\text{only if } i=l\right)$ and $\delta_{jk} = 1$ $\left(\text{only if } i=k\right) \rightarrow \delta_{il} = \delta_{ii}$ and $\delta_{jk} = \delta_{jj}$; therefore, $G\delta_{il}\delta_{jk}\dot{\varepsilon}_{kl} = G\delta_{ii}\delta_{jj}\dot{\varepsilon}_{ji}$.

10
$$J\left(\rho_l^w\phi\right) + J\rho_l^w\phi\nabla\cdot\mathbf{v}_s + J\nabla\cdot\left(\rho_l^w\mathbf{u}\right) = 0$$
$$J\left(\rho_l^w\phi\right) + \overbrace{\left(\rho_l^w\phi\right)\dot{J}}^{\because \dot{J} - J\nabla\cdot V_s} + J\nabla\cdot\left(\rho_l^w\mathbf{u}\right) = 0$$
$$\underbrace{\left(J\rho_l^w\phi\right)}_{\because \upsilon = J\phi} + J\nabla\cdot\left(\rho_l^w\mathbf{u}\right) = 0$$
$$\overbrace{\left(\upsilon\rho_l^w\right)} + J\nabla\cdot\left(\rho_l^w\mathbf{u}\right) = 0$$

11 This equation can also be described as $G\nabla^2 d + \left(\frac{G}{1-2\theta}\right)\nabla\left(\nabla\cdot d\right) - (\zeta - \frac{\omega}{\underbrace{\rho_l^w}_{Swelling}})\frac{\partial p_w}{\partial x_i} = 0$ (Chen & Hicks, 2011), where θ is Poisson's ratio.

REFERENCES

Arnol'd, V. I. (2013) *Mathematical methods of classical mechanics.* New York, Springer Science & Business Media.

Biot, M. A. (1941) General theory of three-dimensional consolidation. *Journal of Applied Physics* 12: 155–164.

Bower, A.F. (2009). *Applied Mechanics of Solids (1st ed.)*. CRC Press. https://doi.org/10.1201/9781439802489

Chen, X. & Hicks, M. A. (2010) Influence of water chemical potential on the swelling of water sensitive materals. *Computers & Structures* 88 (23–24): 1498–1505.

Chen, X., & Hicks, M. A. (2013). Unsaturated hydro-mechanical-chemo coupled constitutive model with consideration of osmotic flow. *Computers and Geotechnics*, 54, 94–103.

Groot, S. R. D. & Mazur, P. (1962) Non-equilibrium thermodynamics. New York, Interscience Publishers.

Haupt, P. (2013) *Continuum mechanics and theory of materials.* Springer Berlin, Heidelberg, Springer Science & Business Media.

Heidug, W. K. & Wong, S. W. (1996) Hydration swelling of water-absorbing rocks: a constitutive model. *International Journal for Numerical and Analytical Methods in Geomechanics* 20: 403–430.

Karnland, O., Muurinen, A. & Karlsson, F. (2005) Bentonite swelling pressure in NaCl solutions-Experimen-tally determined data and model calculations. In *Advances in understanding engineered clay barriers*. (Alonso, E. E., and Ledesma, A. (eds)) London, Balkema, pp. 241–256.

Katachalsky, A. & Curran, P. F. (1965) Nonequilibrium thermodynamics in biophysics. Cambridge, MA, Harvard University Press.

Komine, H. & Ogata, N. (1994) Experimental study on swelling characteristics of compacted bentonite. *Canadian Geotechnical Journal* 31(**4**): 478–490.

Lewis, R. W. & Schrefler, B. A. (1987) *The finite-element method in deformation and consolidation of porous media.* New York, Wiley.

Madsen, F. T. & Muller-Von Moos, M. (1989) The swelling behavior of clays. *Applied Clay Science* 4: 143–156.

Mase, G. T., Smelser, R. E. & Mase, G. E. (2009) Continuum mechanics for engineers. Boca Raton, CRC press.

Nur, A. & Byerlee, J. D. (1971) An exact effective stress law for elastic deformation of rock with fluids. *Journal of Geophysical Research* 76(**26**): 6414–6419.

Rice, J. R. & Cleary, M. P. (1976) Some basic stress diffusion solutions for fluid-saturated elastic porous media with compressible constituents. *Reviews of Geophysics* 14(**2**): 227–241.

Rutqvist, J. & Tsang, C.-F. (2004) A fully coupled three-dimensional THM analysis of the FEBEX in situ test with the ROCMAS code: prediction of THM behavior in a bentonite barrier. In Elsevier *geo-engineering book series*. (Ove Stephanson (ed)). Kidlington, Oxford, Elsevier, vol. 2, pp. 143–148.

Smith, I. M. & Griffiths, D. V. (2004) *Programming the finite element method*. 4th edn. Chichester, Wiley.

Sugita, Y., Chijimatsu, M., Akira, I., Kurikami, H., Kobayashi, A. & Ohnishi, Y. (2004) THM simulation of the full-scale in-situ engineered barrier system experiment in GRIMSEL test site in Switzerland. In Elsevier *Geo-Engineering Book Series.* (Ove Stephanson (ed)). Kidlington, Oxford, Elsevier, vol. 2, pp. 119–124.

Zheng, L. & Samper, J. (2008) A coupled THMC model of FEBEX mock-up test. *Physics and Chemistry of the Earth, Parts A/B/C* 33: S486–S498.

Zheng, L., Samper, J. & Montenegro, L. (2011) A coupled THC model of the FEBEX in situ test with bentonite swelling and chemical and thermal osmosis. *Journal of Contaminant Hydrology* 126(1–2): 45–60.

Zheng, L., Samper, J., Montenegro, L. & Fernández, A. M. (2010) A coupled THMC model of a heating and hydration laboratory experiment in unsaturated compacted FEBEX bentonite. *Journal of Hydrology* 386(1–4): 80–94.

4 Unsaturated hydro-mechanical model for swelling geomaterials

4.1 INTRODUCTION

There often exists air along with water in the pores of soils/rocks. This represents an unsaturated condition. In geotechnical engineering, unsaturated soil mechanics has attracted much attention in recent decades, due to a wide range of engineering applications such as geological disposal, tunnels, and shallow foundations. Consequently, rapid development has been seen in unsaturated soil mechanics.

This chapter uses Mixture-Coupling theory to develop a coupled constitutive model for unsaturated soils/rocks. The final formulations are similar in format with those formulations obtained from the mechanics approach, but offers further advantages with respect to molecular couplings. This chapter demonstrates that the well-recognized unsaturated hydro-mechanical coupled model without considering swelling (Lewis and Schrefler, 1987) is a special case of the model.

In adopting Mixture-Coupling theory, the representative elementary volume (REV), comprising solid, water, and gas phases, is considered within a soil or rock matrix (Figure 4.1). The volume of this domain is denoted as Ω, with its boundary (Γ) attached to the solid phase. Consequently, only fluid movement, such as water and gas, occurs across the domain boundary. Unlike the saturated case discussed in Chapter 3, the influence of air is now accounted for, with the pore fluid pressure (p_{pore}) on the solid being a combination of air and water pressures. The hydration swelling effect remains similar to that in Chapter 3.

DOI: 10.1201/9780429324925-4

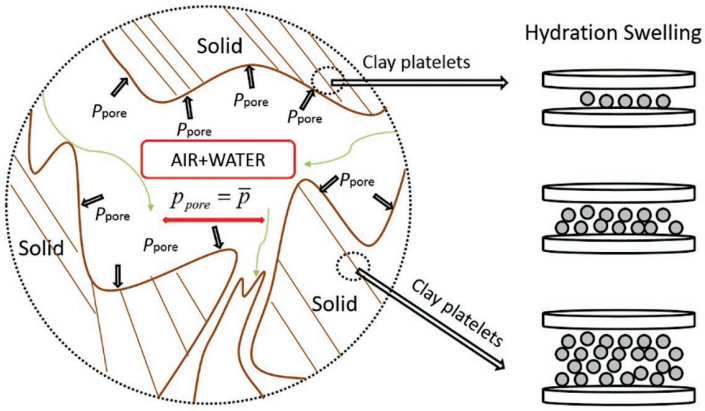

FIGURE 4.1 Conceptual model

4.2 ENERGY IN THE MIXTURE

The balance equation for the Helmholtz free energy density for two-phase coupled flow is

$$\frac{d}{dt}\int_V \psi\, dV = \int_\Gamma \boldsymbol{\sigma}\mathbf{v}_s \cdot \mathbf{n} d\Gamma - \int_\Gamma \mu_w \mathbf{I}_w \cdot \mathbf{n}\, d\Gamma - \int_\Gamma \mu_g \mathbf{I}_g \cdot \mathbf{n}\, d\Gamma - T\int_V \gamma\, dV \tag{4.1}$$

where μ_g is the chemical potential of the gas (i.e., air) and $\mathbf{I}_g$ is the mass flux of the gas defined as

$$\mathbf{I}_g = \rho_g(\mathbf{v}_g - \mathbf{v}_s) \tag{4.2}$$

where ρ_g is the mass density of the gas and $\mathbf{v}_g$ is the velocity of the gas.

Compared with equation (3.1) for the Helmholtz free energy density for the saturated condition, the new terms are the gas-related term $\mathbf{I}_g$ and the gas potential μ_g. To simplify the discussion and allow comparison with the mathematical equation derived using the mechanics approach, it is assumed that the air phase is continuous in the unsaturated zone and remains at atmospheric pressure, $p_{atm} = 0$ (Neuman, 1975; Safai and Pinder, 1979). Since gas transport has not been considered here, $\mathbf{I}_g = 0$, so that the derivative version of the balance equation for the free energy density can be expressed as

$$\dot{\psi} + \psi\nabla\cdot\mathbf{v}_s - \nabla\cdot(\boldsymbol{\sigma}\mathbf{v}_s) + \nabla\cdot(\mu_w\mathbf{I}_w) = -T\gamma \le 0 \tag{4.3}$$

4.3 DISSIPATIVE PROGRESS AND UNSATURATED DARCY'S LAW

By neglecting gas transport and assuming only a single dissipation mechanism at the solid/fluid boundary when water moves through the porous skeleton, a macroscopic expression for the dissipation can be obtained by using standard arguments of nonequilibrium thermodynamics (Katachalsky and Curran, 1965):

$$0 \le T\gamma = -\mathbf{I}_w \cdot \nabla \mu_w \tag{4.4}$$

The driving force of $\mathbf{I}_w$ is the gradient of the chemical potential μ_w. Since μ_w is not commonly used in geotechnical engineering, the relationship between μ_w and the water pressure p_w can be established by using the Gibbs-Duhem equation for the pore fluid, which leads to

$$\nabla \mu_w = \frac{\nabla p_w}{\rho_l^w} \tag{4.5}$$

$\mathbf{I}_w$ links to the Darcy velocity through the definition

$$\mathbf{u} = S_w \phi (\mathbf{v}_w - \mathbf{v}_s) \tag{4.6}$$

which leads to

$$\mathbf{I}_w = \rho_l^w \mathbf{u} \tag{4.7}^1$$

Substitution of equations (4.7) and (4.5) into equation (4.4) leads to a reformed dissipation equation with Darcy's velocity and its corresponding driving force ∇p_w:

$$0 \le T\gamma = -\mathbf{u} \cdot \nabla p_w \tag{4.8}$$

Equation (4.8) is different from equation (3.6) because of the saturation ratio influence. Next, using phenomenological equations (Case, 1994) for the water flow and the corresponding driving force, the unsaturated Darcy's law can be derived as

$$\mathbf{u} = -k \frac{k_{rw}}{v} (\nabla p_w) \tag{4.9}^2$$

where $k \dfrac{k_{rw}}{v} = \dfrac{L_{11}}{(\rho_l^w)^2}$ and k_{rw} is the relative permeability.

4.4 CONSTITUTIVE RELATIONS: SWELLING GEOMATERIALS

In this section, the constitutive equations for the stress and strain response of unsaturated swelling geomaterials (e.g., hydration swelling rock) can be formulated. The same process as followed in Chapter 3 for swelling materials will be adopted. In the material, water resides between individual clay platelets and in the pore space (the gas effect in the clay platelets has not been considered here). Water in the pores is not strongly influenced by intermolecular forces and surface forces, because the pore dimensions are much larger than the distances within which the intermolecular forces are active (Israelachvili, 1991). Hence, bulk fluids in pores can follow thermodynamic relations. Note that multiple chemicals may be involved in the swelling process in real applications (Heidug and Wong, 1996), which can be included in the general structure of the theory.

4.4.1 Free energy evolution path of the mixture

This section is to obtain the balance equation of the free energy density of the mixture system at current configuration and reference configuration.

4.4.1.1 Current configuration

It is assumed that the geomaterial maintains mechanical equilibrium so that $\nabla \cdot \boldsymbol{\sigma} = \mathbf{0}$. Substituting the entropy production equation (4.4) into the Helmholtz free energy density balance equation (4.3), the equation for ψ is

$$\dot{\psi} + \psi \nabla \cdot \mathbf{v}_s - \left(\boldsymbol{\sigma} : \nabla \mathbf{v}_s\right) + \mu_w \nabla \cdot \mathbf{I}_w = 0 \tag{4.10}$$

4.4.1.2 Reference configuration

Multiplying by J, the determinant of the deformation gradient, on both sides of equation (4.10), and using the same process of continuum mechanics as in equations (3.13)–(3.15) (refer to Section 3.4.1), the balance of the Helmholtz free energy density in the reference configuration can be obtained as

$$\dot{\Psi} = tr(\mathbf{T}\dot{\mathbf{E}}) + \mu_w \dot{\rho}_{w,ref} \tag{4.11}$$

where

$$\Psi = J\psi, \; \rho_{w,ref} = J\rho_w = JS_w \phi \rho_l^w \tag{4.12}$$

Compared to equation (3.17), a saturation term (S_w) has been included. Therefore, equation (3.17) represents a specific case of equation (4.12) under the saturated condition ($S_w = 1$). The mechanical deformation is included in equation (4.11).

4.4.2 Helmholtz free energy density of pore water and wetted solid matrix

4.4.2.1 Current configuration (pore water)

The water mass density per unit fluid volume is denoted as ρ_l^{pore} ($\rho_l^{pore} \leq \rho_l^w$, as some water has been absorbed into the clay platelets, see Section 3.4.2), and the Helmholtz free energy density of the pore water is denoted as ψ_{pore}. Based on classical thermodynamics and ignoring gas (i.e., air) chemical potential influence (i.e. $\mu_g \approx 0$), using equation (2.18), the free energy density of the pore fluid can be written as

$$\psi_{pore} = -p_{pore} + S_w \rho_l^{pore} \mu_w \tag{4.13}$$

According to the Gibbs-Duhem equation (2.23) for constant temperature, the relationship between the time derivative of pore pressure and chemical potential can be obtained as

$$\dot{p}_{pore} = S_w \rho_l^{pore} \dot{\mu}_w \tag{4.14}$$

Substituting equation (4.14) into the time derivative of equation (4.13) as

$$\dot{\psi}_{pore} = -\dot{p}_{pore} + \dot{\mu}_w S_w \rho_l^{pore} + \mu_w (S_w \rho_l^{pore}\dot{}) \tag{4.15}$$

it can be concluded that

$$\dot{\psi}_{pore} = \mu_w (S_w \rho_l^{pore}\dot{}) \tag{4.16}$$

which gives the relationship between $\dot{\psi}_{pore}$ and the water content within the pores $S_w \rho_l^{pore}$.

4.4.2.2 Reference configuration (wetted solid matrix)

The free energy density of the unsaturated "wet" solid matrix includes fluid "bound" between the platelets, which follows the principle of molecular forces other than nonequilibrium thermodynamics. Hence,

the free energy density can be obtained by subtracting from the combined solid/fluid system (the total free energy density Ψ) the contribution $J\phi\psi_{pore}$ due to the pore fluids (e.g., water and gas). $\upsilon = J\phi$ is the pore volume per unit reference volume, and $\rho_{bound,ref} = \rho_{w,ref} - JS_w\phi\rho_l^{pore}$ is the reference mass density of the bound water. Note: The air (or gas) may have an influence on the free energy density. The void space is considered; however, its mass density is ignored in this chapter to simplify the discussion ($\rho_g^g \ll \rho_l^w$). Such influence may be accounted for multiphase flow (e.g., gas and liquid).

The time derivative of the free energy density density of the wetted solid matrix (i.e., $\Psi - J\phi\psi_{pore}$) is then described as

$$(\Psi - J\phi\psi_{pore})^{\cdot} = \dot{\Psi} - \upsilon\dot{\psi}_{pore} - \psi_{pore}\dot{\upsilon} \tag{4.17}^3$$

Substitution of equations (4.13) for ψ_{pore}, (4.16) for $\dot{\psi}_{pore}$, and (4.11) for $\dot{\Psi}$ into equation (4.17) leads to the time derivative of the free energy density of the wetted solid matrix:

$$(\Psi - J\phi\psi_{pore})^{\cdot} = tr(\mathbf{T}\dot{\mathbf{E}}) + \mu_w\dot{\rho}_{bound,ref} + p_{pore}\dot{\upsilon} \tag{4.18}^4$$

4.4.3 Constitutive structure

The free energy density of the wetted matrix in the unsaturated condition includes (1) the bounded water on the surface of the solids or between fine grains, (2) the molecules in the clay platelets, and (3) the deformation potential. The deformation potential density can be expressed as

$$W = (\Psi - J\phi\psi_{pore}) - p_{pore}\upsilon - \mu_w\rho_{bound,ref} \tag{4.19}$$

Substituting equation (4.18) into the time derivative of equation (4.19) leads to

$$\dot{W} = tr(\mathbf{T}\dot{\mathbf{E}}) - \dot{p}_{pore}\upsilon - \dot{\mu}_w\rho_{bound,ref} \tag{4.20}^5$$

where W is a function of $\mathbf{E}$, p_{pore}, and μ_w, so that expressions for $\mathbf{T}$, υ, and $\rho_{bound,ref}$ can be obtained as

$$T_{ij} = \left(\frac{\partial W}{\partial E_{ij}}\right)_{p_{pore},\mu_w}, \quad \upsilon = -\left(\frac{\partial W}{\partial p_{pore}}\right)_{E_{ij},\mu_w}, \quad \rho_{bound,ref} = -\left(\frac{\partial W}{\partial \mu_w}\right)_{E_{ij},p_{pore}} \tag{4.21}$$

Equation (4.20) can be rewritten as

$$\dot{W}(\mathbf{E}, p_{pore}, \mu) = \left(\frac{\partial W}{\partial E_{ij}}\right)_{p_{pore},\mu_w} \dot{E}_{ij} + \left(\frac{\partial W}{\partial p_{pore}}\right)_{E_{ij},\mu_w} \dot{p}_{pore} + \left(\frac{\partial W}{\partial \mu_w}\right)_{E_{ij},p_{pore}} \dot{\mu}_w \tag{4.22}$$

or

$$\dot{W}(\mathbf{E}, p_{pore}, \mu_w) = T_{ij}\dot{E}_{ij} - \upsilon \dot{p}_{pore} - \rho_{bound,ref}\dot{\mu}_w \tag{4.23}$$

If equation (4.21) is differentiated with respect to time, the fundamental constitutive equations for the evolution of stress, pore volume fraction, and mass densities in the bound water can be obtained (Appendix 3):

$$\dot{T}_{ij} = L_{ijkl}\dot{E}_{kl} - M_{ij}\dot{p}_{pore} + S_{ij}\dot{\mu}_w \tag{4.24}$$

$$\dot{\upsilon} = M_{ij}\dot{E}_{ij} + Q\dot{p}_{pore} + B\dot{\mu}_w \tag{4.25}$$

$$\dot{\rho}_{bound,ref} = -S_{ij}\dot{E}_{ij} + B\dot{p}_{pore} + Z\dot{\mu}_w \tag{4.26}$$

In a matrix form, these equations can be written as

$$\begin{bmatrix} \dot{T}_{ij} \\ \dot{\upsilon} \\ \dot{\rho}_{bound,ref} \end{bmatrix} = \begin{bmatrix} L_{klij} & -M_{ij} & S_{ij} \\ M_{ij} & Q & B \\ -S_{ij} & B & Z \end{bmatrix} \begin{bmatrix} \dot{E}_{ij} \\ \dot{p}_{pore} \\ \dot{\mu}_w \end{bmatrix} \tag{4.27}$$[6]

where the parameters L_{ijkl}, M_{ij}, S_{ij}, Z, B, and Q are expressed as follows (see equation (3.38) for details):

$$L_{ijkl} = \left(\frac{\partial T_{ij}}{\partial E_{kl}}\right)_{p_{pore},\mu_w} = \left(\frac{\partial T_{kl}}{\partial E_{ij}}\right)_{p_{pore},\mu_w} = L_{klij},\ M_{ij} = -\left(\frac{\partial T_{ij}}{\partial p_{pore}}\right)_{E_{ij},\mu_w} = \left(\frac{\partial \upsilon}{\partial E_{ij}}\right)_{p_{pore},\mu_w}$$

$$S_{ij} = -\left(\frac{\partial T_{ij}}{\partial \mu_w}\right)_{E_{ij},p_{pore}} = -\left(\frac{\partial \rho_{bound,ref}}{\partial E_{ij}}\right)_{p_{pore},\mu_w},\ Z = \left(\frac{\partial \rho_{bound,ref}}{\partial \mu_w}\right)_{E_{ij},p_{pore}}$$

$$B = \left(\frac{\partial \upsilon}{\partial \mu}\right)_{E_{ij},p_{pore}} = \left(\frac{\partial \rho_{bound,ref}}{\partial p_{pore}}\right)_{E_{ij},\mu_w},\ Q = \left(\frac{\partial \upsilon}{\partial p_{pore}}\right)_{E_{ij},\mu_w} \tag{4.28}$$

4.5 COUPLED FIELD EQUATIONS

4.5.1 Solid phase and porosity

The constitutive equations (4.24) and (4.25) define the alteration in solid stress and volume fraction. Following the same assumptions of physical and geometrical linearization, and also small strain, as in Chapter 3, as well as the condition of mechanical equilibrium $\partial\sigma_{ij} / \partial x_j = 0$, equations (4.24) and (4.25) can be changed to

$$\dot{\sigma}_{ij} = \left(K - \frac{2G}{3} \right) \dot{\varepsilon}_{kk}\delta_{ij} + 2G\dot{\varepsilon}_{ij} - \zeta\, \dot{p}_{pore}\delta_{ij} + \omega\dot{\mu}_w\delta_{kl} \tag{4.29}$$

$$\dot{\upsilon} = \zeta\dot{\varepsilon}_{ii} + Q\dot{p}_{pore} + B\ \dot{\mu}_w \tag{4.30}$$

where $\varepsilon_{ij} = \frac{1}{2}(d_{i,j} + d_{j,i})$ and $d_i (i = 1, 2, 3)$ is the displacement component (Note here: The detailed discussion and derivation of the parameters can be found in Section 3.5.1).)

By comparing these equations with the constitutive equations (3.67) and (3.68) for the saturated condition, the water pressure p_w is replaced by the average pressure p_{pore}, which considers the influence of unsaturation. The chemical potential of water μ_w remains the same, even though the relationship with p_{pore} has been changed using equation (4.14), leading to

$$\dot{\mu}_w = \left(\frac{1}{S_w \rho_l^w} \right) \dot{p}_{pore} \tag{4.31}$$

Hence, using equation (4.31), the stress equation (4.29) can be rewritten as

$$\dot{\sigma}_{ij} = \underbrace{(K - \frac{2G}{3})\dot{\varepsilon}_{kk}\delta_{ij} + 2G\dot{\varepsilon}_{ij}}_{1} - \underbrace{(\zeta - \frac{\omega}{S_w \rho_l^w})\dot{p}_{pore}\delta_{ij}}_{2} \tag{4.32}$$

and the porosity evolution equation (4.30) can be changed to

$$\dot{\upsilon} = \underbrace{\zeta\dot{\varepsilon}_{ii}}_{3} + \underbrace{\left(Q + B\ (\frac{1}{S_w \rho_l^w}) \right)}_{4} \dot{p}_{pore} \tag{4.33}$$

Compared with equations (4.29) and (4.30), equations (4.32) and (4.33) have fewer variables (i.e., removing $\dot{\mu}_w$ from the equations) and are more convenient to use in geotechnical engineering.

The physical meanings of the terms in equations (4.32) and (4.33) are as follows:

- 1: This term represents the elastic deformation of the solids.
- 2: This is the coupling term, which describes the influence of water pressure on the deformation of the solids, incorporating the swelling term $\frac{\omega}{S_w \rho_l^w}$. The pore pressure p_{pore} here includes the impact of the saturation ratio within the pores, which differentiates it from equation (3.67).
- 3: This term represents the change in porosity induced by deformation.
- 4: This term represents the pressure-induced porosity change, with the influence of swelling (i.e., the term $B\left(\frac{1}{S_w \rho_l^w}\right)$) included.
- Key novelties: Terms 2 and 4 provide a comprehensive consideration of the swelling influence.

4.5.2 Fluid phase

The balance equation for the water mass is (refer to Section 2.3)

$$\dot{\rho}_w + \rho_w \nabla \cdot \mathbf{v}_s + \nabla \cdot \mathbf{I}_w = 0 \tag{4.34}$$

Since ρ_w is related to the in-phase mass density ρ_l^w through

$$\rho_w = \phi_w \rho_l^w$$

where ϕ_w is the volume fraction of the water, and since the relationship between ϕ_w and the porosity of the medium ϕ is

$$\phi_w = S_w \phi$$

equation (4.34) can be derived as

$$(\rho_l^w \phi S_w)^{\cdot} + \rho_l^w \phi S_w \nabla \cdot \mathbf{v}_s + \nabla \cdot \left(\rho_l^w \phi S_w (\mathbf{v}_l - \mathbf{v}_s)\right) = 0 \tag{4.35}$$

Substitution of the Darcy velocity (equation (1.20))

$$\mathbf{u} = S_w \phi (\mathbf{v}_l - \mathbf{v}_s)$$

into equation (4.35) leads to

$$(\rho_l^w \phi S_w)^{\cdot} + \rho_l^w \phi S_w \nabla \cdot \mathbf{v}_s + \nabla \cdot \left(\rho_l^w \mathbf{u}\right) = 0 \tag{4.36}$$

By multiplying both sides of equation (4.36) by J, and using the Euler identity as

$$\dot{J} = J \nabla \cdot \mathbf{v}_s \text{ and } \upsilon = J\phi,$$

this leads to

$$(S_w \upsilon \rho_l^w)^{\cdot} + \nabla \cdot (\rho_l^w \mathbf{u}) = 0^{7}$$

or

$$\upsilon (S_w \rho_l^w)^{\cdot} + S_w \rho_l^w \dot{\upsilon} + \nabla \cdot (\rho_l^w \mathbf{u}) = 0 \tag{4.37}$$

From equation (4.37), substituting equation (4.30) for υ and equation (4.9) for $\mathbf{u}$ leads to

$$\underbrace{\upsilon (S_w \rho_l^w)^{\cdot}}_{5} + \underbrace{S_w \rho_l^w \left[\zeta \dot{\varepsilon}_{ii} + Q \dot{p}_{pore} + B\ \dot{\mu}_w\right]}_{6} + \underbrace{\nabla \cdot (\rho_l^w \left[-k \frac{k_{rw}}{v} \nabla p_w\right])}_{7} = 0 \tag{4.38}$$

The physical meanings of the terms in equation (4.38) are:

- 5: This term represents the influence of water density and the variation in saturation ratio on water transport.
- 6: This term describes the effect of changes in porosity—due to deformation, water pressure, and the chemical potential of water in the clay platelets—on water transport.
- 7: This term represents Darcy's law, incorporating the effects of water density and the unsaturated conditions.

4.6 NUMERICAL SIMULATION

Equation (1.41) provides the relationship of average pressure and pore pressure. Since the average pressure $\overline{p}$ can be simplified by ignoring the gas pressure as

$$\overline{p} = S_w p_w \tag{4.39}$$

and its time derivative as

$$\dot{\bar{p}} = S_w \dot{p}_w + \dot{S}_w p_w = S_w \frac{\partial p_w}{\partial t} + \frac{\partial S_w}{\partial p_w}\frac{\partial p_w}{\partial t} p_w \tag{4.40}$$

The specific moisture content defined in terms of pressure can be described as

$$C_s^p = \frac{\partial S_w}{\partial p_w}\phi$$

or

$$\frac{\partial S_w}{\partial p_w} = \frac{\phi}{C_s^p} \tag{4.41}$$

Substituting equation (4.41) into equation (4.40) leads to (Lewis and Schrefler, 1987)

$$\dot{\bar{p}} = S_w \frac{\partial p_w}{\partial t} + \frac{C_s^p}{\phi} p_w \frac{\partial p_w}{\partial t} = (S_w + \frac{C_s^p}{\phi} p_w)\frac{\partial p_w}{\partial t} \tag{4.42}$$

The rate of change of saturation function and the rate of change of water density function $\phi(S_w \rho_l^w)^{\cdot}$ can be defined as (Lewis and Schrefler, 1987)

$$\phi(S_w \rho_l^w)^{\cdot} = \phi \rho_l^w \frac{\partial S_w}{\partial t} + \phi S_w \frac{\partial \rho_l^w}{\partial t} = \rho_l^w (C_s^p + \phi \frac{S_w}{K_w})\frac{\partial p_w}{\partial t} \tag{4.43)[8]}$$

where K_w is the bulk modulus of water (liquid) which can be defined as $K_w = \rho_l^w \dfrac{\partial p_w}{\partial \rho_l^w}$.

If the chemicals do not strongly affect p_w (in the absence of chemical reaction), the above equations (4.39)~(4.43) can be applied to the dilute chemical fluid for p_l (defined as the liquid pressure and $p_l \cong p_w$).

4.6.1 Mathematical equation

Mechanical: By using equation (4.42) for $\dot{\bar{p}}$, and the relationship between ε_{ij} and $d_{i,j}$, equation (4.32) can be rewritten as

$$\begin{aligned}(K - \frac{2G}{3})\frac{\partial^2 \dot{d}_k}{\partial x_k \partial x_i} + G\left(\frac{\partial^2 \dot{d}_i}{\partial x_j \partial x_j} + \frac{\partial^2 \dot{d}_j}{\partial x_i \partial x_j}\right) - \\ (\zeta - \frac{\omega}{S_w \rho_l^w})\nabla\left[(S_w + \frac{C_s^p}{\phi} p_w)\dot{p}_w\right] = 0\end{aligned} \tag{4.44}$$

Hydro: Considering the strain and displacement relationship, equation (4.38) can be written as

$$S^w \rho_l^w \zeta \nabla \cdot \dot{\mathbf{d}} + S_w \rho_l^w (Q + B / \rho_l^w) \dot{\bar{p}} + \phi (S_w \rho_l^{w\cdot}) + \rho_l^w \left[-k \frac{k_{rw}}{v} \nabla^2 p_w \right] = 0 \tag{4.45}$$

Using equations (4.42) and (4.43), equation (4.45) can be derived as

$$\begin{aligned} -k \frac{k_{rw}}{v} \nabla^2 p_w + (C_s^p + \phi \frac{S_w}{K_w}) \frac{\partial p_w}{\partial t} + S_w (Q + B / \rho_l^w) \\ (S_w + \frac{C_s^p}{\phi} p_w) \frac{\partial p_w}{\partial t} + S_w \zeta \nabla \cdot \dot{\mathbf{d}} = 0 \end{aligned} \tag{4.46}$$

Equation (4.46) can be arranged as

$$\begin{aligned} -k \frac{k_{rw}}{v} \nabla^2 p_w + \left[(C_s^p + \phi \frac{S_w}{K_w}) + S_w (Q + B / \rho_l^w)(S_w + \frac{C_s^p}{\phi} p_w) \right] \\ \frac{\partial p_w}{\partial t} + S_w \zeta \nabla \cdot \dot{\mathbf{d}} = 0 \end{aligned} \tag{4.47}$$

in which

$$(C_s^p + \phi \frac{S_w}{K_w}) + S_w (Q + B / \rho_l^w)(S_w + \frac{C_s^p}{\phi} p_w) \approx Q S_w^2 + \phi \frac{S_w}{K_w} \tag{4.48}$$

can be obtained through the following assumptions: (1) the term $(Q + B / \rho_l^w)$ can be simplified to Q as discussed in Section 3.5.1.2; (2) C_s^p is assumed to be zero.

Hence, equation (4.47) becomes

$$-k \frac{k_{rw}}{v} \nabla^2 p_w + q S_w^2 \frac{\partial p_w}{\partial t} + S_w \zeta \nabla \cdot \dot{\mathbf{d}} = 0 \tag{4.49}$$

The interations between degree of saturation, pressure, and relative permeability are characterized by the van Genuchten relationship in Section 1.3.1 (van Genuchten, 1980). Since p_{atm} is assumed to be zero leading to $p_c = -p_w$, S_r is assumed to be zero leading to $S_w = S_e$, equation (1.44) becomes

$$S_w = \left[\left(-p_w / M \right)^{\frac{1}{(1-m)}} + 1 \right]^{-m} \tag{4.50}$$

and the relative permeability can be described as

$$k_{rw} = (S_w)^{0.5}\left[1-\left(1-(S_w)^{\frac{m}{m-1}}\right)^{\frac{m-1}{m}}\right]^2 \tag{4.51}$$

where m and M are material constants, e.g., as 0.18 and 20 MPa, respectively, for the sample rock used in this book for the numerical examples in Chapters 4–7 (Wild et al., 2015).

4.6.2 Discussion and comparison

The coupled equations (4.44) and (4.46) can be compared with non-swelling unsaturated hydro-mechanical coupled equations derived by the mechanics approach, which have been tested by a number of researchers (Lewis and Schrefler, 1987). Without considering hydration swelling, equations (4.44) and (4.46) can be reduced to the classic equations from the mechanics approach (Lewis and Schrefler, 1987). The differences are the swelling term in equation (4.44), $\frac{\omega}{S_w \rho_l^w}$, and the flow buffer term B / ρ_l^w in equation (4.46), and these two terms need to be determined by experiments.

The key identification of two stress state variables for unsaturated soil mechanics are matric suction $(p_g - p_w)$ and net normal stress $(\sigma_{ij} - \delta_{ij} p_g)$, which govern the soil behavior (Fredlund and Rahardjo, 1993). They are not used in the derivation process, although they can be obtained through the final equations (4.44) and (4.46), in which the net normal stress has been extended by including molecule-induced swelling.

4.6.3 Model geometry and boundary conditions

The conceptual model and the geomaterial parameters are similar to those used in Chapter 3, apart from some modified parameters as in Table 4.1, and different initial conditions and boundary conditions.

Boundary conditions: Boundary B is fixed (displacement = 0), whereas boundary A is free to move. Both boundaries B and A are permeable (free draining).

Initial conditions: An equilibrium state is assumed at $t = 0$, with an external force at boundary A to maintain the equilibrium (the initial effective stress is assumed to be 0 initially). The water pressure is $p_w = -5$ MPa ($t = 0$) under the unsaturated condition.[9]

TABLE 4.1
Additional parameters for numerical simulation

Parameters	Physical meaning	Values and units
ϕ	Porosity	0.41
m	van Genuchten parameter	0.18
M	van Genuchten parameter	20 MPa

Start of the simulation: The pore water pressure at the fixed boundary B is decreased to −10 MPa (t >0), and the pore water pressure at free boundary A is maintained at −5 Mpa. The external load at boundary A remains the same as it was in the equilibrium condition.

4.6.4 Numerical simulation results

Figure 4.2 illustrates the evolution of pore water pressure in both swelling and non-swelling geomaterials. As discussed in Chapter 3, the influence of water in the clay platelets is assumed to be negligible on the absolute permeability, simplifying the simulation (note: porosity changes are accounted for using equation (4.30)). As a result, the absolute permeability is treated as constant throughout the simulation. This assumption leads to very similar pore water pressure profiles for both swelling and non-swelling geomaterials, as shown in the figure.

The label "Lewis" refers to the numerical simulation based on the classical unsaturated hydro-mechanical model (Lewis and Schrefler, 1987), while "swelling" refers to the simulation results derived from the model developed in this chapter. Notably, the pore water pressures for the swelling geomaterials are slightly lower than those for the non-swelling geomaterials. This difference occurs because the swelling effect reduces the buildup of pore pressure. As the material swells, it expands due to the absorption of water, which dampens the increase in pore pressure compared to the non-swelling material, where the absence of swelling leads to a greater pressure buildup.

Additionally, when the pressure at boundary B drops to −10 MPa, water begins to flow out of the system, influencing the saturation levels, as depicted in Figure 4.3. This change in saturation follows a trend very

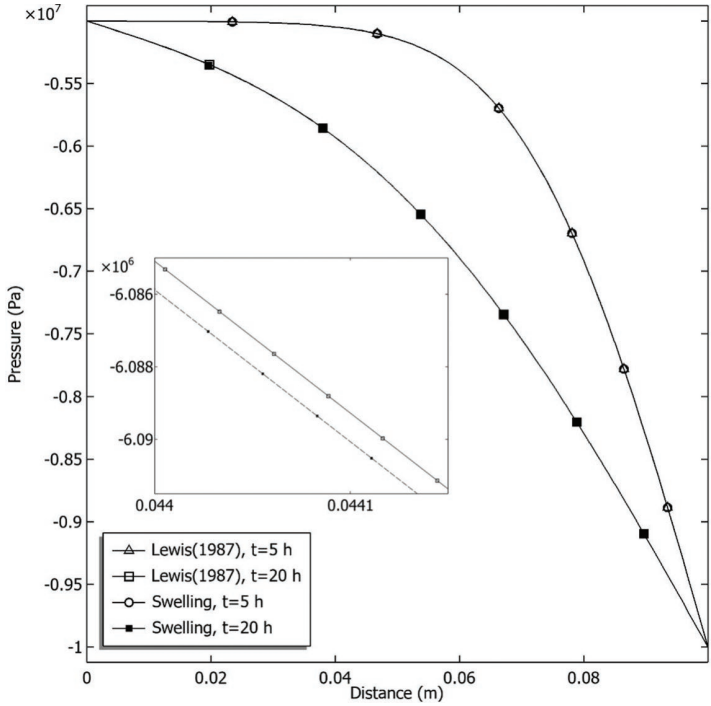

FIGURE 4.2 Evolution of pore water pressure with time

similar to the pore water pressure profile in Figure 4.2, as governed by the van Genuchten relationship. The saturation decreases in response to the pressure drop, reflecting the interconnected nature of pressure and saturation in unsaturated soils and the complex interactions between the water and solid phases within the material. This analysis underscores the importance of swelling effects in modulating both the pore pressure and saturation in porous materials, and highlights the significance of incorporating these effects into models for accurate predictions of geotechnical behavior.

Figures 4.4 and 4.5 illustrate the evolution of effective stress and horizontal displacement, respectively, showing a clear consolidation process. The effective stress increases over time due to the pressure gradient, which drives the movement of water and leads to

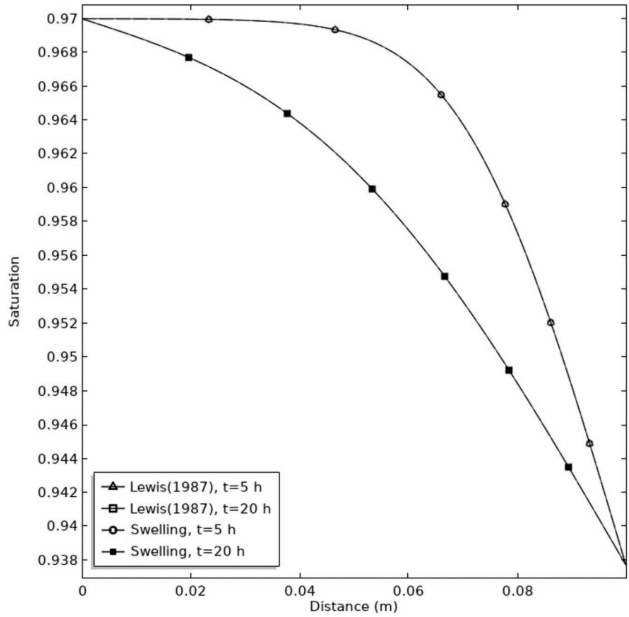

FIGURE 4.3 Evolution of saturation with time

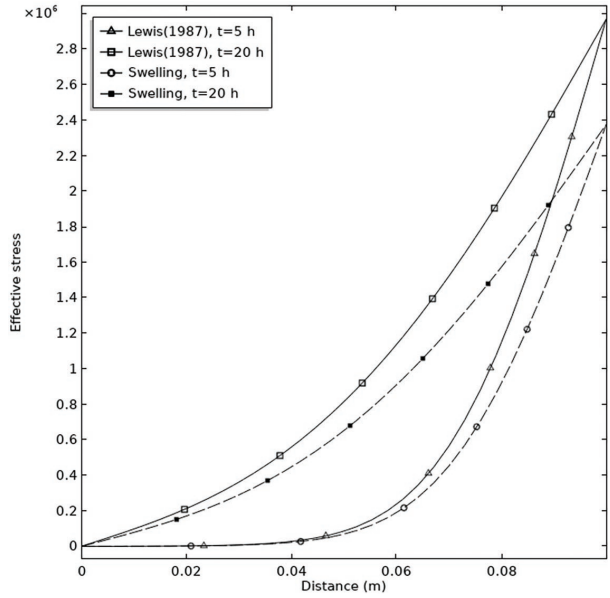

FIGURE 4.4 Evolution of effective stress with time

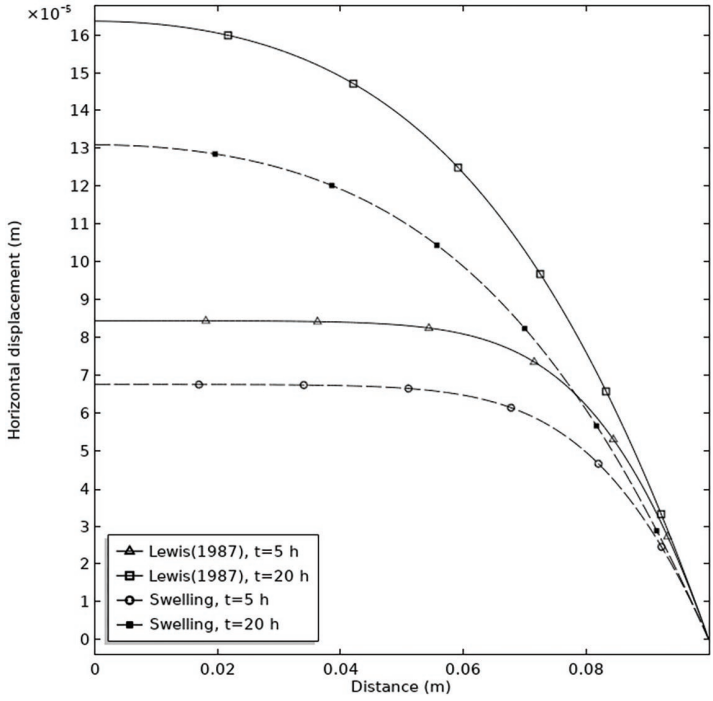

FIGURE 4.5 Evolution of horizontal displacement with time

the consolidation of the geomaterial. As the degree of saturation in the system is very high, the mechanical behavior observed is very similar to that of a saturated condition, as discussed in Chapter 3. However, despite this similarity, there is a notable physical deformation change induced by saturation, which is particularly evident in the swelling geomaterial.

The inclusion of molecular-scale swelling effects in the constitutive model presented in this chapter significantly enhances the understanding of the material's behavior. This model successfully incorporates the swelling influence at the molecular level, which, in turn, reduces the overall deformation compared to the classic unsaturated hydro-mechanical model (Lewis and Schrefler, 1987). In the classic model, the absence of molecular-scale effects such as swelling leads to a larger deformation response under similar conditions.

The incorporation of swelling at the molecular scale in this chapter allows for a more accurate representation of real-world behaviors in unsaturated soils and rocks, where swelling can significantly affect the material's response to changes in pore pressure and saturation. By considering these molecular influences, the model better captures the complex interactions between the solid matrix, pore water, and gas, offering a more comprehensive approach to modeling unsaturated porous media. This refinement is crucial for addressing engineering challenges such as soil expansion, land subsidence, and other phenomena where swelling plays a critical role.

4.7 CONCLUSION

This chapter introduced the theoretical framework of Mixture-Coupling theory applied to unsaturated soils and rocks, providing a coupled model that considers the intricate interactions between the solid matrix, pore water, and air. By incorporating molecular-level effects, such as swelling processes, this model presents a more comprehensive and flexible approach compared to traditional geotechnical models. The integration of these molecular influences allows for a more accurate representation of unsaturated soil behavior, offering a foundation for further advancements in the field of geotechnical engineering.

The model developed in this chapter demonstrates that the coupled interactions between the solid matrix and pore fluids are critical in accurately capturing the behavior of unsaturated materials. This approach extends beyond traditional models by addressing the complexities of molecular interactions, which are often overlooked in standard geotechnical models. Furthermore, the model provides a robust platform for future research into the behavior of unsaturated soils and rocks, paving the way for more refined and predictive modeling in practical engineering applications, such as land subsidence, slope stability, and the design of foundations in unsaturated conditions.

Looking forward, Chapter 5 will build upon the insights presented here by exploring the chemical influences on very low permeability geomaterials, such as clays and shales, which can act as semipermeable membranes. These materials are crucial in applications like landfills and waste disposal, where solute migration is a concern. In such materials, the interaction between chemical diffusion and water flow can lead to chemical osmotic flow, which is not accounted for by Darcy's law.

NOTES

1 $\mathbf{I}_w = \rho_w(\mathbf{v}_w - \mathbf{v}_s) = \phi S_w \rho_l^w(\mathbf{v}_w - \mathbf{v}_s) = \rho_l^w \mathbf{u}$.

2 Equation (4.8) can be reorganized in the form of flow and the corresponding driving force as $0 \le T\gamma = \rho_l^w \mathbf{u} \cdot \left(-\frac{\nabla p_w}{\rho_l^w}\right)$. Using the phenomenological equations leads to $\rho_l^w \mathbf{u} = L_{11}\left(-\frac{\nabla p_w}{\rho_l^w}\right)$, and therefore, $\mathbf{u} = -\frac{L_{11}}{\left(\rho_l^w\right)^2}\nabla p_w$ where $\frac{L_{11}}{\left(\rho_l^w\right)^2} = k\frac{k_{rw}}{v}$.

3 $(\Psi - J\phi\psi_{pore})^{\cdot} = (\Psi - \psi_{pore}\upsilon)^{\cdot} = \dot{\Psi} - (\psi_{pore}\upsilon)^{\cdot} = \dot{\Psi} - \upsilon\dot{\psi}_{pore} - \psi_{pore}\dot{\upsilon}$

4 Substitution of equations (4.13), (4.16), and (4.11) into equation (4.17) leads to

$$
\begin{aligned}
&(\Psi - J\phi\psi_{pore})^{\cdot} = \dot{\Psi} - \upsilon\dot{\psi}_{pore} - \psi_{pore}\dot{\upsilon} \\
&= \left[tr(\mathbf{T}\dot{\mathbf{E}}) + \mu_w \dot{\rho}_{w,ref}\right] - \upsilon\mu_w(S_w\rho_l^{pore})^{\cdot} - \left[-p_{pore} + S_w\rho_l^{pore}\mu_w\right]\dot{\upsilon} \\
&= tr(\mathbf{T}\dot{\mathbf{E}}) + \mu_w\dot{\rho}_{w,ref} - \upsilon\mu_w(S_w\rho_l^{pore})^{\cdot} + p_{pore}\dot{\upsilon} - \dot{\upsilon}(S_w\rho_l^{pore}\mu_w) \\
&= tr(\mathbf{T}\dot{\mathbf{E}}) + \mu_w\dot{\rho}_{w,ref} - \left[\mu_w(S_w\rho_l^{pore}\upsilon)^{\cdot}\right] + p_{pore}\dot{\upsilon} \\
&= tr(\mathbf{T}\dot{\mathbf{E}}) + \mu_w\dot{\rho}_{bound,ref} + p_{pore}\dot{\upsilon}
\end{aligned}
$$

5 The derivation of equation (4.20) can be described as follows:

$$
\begin{aligned}
&\dot{W}(\mathrm{E}, p_{pore}, \mu_w) = (\Psi - J\phi\psi_{pore})^{\cdot} - (p_{pore}\upsilon)^{\cdot} - (\mu_w\rho_{bound,ref})^{\cdot} \\
&= tr(\mathbf{T}\dot{\mathbf{E}}) + \mu_w\dot{\rho}_{bound,ref} + p_{pore}\dot{\upsilon} - (p_{pore}\upsilon)^{\cdot} - (\mu_w\rho_{bound,ref})^{\cdot} \\
&= tr(\mathbf{T}\dot{\mathbf{E}}) + \mu_w\dot{\rho}_{bound,ref} + p_{pore}\dot{\upsilon} - p_{pore}\dot{\upsilon} - \upsilon(p_{pore})^{\cdot} - \mu_w\dot{\rho}_{bound,ref} - \dot{\mu}_w\rho_{bound,ref} \\
&= tr(\mathbf{T}\dot{\mathbf{E}}) - (p_{pore})^{\cdot}\upsilon - \dot{\mu}_w\rho_{bound,ref}
\end{aligned}
$$

6 In order to write in a matrix form as equation (4.27), $L_{ijkl}\dot{E}_{kl}$ in equation (4.28) is written as $L_{klij}\dot{E}_{ij}$, with the definition of $L_{ijkl} = L_{klij}$ in equation (4.28).

$$\overbrace{J\left(\rho_l^w \phi S_w\right) + \rho_l^w \phi S_w J\nabla \cdot \mathrm{v}_s}^{} + J\nabla \cdot \left(\rho_l^w \mathbf{u}\right) = 0$$

7 The derivation is $\overbrace{J\left(\rho_l^w \phi S_w\right) + \rho_l^w \phi S_w J}^{} + J\nabla \cdot \left(\rho_l^w \mathbf{u}\right) = 0$

$$\overbrace{\left(J\rho_l^w \phi S_w\right)}^{} + J\nabla \cdot \left(\rho_l^w \mathbf{u}\right) = 0$$
$$\left(\upsilon \rho_l^w S_w\right) + J\nabla \cdot \left(\rho_l^w \mathbf{u}\right) = 0$$

As the configuration at any given instant has been selected as the reference configuration, it leads to $J = 1$, although the time derivative of J exists (Euler identity).

$$\phi\left(S_w \rho_l^w\right) = \phi S_w \rho_l^w + \phi S_w \rho_l^w = \phi \rho_l^w \frac{\partial S_w}{\partial t} + \phi S_w \frac{\partial \rho_l^w}{\partial t}$$

8 $$= \rho_l^w \left(\phi \frac{\partial S_w}{\partial t} + \frac{\phi S_w}{\rho_l^w} \frac{\partial \rho_l^w}{\partial t}\right) = \rho_l^w (\phi \frac{\partial S_w}{\partial p_w \partial t} + \frac{\phi S_w}{\rho_l^w} \frac{\partial \rho_l^w}{\partial p_w} \frac{\partial p_w}{\partial t}) =$$

$$\rho_l^w (\underbrace{C_s^p}_{=\phi \frac{\partial s_w}{\partial p_w}} + \phi \frac{S_w}{K_w}) \frac{\partial p_w}{\partial t}$$

where $K_w = \rho_l^w \dfrac{\partial p_w}{\partial p_l^w}$.

9 In classic unsaturated soil theory, an unsaturated zone has mixed air and water, and is above a water table. The pore water pressure is negative mainly due to matric suction (Fredlund and Rahardjo, 1993).

REFERENCES

Case, C. M. (1994) *Physical principles of flow in unsaturated porous media*. Oxford, Oxford University Press Inc.

Fredlund, D. G. & Rahardjo, H. (1993) *Soil mechanics for unsaturated soils*. New York, John Wiley & Sons.

Heidug, W. K. & Wong, S. W. (1996) Hydration swelling of water-absorbing rocks: a constitutive model. *International Journal for Numerical and Analytical Methods in Geomechanics* 20: 403–430.

Israelachvili, J. N. (1991) *Intermolecular and surface forces.* London, Academic Press.

Katachalsky, A. & Curran, P. F. (1965) Nonequilibrium thermodynamics in biophysics. Cambridge, MA, Harvard University Press.

Lewis, R. W. & Schrefler, B. A. (1987) *The finite-element method in deformation and consolidation of porous media*. New York, Wiley.

Neuman, S. P. (1975) Galerkin approach to saturated–unsaturated flow in porous media. In Finite elements in fluids. (Gallagher, R. H., Oden, J. T., Taylor, C., andZienkiewicz, O. C. (eds)) New York, John Wiley & Sons, vol. 1.

Safai, N. M. & Pinder, G. F. (1979) Vertical and horizontal land deformation in a desaturating porous medium. Advances in Water Resources 2: 19–25.

Van Genuchten, M. T. (1980) A closed-form equation for predicting the hydraulic conductivity of unsaturated soils. Soil Science Society of America Journal 44: 892–898.

Wild, K. M., Wymann, L. P., Zimmer, S., Thoeny, R. & Amann, F. (2015) Water retention characteristics and state-dependent mechanical and petro-physical properties of a clay shale. Rock Mechanics and Rock Engineering 48**(2)**: 427–439.v

5 Unsaturated hydro-mechanical-chemical coupled modeling with chemical osmosis

5.1 INTRODUCTION

Very low permeable soils and rocks (e.g., clays or shales) can act as actual semipermeable membranes and restrict the migration of large solute molecules. Such membrane-like materials have many engineering applications, such as in landfills and waste disposal. Solute transport in the engineered barrier may result in chemical osmotic flow. The water flow direction is from a lower to a higher chemical concentration. Such a flow is not accounted for by Darcy's law, which is the foundation of much of the existing software used in hydrogeology and groundwater modeling. Hence, false or unrealistic predictions of transient flow may occur in some situations.

This chapter will discuss the dynamical interactions between chemical diffusion driven by chemical concentration and water flow driven by water gradient using Mixture-Coupling Theory, presenting a new hydro-mechanical-chemical coupled model. This chapter demonstrates that Darcy's law is not applicable for predicting chemical osmotic flow in very low permeability geomaterials, and the well-recognized Lewis's unsaturated hydro-mechanical coupled model (Lewis and Schrefler, 1987) is a special case of the model without considering chemical influence (Chen and Hicks, 2013; Chen et al., 2016).

Figure 5.1 shows the representative elementary volume (REV) with air, water, and chemicals in the pores, and a combination of microchannels and macrochannels through the solids. The pore pressure is generated by a combination of air pressure and water (and chemical) pressure. The micro channels may allow small molecules (e.g., water

DOI: 10.1201/9780429324925-5

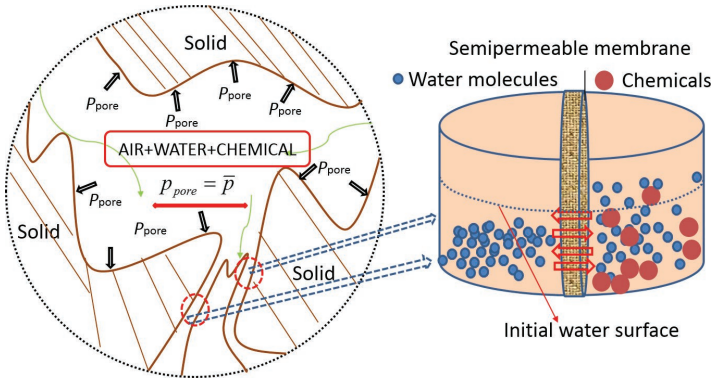

FIGURE 5.1 Conceptual model

molecules) to breakthrough, however, block large molecules (e.g., chemicals). As the actual flux is a combination of flux through both micro- and macro-channels, such materials are regarded as an actual semipermeable membrane.

To focus on the osmosis function and simplify the discussion, this chapter will not include swelling, which has been extensively discussed in Chapters 3 and 4. It is assumed that (1) there is only one solute in the water, and the chemical potential of the solute and solvent (i.e. water) are μ_c and μ_w, respectively. The solution is an ideal solution[1] (Smith et al., 2016); (2) the gas phase is continuous in the unsaturated zone and remains at atmospheric pressure, $p_{atm} = 0$ (Neuman, 1975; Safai and Pinder, 1979) so that the gas transport can be ignored.

5.2 ENERGY IN THE MIXTURE

The balance equation for the Helmholtz free energy density (ψ) considering chemicals transport can be obtained as

$$\frac{d}{dt}\int_V \psi \, dV = \int_\Gamma \boldsymbol{\sigma}\mathbf{v}_s \cdot \mathbf{n} d\Gamma - \int_\Gamma (\mu_w \mathbf{I}_w + \mu_c \mathbf{I}_c) \cdot \mathbf{n} \, d\Gamma - T\int_V \gamma \, dV \quad (5.1)$$

where μ_c is the chemical potential of the chemical, $\boldsymbol{\sigma}$ is the Cauchy stress tensor, $\mathbf{n}$ is the outward unit normal vector, T is the constant temperature, and γ is the entropy production per unit volume, where the material time derivative is given by

$$\frac{D}{Dt} = \partial_t + \mathbf{v}_s \cdot \nabla \quad (5.2)$$

By using equation (5.2) and divergence theorem, the balance equation for the free energy density is

$$\dot{\psi} + \psi \nabla \cdot \mathbf{v}_s - \nabla \cdot (\boldsymbol{\sigma} \mathbf{v}_s) + \nabla \cdot (\mu_w \mathbf{I}_w + \mu_c \mathbf{I}_c) = -T\gamma \leq 0 \tag{5.3}$$

5.3 DISSIPATIVE PROCESS: EXTENDED DARCY'S LAW AND FICK'S LAW

It is assumed that only one dissipation mechanism is present, specifically the friction generated at the solid-fluid boundary (which includes both water and chemicals) when the fluid moves through the porous skeleton. The friction generated by gas flow is neglected. A macroscopic expression for the dissipation caused by the frictional resistance at the interface can be derived using standard principles of nonequilibrium thermodynamics (Katachalsky and Curran, 1965) as follows:

$$0 \leq T\gamma = -\mathbf{I}_w \cdot \nabla \mu_w - \mathbf{I}_c \cdot \nabla \mu_c \tag{5.4}$$

where the fluxes $\mathbf{I}_w$ and $\mathbf{I}_c$ are driven by their corresponding forces $\nabla \mu_w$ and $\nabla \mu_c$, respectively.

5.3.1 Fluxes and driving forces

Equation (5.4) can be rearranged to establish the Darcy velocity (i.e. $\mathbf{u}$) and chemical diffusion flux (i.e. $\mathbf{J}_c$) with respect to their corresponding driving forces. Substituting the relationship between mass flux and diffusion flux obtained using equation (1.33),

$$\mathbf{I}_w = \mathbf{J}_w + \rho_l^w \mathbf{u} \text{ and } \mathbf{I}_c = \mathbf{J}_c + \rho_l^c \mathbf{u}$$

into equation (5.4) leads to

$$T\gamma = -(\mathbf{J}_w + \rho_l^w \mathbf{u}) \cdot \nabla \mu_w - (\mathbf{J}_c + \rho_l^c \mathbf{u}) \cdot \nabla \mu_c$$

which can be reorganized as

$$T\gamma = -\mathbf{u} \cdot (\rho_l^w \nabla \mu_w + \rho_l^c \nabla \mu_c) - \mathbf{J}_w \cdot \nabla \mu_w - \mathbf{J}_c \cdot \nabla \mu_c \tag{5.5}$$

where the fluxes $\mathbf{u}$, $\mathbf{J}_w$, $\mathbf{J}_c$ link with their driving forces $(\rho_l^w \nabla \mu_w + \rho_l^c \nabla \mu_c), \nabla \mu_w, \nabla \mu_c$, respectively.

By introducing the Gibbs-Duhem equation (2.22) for the liquid as

$$\rho_l^w \nabla \mu_w + \rho_l^c \nabla \mu_c = \nabla p_l$$

into equation (5.5), it leads to

$$0 \le T\gamma = -\mathbf{u} \cdot \nabla p_l - (\mathbf{J}_w \cdot \nabla \mu_w + \mathbf{J}_c \cdot \nabla \mu_c) \tag{5.6}$$

Thus, the driving force of $\mathbf{u}$ is simplified from $(\rho_l^w \nabla \mu_w + \rho_l^c \nabla \mu_c)$ in equation (5.5) to ∇p_l. Note that the gas chemical potential is assumed to be zero in equation (5.6) (Sacchetti, 2001).

The diffusion fluxes $\mathbf{J}_w$ and $\mathbf{J}_c$ in equation (5.6) have to satisfy

$$\mathbf{J}_w + \mathbf{J}_c = 0 \text{ or } \mathbf{J}_w - \mathbf{J}_c \tag{5.7}$$

because there is only one independent diffusion flux. Hence, the entropy production (5.6) can be rearranged by substituting equation (5.7) into equation (5.6) to remove $\mathbf{J}_w$ as

$$0 \le T\gamma = -\mathbf{u} \cdot \nabla p_l - \mathbf{J}_c \cdot \nabla (\mu_c - \mu_w) \tag{5.8}$$

where the three variables (e.g., $\mathbf{u}$, $\mathbf{J}_w$, and $\mathbf{J}_c$) are reduced to two variables (e.g., $\mathbf{u}$ and $\mathbf{J}_c$).

The relationship between the flows $\rho_l^l \mathbf{u}$ and $\mathbf{J}_c$, and the corresponding driving forces ∇p_l and $\nabla(\mu_c - \mu_w)$ in equation (5.8), can be obtained using phenomenological equations in Section 2.7 leading to

$$\rho_l^l \mathbf{u} = -(L_{11} / \rho_l^l) \nabla p_l - L_{12} \nabla (\mu_c - \mu_w) \tag{5.9}$$

$$\mathbf{J}_c = -(L_{21} / \rho_l^l) \nabla p_l - L_{22} \nabla (\mu_c - \mu_w) \tag{5.10}$$

where L_{11}, L_{12}, L_{21}, and L_{22} denote a set of phenomenological coefficients.

The term $\nabla(\mu_c - \mu_w)$ in equations (5.9) and (5.10) needs to be expressed in terms of chemical concentration for convenience. Using the Gibbs-Duhem equation (Darken, 1950) for the liquid at constant pressure in the micropore leads to

$$c_c (d\mu_c)_{p_l} + c_w (d\mu_w)_{p_l} = 0 \tag{5.11}$$

where c_c and c_w are the solute and diluent mass fractions, respectively, which can be defined as

$$c_c = \rho_l^c / \rho_l^l = \rho_c / \rho_l \,,\; c_w = \rho_l^w / \rho_l^l = \rho_w / \rho_l \tag{5.12}$$

Using equation (5.11) leads to

$$\nabla(\mu_c - \mu_w) = \frac{1}{c_w}\frac{\partial \mu_c}{\partial c_c}\nabla c_c \tag{5.13}^2$$

Hence, equations (5.9) and (5.10) can be rewritten using chemical concentration rather than chemical potential

$$\mathbf{u} = -k\frac{k_{rl}}{v}(\nabla p_l - r\frac{\rho_l^l}{c_w}\frac{\partial \mu_c}{\partial c_c}\nabla c_c) \tag{5.14}$$

$$\mathbf{J}_c = L\rho_l^l\frac{\nabla p_l}{p_l} - \rho_l^l D\nabla c_c \tag{5.15}$$

where

$$k\frac{k_{rl}}{v} = \frac{L_{11}}{(\rho_l^l)^2}, r = -\frac{L_{12}}{L_{11}}, L = \frac{L_{21}p_l}{\left(\rho_l^l\right)^2}, D = \frac{L_{22}}{c_w\left(\rho_l^l\right)^2}\frac{\partial \mu_c}{\partial c_c} \tag{5.16}$$

where

- $r = -\dfrac{L_{12}}{L_{11}}$ is the chemical reflection coefficient that serves as a measure of the efficiency of the osmotic transport (Heidug and Wong, 1996, Staverman, 1951);
- $L = \dfrac{L_{21}p_l}{\left(\rho_l^l\right)^2}$ is the pressure diffusion coefficient for chemical transport;
- $D = \dfrac{L_{22}}{c_w\rho_l^l}\dfrac{\partial \mu_c}{\partial c_c}$ is the dispersion-diffusion coefficient for chemical transport.

Equation (5.14) is an extended Darcy's law accounting for chemical osmosis, and equation (5.15) is the extended Fick's law of chemical diffusion with consideration of pressure influence.

5.3.2 Chemical potential and mass fraction

The term $\dfrac{\partial \mu_c}{\partial c_c}$ in equation (5.14) can be further interpreted using chemical concentration c_c. The solute chemical potential μ_c is given in

Section 2.2.2. With the assumption of $g_c(p,T)=0$, μ_c can be simplified to give

$$\mu_c = \left(\frac{RT}{M_c}\right)(\ln a_c) \tag{5.17}$$

where R is the gas constant, M_c is the molar mass of the solute, and a_c is the activity of the solute and is a measure of the "effective concentration" of the solute in the mixture. If the solution is assumed to be ideal, it leads to $a_c = x_c$.

The relationship between the molar fraction x_c and the mass fraction c_c described in equation (2.10) can be simplified if the solution is assumed to be diluted as

$$c_c = \frac{M_c}{M_w} x_c \text{ or } x_c = \frac{c_c M_w}{M_c} \text{ (if } x_c \text{ is very small)} \tag{5.18}^{3}$$

By substituting equation (5.18) into equation (5.17), the term $\frac{\partial \mu_c}{\partial c_c}$ can be derived as

$$\frac{\partial \mu_c}{\partial c_c} = \left(\frac{RT}{M_c}\right)\frac{\partial \ln(c_c)}{\partial c_c} \tag{5.19}^{4}$$

Since $\frac{\partial \ln(c_c)}{\partial c_c} = \frac{1}{c_c}$, which can be obtained using Taylor series[5] (Kincaid et al., 2009), equation (5.14) can be transformed as

$$\mathbf{u} = -k\frac{k_{rl}}{v}\left(\nabla p_l - r\frac{\rho_l^l}{c_w c_c}\left(\frac{RT}{M_c}\right)\nabla c_c\right) \tag{5.20}$$

5.4 CONSTITUTIVE RELATIONS

In this section, the constitutive equations for the stress and strain response are formulated.

5.4.1 Free energy density evolution path of the mixture

5.4.1.1 Current configuration

By substituting equation (5.4) into equation (5.3), and assuming that the geomaterial maintains mechanical equilibrium, so that, in the absence of volume forces, $\nabla \cdot \boldsymbol{\sigma} = 0$, the balance of free energy density in the current configuration ψ can be rewritten as

$$\dot{\psi} + \psi \nabla \cdot \mathbf{v}_s - \left(\boldsymbol{\sigma} : \nabla \mathbf{v}_s\right) + \mu_w \nabla \cdot \mathbf{I}_w + \mu_c \nabla \cdot \mathbf{I}_c = 0 \tag{5.21}^{6}$$

5.4.1.2 Reference configuration

Multiplying by J (the Jacobian of $\mathbf{F}$, $\dot{J} = J\nabla \cdot \mathbf{v}_s$) on both sides of equation (5.21) leads to

$$J\dot{\psi} + J\psi \nabla \cdot \mathbf{v}_s - J\left(\boldsymbol{\sigma} : \nabla \mathbf{v}_s\right) + J\mu_w \nabla \cdot \mathbf{I}_w + J\mu_c \nabla \cdot \mathbf{I}_c = 0 \tag{5.22}$$

The time derivative of the free energy density in the reference configuration ($\Psi = J\psi$) can be defined as

$$\dot{\Psi} = (J\psi)^{\cdot} = J\dot{\psi} + J\psi \nabla \cdot \mathbf{v}_s \tag{5.23}$$

By substituting equation (5.23) into equation (5.22), and using the relation of $\boldsymbol{\sigma} : \nabla \mathbf{v}_s = \mathrm{tr}(\boldsymbol{\sigma}^{\mathrm{T}} \nabla \mathbf{v}_s)$ in appendix 1, as well as the equation (3.15) of $J\mathrm{tr}\left(\boldsymbol{\sigma}^{\mathrm{T}} \nabla \mathbf{v}_s\right) = tr(\mathbf{T}\dot{\mathbf{E}})$ from continuum mechanics, in which $\mathbf{T}$ is the second Piola-Kirchhoff stress and $\mathbf{E}$ is the grain strain tensor, equation (5.22) can be reorganized as

$$\dot{\Psi} - tr(\mathbf{T}\dot{\mathbf{E}}) + J\mu_w \nabla \cdot \mathbf{I}_w + J\mu_c \nabla \cdot \mathbf{I}_c = 0 \tag{5.24}$$

where $J\mu_w \nabla \cdot \mathbf{I}_w$ and $J\mu_c \nabla \cdot \mathbf{I}_c$ can be transferred using the general balance law for liquids (2.31), leading to

$$J\mu_w \nabla \cdot \mathbf{I}_w = -\mu_w \dot{\rho}_{w,ref} \text{ and } J\mu_c \nabla \cdot \mathbf{I}_c = -\mu_c \dot{\rho}_{c,ref} \tag{5.25}^{7}$$

where $\rho_{w,ref} = J\rho_w = J\phi_w \rho_l^w$ and $\rho_{c,ref} = J\rho_c = J\phi_c \rho_l^c$ are the densities at the reference configuration.

Substituting equation (5.25) into equation (5.24) leads to

$$\dot{\Psi} = tr(\mathbf{T}\dot{\mathbf{E}}) + \mu_w \dot{\rho}_{w,ref} + \mu_c \dot{\rho}_{c,ref} \tag{5.26}$$

5.4.2 Helmholtz free energy density of the pore water and solid matrix

5.4.2.1 Current configuration (pore water)

Thermodynamic relations can be used for the bulk fluids in the pore spaces. Hence, the Helmholtz free energy density of the pore fluid, ψ_{pore}, can be derived using equation (2.18) in the absence of gas transport, as

$$\psi_{pore} = -p_{pore} + S_l(\mu_c \rho_l^c + \mu_w \rho_l^w) \tag{5.27}$$

According to the Gibbs-Duhem equation, this leads to

$$\dot{p}_{pore} = \dot{\mu}_c(S_l \rho_l^c) + \dot{\mu}_w(S_l \rho_l^w) \tag{5.28}$$

The time derivative of equation (5.27) gives

$$\dot{\psi}_{pore} = -\dot{p}_{pore} + \dot{\mu}_c(S_l \rho_l^c) + \dot{\mu}_w(S_l \rho_l^w) + \mu_c(S_l \rho_l^c)^{\cdot} + \mu_w(S_l \rho_l^w)^{\cdot} \tag{5.29}$$

Substituting equation (5.28) into equation (5.29) leads to

$$\dot{\psi}_{pore} = \mu_c(S_l \rho_l^c)^{\cdot} + \mu_w(S_l \rho_l^w)^{\cdot} \tag{5.30}$$

Equation (5.30) gives the dynamic change of free energy density in the current configuration, providing a useful function for free energy density analysis in the reference configuration in the following section.

5.4.2.2 Reference configuration (Solid matrix)

The free energy density of the matrix may be found by subtracting the contribution $J\phi\psi_{pore}$ due to the pore fluid from the total free energy density Ψ (note: even though the swelling is not considered here, the matrix still includes water molecules attached on the solid surfaces, which follow the principle of molecular forces rather than nonequilibrium thermodynamics). If $\upsilon = J\phi$ is the pore volume per unit reference volume, the free energy density of the matrix may be written as

$$(\Psi - J\phi\psi_{pore})^{\cdot} = tr(\mathbf{T}\dot{\mathbf{E}}) + p_{pore}\dot{\upsilon} \tag{5.31}[8]$$

By comparing equation (5.31) with equation (4.18), the swelling term is not included.

5.4.3 Constitutive structure

The deformation potential density, which is used for reasons of convenience, can be written as

$$W = (\Psi - J\phi\psi_{pore}) - p_{pore}\upsilon \tag{5.32}$$

Substituting equation (5.31) into the time derivative of equation (5.32) leads to

$$\dot{W}(\mathbf{E}, p_{pore}) = \mathrm{tr}(\mathbf{T}\dot{\mathbf{E}}) - \dot{p}_{pore}\upsilon \tag{5.33}$$

where W is a function of $\mathbf{E}$ and p_{pore}. The expressions for T and υ can be derived as

$$T_{ij} = \left(\frac{\partial W}{\partial E_{ij}}\right)_{p_{pore}}, \upsilon = -\left(\frac{\partial W}{\partial p_{pore}}\right)_{E_{ij}} \tag{5.34}$$

and also

$$\dot{W}(\mathbf{E}, p_{pore}) = \left(\frac{\partial W}{\partial E_{ij}}\right)_{p_{pore}} \dot{E}_{ij} + \left(\frac{\partial W}{\partial p_{pore}}\right)_{E_{ij}} \dot{p}_{pore} \tag{5.35}$$

The fundamental constitutive equations for the evolution of stress and pore volume fraction can be obtained by differentiating equation (5.34) with respect to time and substitution of equation (5.35) to give (refer to Appendix 4)

$$\dot{T}_{ij} = L_{ijkl}\dot{E}_{kl} - M_{ij}\dot{p}_{pore} \tag{5.36}$$

$$\dot{\upsilon} = M_{ij}\dot{E}_{ij} + Q\dot{p}_{pore} \tag{5.37}$$

where the parameters L_{ijkl}, M_{ij}, and Q are defined by the following equations:

$$\begin{aligned} L_{ijkl} &= \left(\frac{\partial T_{ij}}{\partial E_{kl}}\right)_{p_{pore}} = \left(\frac{\partial T_{kl}}{\partial E_{ij}}\right)_{p_{pore}} = L_{klij}, \\ M_{ij} &= -\left(\frac{\partial T_{ij}}{\partial p_{pore}}\right)_{E_{ij}} = \left(\frac{\partial \upsilon}{\partial E_{ij}}\right)_{p_{pore}}, \\ Q &= \left(\frac{\partial \upsilon}{\partial p_{pore}}\right)_{E_{ij}} \end{aligned} \tag{5.38}$$

Equations (5.36) and (5.37) can be written in the matrix form:

$$\begin{bmatrix} \dot{T}_{ij} \\ \dot{\upsilon} \end{bmatrix} = \begin{bmatrix} L_{klij} & -M_{ij} \\ M_{ij} & Q \end{bmatrix} \begin{bmatrix} \dot{E}_{ij} \\ \dot{p}_{pore} \end{bmatrix} \tag{5.39}$$

Compared with equations (4.27) and (3.44) for swelling materials, this matrix is much simpler. Swelling can be included in an Hydro-Mechanical-Chemical (HMC) model with consideration of chemical osmosis (Chen et al., 2016).

5.5 COUPLED FIELD EQUATIONS

The constitutive equations, (5.36) and (5.37), define changes in solid stress ($\dot{T}_{ij}$) and volume fraction ($\dot{\upsilon}$) in terms of independent variables such as $\dot{E}_{kl}$ and $\dot{p}_{pore}$.

5.5.1 Solid phase and porosity

Following the same assumptions of physical and geometrical linearization, and small strain, as in Section 3.5, the equations for the solid phase and pore volume fraction, respectively, can be written as

$$\dot{\sigma}_{ij} = \underbrace{(K - \frac{2G}{3})\dot{\varepsilon}_{kk}\delta_{ij} + 2G\dot{\varepsilon}_{ij}}_{1} - \underbrace{\zeta \dot{p}_{pore}\delta_{ij}}_{2} \tag{5.40}$$

$$\dot{\upsilon} = \underbrace{\zeta\dot{\varepsilon}_{ii}}_{3} + \underbrace{Q\dot{p}_{pore}}_{4} \tag{5.41}$$

(Note here: The detailed discussion and derivation of the parameters can be found in Section 3.5.1.)

Physical meanings of terms in equations (5.40) and (5.41) are:

- 1: Elastic deformation of the solids.
- 2: The coupling term, describing the influence of the water pressure on the deformation of the solids. Note: Since swelling is not considered in this chapter (in contrast to Chapters 3 and 4), there is no swelling term present in this equation.
- 3: Deformation-induced porosity change.
- 4: Pressure-induced porosity change, with consideration of only pore pressure influence (i.e. $B = 0$, compared with equation (4.33)).

5.5.2 Fluid phase

The local balance equation for the fluid is described in equation (2.49) as

$$(\upsilon S_l \rho_l^l)^{\cdot} + \nabla \cdot (\rho_l^l \mathbf{u}) = 0 \tag{5.42}$$

Substitution of equation (5.20) for **u** into equation (5.42) leads to fluid transport equation:

$$(S_l\rho_l^l)\dot{\upsilon}+\upsilon(S_l\rho_l^l)^{\cdot}-\nabla\cdot(\rho_l^l\left[k\frac{k_{rl}}{v}(\nabla p_l-\rho_l^l r\frac{RT}{M_c}\frac{1}{c_c c_w}\nabla c_c)\right])=0 \quad (5.43)$$

Substituting equation (5.41) into equation (5.43) leads to

$$\underbrace{(S_l\rho_l^l)(\zeta\dot{\varepsilon}_{ii}+Q\dot{p}_{pore})}_{5}+\underbrace{\upsilon(S_l\rho_l^l)^{\cdot}}_{6}-\underbrace{\nabla\cdot(\rho_l^l\left[k\frac{k_{rl}}{v}(\nabla p_l-\rho_l^l r\frac{RT}{M_c}\frac{1}{c_c c_w}\nabla c_c)\right])}_{7}=0 \quad (5.44)$$

Equation (5.44) is the liquid transport equation, with physical meanings of terms in the equation:

- 5: Liquid variation caused by the porosity change, due to deformation and pore pressure time-dependent variation.
- 6: Liquid change within a pore caused by liquid mass density and saturation ratio change.
- 7: Extended Darcy's law with consideration of chemical osmosis, which is one of the key novelties of the equation.

5.5.3 Chemical

The balance equation for chemicals is described in equation (2.50) as

$$(\upsilon S_l\rho_l^l)\dot{c}_c+\rho_l^l\mathbf{u}\cdot\nabla c_c+\nabla\cdot\mathbf{J}_c=0 \quad (5.45)$$

Substitution of equations (5.14) and (5.15) into (5.45) leads to the chemical transport equation:

$$\underbrace{(\upsilon S_l\rho_l^l)\dot{c}_c}_{8}-\underbrace{\rho_l^l\left[k\frac{k_{rw}}{v}(\nabla p_l-\rho_l^l r\frac{RT}{M_c}\frac{1}{c_c c_w}\nabla c_c)\right]\cdot\nabla c_c}_{9}+\underbrace{\nabla\cdot\left[L\rho_l^l\frac{\nabla p}{p}-\rho_l^l D\nabla c_c\right]}_{10}=0 \quad (5.46)$$

Physical meanings of terms in equation (5.46) are:

- 8: Chemical concentration change over time.

- 9: The chemical transport caused by the liquid flow (convection flux). The novelty in this term is that chemical osmotic flow is embedded.
- 10: The extended Fick's law of the chemical diffusion process. The novelty of this term is that the pressure gradient may have an influence on the chemical diffusion.

5.6 NUMERICAL SIMULATIONS

In this section, a simple numerical simulation is presented for illustrative purposes, especially for the influence of nanoscale chemical osmosis.

5.6.1 Mathematical equations

Mechanical: By considering the mechanical equilibrium condition ($\partial\sigma_{ij} / \partial x_j = 0$), equation (5.40) leads to

$$(K - \frac{2G}{3})\dot{\varepsilon}_{kk}\delta_{ij} + 2G\dot{\varepsilon}_{ij} - \zeta\nabla\dot{p}_{pore} = 0 \tag{5.47}$$

Considering equations (1.41) and (4.42) for the average pressure of a dilute chemical fluid, and using the strain-displacement relationship, equation (5.47) can be written as

$$(K - \frac{2G}{3})\frac{\partial^2 \dot{d}_k}{\partial x_k \partial x_i} + G\left(\frac{\partial^2 \dot{d}_i}{\partial x_j \partial x_j} + \frac{\partial^2 \dot{d}_j}{\partial x_i \partial x_j}\right) - \zeta\nabla\left[(S_l + \frac{C_s}{\phi}p_l)\dot{p}_l\right] = 0 \tag{5.48}$$

Hydro: Using the strain-displacement relationship $\dot{\varepsilon}_{ii} = \nabla \cdot \dot{\mathbf{d}}$, and substituting the term $(S_l\rho_l^l\dot{)} = \rho_l^l\frac{\partial S_l}{\partial t} + S_l\frac{\partial \rho_l^l}{\partial t}$ into equation (5.44) leads to

$$S_l\rho_l^l\zeta\nabla\cdot\dot{\mathbf{d}} + S_l\rho_l^l Q\dot{p}_{pore} + \phi\rho_l^l\frac{\partial S_l}{\partial t} + \phi S_l\frac{\partial \rho_l^l}{\partial t} + \rho_l^l\left[-\nabla\cdot k\frac{k_{rl}}{v}(\nabla p_l - \rho_l^l r\frac{RT}{M_c}\frac{1}{c_c c_w}\nabla c_c)\right] = 0 \tag{5.49}$$

By using the rate of change of saturation function and the rate of change of liquid density function equations (4.42) and (4.43), and by assuming these two equations apply liquid containing chemicals (This applies to Chapters 6 and 7.), dividing ρ_l^l from both sides of equation (5.49), and invoking equations (1.41) and (4.42) for the average pressure ($p_{pore} \approx \overline{p}$), equation (5.49) can be rewritten as

$$S_l\zeta\nabla\cdot\dot{\mathbf{d}} + S_lQ(S_l + \frac{C_s^p}{\phi}p_l)\frac{\partial p_l}{\partial t} + (C_s^p + \phi\frac{S_l}{K_w})\frac{\partial p_l}{\partial t} + \left[-\nabla\cdot k\frac{k_{rl}}{v}(\nabla p_l - \rho_l^l r\frac{RT}{M_c}\frac{1}{c_c c_w}\nabla c_c)\right] = 0 \tag{5.50}$$

The degree of saturation and relative permeability are characterized by the van Genuchten relationship (van Genuchten, 1980) in equation (4.50). Note: The parameters M and m are assumed as the same for unsaturated water as in Chapter 4.

Chemical: By assuming the density ρ_l^l is constant, equation (5.46) can be written as

$$S_l\phi\dot{c}_c - \left[k\frac{k_{rl}}{v}(\nabla p_l - \rho_l^l r\frac{RT}{M^c}\frac{1}{c_c c_w}\nabla c_c)\right]\cdot\nabla c_c - L\nabla\cdot\left(\frac{1}{p_l}\nabla p_l\right) - D\nabla^2 c_c = 0 \tag{5.51}$$

5.6.2 Discussion and comparison

The simplified equations (5.48), (5.50), and (5.51) of the coupled HMC model are based on a more comprehensive group of equations developed in Section 5.5. Comparing these simplified equations with the HMC model developed using the mechanics approach, the major advantage is the inclusion of chemical osmosis in equation (5.50), which consequently affects the chemical transport and mechanical deformation.

The following sections will be focusing on the discussion of chemical osmosis influences.

5.6.3 Model geometry and boundary conditions

Figure 5.2 shows a simple (plane strain) experimental setup (0.1 m × 0.1 m) with an unsaturated geomaterial sample (e.g., unsaturated rock). The top and bottom boundaries are fixed, stiff, and frictionless, allowing movement only in the horizontal (i.e., x) direction.

Boundary conditions: Boundary B is fixed (displacement=0) and impermeable, whereas boundary A allows movement and permeable, so that water is free to flow in or out.

Initial conditions: An equilibrium state is assumed at $t = 0$, with an external force applied at boundary A to maintain equilibrium (it is assumed that the initial effective stress = 0). The initial water pressure is $p_w = -5$ MPa ($t = 0$) in unsaturated conditions. The initial chemical mass fraction in the domain is 0.1.

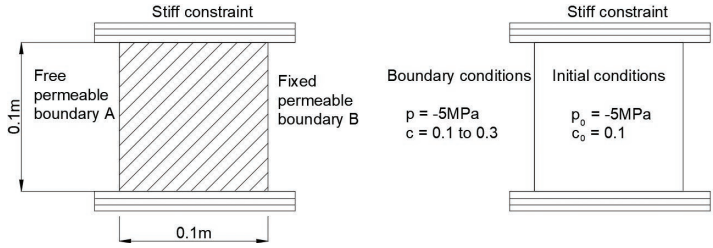

FIGURE 5.2 Geometry and boundary conditions

Start of the simulation: Since the numerical simulation is focused on the influence of chemical osmosis, only chemical gradient is applied to the model (fluid convection is ignored). At the beginning of the simulation, the mass fraction at boundary A rises to 0.3. The initial water pressure in the domain is –5 MPa, and the water pressure at boundary A is maintained at –4 MPa throughout the analysis. The van Genuchten relationship for unsaturated conditions is used, as given by equations (4.50) and (4.51).

The parameters adopted in the simulation are listed in Table 5.1.

5.6.4 Numerical simulation results

The numerical simulation results are compared with classic Fick's law for chemical transport and with equations from an unsaturated hydro-mechanical coupled model developed using the classical mechanics approach (Lewis and Schrefler, 1982) for comparison of interactions between solids and fluids.

Figures 5.3 and 5.4 show the distribution of chemical mass fraction over time (short term and long term, respectively). The chemical species move from areas of higher chemical fraction to areas of lower fraction, from boundary A to boundary B, driven by the diffusion process. As time progresses, the chemical mass fraction increases gradually throughout the domain and eventually reaches a steady state. These results align with predictions made by Fick's law, which is applicable since the pressure influence on the chemical diffusion process is not considered in equation (5.51). In this case, Fick's law can be seen as a special case of the more general formulation used in this chapter.

Figures 5.5 and 5.6 depict the changes in pore water pressure caused by chemical osmosis. Chemical osmosis occurs due to the chemical gradient, which drives water molecules to flow out from the domain through boundary A, leading to a more negative pore water pressure. At

TABLE 5.1
Material parameters for shale

Parameter	Physical meaning	Value and units
k	Absolute permeability	2.75E–21 m^2
v	Dynamic viscosity	8.54E–4 Pa·s
G	Shear modulus	239.08 MPa (SUGITA et al., 2004)
E	Young's modulus	645.52 MPa
θ	Poisson's ratio	0.35 (Rutqvist and Tsang, 2004)
ϕ	Porosity	0.41
ζ	Biot's coefficient	1 (assumed)
K_s	Bulk modulus of solid	∞ (assumed)
K_w	Bulk modulus of water	2E3 MPa
R	Gas constant	8.314
M_c	Molar mass	0.0585 kg/mol
ρ_l^w	Density of fluid	998.2 kg/m^3
r	Chemical reflection	0.2
D	Diffusion coefficient	5 E–9 m^2/s ①

Zheng and Samper (2008), Zheng et al. (2010, 2011).
Table note: ①: calculated at T = 300 K.

t = 3,600 s, the pressure at boundary B reaches a maximum. As boundary A is fixed at –5 MPa, water eventually flows back into the domain, driven by the decreasing chemical gradient. These results are compared with those obtained using the classical unsaturated hydro-mechanical coupled model (Lewis and Schrefler, 1987), which does not account for osmotic effects and thus fails to predict the osmotic flow behavior.

Figures 5.7 and 5.8 illustrate the displacement changes associated with the chemical transport process and the evolution of saturation. The sample undergoes a shrinking and recovering process as chemical osmosis takes place, highlighting the complex relationship between chemical processes and material deformation.

Chemical osmosis may occasionally occur in the opposite direction, driven by processes such as ion exchange (Roettger and Woermann, 1993) or multiple chemical osmosis interactions (Chen et al., 2018). In such cases, flow may occur from regions of higher chemical concentration to lower concentration (i.e., negative osmosis). This phenomenon, however, is distinct from reverse osmosis, which is commonly discussed in water desalination (Ghaffour et al., 2013). Reverse osmosis involves

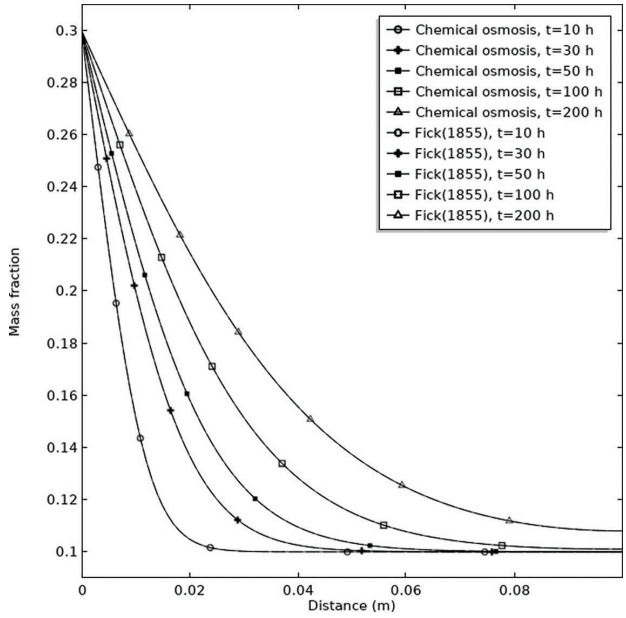

FIGURE 5.3 Evolution of chemical mass fraction with time (short term)

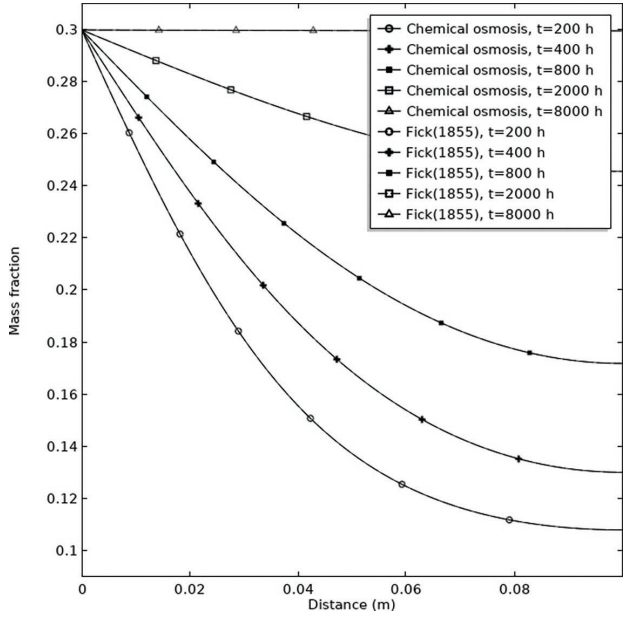

FIGURE 5.4 Evolution of chemical mass fraction with time (long term)

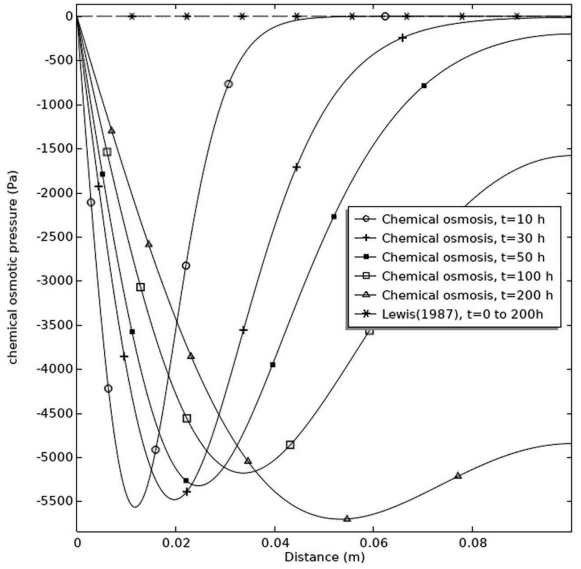

FIGURE 5.5 Pore water pressure change induced by chemical osmosis (short term)

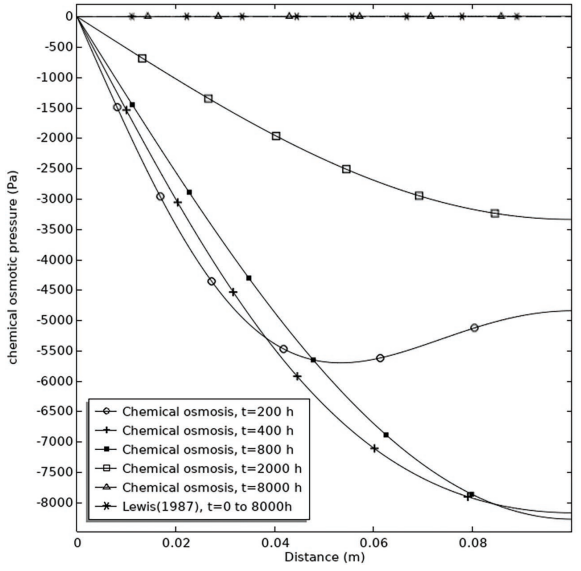

FIGURE 5.6 Pore water pressure change induced by chemical osmosis (long term)

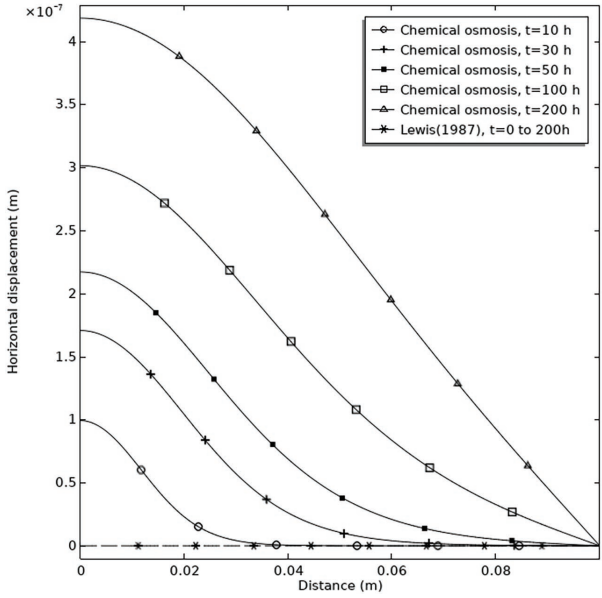

FIGURE 5.7 Displacement change induced by chemical osmosis (short term)

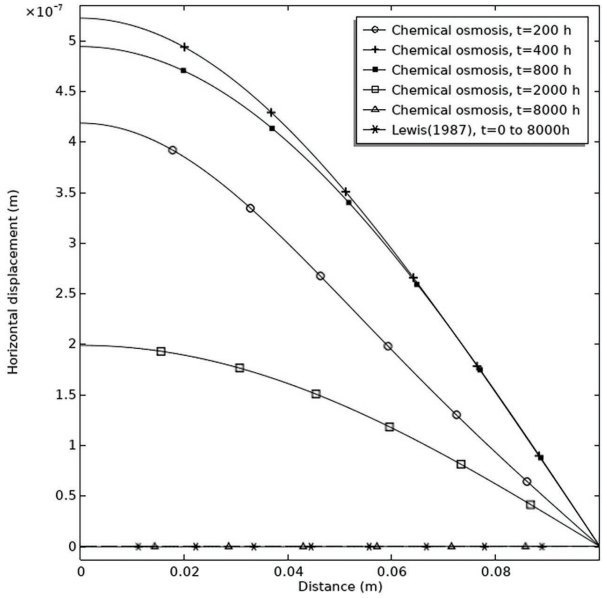

FIGURE 5.8 Displacement change induced by chemical osmosis (long term)

the transport of water against the natural osmotic flow, typically driven by higher external pressure than osmotic pressure. Research into negative osmosis in geotechnical and environmental engineering is still limited.

For the sake of completeness, the simulation includes both positive and negative osmosis scenarios. A chemical reflection coefficient of $r = -0.2$ is used to represent the opposing flow, modeling the reverse transport process. The result is shown in Figure 5.9. The results for this scenario are compared with those for a positive reflection coefficient ($r = 0.2$). In both cases, chemical osmosis causes changes in pore water pressure. However, in the positive osmosis case ($r = 0.2$), the water pressure decreases, whereas, in the negative osmosis case ($r = -0.2$), the water pressure increases

Figure 5.10 shows the positive and negative displacement changes associated with the selection of reflection coefficient. These findings demonstrate that the direction of osmotic flow has a significant impact

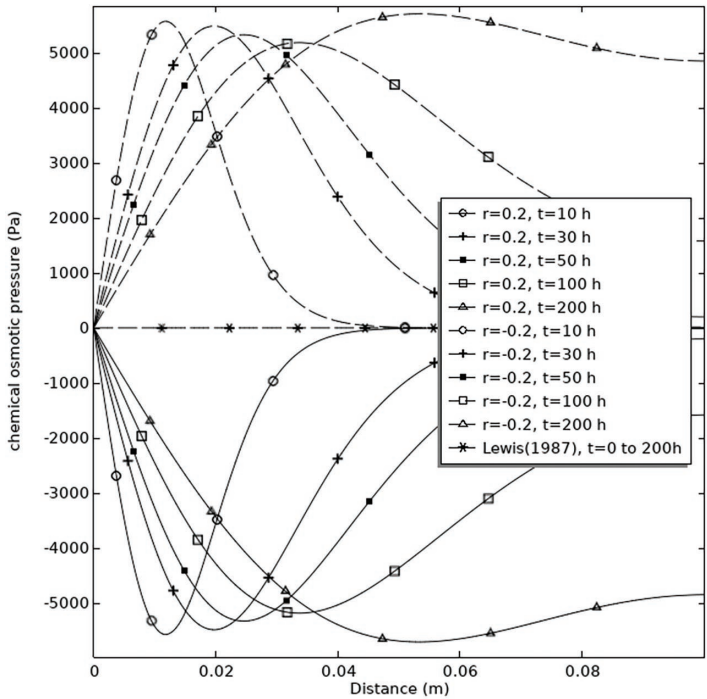

FIGURE 5.9 Pore water pressure change induced by chemical osmosis ($r = 0.2$ and $r = -0.2$)

on the deformation of geomaterials, influencing the overall behaviour of soils and rocks in various environmental conditions.

These findings demonstrate that the direction of osmotic flow has a significant impact on the deformation of geomaterials, influencing the overall behaviour of soils and rocks in various environmental conditions.

5.7 CONCLUSION

This chapter has introduced the Mixture-Coupling Theory framework to account for chemical influences in geomaterials, resulting in fully coupled constitutive equations for hydro-mechanical-chemical behavior. By integrating chemical effects with hydro-mechanical processes, the model offers a more comprehensive understanding of material behavior in low-permeability geomaterials, such as clays and shales,

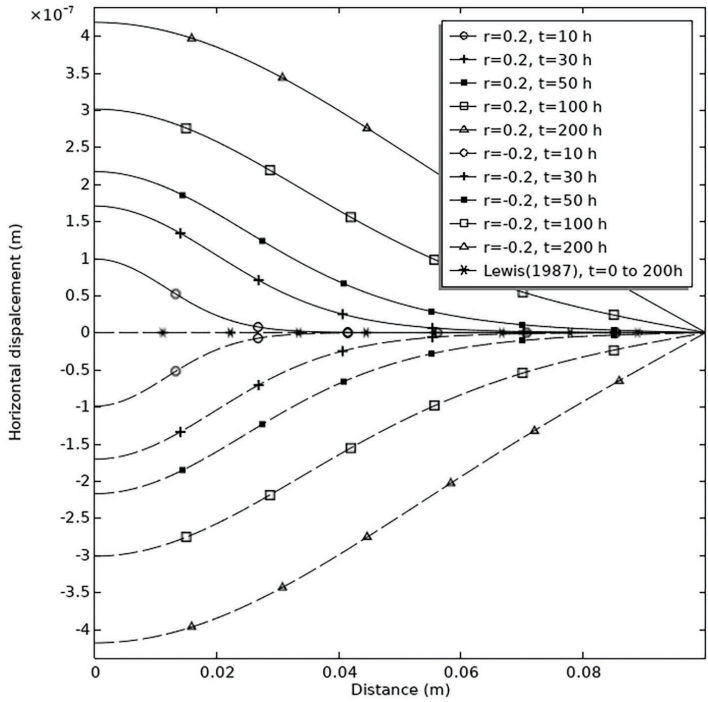

FIGURE 5.10 Displacement change induced by chemical osmosis ($r = 0.2$ and $r = -0.2$)

which are commonly involved in applications like landfills, waste disposal, and groundwater modeling.

When compared to the models presented in Chapters 3 and 4, the structure of the equations in this chapter follows a similar format, demonstrating one of the key advantages of the Mixture-Coupling Theory: its ability to consistently extend previous models to incorporate additional physical processes, such as chemical influences. This consistency makes the theory highly adaptable, allowing for the inclusion of more complex chemical interactions in future research. For instance, dual chemical osmosis has been successfully explored in previous studies (Chen et al., 2018), where the coupling of chemical concentration gradients and osmotic flow was integrated into the framework.

Although this chapter has focused on the theoretical and mathematical modeling aspects, further experimental research is encouraged to validate and expand these findings. Experimental studies will provide a deeper understanding of how these coupled processes manifest in real-world applications, ensuring that the theoretical models can be refined and better aligned with practical engineering needs. As the research advances, it will be crucial to explore the potential implications of chemical coupling in a wider range of geotechnical applications, from the design of waste containment systems to understanding the long-term stability of geological formations. This chapter lays the groundwork for future exploration of these complex interactions and invites further interdisciplinary research to continue developing robust, predictive models for geotechnical engineering.

NOTES

1 In chemistry, an ideal solution or ideal mixture is defined as a solution in which the enthalpy of the solution (or "enthalpy of mixing") is zero (Smith et al., 2016). In an ideal solution, the activity coefficients (which measure the deviation from ideality) are equal to one.

2 Equation (5.11) leads to $\nabla\mu_w = -\frac{c_c}{c_w}\nabla\mu_c$,

$$\therefore \nabla\left(\mu_c - \mu_w\right) = \nabla\mu_c - \left(-\frac{c_c}{c_w}\nabla\mu_c\right) = \frac{c_c + c_w}{c_w}\nabla\mu_c;\ \because c_c + c_w = 1,$$

$$\therefore \nabla\left(\mu_c - \mu_w\right) = \frac{1}{c_w}\nabla\mu_c. \text{ Since } \nabla\mu_c = \frac{\partial\mu_c}{\partial c_c}\nabla c_c, \text{ therefore}$$

$$\nabla\left(\mu_c - \mu_w\right) = \frac{1}{c_w}\frac{\partial\mu_c}{\partial c_c}\nabla c_c.$$

3 Equation (2.10) $c_c = x_x M_c / \left(x_c M_c + \left(1 - x_c\right) M_w\right)$ can be reformed as $c_c = x_c M_c / \underbrace{\left(M_w + x_c\left(M_c - M_w\right)\right)}_{x_c M_c + \left(1-x_c\right) M_w}$. If $x_c << 1$, it leads to $x_c\left(M_c - M_w\right) \approx 0$ and equation can be simplified as $c_c = \dfrac{M_c}{M_w} x_c$

(Note: This assumption is only applied to molecules with small molemass (e.g., Na^+). If, for big molecules, the original equation should be applied.)

4 $$\frac{\partial \mu_c}{\partial c_c} = \left(\frac{RT}{M_c}\right)\frac{\partial\left(ln\, a_c\right)}{\partial c_c} = \left(\frac{RT}{M_c}\right)\frac{\partial\left(ln\left(\dfrac{r_c c_c M_w}{M_c}\right)\right)}{\partial c_c}$$

$$= \left(\frac{RT}{M_c}\right)\frac{\partial\left(ln(\dfrac{r_c M_w}{M_c}) + ln\left(c_c\right)\right)}{\partial c_c}$$

$$= \left(\frac{RT}{M_c}\right)\frac{\partial ln\left(c_c\right)}{\partial c_c}$$

Note: During the derivation process, the $\dfrac{\partial\left(ln\left(\dfrac{r_c M_w}{M_c}\right)\right)}{\partial c_c} = 0$ is obtained as r_c, M_w, and M_c are all constants, independing on c_c. r_c is the activity coefficient, which is assumed to be 1 for ideal solution.

5 Taylor series: $d\left(ln\, x\right)/dx = 1/x$. Since, for an ideal solution,

$$\mu_c = \frac{RT}{M^c} ln\, c_c \text{, thus } \frac{1}{c_w}\frac{\partial\left(\dfrac{RT}{M_c} ln\, \mathrm{c}_c\right)}{\partial c_c}\nabla c_c = \frac{RT}{M_c}\frac{1}{c_w}\frac{\partial\left(ln\, c_c\right)}{\partial c_c} = \frac{RT}{M_c}\frac{1}{c_w c_c}$$

Substitution into equation leads to

$$\mathbf{u} = -k\frac{k_{rl}}{v}\left(\nabla p_l - r\frac{\rho_l^l}{c_w}\frac{\partial \mu_c}{\partial c_c}\nabla \mathrm{c}_c\right) = -k\frac{k_{rl}}{v}\left(\nabla p_l - r\frac{\rho_l^l}{c_w}\left(\frac{RT}{M^c}\right)\frac{\partial\left(ln\, a^c\right)}{\partial c_c}\nabla \mathrm{c}_c\right)$$

$$= -k\frac{k_{rl}}{v}\left(\nabla\, p_l - r\frac{\rho_l^l}{c_w c_c}\left(\frac{RT}{M^c}\right)\nabla c_c\right)$$

6 Since $\nabla\cdot\left(\boldsymbol{\sigma}\cdot\mathbf{v}_s\right) = \boldsymbol{\sigma}\cdot\nabla\mathbf{v}_s + (\nabla\cdot\boldsymbol{\sigma})\cdot\mathbf{v}_s$, and $\because \nabla\cdot\boldsymbol{\sigma} = 0$, therefore, $\nabla\cdot\left(\boldsymbol{\sigma}\cdot\mathbf{v}_s\right) = \boldsymbol{\sigma}\cdot\nabla\mathbf{v}_s$.

7 $$J\mu_k \nabla \cdot \mathbf{I}_k = -J\mu_k(\dot{\rho}_k + \rho_k \cdot \nabla \mathbf{v}_s) = -\mu_k(J\dot{\rho}_k + \rho_k J \cdot \nabla \mathbf{v}_s)$$
$$= -\mu_k(J\rho_k\dot{)} = -\mu_k \dot{\rho}_{k,ref}.$$

8 $$(\Psi - J\phi\psi_{pore}\dot{)} = \dot{\Psi} - \upsilon\dot{\psi}_{pore} - \psi_{pore}\dot{\upsilon}$$
$$= \overbrace{\left[tr(\mathbf{T}\dot{\mathbf{E}}) + \mu_w\dot{\rho}_{w,ref} + \mu_c\dot{\rho}_{c,ref}\right]}^{\dot{\Psi}} - \overbrace{\upsilon\mu_w(S_l\rho_l^w\dot{)} - \upsilon\mu_c(S_l\rho_l^c\dot{)}}^{\upsilon\dot{\psi}_{pore}} - \overbrace{\left[-p_{pore} + S_l\rho_l^w\mu_w + S_l\rho_l^c\mu_c\right]}^{\psi_{pore}}\dot{\upsilon}$$
$$= tr(\mathbf{T}\dot{\mathbf{E}}) + \mu_w\dot{\rho}_{w,ref} \overbrace{-\upsilon\mu_w(S_l\rho_l^w\dot{)} - \dot{\upsilon}(S_l\rho_l^w\mu_w)}^{1} + p_{pore}\dot{\upsilon} + \mu_c\dot{\rho}_{c,ref} \overbrace{-\upsilon\mu_c(S_l\rho_l^c\dot{)} - \dot{\upsilon}(S_l\rho_l^c\mu_c)}^{2}$$
$$= tr(\mathbf{T}\dot{\mathbf{E}}) + \underbrace{\mu_w\dot{\rho}_{w,ref} - \mu_w(S_l\rho_l^w\dot{\upsilon})}_{=0} + p_{pore}\dot{\upsilon} + \underbrace{\mu_c\dot{\rho}_{c,ref} - \mu_c(S_l\rho_l^c\dot{\upsilon})}_{=0}$$
$$= tr(\mathbf{T}\dot{\mathbf{E}}) + p_{pore}\dot{\upsilon}$$

Note: The superscripts 1 and 2 indicate the major devrivation pathway.

Since $\rho_{k,ref} = J\rho_k = J\phi_k\rho_l^k$, it leads to $\rho_{k,ref} = JS_l\phi\rho_l^k = \upsilon S_l\rho_l^k$, which indicates the terms $\mu_w\dot{\rho}_{w,ref} - \mu_w(S_l\rho_l^w\upsilon\dot{)} = 0$ and $\mu_c\dot{\rho}_{c,ref} - \mu_c(S_l\rho_l^c\upsilon\dot{)} = 0$.

REFERENCES

Chen, X. & Hicks, M. A. (2013) Unsaturated hydro-mechanical-chemo coupled constitutive model with consideration of osmotic flow. *Computers and Geotechnics* 54: 94–103.

Chen, X., Pao, W., Thornton, S. & Small, J. (2016) Unsaturated hydro-mechanical–chemical constitutive coupled model based on mixture coupling theory: hydration swelling and chemical osmosis. *International Journal of Engineering Science* 104: 97–109.

Chen, X., Thornton, S. F. & Pao, W. (2018) Mathematical model of coupled dual chemical osmosis based on mixture-coupling theory. *International Journal of Engineering Science* 129: 145–155.

Darken, L. (1950) Application of the Gibbs-Duhem equation to ternary and multicomponent systems. *Journal of the American Chemical Society* 72(**7**): 2909–2914.

Ghaffour, N., Missimer, T. M. & Amy, G. L. J. D. (2013) Technical review and evaluation of the economics of water desalination: current and future challenges for better water supply sustainability. *Desalination* 309: 197–207.

Heidug, W. K. & Wong, S. W. (1996) Hydration swelling of water-absorbing rocks: a constitutive model. *International Journal for Numerical and Analytical Methods in Geomechanics* 20: 403–430.

Katachalsky, A. & Curran, P. F. (1965) Nonequilibrium thermodynamics in biophysics. Cambridge, MA, Harvard University Press.

Kincaid, D., Kincaid, D. R. & Cheney, E. W. (2009) *Numerical analysis: mathematics of scientific computing*. Providence, American Mathematical Soc.

Lewis, R. W. & Schrefler, B. A. (1982) *A finite element simulation of the subsidence of gas reservoirs undergoing a waterdrivem in Finite Elements in Fluids.* London, Wiley.

Lewis, R. W. & Schrefler, B. A. (1987) *The finite-element method in deformation and consolidation of porous media.* New York, Wiley.

Neuman, S. P. (1975) Galerkin approach to saturated–unsaturated flow in porous media. In *Finite elements in fluids*. (Gallagher, R. H., Oden, J. T., Taylor, C., andZienkiewicz, O. C. (eds)) New York, John Wiley & Sons, vol. 1.

Roettger, H. & Woermann, D. (1993) Osmotic properties of polyelectrolyte membranes: positive and negative osmosis. *Langmuir* 9(**5**): 1370–1377.

Rutqvist, J. & Tsang, C.-F. (2004) A fully coupled three-dimensional THM analysis of the FEBEX in situ test with the ROCMAS code: prediction of THM behavior in a bentonite barrier. In *Elsevier geo-engineering book series.* (Ove Stephanson (ed)). Potsdam, Germany, Elsevier, vol. 2, pp. 143–148.

Sacchetti, M. (2001) The general form of the Gibbs-Duhem equation for multiphase/multicomponent systems and Its application to solid-state activity measurements. *Journal of Chemical Education* 78(**2**): 260–263.

Safai, N. M. & Pinder, G. F. (1979) Vertical and horizontal land deformation in a desaturating porous medium. *Advances in Water Resources* 2: 19–25.

Smith, P. E., Matteoli, E. & O'connell, J. P. (2016) *Fluctuation theory of solutions: applications in chemistry, chemical engineering, and biophysics*. Boca Raton, CRC Press.

Staverman, A. (1951) The theory of measurement of osmotic pressure. Recueil des Travaux Chimiques des Pays-Bas 70(**4**): 344–352.

Sugita, Y., Chijimatsu, M., Akira, I., Kurikami, H., Kobayashi, A. & Ohnishi, Y. (2004) THM simulation of the full-scale in-situ engineered barrier system experiment in GRIMSEL test site in Switzerland. In Elsevier *geo-engineering book series.* (Ove Stephanson (ed)). Boulevard, Elsevier, vol. 2, pp. 119–124.

Van Genuchten, M. T. (1980) A closed-form equation for predicting the hydraulic conductivity of unsaturated soils. *Soil Science Society of America Journal* 44: 892–898.

Zheng, L. & Samper, J. (2008) A coupled THMC model of FEBEX mock-up test. *Physics and Chemistry of the Earth, Parts A/B/C* 33: S486–S498.

Zheng, L., Samper, J. & Montenegro, L. (2011) A coupled THC model of the FEBEX in situ test with bentonite swelling and chemical and thermal osmosis. *Journal of Contaminant Hydrology* 126(1–2): 45–60.

Zheng, L., Samper, J., Montenegro, L. & Fernández, A. M. (2010) A coupled THMC model of a heating and hydration laboratory experiment in unsaturated compacted FEBEX bentonite. *Journal of Hydrology* 386(1–4): 80–94.

6 Unsaturated thermo-hydro-mechanical coupled modelling with thermal osmosis

6.1 INTRODUCTION

Thermo transport caused by a temperature gradient (e.g., A to B in Figure 6.1 of the representative elementary volume (REV)) has an influence on all components (e.g., water and solid) within the geomaterial and is significant in geoengineering applications. For example, during the drilling process in the petroleum industry, the high-temperature gradient generated between the drilling mud and the wellbore will place a thermal field on the formation of the wellbore. This consequently affects the deformation of the geomaterials (e.g., wellbore instability) (Steiger and Leung, 1988) and water flow. The water flow caused by thermal effects is known as osmotic flow and can flow directly from warmer to cooler or from cooler to warmer zones (Dirksen, 1969), influenced by electrical phenomena or chemical solution (Barragán and Kjelstrup, 2017).

The traditional analysis ignores thermal osmosis, even though it is found to be very important for controlling flow in very low-permeability geomaterials (e.g., shales), and consequently on impacting deformation. Based on a temperature gradient of 2 K/m, a hydraulic gradient of 10 J/m^4, and the experimental study (Srivastava and Avasthi, 1975), it was estimated that the thermo-osmotic flow through Kaolinite can be 800 times larger than Darcy's flow (Carnahan, 1983). An analysis of mud filtrate invasion due to a temperature gradient found that the thermal osmotic flow can be several times larger than hydraulic flow (Ghassemi and Diek, 2003). Thus, thermal effects will alter the pore pressure and geomaterial strength.

DOI: 10.1201/9780429324925-6

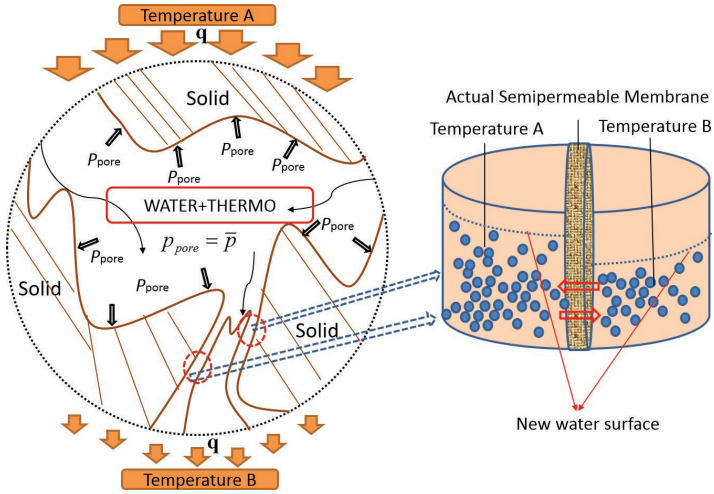

FIGURE 6.1 Conceptual model

Research on coupled thermo-hydro-mechanical (THM) models has been based on the mechanics approach and the mixture theory approach. The mechanics approach originated from hydro-mechanical coupled theory (Terzaghi, 1943; Biot, 1962, 1972) and was extended for THM coupling (Lewis and Schrefler, 1987). This chapter will discuss a THM model for unsaturated conditions extended from a saturated THM model (Chen et al., 2013) with consideration of thermal osmosis. The chapter demonstrates that Darcy's law is not applicable for predicting thermal osmotic flow in very low-permeability geomaterials, and the well-known Lewis's unsaturated THM coupled model (Lewis and Schrefler, 1987) is a special case of the model not considering thermal osmotic influence (Chen et al., 2013).

6.2 ENERGY IN THE MIXTURE

6.2.1 Internal energy and entropy balance equation

The transport of thermal flow changes the energy in the mixture. In the absence of chemical reactions (as these will generate or absorb heat), it is still convenient to use the Helmholtz free energy density (Haase, 1969), which combines both internal energy and entropy. Following the discussion in Section 2.4.2, the balance equation for internal energy is

$$\frac{d}{dt}\int_{V(t)} \varepsilon \, dV = \int_{\Gamma} (\boldsymbol{\sigma}\mathbf{v}_s - \mathbf{I}'_q)\cdot \mathbf{n}\, d\Gamma - \underbrace{\int_{\Gamma} h_w \mathbf{I}_w \cdot \mathbf{n}\, d\Gamma}_{\text{Heat carried by water flow}} \tag{6.1}$$

Compared with previous chapters for isothermal condition, reduced heat flow (heat by conduction) $\mathbf{I}'_q$ is included in equation (6.1) which is expressed as

$$\mathbf{I}'_q = \mathbf{I}_q - \sum_{\alpha=1}^{n-1} h_\alpha \mathbf{I}_\alpha$$

In equation (6.1), as $\frac{d}{dt}\int_{V(t)} \varepsilon \, dV = \int_{V(t)} (\dot{\varepsilon} + \varepsilon \nabla \cdot \mathbf{v}_s)\, dV$ (see equation (1.107)), and using divergence theorem (1.105), the local form of equation (6.1) is obtained as

$$\dot{\varepsilon} + \varepsilon \nabla \cdot \mathbf{v}_s = \nabla \cdot \boldsymbol{\sigma}\mathbf{v}_s - \nabla \cdot \mathbf{I}'_q - h_w \nabla \cdot \mathbf{I}_w \tag{6.2}$$

which can be rewritten using the total heat flow $\mathbf{I}_q = \mathbf{I}'_q + h_w \mathbf{I}_w$ as

$$\dot{\varepsilon} + \varepsilon \nabla \cdot \mathbf{v}_s = \nabla \cdot \boldsymbol{\sigma}\mathbf{v}_s - \nabla \cdot \mathbf{I}_q \tag{6.3}$$

The entropy balance equation is

$$\frac{d}{dt}\int_{V} \eta \, dV = \underbrace{\int_{\Gamma} -\mathbf{I}_\eta \cdot \mathbf{n}\, d\Gamma}_{\text{Entropy exchange}} + \underbrace{\int_{V} \gamma \, dV}_{\text{Entropy production}} \tag{6.4}$$

where $\mathbf{I}_\eta$ is the entropy flow described as

$$\mathbf{I}_\eta = \frac{\mathbf{I}_q - \mu_w \mathbf{I}_w}{T} = \frac{\mathbf{I}_q - h_w \mathbf{I}_w + T\eta_w \mathbf{I}_w}{T} = \frac{\mathbf{I}'_q + T\eta_w \mathbf{I}_w}{T} \tag{6.5}$$

and the local version of equation (6.4) can be obtained as

$$\dot{\eta} + \eta \nabla \cdot \mathbf{v}_s = -\nabla \cdot \mathbf{I}_\eta + \gamma \tag{6.6}$$

6.2.2 Helmholtz free energy density balance equation

Since Helmholtz free energy density ψ is defined as $\psi = \varepsilon - T\eta$, it leads to

$$\frac{d}{dt}\int_{V(t)}\psi\,dV=\frac{d}{dt}\int_{V(t)}\left(\varepsilon-T\eta\right)dV=\frac{d}{dt}\int_{V(t)}\varepsilon\,dV-\frac{d}{dt}\int_{V(t)}T\eta\,dV \quad (6.7)$$

Using similar derivation process of footnote (13) in Chapter 1, the term $\frac{d}{dt}\int_{V(t)}T\eta\,dV$ leads to

$$\frac{d}{dt}\int_{V}T\eta\,dV=\int_{V}\left((T\eta)^{\cdot}+T\eta\nabla\cdot\mathbf{v}_s\right)dV=\int_{V}\left(\dot{T}\eta+\dot{\eta}T+T\eta\nabla\cdot\mathbf{v}_s\right)dV \quad (6.8)$$

Substituting equation (6.8) into equation (6.7) leads to

$$\dot{\psi}+\psi\nabla\cdot\mathbf{v}_s=\dot{\varepsilon}+\varepsilon\nabla\cdot\mathbf{v}_s-\dot{T}\eta-T\left(\dot{\eta}+\eta\nabla\cdot\mathbf{v}_s\right) \quad (6.9)^{1}$$

Introducing local form of entropy balance equation (6.6), equation (6.9) can be rewritten as

$$\begin{aligned}\dot{\psi}+\psi\nabla\cdot\mathbf{v}_s&=\dot{\varepsilon}+\varepsilon\nabla\cdot\mathbf{v}_s-\dot{T}\eta-T\left(-\nabla\cdot\mathbf{I}_\eta+\gamma\right)\\&=\dot{\varepsilon}+\varepsilon\nabla\cdot\mathbf{v}_s-\dot{T}\eta+T\nabla\cdot\mathbf{I}_\eta-T\gamma\end{aligned} \quad (6.10)$$

and reformed as

$$\dot{\psi}+\psi\nabla\cdot\mathbf{v}_s-(\dot{\varepsilon}+\varepsilon\nabla\cdot\mathbf{v}_s)+\dot{T}\eta-T\nabla\cdot\mathbf{I}_\eta=-T\gamma\le 0 \quad (6.11)$$

6.3 DISSIPATIVE PROCESS: EXTENDING DARCY'S LAW AND THERMAL DIFFUSION LAW

A macroscopic expression for the dissipation generated by the frictional resistance at the solid and fluid interface, along with thermo transport, can be obtained by using standard arguments of nonequilibrium thermodynamics in equation (2.18) (Katachalsky and Curran, 1965; Chen et al., 2018). The entropy production $T\gamma$ can be obtained in terms of entropy flow from equation (2.92) in the absence of chemical reaction as

$$T\gamma=-\mathbf{I}_\eta\cdot\nabla T-\mathbf{I}_w\cdot\nabla\mu_w \quad (6.12)$$

or in terms of reduced heat flow from equation (2.97) as

$$T\gamma = \mathbf{I}'_q \cdot \frac{\nabla(-T)}{T} + \mathbf{I}_w \cdot \nabla(-\mu_w) \tag{6.13}$$

in which the reduced heat flow is expressed as

$$\mathbf{I}'_q = \mathbf{I}_q - h_w \mathbf{I}_w$$

Equation (6.13) is different from the dissipation function for the isothermal condition (3.3) because of the term $\mathbf{I}'_q \cdot \frac{\nabla(-T)}{T}$.

Equation (6.13) is based on the assumption of mechanical equilibrium with constant pressure. The relationship between water chemical potential μ_w and water pressure p_w can be derived by using the Gibbs-Duhem equation (Moran and Shapiro, 2000), equation (2.21), hence,

$$\rho_l^w \nabla \mu_w = \nabla p_w \tag{6.14}^2$$

Introducing equation (6.14) into equation (6.13) and using the relationship between Darcy velocity and $\mathbf{I}_w$ leads to

$$0 \le T\gamma = \mathbf{I}'_q \cdot \frac{\nabla(-T)}{T} - \mathbf{u} \cdot \nabla p_w \tag{6.15}^3$$

Since $\mathbf{u}$ is velocity, the term $\mathbf{u} \cdot \nabla p_w$ should be rewritten by introducing ρ_l^w as

$$\mathbf{u} \cdot \nabla p_w = (\rho_l^w \mathbf{u}) \cdot \left(\frac{\nabla p_w}{\rho_l^w} \right)$$

Thus, the dissipation function (6.15) can be written as

$$T\gamma = -(\rho_l^w \mathbf{u}) \cdot \left(\frac{\nabla p_w}{\rho_l^w} \right) + \mathbf{I}'_q \cdot \frac{\nabla(-T)}{T} \tag{6.16}$$

The relationships between the water flow $\rho_l^w \mathbf{u}$ and the thermal flow $\mathbf{I}'_q$, and their driving forces $\frac{\nabla p_w}{\rho_l^w}$ and $\frac{\nabla(-T)}{T}$, respectively, are obtained with phenomenological equations, which express the linear dependence of flow on the corresponding force as

$$(\rho_l^w \mathbf{u}) = -L_{11}\left(\frac{\nabla p_w}{\rho_l^w}\right) + L_{12}\frac{\nabla(-T)}{T} \tag{6.17}$$

$$\mathbf{I}_q' = -L_{21}\left(\frac{\nabla p_w}{\rho_l^w}\right) + L_{22}\frac{\nabla(-T)}{T} \tag{6.18}$$

where L_{11}, L_{12}, L_{21}, L_{22} are phenomenological coefficients.

Darcy's law in equation (6.17) can be derived as

$$\mathbf{u} = -\left(\frac{L_{11}}{(\rho_l^w)^2}\right)\left[\nabla p_w + \left(\frac{L_{12}}{L_{11}}\right)\frac{\rho_l^w \nabla T}{T}\right] \tag{6.19}$$[4]

where $\frac{L_{11}}{(\rho_l^w)^2} = k\frac{k_{rw}}{v}$, and $\frac{L_{12}}{L_{11}} = r_q$ can be defined as the reflection coefficient, which serves as a measure of the efficiency of the osmotic transport (Chen et al., 2013).

Consequently, Darcy's law is changed to

$$\mathbf{u} = -k\frac{k_{rw}}{v}\left[\nabla p_w + r_q\frac{\rho_l^w \nabla T}{T}\right] \tag{6.20}$$

in which the thermal osmosis reflection coefficient r_q has been included.

The thermal flow equation (6.18) can be expressed as

$$\mathbf{I}_q' = -L_q\left(\rho_l^w \frac{\nabla p_w}{p_w}\right) - \frac{L_{22}}{T}\nabla T \tag{6.21}$$[5]

where $L_q = \left(\frac{L_{21}p_w}{(\rho_l^w)^2}\right)$ is pressure diffusion coefficient for thermal effects and $\frac{L_{22}}{T} = \lambda$ is the conduction coefficient.

A coupling matrix can be written based on equations (6.17) and (6.18) as

$$\begin{pmatrix} \mathbf{u} \\ \mathbf{I}'_q \end{pmatrix} = -\begin{pmatrix} k\dfrac{k_{rw}}{v} & \dfrac{kk_{rw}r_q\rho_l^w}{vT} \\ \dfrac{L_q\rho_l^w}{p_w} & \lambda \end{pmatrix}\begin{pmatrix} \nabla p_w \\ \nabla T \end{pmatrix} \tag{6.22}$$

If the coupling term relating heat flow and water flow is not considered, the matrix equation can be written as

$$\begin{pmatrix} \mathbf{u} \\ \mathbf{I}'_q \end{pmatrix} = -\begin{pmatrix} k\dfrac{k_{rw}}{v} & 0 \\ 0 & \lambda \end{pmatrix}\begin{pmatrix} \nabla p_w \\ \nabla T \end{pmatrix} \tag{6.23}$$

which comprises the traditional Darcy's law and Fourier's law.

6.4 CONSTITUTIVE RELATIONS

The constitutive equations for the stress, strain, and temperature responses are formulated here by considering the dissipation function and free energy in the mixture.

6.4.1 Free energy density evolution path of the mixture

6.4.1.1 Current configuration

Equation (6.10) gives the balance equation of the Helmholtz free energy density as

$$\dot{\psi} + \psi\nabla\cdot\mathbf{v}_s = \dot{\varepsilon} + \varepsilon\nabla\cdot\mathbf{v}_s - \dot{T}\eta + T\nabla\cdot\mathbf{I}_\eta - T\gamma$$

Substituting the entropy production $T\gamma$ that described in equation (6.12) as

$$T\gamma = -\mathbf{I}_\eta\cdot\nabla T - \mathbf{I}_w\cdot\nabla\mu_w$$

The Helmholtz free energy density balance equation becomes

$$\dot{\psi} + \psi\nabla\cdot\mathbf{v}_s = \dot{\varepsilon} + \varepsilon\nabla\cdot\mathbf{v}_s - \dot{T}\eta + T\nabla\cdot\mathbf{I}_\eta - \underbrace{\left(-\mathbf{I}_\eta\cdot\nabla T - \mathbf{I}_w\cdot\nabla\mu_w\right)}_{T\gamma} \tag{6.24}$$

Since $T\nabla\cdot\mathbf{I}_\eta + \mathbf{I}_\eta\cdot\nabla T = \nabla\cdot\left(T\mathbf{I}_\eta\right)$, it leads to

$$\dot{\psi} + \psi\nabla\cdot\mathbf{v}_s = \dot{\varepsilon} + \varepsilon\nabla\cdot\mathbf{v}_s - \dot{T}\eta + \nabla\cdot\left(T\mathbf{I}_\eta\right) + \mathbf{I}_w\cdot\nabla\mu_w \tag{6.25}$$

Invoking $\mathbf{I}_\eta = \dfrac{\mathbf{I}_q - \mu_w\mathbf{I}_w}{T}$ into equation (6.25) leads to

$$\dot{\psi} + \psi\nabla\cdot\mathbf{v}_s = \dot{\varepsilon} + \varepsilon\nabla\cdot\mathbf{v}_s - \dot{T}\eta + \nabla\cdot\left(T\,\frac{\mathbf{I}_q - \mu_w\mathbf{I}_w}{T}\right) + \mathbf{I}_w\cdot\nabla\mu_w \tag{6.26}$$

which can be rearranged as

$$\begin{aligned}\dot{\psi} + \psi\nabla\cdot\mathbf{v}_s &= \dot{\varepsilon} + \varepsilon\nabla\cdot\mathbf{v}_s - \dot{T}\eta + \nabla\cdot\mathbf{I}_q - \nabla\cdot\left(\mu_w\mathbf{I}_w\right) + \mathbf{I}_w\cdot\nabla\mu_w \\ &= \dot{\varepsilon} + \varepsilon\nabla\cdot\mathbf{v}_s - \dot{T}\eta + \nabla\cdot\mathbf{I}_q - \mu_w\nabla\cdot\mathbf{I}_w\end{aligned} \tag{6.27}$$

Substituting the energy balance equation (6.3) $\dot{\varepsilon} + \varepsilon\nabla\cdot\mathbf{v}_s = \nabla\cdot\boldsymbol{\sigma}\mathbf{v}_s - \nabla\cdot\mathbf{I}_q$ into equation (6.27) leads to

$$\dot{\psi} + \psi\nabla\cdot\mathbf{v}_s = \nabla\cdot\boldsymbol{\sigma}\mathbf{v}_s - \dot{T}\eta - \mu_w\nabla\cdot\mathbf{I}_w \tag{6.28}$$

6.4.1.2 Reference configuration

Multiplying by J on both sides of equation (6.28) leads to

$$J\dot{\psi} + J\psi\nabla\cdot\mathbf{v}_s = J\nabla\cdot\boldsymbol{\sigma}\mathbf{v}_s - J\dot{T}\eta - J\mu_w\nabla\cdot\mathbf{I}_w \tag{6.29}$$

and using $\dot{\Psi} = J\dot{\psi} + J\psi\nabla\cdot\mathbf{v}_s$, equation (6.29) becomes

$$\dot{\Psi} = \mathrm{tr}(\mathbf{T}\dot{\mathbf{E}}) - \dot{T}J\eta - J\mu_w\nabla\cdot\mathbf{I}_w \tag{6.30}$$

where $\Psi = J\psi$ is the free energy density at the reference configuration and $\mathbf{T}$ is the second Piola-Kirchhoff stress.

By substituting Euler's identity $\dot{J} = J\nabla\cdot\mathbf{v}_s$, and the balance equations for $\mathbf{I}_w$ from Section 2.2, equation (6.30) becomes

$$\dot{\Psi} = tr(\mathbf{T}\dot{\mathbf{E}}) - \dot{T}J\eta + \mu_w\dot{\rho}_{w,ref} \tag{6.31}$$

where $\rho_{w,ref} = J\rho^w = J\phi_w\rho_l^w$ is the mass of water per unit reference volume (or density of pore water at the reference configuration).

6.4.2 Helmholtz free energy density of the pore water and solid matrix

6.4.2.1 Current configuration (pore water)

If the mass and entropy density per unit fluid volume are defined as ρ_l^{pore} (=ρ_l^w in this chapter for nonswelling geomaterials) and η_l^{pore} (= η_l^w), respectively, and the Helmholtz free energy density of the pore water is ψ_{pore}, then, based on classical thermodynamics and using equation (2.18), the free energy density can be expressed as

$$\psi_{pore} = -p_{pore} + S_w \mu_w \rho_l^w \tag{6.32}$$

(note here: the ψ_{pore} is relative to the volume of the pore space, and ρ_l^w is the "partial density") and its time derivative as

$$\dot{\psi}_{pore} = -\dot{p}_{pore} + \dot{\mu}_w S_w \ \rho_l^w + \mu_w (S_w \rho_l^w)^{\cdot} \tag{6.33}$$

According to the Gibbs-Duhem equation (2.21),

$$\dot{p}_{pore} - \dot{T} S_w \eta_l^w = S_w \rho_l^w \dot{\mu} \tag{6.34}$$

and by introducing equation (6.34) into equation (6.33), it leads to

$$\dot{\psi}_{pore} = -\dot{T} S_w \eta_l^w + \mu_w (S_w \rho_l^w)^{\cdot} \tag{6.35}$$

6.4.2.2 Reference configuration (solid matrix)

The free energy density of the solid matrix can be derived by subtracting from the free energy density Ψ of the combined material/fluid system the contribution $J\phi\psi_{pore}$ due to the pore water. Using the time derivative of ψ_{pore} in equation (6.35) leads to

$$(\Psi - J\phi\psi_{pore})^{\cdot} = tr(\mathbf{T}\dot{\mathbf{E}}) + p_{pore}\dot{\upsilon} - \dot{T} H_s \tag{6.36}^{6}$$

where $\upsilon = J\phi$ is the pore volume per unit reference volume, and $H_s = J\eta - J(S_w \phi \eta_l^{pore}) = J\phi_s \eta_s^s = J\eta_s$ is the reference entropy density of the solid.

6.4.3 Constitutive equation structure

The deformation potential density is defined as

$$W = (\boldsymbol{\psi} - J\phi\psi_{pore}) - p_{pore}\upsilon \tag{6.37}$$

The time derivative of equation (6.37) becomes

$$\begin{aligned}\dot{W} &= \mathrm{tr}(\mathbf{T}\dot{\mathbf{E}}) - \dot{T}H_s + \dot{\upsilon}p_{pore} - \dot{\upsilon}p_{pore} - \upsilon\dot{p}_{pore} \\ &= \mathrm{tr}(\mathbf{T}\dot{\mathbf{E}}) - \dot{T}H_s - \upsilon\dot{p}_{pore}\end{aligned} \tag{6.38}$$

Substituting equation (6.36) into equation (6.38) leads to

$$\dot{W} = \mathrm{tr}(\mathbf{T}\dot{\mathbf{E}}) - \dot{p}_{pore}\upsilon - \dot{T}H_s \tag{6.39}$$

which indicates that W is a function of $\mathbf{E}$, p_{pore}, and T, so that the following equations are also obtained:

$$T_{ij} = \left(\frac{\partial W}{\partial E_{ij}}\right)_{p_{pore},T}, \quad \upsilon = -\left(\frac{\partial W}{\partial p_{pore}}\right)_{E_{ij},T}, \quad H_s = -\left(\frac{\partial W}{\partial T}\right)_{E_{ij},p_{pore}} \tag{6.40}$$

By substituting equation (6.40) into equation (6.39), the expressions of $\dot{W}$ for $\mathbf{T}$ (or T_{ij}), υ, and H_s may be obtained:

$$\dot{W}(\mathbf{E}, p_{pore}, T) = \left(\frac{\partial W}{\partial E_{ij}}\right)_{p_{pore},T}\dot{E}_{ij} + \left(\frac{\partial W}{\partial p_{pore}}\right)_{E_{ij},T}\dot{p}_{pore} + \left(\frac{\partial W}{\partial T}\right)_{E_{ij},p_{pore}}\dot{T} \tag{6.41}$$

If equation (6.40) is differentiated with respect to time, the fundamental constitutive equations for the evolution of stress, pore volume fraction, and temperature can be expressed as

$$\dot{T}_{ij} = L_{ijkl}\dot{E}_{kl} - M_{ij}\dot{p}_{pore} + S_{ij}^{q}\dot{T} \tag{6.42}$$

$$\dot{\upsilon} = M_{ij}\dot{E}_{ij} + Q\dot{p}_{pore} + B_q\dot{T} \tag{6.43}$$

$$\dot{H}_s = -S_{ij}^{q}\dot{E}_{ij} + B_q\dot{p}_{pore} + Z_q\dot{T} \tag{6.44}$$

where the parameters L_{ijkl}, M_{ij}, S_{ij}^{q}, Z_q, B_q, and Q are material-dependent constants defined by the following group of equations (note: the derivation process can be found in Appendix 5):

$$L_{ijkl} = \left(\frac{\partial T_{ij}}{\partial E_{kl}}\right)_{p_{pore},T} = \left(\frac{\partial T_{kl}}{\partial E_{ij}}\right)_{p_{pore},T}, M_{ij} = -\left(\frac{\partial T_{ij}}{\partial p_{pore}}\right)_{E_{ij},T} = \left(\frac{\partial \upsilon}{\partial E_{ij}}\right)_{p_{pore},T},$$

$$S_{ij}^{q} = -\left(\frac{\partial T_{ij}}{\partial T}\right)_{E_{ij},p_{pore}} = -\left(\frac{\partial H_s}{\partial E_{ij}}\right)_{p_{pore},T} \tag{6.45}$$

$$Z_q = \left(\frac{\partial H_s}{\partial T}\right)_{E_{ij},p_{pore}}, B_q = \left(\frac{\partial \upsilon}{\partial T}\right)_{E_{ij},p_{pore}} = \left(\frac{\partial H_s}{\partial p_{pore}}\right)_{E_{ij},T}, Q = \left(\frac{\partial \upsilon}{\partial p_{pore}}\right)_{E_{ij},T}$$

The matrix format of equations (6.42)–(6.44) can be obtained as

$$\begin{bmatrix} \dot{T}_{ij} \\ \dot{\upsilon} \\ \dot{H}_s \end{bmatrix} = \begin{bmatrix} L_{ijkl} & -M_{ij} & S_{ij}^{q} \\ M_{ij} & Q & B_q \\ -S_{ij}^{q} & B_q & Z_q \end{bmatrix} \begin{bmatrix} \dot{E}_{kl} \\ \dot{p}_{pore} \\ \dot{T} \end{bmatrix} \tag{6.46}$$

6.5 COUPLED FIELD EQUATIONS

6.5.1 Solid phase and porosity

Following the same assumption of physical and geometrical linearization and small strain as in Section 3.5, and assuming an isotropic relationship $S_{ij}^{q} = \omega_T \delta_{ij}$ for the thermal coefficient, the governing stress, and pore fraction equations, (6.42) and (6.43), can be changed to the form

$$\dot{\sigma}_{ij} = \underbrace{(K - \frac{2G}{3})\dot{\varepsilon}_{kk}\delta_{ij} + 2G\dot{\varepsilon}_{ij}}_{1} - \underbrace{\zeta \dot{p}_{pore}\delta_{ij}}_{2} + \underbrace{\omega_T \dot{T}\delta_{ij}}_{3} \tag{6.47}$$

$$\dot{\upsilon} = \underbrace{\zeta \dot{\varepsilon}_{ii}}_{4} + \underbrace{Q\dot{p}_{pore}}_{5} + \underbrace{B_q \dot{T}}_{6} \tag{6.48}$$

Physical meanings of terms in equations (6.47) and (6.48) are:

- 1: Elastic deformation of the solids.
- 2: The coupling term associated with pore pressure, describing the influence of the pore pressure on the deformation of

the solids. Note: Since swelling is not considered in this chapter, there is no swelling term present in this equation.
- 3: The temperature coupling term, describing the influence of the temperature variation on the deformation of the solids.
- 4: Deformation-induced porosity change.
- 5: Pressure-induced porosity change, with only consideration of pore pressure influence (i.e., $B = 0$, compared with equation (4.33)).
- 6: Temperature-induced porosity change (e.g., thermal expansion).

The detailed discussion and derivation of parameters (e.g., ζ, Q, etc.) can be found in Section 3.5.1. The discussion will be focused on B_q and its relationship with ω_T, using a similar process to that followed in Section 3.5.1, for a fully saturated condition.

At equilibrium, when $\dot{p}_{pore} = 0$ and $\dot{\sigma}_{ij} = 0$, equation (6.47) can be simplified to

$$\left(K - \frac{2G}{3}\right)\dot{\varepsilon}_{kk}\delta_{ij} + 2G\dot{\varepsilon}_{ij} + \delta_{ij}\omega_T\dot{T} = 0 \tag{6.49}$$

where ω_T is the thermal expansion coefficient of the solid. Since $\omega_T\dot{T}\delta_{ij}$ must exist ($i = j$), equation (6.48) can be written as

$$\left(K - \frac{2G}{3}\right)\dot{\varepsilon}_{kk}\delta_{ii} + 2G\dot{\varepsilon}_{ii} + \delta_{ii}\omega_T\dot{T} = 0 \tag{6.50}$$

Since $\delta_{ii} = 3$, it leads to

$$3\left(K - \frac{2G}{3}\right)\dot{\varepsilon}_{kk} + 2G\dot{\varepsilon}_{ii} + 3\omega_T\dot{T} = 0 \tag{6.51}$$

Because $\dot{\varepsilon}_{kk} = \dot{\varepsilon}_{ii}$,

$$\dot{\varepsilon}_{ii} = -\frac{1}{K}\omega_T\dot{T} \tag{6.52}$$

As $\dot{\varepsilon}_{ii} = \beta_s\dot{T}$ in which β_s is the thermal expansion coefficient, it leads to $\omega_T = -K\beta_s$.

From equation (6.48), when there is no mechanical loading and $\dot{p}_{pore} = 0$, and by substituting (6.52) into (6.48), this leads to

$$\dot{\upsilon} = -\frac{\zeta}{K}\omega_T \dot{T} + B_q \dot{T} \tag{6.53}$$

Because $\dot{\varepsilon}_{ii} = \dot{\upsilon}$ (when $\dot{p}_{pore} = 0$, $\dot{T} = 0$ in equation (6.48) and assuming $\zeta \approx 1$),

$$-\frac{1}{K}\omega_T \dot{T} = -\frac{\zeta}{K}\omega_T \dot{T} + B_q \dot{T}. \tag{6.54}$$

By eliminating $\dot{T}$ from the above equation, this leads to the relationship

$$-\frac{1}{K}\omega_T = -\frac{\zeta}{K}\omega_T + B_q$$

and finally to

$$B_q = (1/K)(\zeta - 1)\omega_T \tag{6.55}$$

Equation (6.55) is very similar to the coefficient B (Chapter 3) for water-molecular induced swelling.

6.5.2 Fluid phase

Since the balance equation (equation (2.49) in Section 2.2) for the water can be described as

$$(S_w \upsilon \rho_l^w)^{\cdot} + \nabla \cdot (\rho_l^w \mathbf{u}) = 0$$

or

$$S_w \rho_l^w \dot{\upsilon} + \upsilon (S_w \rho_l^w)^{\cdot} + \nabla \cdot (\rho_l^w \mathbf{u}) = 0 \tag{6.56}$$

by substituting equation (6.43) for $\mathbf{u}$ into equation (6.56), the control equation for the fluid phase can be written as

$$\underbrace{S_w \rho_l^w \left[\zeta \dot{\varepsilon}_{ii} + Q\dot{p}_{pore} + B_q \dot{T}\right]}_{7} + \underbrace{\upsilon (S_w \rho_l^w)^{\cdot}}_{8} - \underbrace{\nabla \cdot \left(\rho_l^w \left[\frac{k_{rw} k}{v}\left(\nabla p + \frac{r_q \rho_l^w}{T}\nabla T\right)\right]\right)}_{9} = 0 \tag{6.57}$$

Physical meanings of terms in equation (6.57) are:

- 7: Water flow caused by porosity change, due to deformation of the solid, and pore pressure and temperature time-dependent variation.
- 8: Water flow caused by its mass density and saturation ratio change.
- 9: Extended Darcy's law with consideration of thermal osmosis, which is one of the key novelties of the equation.

6.5.3 Thermal

The balance equation for heat transport can be obtained from the general equation (2.62) (refer to Section 2.2) as

$$(S_w \upsilon q_l^w + (J-\upsilon)q_s^s)^{\cdot} + J\nabla\cdot(\mathbf{I}_q' + h_w \mathbf{I}_w) = 0 \tag{6.58}$$

By substituting equation (6.22), and invoking equation (1.21) $\left(\mathbf{I}_w = \dfrac{\mathbf{u}\rho_w}{S_w\phi} = \mathbf{u}\rho_l^w\right)$ so that equation (6.58) can be rearranged as

$$\underbrace{(S_w \upsilon q_l^w + (1-\upsilon)q_s^s)^{\cdot}}_{10} + \underbrace{J\nabla\cdot\left[-\frac{L_q\rho_l^w}{p}\nabla p - \lambda\nabla T\right]}_{11} + \underbrace{J\nabla\cdot(\rho_l^w \mathbf{u} C_w T)}_{12} = 0 \tag{6.59}$$

Physical meaning of terms in equation (6.59) are:

- 10: Thermal density change over time.
- 11: The thermo transport caused by the temperature difference (conduction), which is an extended Fourier's law. The novelty in this term is that the water pressure gradient has an influence on the conduction process.
- 12: The heat transport caused by convection of the water flow.

6.6 NUMERICAL SIMULATIONS

This section presents a simple numerical simulation to illustrate the influence of thermal osmosis. Particularly, attention is focused on the pressure change induced by thermal osmosis.

6.6.1 Mathematical equations

Mechanical: By considering equations (1.41) and (4.42) in Section 1.3.2 for the average pressure, and assuming the mechanical equilibrium condition $\partial\sigma_{ij} / \partial x_{ij} = 0$, equation (6.47) can be rewritten as

$$\left(K - \frac{2G}{3}\right)\frac{\partial^2 \dot{d}_k}{\partial x_k \partial x_i} + G\left(\frac{\partial^2 \dot{d}_i}{\partial x_j \partial x_j} + \frac{\partial^2 \dot{d}_j}{\partial x_i \partial x_j}\right) - \zeta\nabla\left[(S_w + \frac{C_s^p}{\phi} p_w)\dot{p}_w\right] + \omega_T \frac{\partial \dot{T}}{\partial x_i} = 0 \tag{6.60}$$

Hydro: By assuming the porosity is constant and using the rate of change of saturation function and the rate of change of water density function, equation (6.57) can be rewritten as

$$S_w \rho_l^w \zeta\nabla \cdot \dot{d} + S_w \rho_l^w (Q + B / \rho_l^w)\dot{p}_{pore} + \phi\rho_l^w \frac{\partial S_w}{\partial t} + \phi S_w \frac{\partial \rho_l^w}{\partial t} + \rho_l^w \left[-\nabla \cdot \frac{k_{rw} k}{v}(\nabla p + \frac{r_q \rho_l^w}{T}\nabla T)\right] + B_q \dot{T} = 0 \tag{6.61}$$

Considering equations (1.41) and (4.42) for average pressure leads to

$$-\nabla \cdot \frac{k_{rw} k}{v}\left(\nabla p + \frac{r_q \rho_l^w}{T}\nabla T\right) + \left(C_s^p + \phi\frac{S_w}{K_w}\right)\frac{\partial p_w}{\partial t} + S_w(Q + B / \rho_l^w)\left(S_w + \frac{C_s^p}{\phi} p_w\right)\frac{\partial p_w}{\partial t} + S_w \zeta\nabla \cdot \dot{d} + B_q \dot{T} = 0 \tag{6.62}$$

Thermal: By assuming the porosity is constant, and neglecting the thermal coupling term due to pressure, equation (6.59) can be rearranged as

$$\frac{\partial}{\partial t}\left\{\left[(1-\phi)\rho_s^s C_s + S_w \phi \rho_l^w C_w\right]T\right\} - \nabla^T \lambda \nabla T = 0 \tag{6.63}$$

which is the same function as that derived based on Fourier's law.

6.6.2 Discussion and comparison

The simplified THM equations (6.60), (6.62) and (6.63) are nearly the same as those developed via the mechanics approach (Lewis and

Schrefler, 1987). The major advantage is the inclusion of a nanoscale thermal osmosis in equation (6.61), which will consequently affect mechanical deformation.

Considering the more comprehensive equations in Section 6.5 (e.g., equation (6.47)), the classic THM is a simplified case without considering the porosity change and thermal osmosis. Since thermal osmosis is a complicated phenomenon, more research in theoretical and experimental studies will be needed. The following section will present a simple numerical example to demonstrate the potential thermal osmosis influence.

6.6.3 Model geometry and boundary condition

The geometry of the model (Figure 6.2) is the same as that used in Chapter 5: a simple (plane strain) experimental setup (0.15 m × 0.3 m) with an unsaturated geomaterial sample (e.g., unsaturated rock).

Boundary conditions: The top and bottom boundaries are fixed, stiff, and frictionless, allowing movement only in the horizontal (i.e., x) direction. Boundary B is fixed (displacement = 0) and impermeable for water, whereas boundary A allows free movement and water flow in and out of the sample.

Initial conditions: An equilibrium state is assumed at $t = 0$, with an external force applied at boundary A to maintain the equilibrium (the initial effective stress = 0). The initial water pressure is $p_w = -5$ MPa ($t = 0$) in unsaturated conditions. The initial temperature in the domain is 300 K.

Start of the simulation: Similar to Chapter 5 which is focused on chemical osmosis, the numerical modeling is now focused on the influence of thermal osmosis, and no water pressure gradient is applied initially. An external temperature of 380 K is applied to boundary A to generate a temperature gradient (Figure 6.2). The water pressure in the

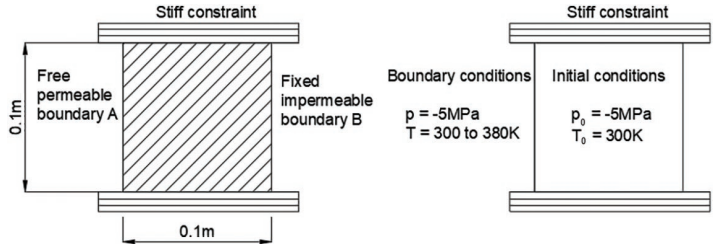

FIGURE 6.2 Model geometry and boundary conditions

domain is set to –5 MPa, and a constant value of –5 MPa is maintained at boundary A.

The parameters adopted in the simulation are listed in Table 6.1.

6.6.4 Numerical simulation results

The temperature distribution over time is illustrated in Figure 6.3. As heat is conducted from boundary A to boundary B, the temperature throughout the domain gradually rises. Eventually, the temperature reaches a stable state. These predictions align with the results derived from Fourier's law, as the influence of pressure on thermal transport is ignored in equation (6.63). This confirms that Fourier's law represents a specific case of the more general thermal transport equation for porous media presented in equation (6.59).

As a result of the temperature gradient within the domain, thermal osmosis occurs. This phenomenon causes water to move into or out of the sample, leading to changes in the water pressure. Previous studies

TABLE 6.1
Material parameters

Parameters	Physical meaning	Values and units
C_s	Specific heat of solid	835.5 J/kg℃
C_w	Specific heat of water	4,202 J/kg℃
β_s	Thermal expansion coefficient for solid	2E–5/K
λ_s	Thermal conductivity of solid	1.5 W/m℃①
λ_w	Thermal conductivity of liquid	1.23 W/m℃①
r_q	Thermal reflection coefficient	5.21E5②

Table notes: ①: The conduction coefficient λ is obtained through $\lambda = \lambda_s\left(1-\phi\right)+\lambda_w\phi$; ②: calculated from the relationship between the thermal reflection coefficient and the thermal osmotic permeability with T = 300 K and relative permeability = 0.927.

Note: The r_q is normally determined by experimental studies. Whether the osmosis is positive (e.g., +1) or negative (e.g. –1) is determined by the chemicals present in the fluid and the physical/chemical (e.g., ion charged membrane) properties of the geomaterials.

have indicated that thermal osmosis-driven water flow typically moves from regions of lower temperature to higher temperature (Gonçalvès et al., 2012).

The evolution of water pressure is depicted in Figure 6.4. Two different reflection coefficients r_q = 5.21E5 or r_q = –5.21E5 are selected, causing the water pressure to either decrease or increase within the domain, respectively. At the early stages, the pressure near boundary A exhibits more significant changes than that near boundary B due to the higher temperature gradient at boundary A. As time progresses, the pressure near boundary A begins to decrease after reaching its maximum value, while the pressure near boundary B also decreases.

The corresponding displacement changes are shown in Figure 6.5, reflecting the expansion or contraction of the sample. In contrast to the traditional mechanics approach (Lewis and Schrefler, 1987), which predicts no change in pressure or displacement, as indicated by the constant horizontal lines in both Figures 6.4 and 6.5, the constitutive model

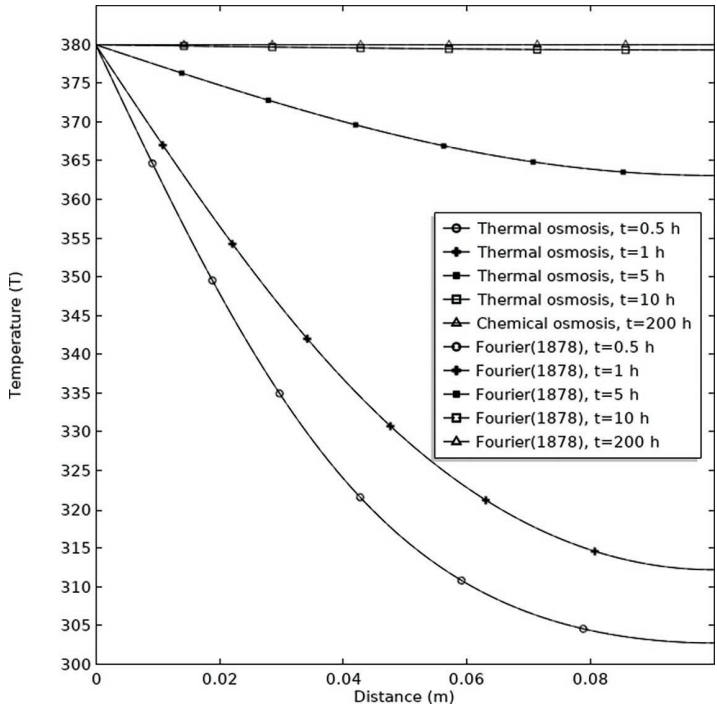

FIGURE 6.3 Evolution of temperature with time

developed in this chapter accurately predicts the thermal osmotic effects.

Finally, once the temperature reaches a steady state and the temperature gradient diminishes, the water pressure within the domain returns to its initial state, and no further water flow occurs. This highlights the effective role of thermal osmosis in influencing the physical behavior of porous media under thermal gradients, a key aspect that is not captured in traditional models.

6.7 CONCLUSION

This chapter has provided a comprehensive derivation of an unsaturated THM model, incorporating thermal osmosis, within the framework established in Chapters 3–5. By utilizing the Mixture-Coupling theory, the chapter illustrates how nanoscale influences in geomaterials can be integrated into the model, offering a significant advantage over traditional models derived from mechanics approaches. These nanoscale

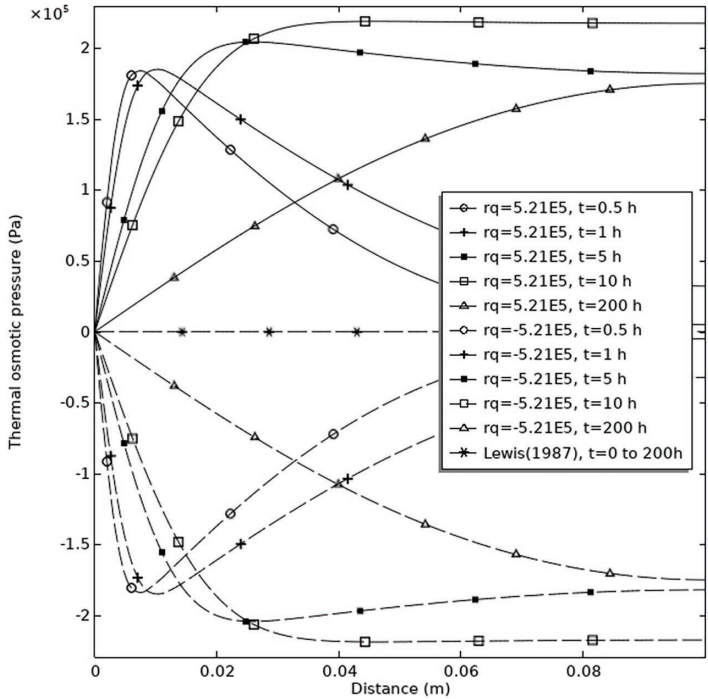

FIGURE 6.4 Evolution of water pressure with time

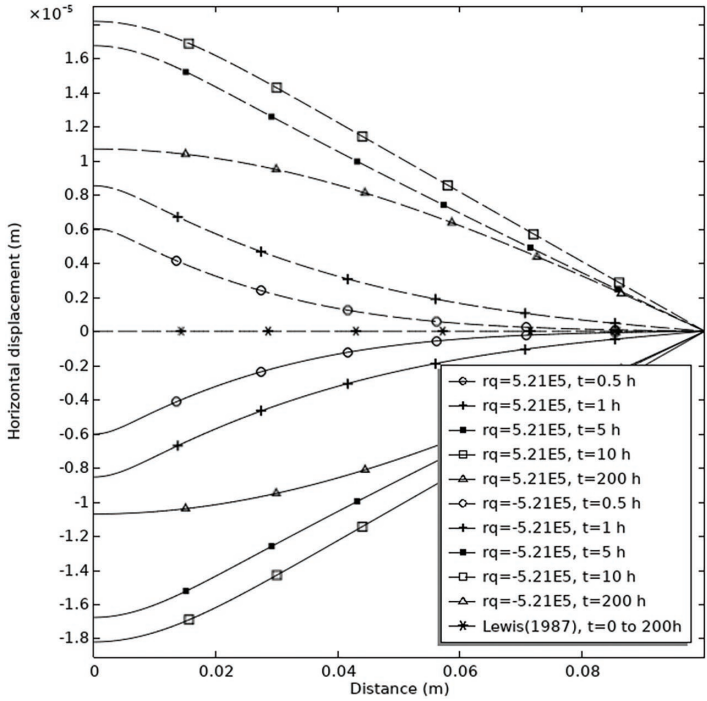

FIGURE 6.5 Displacement change induced by thermal osmosis

effects, such as the impact of molecular interactions on material behavior, are often difficult to capture through experimental means, making this theoretical framework especially valuable in advancing our understanding of complex geomaterials.

The focus of this chapter has been primarily on thermal osmosis, and as such, swelling effects have not been included in the model. However, the foundation laid here provides a clear path for incorporating swelling into the model, drawing from the theory presented in Chapters 3 and 4. By building on this foundation, readers can extend the current model to include swelling materials, further enhancing its applicability to a wide range of geotechnical and geoenvironmental problems.

Looking forward, Chapter 7 will build upon this work by exploring the chemical influence within an unsaturated thermo-hydro-mechanical-chemical (THMC) model, developed within the same theoretical framework. This extension will allow for a more comprehensive understanding of the coupled processes that govern the behavior of

geomaterials, particularly in low-permeability soils and rocks, where chemical interactions and transport processes play a critical role. This progression will help bridge the gap between fundamental theory and practical applications in geotechnical engineering, advancing the ability to model complex environmental systems and improving predictive capabilities in areas such as waste disposal, soil stabilization, and natural resource management.

NOTES

1 Since $\frac{d}{dt}\int_{\mathrm{v}(t)} \psi \, dV = \int_{V(t)} \left(\psi + \psi \nabla \cdot \mathbf{v}_s\right)$ and

$$\frac{d}{dt}\int_{V(t)} \varepsilon \, dV = \int_{V(t)} \left(\varepsilon + \varepsilon \nabla \cdot \mathbf{v}_s\right) dV,$$

using equation (6.7), it leads to

$$\begin{aligned}\int_{V(t)} \left(\psi + \psi \nabla \cdot \mathrm{v}_s\right) &= \int_{V(t)} \left(\dot{\varepsilon} + \varepsilon \nabla \cdot \mathrm{v}_s\right) dV - \int_{V(t)} \left(T\eta + \eta T + T\eta \nabla \cdot \mathrm{v}_s\right) dV \\ &= \int_{V(t)} \left(\dot{\varepsilon} + \varepsilon \nabla \cdot \mathrm{v}_s - T\eta - T\left(\eta + \eta \nabla \cdot \mathrm{v}_s\right)\right) dV\end{aligned}$$

2 The influence of temperature variation on the chemical potential is ignored here.

3 $$T\gamma = \mathbf{I}_q^{'} \cdot \frac{\nabla(-T)}{T} - \mathbf{I}_w \cdot \left(\frac{\nabla p_w}{\rho_l^w}\right)$$

$$\because \ \mathbf{I}_w = \mathrm{u}\,\rho_l^w, \therefore T\gamma = \mathbf{I}_q^{'} \cdot \frac{\nabla(-T)}{T} - \mathbf{u} \cdot \left(\nabla p_w\right)$$

4 $$\mathbf{u} = -\frac{L_{11}}{\left(\rho_l^w\right)^2}\left(\nabla p_w\right) - \frac{L_{12}}{\rho_l^w}\frac{\nabla T}{T} = -\left(\frac{L_{11}}{\left(\rho_l^w\right)^2}\right)\left[\nabla p_w + \left(\frac{L_{12}}{L_{11}}\right)\frac{\rho_l^w \nabla T}{T}\right]$$

5 $$\mathbf{I}_q' = -L_{21}\left(\frac{\nabla p_w}{\rho_l^w}\right) - L_{22}\left(\frac{\nabla T}{T}\right) = -\left(\frac{L_{21} p_w}{\left(\rho_l^w\right)^2}\right)\left(\rho_l^w \frac{\nabla p_w}{p_w}\right) - L_{22}\left(\frac{\nabla T}{T}\right) =$$
$$-L_q\left(\rho_l^w \frac{\nabla p_w}{p_w}\right) - \frac{L_{22}}{T}\nabla T$$

6 $$
\begin{aligned}
&(\Psi - J\phi\psi_{pore})^{\cdot} = \dot{\Psi} - \upsilon\dot{\psi}_{pore} - \psi_{pore}\dot{\upsilon} \\
&= \overbrace{\left[tr(\mathbf{T}\dot{\mathbf{E}}) + \mu_w\dot{\rho}_{w,ref} - \dot{T}J\eta\right]}^{\dot{\Psi}} - \overbrace{\left[\upsilon\mu_w(S_w\rho_l^{pore})^{\cdot} - \upsilon\dot{T}S_w\eta_l^w\right]}^{\upsilon\dot{\psi}_{pore}} \\
&- \overbrace{\left[-p_{pore} + S_w\rho_l^{pore}\mu_w\right]}^{\psi_{pore}}\dot{\upsilon} \\
&= tr(\mathbf{T}\dot{\mathbf{E}}) + \mu_w\dot{\rho}_{w,ref} \overbrace{-\upsilon\mu_w(S_w\rho_l^{pore})^{\cdot} - \dot{\upsilon}(S_w\rho_l^{pore}\mu_w)}^{1} + p_{pore}\dot{\upsilon} \\
&- \overbrace{\left[\dot{T}J\eta - \upsilon\dot{T}S_w\eta_l^w\right]}^{2} \\
&= tr(\mathbf{T}\dot{\mathbf{E}}) + \overbrace{\mu_w\dot{\rho}_{w,ref} - \mu_w(S_w\rho_l^{pore}\upsilon)^{\cdot}}^{1} + p_{pore}\dot{\upsilon} - \overbrace{\left[\dot{T}J\eta - J\phi\dot{T}S_w\eta_l^w\right]}^{2} \\
&= tr(\mathbf{T}\dot{\mathbf{E}}) + p_{pore}\dot{\upsilon} - \underbrace{\overbrace{\dot{T}J\eta_s}^{2}}_{=T\mathrm{H}_s}
\end{aligned}
$$

Note: Compared with the note 4 in Chapter 4, the bounded mass density vanishes as swelling phenomenon is not considered in this chapter. $\dot{T}J\eta_s$ has been included.

REFERENCES

Barragán, V. M. & Kjelstrup, S. (2017) Thermo-osmosis in membrane systems: a review. *Journal of Non-equilibrium Thermodynamics* **42(3)**: 217–236.

Biot, M. A. (1962) Mechanics of deformation and acoustic propagation in porous media. *Journal of Applied Physics* **33**: 1482–1498.

Biot, M. A. (1972) Theory of finite deformations of porous solids. *Indiana University Mathematics Journal* **21**: 597–620.

Carnahan, C. L. (1983) Thermodynamic coupling of heat and matter flows in near-field regions of nuclear waste repositories. *MRS Proceedings* **26**: 1023.

Chen, X., Pao, W. & Li, X. (2013) Coupled thermo-hydro-mechanical model with consideration of thermal-osmosis based on modified mixture theory. *International Journal of Engineering Science* **64**: 1–13.

Chen, X., Wang, M., Hicks, M. A. & Thomas, H. R. (2018) A new matrix for multiphase couplings in a membrane porous medium. *International Journal for Numerical Analytical Methods in Geomechanics* **42(10)**: 1144–1153.

Dirksen, D. (1969) Thermo-osmosis through compacted saturated clay membranes. *Soil Science Society of America, Proceedings* **33(6)**: 821–826.

Ghassemi, A. & Diek, A. (2003) Linear chemo-poroelasticity for swelling shales: theory and application. *Journal of Petroleum Engineering* **38**: 199–212.

Gonçalvès, J., De Marsily, G., Tremosa, J. J. E. & Letters, P. S. (2012) Importance of thermo-osmosis for fluid flow and transport in clay formations hosting a nuclear waste repository. *Earth and Planetary Science Letters* **339**: 1–10.

Haase, R. (1969) *Thermodynamics of irreversible processes*. Reading, MA, Addison-Wesley.

Katachalsky, A. & Curran, P. F. (1965) Nonequilibrium thermodynamics in biophysics. Cambridge, MA, Harvard University Press.

Lewis, R. W. & Schrefler, B. A. (1987) *The finite-element method in deformation and consolidation of porous media.* New York, Wiley.

Moran, M. J. & Shapiro, H. N. (2000) *Fundamentals of engineering thermodynamics*. 4th edn. Ontario, Canada, John Wiley & Sons Canada, Ltd.

Srivastava, R. C. & Avasthi, P. K. (1975) Non-equilibrium thermodynamics of thermo-osmosis of water through kaolinite. *Journal of Hydrology* **24(1)**: 111–120.

Steiger, R. P. & Leung, P. K. (1988) Quantitative determination of the mechanical properties of shales. In *The 63rd Annual Technical Conference and Exhibition of SPE*. Houston, TX.

Terzaghi, K. (1943) Theore*tical soil mechanics*. New York, John Wiley & Sons.

7 Unsaturated thermo-hydro-mechanical-chemical coupled model

7.1 INTRODUCTION

Chapters 3 and 4 introduce the use of Mixture-Coupling Theory in molecular induced swelling, while Chapters 5 and 6 introduce chemical osmosis and thermal osmosis at the nanoscale. In this chapter, Mixture-Coupling Theory is used to develop constitutive coupled thermal (T), hydro (H), mechanical (M), and chemical (C) processes in geomaterials.

The conceptual model of the representative elementary volume (REV) for thermo-hydro-mechanical-chemical (THMC) is shown in Figure 7.1: a microscopic region (Ω) is selected with the solid phases attached to the boundary (Γ) to ensure no movement of solid across the boundary. The thermo transport caused by the temperature difference between A and B, the chemical transport due to the change in concentration from c_a to c_b, and their influence on pore water pressure and solid deformation are analyzed.

The structure of the THMC formulation based on Mixture-Coupling Theory remains the same as the structure described in Chapters 3–6, demonstrating one of the major advantages of Mixture-Coupling Theory: a unified theoretical framework for multiphase physical-chemical coupling.

7.2 ENERGY BALANCE IN THE MIXTURE

The balance of the Helmholtz free energy density combines both internal energy and dissipative energy.

DOI: 10.1201/9780429324925-7

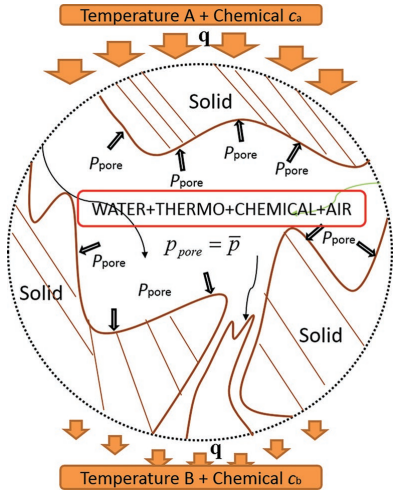

FIGURE 7.1 Conceptual model of THMC coupled behavior in the porous media

7.2.1 Internal energy and entropy density balance equation

For a non-isothermal unsaturated field in the absence of chemical reactions and gas transport, the internal energy density balance equation may be described as

$$\frac{d}{dt}\int_{V(t)} \varepsilon\, dV = \int_{\Gamma} (\boldsymbol{\sigma}\mathbf{v}_s - \mathbf{I}'_q)\cdot \mathbf{n}\, d\Gamma - \underbrace{\int_{\Gamma} \sum_{\alpha}\sum_{k} h_{\alpha}^{k}\mathbf{I}_{\alpha}^{k}\cdot \mathbf{n} d\Gamma}_{\substack{\text{Heat carried by fluids } (\alpha) \\ \text{each contains } k \text{ chemicals}}} \tag{7.1}$$

where the reduced heat flow (heat by conduction) in equation (6.1) can be expanded to accommodate multiple phases and chemicals as

$$\mathbf{I}'_q = \mathbf{I}_q - \sum_{\alpha}\sum_{k} h_{\alpha}^{k}\mathbf{I}_{\alpha}^{k} \tag{7.2}$$

By using Reynolds transport theorem and divergence theorem, the local form of equation (7.1) is obtained as

$$\dot{\varepsilon} + \varepsilon \nabla \cdot \mathbf{v}_s = \nabla \cdot \boldsymbol{\sigma} \mathbf{v}_s - \nabla \cdot \mathbf{I}'_q - \sum_{\alpha} \sum_{k} h_{\alpha}^{k} \nabla \cdot \mathbf{I}_{\alpha}^{k} \tag{7.3}$$

which can be rewritten by using the total heat flow, $\mathbf{I}_q = \mathbf{I}'_q + \sum_{\alpha} \sum_{k} h_{\alpha}^{k} \mathbf{I}_{\alpha}^{k}$, leading to

$$\dot{\varepsilon} + \varepsilon \nabla \cdot \mathbf{v}_s = \nabla \cdot \boldsymbol{\sigma} \mathbf{v}_s - \nabla \cdot \mathbf{I}_q \tag{7.4}$$

The entropy density balance equation is

$$\frac{d}{dt} \int_{V(t)} \eta \, dV = \underbrace{\int_{\Gamma} -\mathbf{I}_{\eta} \cdot \mathbf{n} \, d\Gamma}_{\text{Entropy exchange}} + \underbrace{\int_{V} \gamma \, dV}_{\text{Entropy production}} \tag{7.5}$$

where $\mathbf{I}_{\eta}$ is the entropy flow described as

$$\begin{aligned} \mathbf{I}_{\eta} &= \frac{\mathbf{I}_q - \sum_{\alpha} \sum_{k} \mu_{\alpha}^{k} \mathbf{I}_{\alpha}^{k}}{T} = \frac{\mathbf{I}_q - \sum_{\alpha} \sum_{k} h_{\alpha}^{k} \mathbf{I}_{\alpha}^{k} + \sum_{\alpha} \sum_{k} T \eta_{\alpha}^{k} \mathbf{I}_{\alpha}^{k}}{T} \\ &= \frac{\mathbf{I}'_q + \sum_{\alpha} \sum_{k} T \eta_{\alpha}^{k} \mathbf{I}_{\alpha}^{k}}{T} \end{aligned} \tag{7.6}$$

The local version of equation (6.4) can be obtained as

$$\dot{\eta} + \eta \nabla \cdot \mathbf{v}_s = -\nabla \cdot \mathbf{I}_{\eta} + \gamma \tag{7.7}$$

7.2.2 Helmholtz free energy density balance equation

Since the Helmholtz free energy density ψ is defined as $\psi = \varepsilon - T\eta$, its time derivation for non-isothermal conditions (following Chapter 6) is

$$\frac{d}{dt} \int_{V(t)} \psi \, dV = \frac{d}{dt} \int_{V(t)} (\varepsilon - T\eta) dV = \frac{d}{dt} \int_{V(t)} \varepsilon \, dV - \frac{d}{dt} \int_{V(t)} T\eta \, dV \tag{7.8}$$

Using a similar derivation process to footnote (13) in Chapter 1, leads to

$$\psi + \dot{\psi} \nabla \cdot \mathbf{v}_s = \dot{\varepsilon} + \varepsilon \nabla \cdot \mathbf{v}_s - \dot{T}\eta - T\left(\dot{\eta} + \eta \nabla \cdot \mathbf{v}_s\right) \tag{7.9}$$

Introducing a local form of the entropy balance equation (6.6), equation (6.9) can be rewritten as

$$\begin{aligned}\dot{\psi}+\psi\nabla\cdot\mathbf{v}_s &= \dot{\varepsilon}+\varepsilon\nabla\cdot\mathbf{v}_s-\dot{T}\eta-T\left(-\nabla\cdot\mathbf{I}_\eta+\gamma\right)\\ &= \dot{\varepsilon}+\varepsilon\nabla\cdot\mathbf{v}_s-\dot{T}\eta+T\nabla\cdot\mathbf{I}_\eta-T\gamma\end{aligned} \tag{7.10}$$

and

$$\dot{\psi}+\psi\nabla\cdot\mathbf{v}_s-(\dot{\varepsilon}+\varepsilon\nabla\cdot\mathbf{v}_s)+\dot{T}\eta-T\nabla\cdot\mathbf{I}_\eta=-T\gamma\le 0 \tag{7.11}$$

7.3 DISSIPATIVE PROCESS IN THE MIXTURE

Here, a macroscopic expression for the dissipation generated by the frictional resistance at the solid-fluid interface under non-isothermal conditions can be obtained by using standard arguments of nonequilibrium thermodynamics as

$$T\gamma=-\mathbf{I}_\eta\cdot\nabla T-\sum_\alpha\sum_k\mathbf{I}_\alpha^k\cdot\nabla\mu_\alpha^k \tag{7.12}$$

or in the form of reduced heat flow as

$$T\gamma=-\mathbf{I}_q'\cdot\frac{\nabla(-T)}{T}+\sum_\alpha\sum_k\mathbf{I}_\alpha^k\cdot\nabla\left(-\mu_\alpha^{k,c}\right) \tag{7.13}$$

where $-\mu_\alpha^k$ is the chemical potential depending on the concentration of the kth chemical.

If only one chemical and one solvent are considered, equations (7.12) and (7.13) become (Chen et al., 2018b)

$$T\gamma=-\mathbf{I}_\eta\cdot\nabla T-\mathbf{I}_w\cdot\nabla\mu_w-\mathbf{I}_c\cdot\nabla\mu_c \tag{7.14}$$

or

$$T\gamma=-\mathbf{I}_q'\cdot\frac{\nabla(-T)}{T}-\mathbf{I}_w\cdot\nabla\mu_w-\mathbf{I}_c\cdot\nabla\mu_c \tag{7.15}$$

where the reduced heat flow, which is the difference between the total heat flow and the heat flow caused by the water and chemical flux, can be simplified as

$$\mathbf{I}_q'=q-h_w\mathbf{I}_w-h_c\mathbf{I}_c$$

To discuss the interactions between heat and the multiphase flow, it is more convenient to use equation (7.15). Substituting the relationship between mass flux and diffusion flux from equation (1.33), $\mathbf{I}_k = \mathbf{J}_k + \rho_l^k \mathbf{u}$, into equation (7.15) leads to

$$T\gamma = -\mathbf{u} \cdot (\rho_l^w \nabla \mu_w + \rho_l^c \nabla \mu_c) - \mathbf{J}_w \cdot \nabla \mu_w - \mathbf{J}_c \cdot \nabla \mu_c + \mathbf{I}_q' \cdot \frac{\nabla(-T)}{T} \quad (7.16)$$

In order to obtain a relationship between chemical potential and liquid pressure, by introducing the Gibbs-Duhem equation (2.22) for the liquid and assuming the temperature influence on nonreactive chemicals (e.g., water) can be ignored, it leads to

$$\rho_l^w \nabla \mu_w + \rho_l^c \nabla \mu_c = \nabla p_l \quad (7.17)$$

Substituting equation (7.17) into equation (7.16) results in (Chen et al., 2018b)

$$0 \le T\gamma = -\mathbf{u} \cdot (\nabla p_l) - (\mathbf{J}_w \cdot \nabla \mu_w + \mathbf{J}_c \cdot \nabla \mu_c) + \mathbf{I}_q' \cdot \frac{\nabla(-T)}{T} \quad (7.18)$$

Since the diffusion fluxes $\mathbf{J}_w$ and $\mathbf{J}_c$ in equation (7.18) have to satisfy

$$\mathbf{J}_w + \mathbf{J}_c = 0$$

because there is one independent diffusion flux, the entropy production (7.18) can be rearranged as

$$0 \le T\gamma = -\mathbf{u} \cdot \nabla p_l - \mathbf{J}_c \cdot \nabla (\mu_c - \mu_w) + \mathbf{I}_q' \cdot \frac{\nabla(-T)}{T} \quad (7.19)$$

By substituting the relationship between μ_c and μ_w in equation (5.13), equation (7.19) can be rewritten as

$$0 \le T\gamma = -(\rho_l^w \mathbf{u}) \cdot \left(\frac{\nabla p_l}{\rho_l^w}\right) - \mathbf{J}_c \cdot \left[\frac{1}{c_w} \frac{\partial \mu_c}{\partial c_c} \nabla c_c\right] - \mathbf{I}_q' \cdot \frac{\nabla(T)}{T} \quad (7.20)$$

By using phenomenological equations and following similar steps as in previous chapters, the complete coupling matrix for multiphase flow with corresponding driving forces (including the major driving force and the coupled driving force) can be written as (Chen et al., 2018c),

$$\begin{pmatrix} \mathbf{u} \\ \mathbf{J}_c \\ \mathbf{I}_q^{'} \end{pmatrix} = -\begin{bmatrix} k\dfrac{k_{rl}}{v} & -k\dfrac{k_{rl}}{v}\dfrac{r_l\rho_l^l}{c_w}\dfrac{\partial\mu_c}{\partial c_c} & k\dfrac{k_{rl}}{v}\dfrac{r_q\rho_l^l}{T} \\ \dfrac{L\rho_l^l}{p_l} & \rho_l^l D & \dfrac{L_T}{T} \\ \dfrac{L_q\rho_l^l}{p_l} & \rho_l^l D_q & \lambda \end{bmatrix} \begin{pmatrix} \nabla p_l \\ \nabla c_c \\ \nabla T \end{pmatrix} \tag{7.21}$$

where

- $k\dfrac{k_{rl}}{v} = \dfrac{L_{11}}{\left(\rho_l^l\right)^2}$; k is the absolute permeability and k_{rl} is the relative permeability;
- $r_l = -\dfrac{L_{12}}{L_{11}}$ is the chemical reflection coefficient (Heidug and Wong, 1996; Staverman, 1951);
- $r_q = \dfrac{L_{13}}{L_{11}}$ is the thermal reflection coefficient (Chen et al., 2013);
- $L = \dfrac{L_{21}p_l}{\rho_l^{\,2}}$ is the pressure diffusion coefficient for chemical transport;
- L_T is the thermal conduction coefficient for chemical transport;
- $D = \dfrac{L_{22}}{c_w\rho_l^l}\dfrac{\partial\mu_c}{\partial c_c}$ is the dispersion-diffusion coefficient for chemical transport;
- $L_q = \left(\dfrac{L_{31}p_l}{\left(\rho_l^l\right)^2}\right)$ is the pressure diffusion coefficient for thermal transport;
- $D_q = \left(\dfrac{L_{32}}{c_w\rho_l^l}\dfrac{\partial\mu_c}{\partial c_c}\right)$ is the dispersion-diffusion coefficient for thermal transport, which links to the Dufour effect (Ingle and Horne, 1973) in Table 2.1;
- $\lambda = \dfrac{L_{33}}{T}$ is the conduction coefficient;
- $\dfrac{L_{33}}{T}$ is the thermal influence on the chemical transport which links to the Soret effect (Eastman, 1928) in Table 2.1.

Equation (7.21) extends Darcy's law, Fick's law, and Fourier's law by including the coupled influence. If this matrix is used in

Mixture-Coupling Theory, the coupled thermo-chemical osmosis for the THMC model can be obtained (Chen et al., 2020). However, as this section is to build the foundation for THMC coupling, a simplified matrix, which incorporates the traditional Darcy's law, Fick's law, and Fourier law, is used:

$$\begin{pmatrix} \mathbf{u} \\ \mathbf{J}_c \\ \mathbf{I}_q^{'} \end{pmatrix} = -\begin{bmatrix} k\dfrac{k_{rl}}{v} & 0 & 0 \\ 0 & \rho_l^l D & 0 \\ 0 & 0 & \lambda \end{bmatrix} \begin{pmatrix} \nabla p_l \\ \nabla c_c \\ \nabla T \end{pmatrix} \tag{7.22}$$

7.4 CONSTITUTIVE RELATIONS OF THE MIXTURE

7.4.1 Free energy density evolution path of the mixture

7.4.1.1 Current configuration

It is assumed that the material maintains mechanical equilibrium, so that $\nabla \cdot \sigma = 0$. By substituting the entropy production equation (7.14) into the Helmholtz free energy density balance equation (7.11), The Helmholtz free energy density balance equation becomes

$$\dot{\psi} + \psi \nabla \cdot \mathbf{v}_s = \dot{\varepsilon} + \varepsilon \nabla \cdot \mathbf{v}_s - \dot{T}\eta + T\nabla \cdot \mathbf{I}_\eta - \underbrace{\left(-\mathbf{I}_\eta \cdot \nabla T - \mathbf{I}_w \cdot \nabla \mu_w - \mathbf{I}_c \cdot \nabla \mu_c\right)}_{T\gamma} \tag{7.23}$$

Since $T\nabla \cdot \mathbf{I}_\eta + \mathbf{I}_\eta \cdot \nabla T = \nabla \cdot \left(T\mathbf{I}_\eta\right)$, it leads to

$$\dot{\psi} + \psi \nabla \cdot \mathbf{v}_s = \dot{\varepsilon} + \varepsilon \nabla \cdot \mathbf{v}_s - \dot{T}\eta + \nabla \cdot \left(T\mathbf{I}_\eta\right) + \mathbf{I}_w \cdot \nabla \mu_c \tag{7.24}$$

Invoking $\mathbf{I}_\eta = \dfrac{\mathbf{I}_q - \mu_w \mathbf{I}_w - \mathbf{I}_c \cdot \nabla \mu_c}{T}$ into equation (7.24) leads to

$$\begin{aligned} \dot{\psi} + \psi \nabla \cdot \mathbf{v}_s = \dot{\varepsilon} + \varepsilon \nabla \cdot \mathbf{v}_s - \dot{T}\eta + \nabla \cdot (T \underbrace{\frac{\mathbf{I}_q - \mu_w \mathbf{I}_q - \mu_w \mathbf{I}_c}{T}}_{\mathbf{I}_\eta}) \\ + \mathbf{I}_w \cdot \nabla \mu_w + \mathbf{I}_c \cdot \nabla \mu_c \end{aligned} \tag{7.25}$$

which can be rearranged as

$$\begin{aligned}\dot{\psi} + \psi\nabla\cdot\mathbf{v}_s &= \dot{\varepsilon} + \varepsilon\nabla\cdot\mathbf{v}_s - \dot{T}\eta + \nabla\cdot\mathbf{I}_q - \nabla\cdot\left(\mu_w\mathbf{I}_w + \mu_w\mathbf{I}_c\right) + \mathbf{I}_w\cdot\nabla\mu_w + \mathbf{I}_c\cdot\nabla\mu_c \\ &= \dot{\varepsilon} + \varepsilon\nabla\cdot\mathbf{v}_s - \dot{T}\eta + \nabla\cdot\mathbf{I}_q - \mu_w\nabla\cdot\mathbf{I}_q - \mu_c\nabla\cdot\mathbf{I}_q\end{aligned} \tag{7.26}$$

Substituting the energy balance equation (7.4) into equation (7.26) leads to

$$\dot{\psi} + \psi\nabla\cdot\mathbf{v}_s = \nabla\cdot\sigma\mathbf{v}_s - \dot{T}\eta - \mu_w\nabla\cdot\mathbf{I}_w - \mu_c\nabla\cdot\mathbf{I}_c \tag{7.27}$$

7.4.1.2 Reference configuration

Multiplying by J on both sides of equation (7.27) leads to

$$J\dot{\psi} + J\psi\nabla\cdot\mathbf{v}_s = J\nabla\cdot\sigma\mathbf{v}_s - J\dot{T}\eta - J\mu_w\nabla\cdot\mathbf{I}_w - J\mu_w\nabla\cdot\mathbf{I}_c \tag{7.28}$$

and by using $\dot{\Psi} = J\dot{\psi} + J\psi\nabla\cdot\mathbf{v}_s$, equation (7.28) becomes

$$\dot{\Psi} = tr(\mathbf{T}\dot{\mathbf{E}}) - \dot{T}J\eta - J\mu_w\nabla\cdot\mathbf{I}_w - J\mu_c\nabla\cdot\mathbf{I}_c \tag{7.29}$$

in which $\Psi = J\psi$ is the free energy and $\mathbf{T}$ is the second Piola-Kirchhoff stress.

By substituting Euler's identity, and the balance equations for $\mathbf{I}_w$ and $\mathbf{I}_c$ from Section 2.2, equation (7.29) becomes

$$\dot{\Psi} = tr(\mathbf{T}\dot{\mathbf{E}}) - \dot{T}J\eta + \mu_w\dot{\rho}_{w,ref} + \mu_c\dot{\rho}_{c,ref} \tag{7.30}$$

where

- $\rho_{w,ref} = J\rho_w = J\phi\rho_l^w$ is the mass of the water per unit reference volume;
- $\rho_{c,ref} = J\rho_c = J\phi\rho_l^c$ is the mass of the chemical per unit reference volume.

7.4.2 Helmholtz free energy density of the pore water and solid matrix

The free energy density of the solid matrix can be derived by subtracting from the free energy Ψ of the combined material/fluid system the contribution $J\phi\psi_{pore}$ due to the pore water.

7.4.2.1 Current configuration (pore water)

The Helmholtz free energy density of the pore water, ψ_{pore}, can be obtained using equation (2.18) based on classical thermodynamics as

$$\psi_{pore} = -p_{pore} + \mu_c S_l \rho_l^c + \mu_w S_l \rho_l^w \tag{7.31}$$

and its time derivative as

$$\dot{\psi}_{pore} = -\dot{p}_{pore} + \mu_c \dot{S}_l \rho_l^c + \mu_w \dot{S}_l \rho_l^w + \mu_c \left(S_l \dot{\rho}_l^c \right) + \mu_w \left(S_l \dot{\rho}_l^w \right) \tag{7.32}$$

Also, according to the Gibbs-Duhem equation (equation (2.21), refer to Section 2.6),

$$\dot{p}_{pore} = \mu_c \dot{S}_l \rho_l^c + \mu_w \dot{S}_l \rho_l^w + T S_l \dot{\eta}_l^l \tag{7.33}$$

and by introducing equation (7.33) into (7.32), this leads to

$$\dot{\psi}_{pore} = \mu_c \left(S_l \dot{\rho}_l^c \right) + \mu_w \left(S_l \dot{\rho}_l^w \right) - \dot{T} \left(S_l \eta_l^l \right) \tag{7.34}$$

7.4.2.2 Reference configuration (solid matrix)

From equations (7.30) and (7.34), the following equation can be obtained:

$$\left(\Psi - J\phi\psi_{pore} \right) = tr(\mathbf{TE}) + p_{pore}\upsilon - TH_s \tag{7.35}^{1}$$

where $H_s = J\eta_s = J\eta - J\left(S_l \phi \eta_l^l\right)$ is the entropy density of the solid at the reference configuration and H is the entropy per unit reference volume of the solid and fluid mixture, given by

$$H = \left((1-\upsilon)\eta_s^s + S_l \upsilon \eta_l^l \right) = \left((1-\upsilon)\rho_s^s C_l + S_l \upsilon \rho_l^l C_s \right)$$

Note: The relationship between η_α and ρ_α can be found in equation (2.70).

7.4.3 Constitutive structure

The deformation potential W of the solid matrix is

$$W = \left(\Psi - J\phi\psi_{pore}\right) - p_{pore}\upsilon \tag{7.36}$$

Substituting equation (7.35) into the time derivative of equation (7.36) leads to

$$\dot{W} = tr\left(\mathbf{T}\dot{\mathbf{E}}\right) - \dot{T}H_s - \upsilon\dot{p}_{pore} \tag{7.37}^{2}$$

which indicates that W is a function of $\mathbf{E}$, p_{pore}, and T, and thus, expressions of $\dot{W}$ for $\mathbf{T}$ (or T_{ij}), υ, and H_s are obtained:

$$\dot{W}\left(\mathbf{E}, p_{pore}, \mathbf{T}\right) = \left(\frac{\partial W}{\partial E_{ij}}\right)_{p_{pore},T}\dot{E}_{ij} + \left(\frac{\partial W}{\partial p_{pore}}\right)_{E_{ij},T}\dot{p}_{pore} + \left(\frac{\partial W}{\partial T}\right)_{E_{ij},p_{pore}}\dot{T} \tag{7.38}$$

the following equations are also obtained:

$$T_{ij} = \left(\frac{\partial W}{\partial E_{ij}}\right)_{p_{pore},T}, \upsilon = -\left(\frac{\partial W}{\partial p_{pore}}\right)_{E_{ij},T}, H_s = -\left(\frac{\partial W}{\partial T}\right)_{E_{ij},p_{pore}} \tag{7.39}$$

If equation (7.39) is differentiated with respect to time, the fundamental constitutive equations for the evolution of stress, pore volume fraction, and temperature can be expressed as

$$\dot{T}_{ji} = L_{ijkl}\dot{E}_{kl} - M_{ij}\dot{p}_{pore} + S_{ij}^{q}\dot{T} \tag{7.40}$$

$$\dot{\upsilon} = M_{ij}\dot{E}_{ij} + Q\dot{p}_{pore} + B_q\dot{T} \tag{7.41}$$

$$\dot{H}_s = -S_{ij}^{q}\dot{E}_{ij} + B_q\dot{p}_{pore} + Z_q\dot{T} \tag{7.42}$$

where the parameters L_{ijkl}, M_{ij}, S_{ij}^{q}, Z_q, B_q, and Q are material-dependent constants defined by the following group of equations (the derivation process can be found in the Appendix 6)

$$L_{ijkl} = \left(\frac{\partial T_{ij}}{\partial E_{kl}}\right)_{p_{pore},T} = \left(\frac{\partial T_{kl}}{\partial E_{ij}}\right)_{p_{pore},T}$$

$$M_{ij} = -\left(\frac{\partial T_{ij}}{\partial p_{pore}}\right)_{E_{ij},T} = \left(\frac{\partial \upsilon}{\partial E_{ji}}\right)_{p_{pore},T}$$

$$S_{ij}^{q} = \left(\frac{\partial T_{ij}}{\partial T}\right)_{E_{ij},P_{pore}} = -\left(\frac{\partial H_s}{\partial E_{ij}}\right)_{p_{pore},T} \tag{7.43}$$

$$Z_q = \left(\frac{\partial H_s}{\partial T}\right)_{E_{ij},p_{pore}}, B_q = \left(\frac{\partial \upsilon}{\partial T}\right)_{E_{ij},p_{pore}} = \left(\frac{\partial H_s}{\partial p_{pore}}\right)_{E_{ij},T}, Q = \left(\frac{\partial \upsilon}{\partial p_{pore}}\right)_{E_{ij},\mu}$$

The matrix format of equation (7.43) is

$$\begin{bmatrix} \dot{T}_{ij} \\ \dot{\upsilon} \\ \dot{H}_s \end{bmatrix} = \begin{bmatrix} L_{ijkl} & -M_{ij} & S_{ij}^{q} \\ M_{ij} & Q & B_q \\ -S_{ij}^{q} & B_q & Z_q \end{bmatrix} \begin{bmatrix} \dot{E}_{kl} \\ \dot{p}_{pore} \\ \dot{T} \end{bmatrix} \tag{7.44}$$

Equation (7.44) looks the same as equation (6.46), and it does not include the chemical influence. This is because nonreactive chemicals do not directly engage with solids (unlike swelling materials or osmotic function influence), but link only with water transport as an internal coupling (Chen et al., 2016).

7.5 COUPLED FIELD EQUATIONS

7.5.1 Solid-phase and porosity

Following the same assumption of physical and geometrical linearization, and small strain as in Chapter 3 (Section 3.5), the governing stress and pore fraction equations, (7.40) and (7.41), can be changed to

$$\dot{\sigma}_{ij} = \underbrace{\left(K - \frac{2G}{3}\right)\dot{\varepsilon}_{kk}\delta_{ij} + 2G\dot{\varepsilon}_{ij}}_{1} - \underbrace{\zeta \dot{p}_{pore}\delta_{ij}}_{2} + \underbrace{\omega_T \dot{T}\delta_{ij}}_{3} \tag{7.45}$$

$$\dot{\upsilon} = \underbrace{\zeta\dot{\varepsilon}_{ii}}_{4} + \underbrace{Q\dot{p}_{pore}}_{5} + \underbrace{B_q\dot{T}}_{6} \tag{7.46}$$

where

- $\omega_T = \beta_s / 3$ and β_s is the thermal expansion coefficient of the solid;
- B_q is the thermal expansion coefficient. (Note here: The detailed discussion and derivation of other parameters can be found in Section 3.5.1. and Chapter 6.)

Since reactive chemicals are not considered, these two equations are very similar to equations (6.47) and (6.48). For the purpose of completeness of the chapter, the physical meanings of the terms in equations (7.45) and (7.46) have been included as follows:

- 1: Elastic deformation of the solids.
- 2: The pore pressure coupling term, describing the influence of the pore pressure on the deformation of the solids. Note: The pore pressure comprises pore liquid pressure and gas pressure (assumed to be zero).
- 3: The temperature coupling term, describing the influence of the temperature variation on the deformation of the solids.
- 4: Deformation-induced porosity change.
- 5: Pressure-induced porosity change, without consideration of swelling influence (i.e., $B = 0$, compared with equation (4.33)).
- 6: Temperature-induced porosity change (e.g., thermal expansion).

7.5.2 Fluid phase

In the absence of chemical reaction, the balance equation (2.49) for the liquid is

$$\left(\upsilon S_l \rho_l^l\right) + \nabla \cdot \left(\rho_l^l \mathbf{u}\right) = 0 \tag{7.47}$$

By introducing equations (7.46) and (7.21) for $\mathbf{u}$ as

$$\mathbf{u} = -k\frac{k_{rl}}{v}\nabla p_l - k\frac{k_{rl}}{v}\frac{r_l \rho_l^l}{c_w}\frac{\partial \mu_c}{\partial c_c}\nabla c_c - k\frac{k_{rl}}{v}\frac{r_q \rho_l^l}{T}\nabla T$$

the control equation for the liquid phase can be written as

$$\begin{aligned}&\underbrace{S_l \rho_l^l \left(\zeta \varepsilon_{ii} + Q p_{pore} + B_q T\right)}_{7} + \underbrace{\upsilon\left(S_l \rho_l^l\right)}_{8} \\ &+ \underbrace{\nabla^T \cdot \rho_l^l \left[-k\frac{k_{rl}}{v}\nabla p_l - k\frac{k_{rl}}{v}\frac{r_l \rho_l^l}{c_w}\frac{\partial \mu}{\partial c_c}\nabla c_c - k\frac{k_{rl}}{v}\frac{r_q \rho_l^l}{T}\nabla T\right]}_{9} = 0\end{aligned} \tag{7.48}$$

The physical meaning of terms in equation (7.48) are:

- 7: Liquid flow caused by porosity change, due to the time-dependent variations of the solid deformation, the pore pressure, and the temperature.

- 8: Liquid flow caused by liquid mass density and saturation ratio change.
- 9: Extended Darcy's law with consideration of chemical osmosis and thermal osmosis, which is one of the key novelties of the equation.

7.5.3 Chemical

The balance equation for the chemical transport is equation (2.50) (refer to Section 2.2), i.e.

$$\left(\upsilon S_l \rho_l^l\right)\dot{c}_k + \rho_l^l \mathbf{u}\cdot\nabla c_k + J\nabla\cdot\mathbf{J}_k = 0 \tag{7.49}$$

By assuming only one chemical is present ($c_k = c_c$ in equation (7.49)), and substituting the equations for modified Darcy's law and chemical diffusion from equation (7.21), equation (7.49) can be written as

$$\underbrace{S_l\rho_l^l\upsilon c_c}_{10} + \underbrace{\rho_l^l\left[-k\frac{k_{rl}}{v}\nabla p_l - k\frac{k_{rl}}{v}\frac{r_l\rho_l^l}{c_w}\frac{\partial\mu_c}{\partial c_c}\nabla c_c - k\frac{k_{rl}}{v}\frac{r_q\rho_l^l}{T}\nabla T\right]\cdot\nabla c_c}_{11} + \underbrace{\nabla\cdot\left[-\frac{L\rho_l^l}{p_1}\nabla p_l - \rho_l D\nabla c_c - \frac{L_T}{T}\nabla T\right]}_{12} = 0 \tag{7.50}$$

The physical meaning of terms in equation (7.50) are:

- 10: Chemical concentration change over time.
- 11: The chemical transport caused by the liquid flow (convection flux). The novelty in this term is that the chemical and thermo osmotic flows have been embedded.
- 12: The extended Fick's law of the chemical diffusion process. The novelty of this term is that the pressure and temperature gradient may have an influence on the chemical diffusion process.

7.5.4 Thermal

The balance equation for heat transport is equation (2.62) (refer to Section 2.2), i.e.

$$\left(q_s^s\left(1-\upsilon\right)+\upsilon q_l^l S_l\right)+J\nabla\cdot\left(\mathbf{I}_q'+h_w\mathbf{I}_w+h_c\mathbf{I}_c\right)=0 \tag{7.51}$$

By substituting equation (7.21) in the form

$$\mathbf{I}_q'=-\frac{L_q\rho_l^l}{p}\nabla p_l-\rho_l^l D_q\nabla c_c-\lambda\nabla T$$

and summarizing all the chemical components into one phase as

$$\sum h_k\mathbf{I}_k=h_\alpha\mathbf{I}_\alpha=h_\alpha\rho_\alpha^\alpha\mathbf{u}_\alpha \tag{7.52}$$

into equation (7.51), it leads to

$$\underbrace{\frac{\partial}{\partial t}\left\{\left[\left(1-\upsilon\right)\rho_s^s C_s+S_l\upsilon\rho_l^l C_f\right]T\right\}}_{13}+\underbrace{\nabla^T\cdot\left(-\frac{L_q\rho_l^l}{p}\nabla p_l-\rho_l^l\,\mathrm{D}_q\,\nabla\,\mathrm{c}_c-\lambda\nabla\,\mathrm{T}\right)}_{14}$$

$$+\underbrace{J\nabla\cdot\left(\rho_l^l\mathbf{u}_l C_l T\right)}_{15}=0 \tag{7.53}$$

The physical meaning of terms in equation (7.53) are:

- 13: Thermal density in a pore changes over time.
- 14: The thermo transport caused by the temperature difference (conduction), which is an extension of Fourier's law. The novelty in this term is that the water pressure and chemical gradient have an influence on the conduction process.
- 15: The thermo transport by the fluid (e.g., liquid).

7.6 NUMERICAL SIMULATION

7.6.1 Mathematical equations

Mechanical: If the mechanical equilibrium condition, $\frac{\partial\sigma_{ij}}{\partial x_{ij}}=0$, is introduced into equation (7.45), and considering equations (1.41) and (4.42) for the average pressure (assuming these equations apply to a liquid with chemicals), the final equation for the mechanical deformation is

$$\left(K-\frac{2G}{3}\right)\frac{\partial^2 \dot{d}_k}{\partial x_k \partial x_i}+G\left(\frac{\partial^2 \dot{d}_i}{\partial x_j \partial x_j}+\frac{\partial^2 \dot{d}_j}{\partial x_i \partial x_j}\right)-\zeta\nabla\left[(S_l+\frac{C_s}{\phi}p_l)\dot{p}_l\right]+\omega_T\frac{\partial \dot{T}}{\partial x_i}=0 \quad (7.54)$$

To simplify the discussion, the porosity is assumed to be constant, and equation (7.46) for porosity change is not used in the simulation.

Hydro: By simplifying equation (7.48) using equation (7.22) for u (simplified from equation (7.21) by ignoring the chemical osmosis and thermo-osmosis), and considering equations for the rate of change of saturation function and the rate of change of water density function (4.43) (with the assumption that the chemicals do not present significant influence), the control equation for the liquid phase can be written as

$$\begin{aligned}&S_l\rho_l^l\zeta\nabla\cdot d+S_l\rho_l^l\left(Q+B/\rho_l^l\right)p_{pore}+\phi\rho_l^l\frac{\partial S_l}{\partial t}+\phi S_l\frac{\partial \rho_l^l}{\partial t}\\&+\rho_l^l\left[-\nabla\cdot\frac{k_{rl}k}{v}(\nabla p_l)\right]+B_qT=0\end{aligned} \quad (7.55)$$

By substituting equations (1.41) and (4.42) for the average pressure, equation (7.55) can be rewritten as

$$\begin{aligned}&S_l\zeta\nabla\cdot d-\nabla\cdot\frac{k_{rl}k}{v}(\nabla p_l)+\left(C_s^p+\phi\frac{S_l}{K_l}\right)\frac{\partial p_l}{\partial t}\\&+S_l\left(Q+B/\rho_l^l\right)\left(S_l+\frac{C_s^p}{\phi}p_l\right)\frac{\partial p_l}{\partial t}+B_qT=0\end{aligned} \quad (7.56)$$

Chemical: By assuming that the chemical osmosis and thermo-osmosis can be ignored (for high-permeability porous media $r_l=0=r_q$), and the influence of temperature gradient on c_c is zero, equation (7.50) can be simplified as

$$S_l\phi c_c-\left[k\frac{k_{rl}}{v}(\nabla p_l)\right]\cdot\nabla c_c-\nabla\left(\frac{L}{p_l}\nabla p_l\right)-D\nabla^2 c_c=0 \quad (7.57)^3$$

Thermo: If the coupling terms of p_l and c_c in equation (7.53) are ignored (and assuming the fluid transport influence term is $\nabla\cdot\left(\rho_l^l\mathbf{u}_lC_lT\right)\approx 0$), then the same function as derived using Fourier's law is obtained:

$$\frac{\partial}{\partial t}\left\{\left[(1-\phi)\rho_s^sC_s+S_l\phi\rho_l^lC_l\right]T\right\}-\nabla^T\lambda\nabla T=0 \quad (7.58)$$

where λ is the material thermal conductivity.

7.6.2 Discussion and comparison

The simplified unsaturated THMC coupled model equations (7.54), (7.56), (7.57), and (7.58) are essentially the same as those developed via the mechanics approach (Thomas et al., 2001, 2002), establishing a direct validation of the theory. These equations are simplified without consideration of swelling, chemical osmosis, thermal osmosis, etc. Relevant research has already been done on the extra features not considered in the validation (Chen et al., 2018a), which shows the great advantage of the theory.

For those who are not familiar with THMC coupled modeling, the following section will again focus on comparing with classic laws (e.g., Darcy's law, etc.) and the model previously used as a comparison (Lewis and Schrefler, 1987).

7.6.3 Model geometry and boundary conditions

The model geometry and boundary conditions are presented in Figure 7.2 and are similar to those for the models in Chapters 5 and 6: a simple (plane strain) experimental setup (0.15 m × 0.3 m) with an unsaturated geomaterial sample (e.g., unsaturated rock) has been analyzed. Other details are as follows:

Boundary conditions: The top and bottom boundaries are fixed, stiff, and frictionless, allowing movement only in the horizontal (i.e., x) direction. Boundary B is fixed (displacement=0), whereas boundary A allows free movement. Boundaries A and B are both permeable and allow water to flow in and out of the sample.

Initial conditions: An equilibrium state is assumed at $t = 0$, with an external force applied at boundary A to maintain the equilibrium. The initial effective stress of the domain is assumed to be zero. The domain is assumed to contain water at a pressure of –5 MPa with a degree of saturation of 0.97 and has been modelled using the same van Genuchten relationship as used in Chapter 4. The initial temperature in the domain is 300 K and the chemical mass fraction is 0.1.

Start of the simulation: As for the numerical simulations in Chapters 5 and 6, no pressure gradient is applied initially. At boundary A, the water pressure is set at –5 MPa and remains constant during the modeling process. At boundary B, the pressure drops to –10 MPa as in Chapter

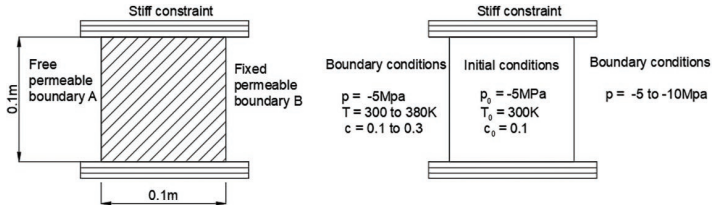

FIGURE 7.2 Geometry and boundary conditions

4. A chemical mass fraction of 0.3 is applied to boundary A ($t > 0$) to simulate the chemical gradient, and the temperature at boundary A is increased to 380 K to set up the thermal gradient.

The parameters adopted in this numerical simulation are a combination of the parameters adopted in Chapters 5 and 6, and are listed in Table 7.1.

7.6.4 Numerical simulation results

In this chapter, the classical finite element method has been employed to solve the governing equations, with results compared to those obtained using Lewis's THM (thermo-hydro-mechanical) equation and fundamental laws such as Fick's law, Fourier's law, and Darcy's law. This approach demonstrates how these classical equations fit within the broader framework of the more comprehensive model developed here.

Figure 7.3 illustrates the evolution of chemical mass fraction over time. Initially, the chemical mass fraction at boundary A is increased from 0.1 to 0.3, which drives the chemical transport from regions of higher to lower mass fraction within the domain. As time progresses, the chemical mass fraction gradually increases in the domain. By t = 200 hours, the chemical mass fraction reaches a steady state, after which it stabilizes. This behavior mirrors the predictions made by Fick's Law, as the influence of temperature and pressure on chemical transport is assumed to be negligible in equation (7.57).

Next, Figure 7.4 shows the temperature change over time. The temperature evolution follows a pattern very similar to the chemical mass fraction change, but with a faster rate of temperature change compared to the mass fraction, given the specific coefficients selected for the simulation. As with the chemical mass transport, the absence of pressure

TABLE 7.1
Material parameters (Rutqvist and Tsang, 2004)

Parameter	Physical meaning	Value and units
k	Absolute permeability	2.75E−21 m^2
η	Dynamic viscosity	8.54E−4 Pa·s
G	Shear modulus	239.08 MPa (Sugita et al., 2004)
E	Young's modulus	645.52 MPa
θ	Poisson's ratio	0.35 (Rutqvist and Tsang, 2004)
ϕ	Porosity	0.41
ζ	Biot's coefficient	1 (assumed)
K_s	Bulk modulus of solid	∞ (assumed)
K_w	Bulk modulus of water	2E3 MPa
R	Gas constant	8.314
M_c	Molar mass	0.0585 kg/mol
ρ_l^w	Density of fluid	998.2 kg/m^3
ρ_l^s	Density of solid	2,780 kg/m^3
r	Chemical reflection	0.2
D	Diffusion coefficient	4.48E−10 m^2/s①
m	van Genuchten parameter	0.18
M	van Genuchten parameter	20 MPa
C_s	Specific heat of solid	835.5 J/kg°C
C_w	Specific heat of water	4,202 J/kg°C
β_s	Thermal expansion coefficient for solid	2E−5/K
λ_s	Thermal conductivity of solid	1.5 W/m°C①
λ_w	Thermal conductivity of liquid	1.23 W/m°C①
r_q	Thermal reflection coefficient	5.21E5②

Table notes:
① calculated at T = 300 K.
② calculated from the relationship between thermal reflection coefficient and thermal osmotic permeability with T=300K and relative permeability=0.927.

and chemical influences on thermal transport results in predictions consistent with Fourier's law.

Figures 7.5–7.7 show the evolution of pressure, saturation, and displacement within the domain. As saturation and pressure are coupled

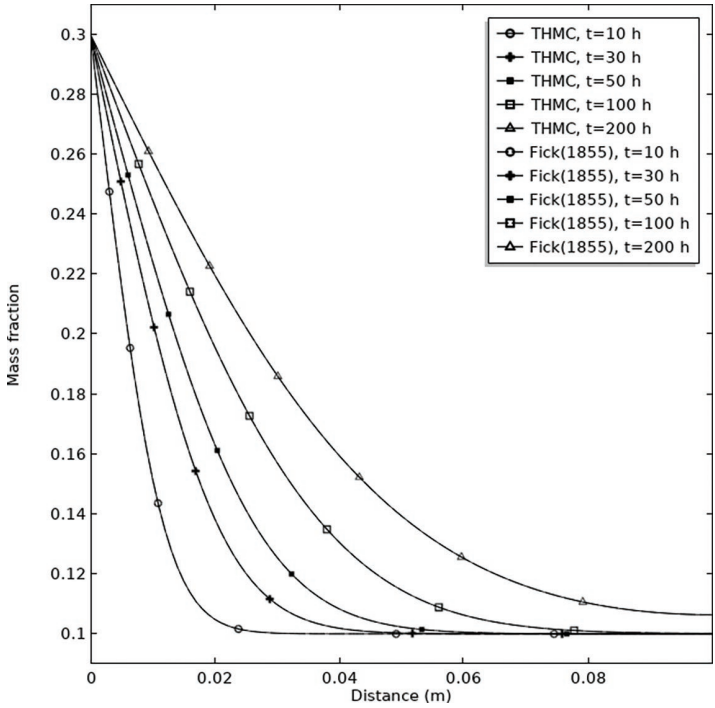

FIGURE 7.3 Evolution of chemical mass fraction with time

through the van Genuchten relationship, their trends are closely aligned, reflecting similar changes over time. Since swelling and osmotic phenomena, discussed in previous chapters, are not considered in this simulation, the results align closely with those obtained using the classical mechanics approach. These results suggest that the influence of osmotic and swelling effects, when excluded, leads to a behavior in agreement with traditional mechanical models.

The simulations confirm that classical equations such as Darcy's law, Fick's law, and Fourier's law are indeed special cases within the broader framework developed in this chapter. Additionally, the THM equations derived from the classical mechanics approach provide a simplified version of the full constitutive equations presented in equations (7.45), (7.46), (7.48), (7.50), and (7.53). These results demonstrate that the newly developed Mixture-Coupling Theory offers a more general, comprehensive framework for modeling the behavior of multiphase, multicomponent, and deformable porous media.

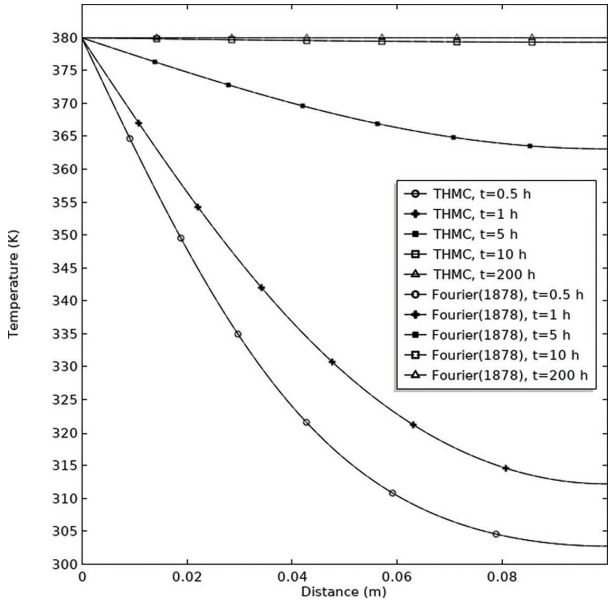

FIGURE 7.4 Evolution of temperature with time

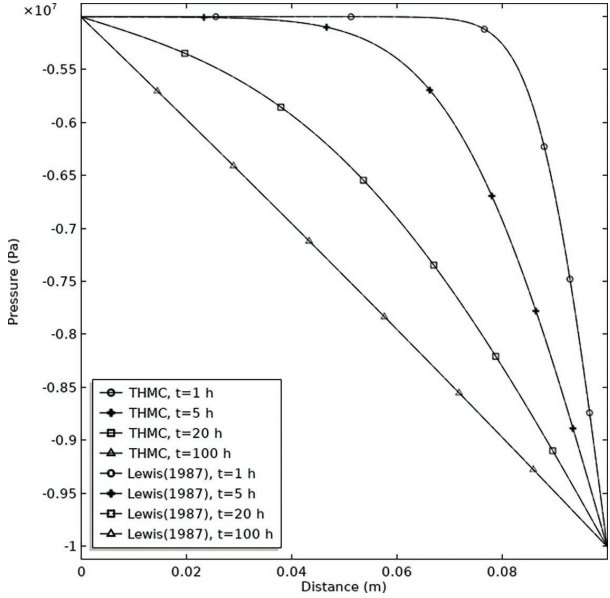

FIGURE 7.5 Pressure change

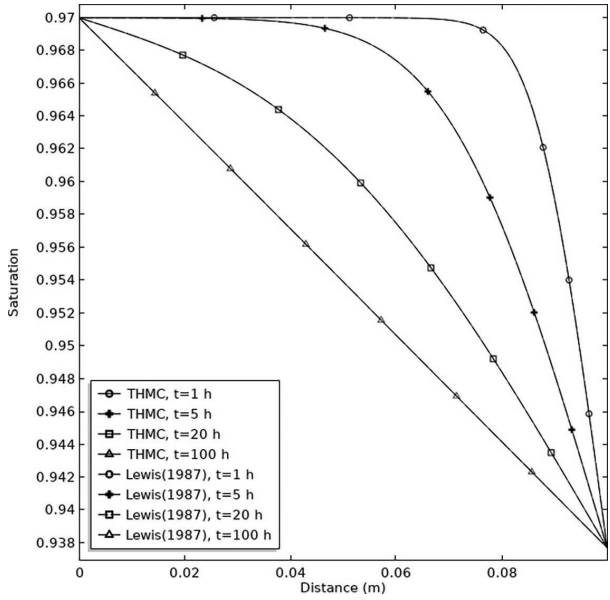

FIGURE 7.6 Saturation change

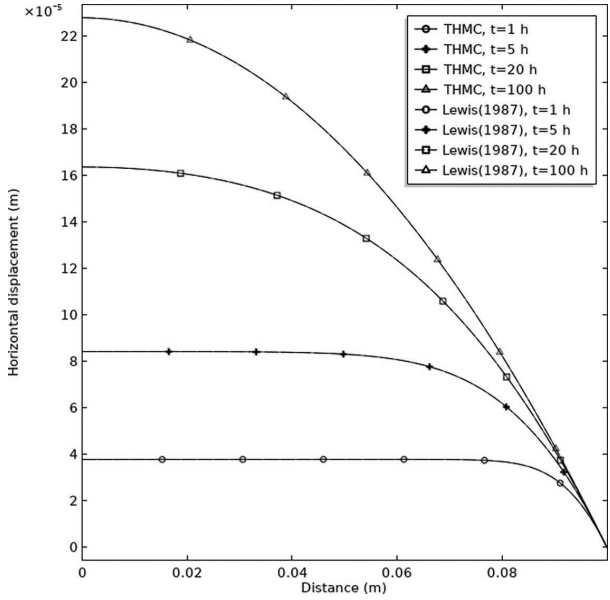

FIGURE 7.7 Horizontal displacement change

7.7 CONCLUSION

This chapter builds upon Mixture-Coupling Theory to establish a comprehensive, fully coupled unsaturated THMC model. The equations derived in this chapter, although simplified, retain the fundamental structure and key insights of the classical mechanics-based models while introducing more intricate coupling mechanisms and coefficients that were previously unaccounted for. These advanced couplings provide a deeper understanding of the interactions between the various phases and processes within geomaterials. Notably, the model accommodates both large strain formulations and small strain as a special case, offering a versatile approach to modeling complex material behaviors.

The inclusion of large strain mechanics allows for the development of a matrix with symmetric coefficients, ensuring that the model captures realistic material deformations under a wide range of conditions. Furthermore, by reducing the number of coefficients, this model exhibits significant advantages over traditional approaches to THMC modeling, streamlining the computational process while maintaining accuracy.

The current model lays a solid foundation for further development. It can be extended to incorporate additional physical processes, such as chemical osmosis, thermal osmosis, swelling, chemical reactions, and biological reactions. Each of these processes can be integrated into the existing framework, following the same rigorous mathematical derivations used in this chapter. This flexibility makes the model a powerful tool for advancing the study and application of coupled processes in geotechnical engineering, environmental management, and other fields where understanding the interactions between multiple physical phenomena is crucial.

In conclusion, this THMC model represents a significant step forward in the integration of complex physical processes in unsaturated geomaterials. It offers a more comprehensive and accurate modeling approach compared to traditional methods, with the potential to address a wide range of engineering challenges in areas such as waste disposal, resource management, and environmental remediation. Future research can continue to refine and extend this model, further enhancing its predictive capabilities and practical applications.

NOTES

1 $$(\Psi - J\phi\psi_{pore})^{\cdot} = \overbrace{\dot{\Psi}}^{\dot{\Psi}} - \upsilon\dot{\psi}_{pore} - \psi_{pore}\dot{\upsilon}$$

$$= \overbrace{\left[\mathrm{tr}(\mathbf{T}\dot{\mathbf{E}}) + \mu_w\dot{\rho}_{w,ref} + \mu_c\dot{\rho}_{c,ref} - \dot{T}J\eta\right]}^{\dot{\Psi}} - \overbrace{\left[\upsilon\left(\mu_c(S_l\rho_l^c)^{\cdot} + \mu_w(S_l\rho_l^w)^{\cdot}\right) - \upsilon\dot{T}S_l\eta_l^l\right]}^{\upsilon\dot{\psi}_{pore}}$$

$$- \overbrace{\left[-p_{pore} + \mu_c S_l\rho_l^c + \mu_w S_l\rho_l^w\right]}^{\psi_{pore}}\dot{\upsilon}$$

$$= \mathrm{tr}(\mathbf{T}\dot{\mathbf{E}}) + \overbrace{\mu_w\dot{\rho}_{w,ref} - \upsilon\mu_w(S_l\rho_l^w)^{\cdot} - \dot{\upsilon}(S_l\rho_l^w\mu_w)}^{1} + \overbrace{\mu_c\dot{\rho}_{c,ref} - \upsilon\mu_c(S_l\rho_l^c)^{\cdot} - \dot{\upsilon}(S_l\rho_l^c\mu_c)}^{2}$$

$$+ p_{pore}\dot{\upsilon} - \overbrace{\left[\dot{T}J\eta - \upsilon\dot{T}S_l\eta_l^l\right]}^{3}$$

$$= \mathrm{tr}(\mathbf{T}\dot{\mathbf{E}}) + \underbrace{\overbrace{\mu_w\dot{\rho}_{w,ref} - \mu_w(S_w\rho_l^w\upsilon)^{\cdot}}^{1}}_{=0} + \underbrace{\overbrace{\mu_c\dot{\rho}_{c,ref} - \mu_c(S_l\rho_l^c\upsilon)^{\cdot}}^{2}}_{=0} + p_{pore}\dot{\upsilon}$$

$$- \overbrace{\left[\dot{T}J\eta - J\phi\dot{T}S_w\eta_l^l\right]}^{3}$$

$$= \mathrm{tr}(\mathbf{T}\dot{\mathbf{E}}) + p_{pore}\dot{\upsilon} - \overbrace{\dot{T}J\eta_s}^{3}$$

2 $$\dot{W} = \mathrm{tr}\left(\mathbf{T}\dot{\mathbf{E}}\right) - \dot{T}H_s + \dot{\upsilon}p_{pore} - \dot{\upsilon}p_{pore} - \upsilon\dot{p}_{pore}$$

$$= \mathrm{tr}\left(\mathbf{T}\dot{\mathbf{E}}\right) - \dot{T}H_s - \upsilon\dot{p}_{pore}$$

3 $r_l = 0 = r_q$, equation (7.50) becomes $S_l\rho_l^l\upsilon c_c + \rho_l^l\left[-k\frac{k_{rl}}{v}\nabla p_l\right]\cdot\nabla c_c +$ $\nabla\cdot\left[-\frac{L\rho_l^l}{p_l}\nabla p_l - \rho_l^l D\nabla c_c - \frac{L_T}{T}\nabla T\right] = 0$. By assuming that ρ_l^l is only time dependent and dividing ρ_l^l from both sides of the equation, and by assuming the influence of temperatura gradience on c_c is zero ($L_T = 0$), it leads to $S_l\upsilon c_c + \left[-k\frac{k_{rl}}{v}\nabla p_l\right]\cdot\nabla c_c + \nabla\cdot\left[-\frac{L}{p_l}\nabla p_l - D\nabla c_c\right] = 0$.

REFERENCES

Chen, X., Ma, Y., Hosking, L., Yu, H.-S. & Thomas, H. (2020) THMC constitutive model for membrane geomaterials based on mixture coupling theory. *International Journal of Engineering Science*, 171, 103605.

Chen, X., Pao, W. & Li, X. (2013) Coupled thermo-hydro-mechanical model with consideration of thermal-osmosis based on modified mixture theory. *International Journal of Engineering Science* **64**: 1–13.

Chen, X., Pao, W., Thornton, S. & Small, J. (2016) Unsaturated hydro-mechanical–chemical constitutive coupled model based on mixture coupling theory: hydration swelling and chemical osmosis. *International Journal of Engineering Science* **104**: 97–109.

Chen, X., Thornton, S. F. & Pao, W. (2018a) Mathematical model of coupled dual chemical osmosis based on mixture-coupling theory. *International Journal of Engineering Science* **129**: 145–155.

Chen, X., Wang, M., Hicks, M. A. & Thomas, H. R. (2018b) A new matrix for multiphase couplings in a membrane porous medium. *International Journal for Numerical Analytical Methods in Geomechanics* **42(10)**: 1144–1153.

Chen, X., Wang, M., Hicks, M. A. & Thomas, H. R. (2018c) A new matrix for multiphase couplings in a membrane porous medium. *International Journal for Numerical and Analytical Methods in Geomechanics*, 42: 1144–1153.

Eastman, E. (1928) Theory of the Soret effect. *Journal of the American Chemical Society* **50(2)**: 283–291.

Heidug, W. K. & Wong, S. W. (1996) Hydration swelling of water-absorbing rocks: a constitutive model. *International Journal for Numerical and Analytical Methods in Geomechanics* **20**: 403–430.

Ingle, S. E. & Horne, F. H. (1973) The Dufour effect. *The Journal of Chemical Physics* **59(11)**: 5882–5894.

Lewis, R. W. & Schrefler, B. A. (1987) *The finite-element method in deformation and consolidation of porous media*. New York, Wiley.

Rutqvist, J. & Tsang, C.-F. (2004) A fully coupled three-dimensional THM analysis of the FEBEX in situ test with the ROCMAS code: prediction of THM behavior in a bentonite barrier. In Elsevier *geo-engineering book series*. (Ove Stephanson (ed)) Langford Lane, Kidlington, Oxford OX5 1GB, UK, ELSEVIER Ltd. The Boulevard, vol. 2, pp. 143–148.

Staverman, A. (1951) The theory of measurement of osmotic pressure. Recueil des Travaux Chimiques des Pays-Bas **70(4)**: 344–352.

Sugita, Y., Chijimatsu, M., Akira, I., Kurikami, H., Kobayashi, A. & Ohnishi, Y. (2004) THM simulation of the full-scale in-situ engineered barrier system experiment in GRIMSEL test site in Switzerland. In Elsevier *geo-engineering book series*. (Ove Stephanson (ed)) Langford Lane, Kidlington, Oxford OX5 1GB, UK, ELSEVIER Ltd. The Boulevard, vol. 2, pp. 119–124.

Thomas, H. R., Cleall, P. J. & Hashm, A. A. (2001) Thermal hydraulic chemical mechanical (THCM) behaviour of partly saturated soil. In *The 10th International Conference on Computer Methods and Advances on Geomechanics*. (Desai, C. S. E. A. (ed)) Balkema, AZ, vol. 1, pp. 757–763.

Thomas, H. R., Cleall, P. J. & Seetharam, S. (2002) Numerical modelling of the thermalhydraulic-chemical-mechanical behaviour of unsaturated clay. In *Environmental Geomechanics.* (Vulliet, L., Laloui, L., & Schrefler, B. A. (eds)) Lausanne, EPFL, pp. 125–136.

8 Conclusions and future research

This book presents a unified theoretical framework for multiphase-multicomponent deformable porous media, termed Mixture-Coupling Theory. The theory offers several advantages, making it a significant contribution to the field of porous media research:

1. **Bridging multiscale physics and chemistry:** Mixture-Coupling Theory effectively addresses the long-standing challenge of integrating multiscale physical and chemical processes in porous media. This is achieved by unifying thermodynamic principles and extending their applicability to a range of coupled phenomena, including molecular-scale interactions and macroscopic flow behaviors.
2. **Flexibility in model development:** The theory provides a coherent and unified structure, allowing for the development of constitutive models across various engineering scenarios. These scenarios include large deformation, porosity evolution, gas migration, and the interaction of multiple reactive chemicals. The flexibility of the theory allows it to adapt to different applications in geotechnical engineering, environmental science, and other fields involving porous materials.
3. **Filling the 100-nanometer gap in geoscience and geoengineering:** Mixture-Coupling Theory addresses the gap in understanding processes at the nanometer scale, a critical area in geoscience and geoengineering. This theory provides a theoretical foundation that could potentially open new avenues of research, particularly in coupled geomechanics and geochemistry, including biochemistry.

While Mixture-Coupling Theory provides a robust foundation for analyzing multiphase-multicomponent systems, further research is needed to refine and expand the theory. Based on the author's experience, the following directions are proposed for the future development of the theory:

DOI: 10.1201/9780429324925-8

1. **Large deformation:** Although the basic equations for large deformation have been developed, including those in equation (3.31), the numerical modeling and coupled influences remain at an early stage. This research is especially relevant for applications in landfill design and waste management, where clay materials are commonly used. The exploration of large deformation coupled with other processes will enhance the model's applicability.
2. **Moisture and gas transport:** The unsaturated model presented in this book does not account for gas flow, which is an important consideration for research in shale gas extraction, landfills, and similar applications. Future work could focus on the inclusion of gas transport mechanisms to further enhance the versatility of Mixture-Coupling Theory.
3. **Reactive chemistry:** This book primarily addresses nonreactive chemicals, leaving out reactive chemical processes. Future versions of this theory could include reactive chemistry, considering the interactions and transformations between different chemical species, which are common in many environmental and engineering applications.
4. **Liquefaction, debris flow, landslides, and nanoparticle transport:** In this book, the assumption is made that solid phases are attached to the boundary and that no solids move across the boundary. This assumption can be relaxed to enable the analysis of solid particle transport, which is crucial for understanding phenomena like liquefaction, debris flow, landslides, and the transport of nanoparticles.
5. **Biological and chemical industry applications:** While this book focuses on geomaterials, Mixture-Coupling Theory has the potential for broader applications, including the analysis of biological tissues. Exploring the theory's application in biological and chemical industries could lead to new research directions and advancements in tissue engineering and related fields.
6. **Applicability to soft and hard porous media:** Mixture-Coupling Theory can be applied to both soft porous media (e.g., soils, clays, biological tissues, fluids) and hard porous media (e.g., rocks, bones). In large deformation theory, where finite strains and rotations are involved, the undeformed (reference) and deformed (current) configurations differ significantly.

> This makes it necessary to move beyond infinitesimal strain theory (Atkin and Craine, 1976), which Mixture-Coupling Theory is well equipped to handle.

In conclusion, Mixture-Coupling Theory offers a comprehensive, adaptable framework for understanding and modeling the complex interactions within multiphase-multicomponent porous media. The areas highlighted for future research will allow for the continued refinement of the theory and its application across a variety of disciplines, driving further advancements in both theory and practical engineering solutions.

Appendixes

APPENDIX 1: FUNDAMENTAL TENSORS

Scalar, vector, matrix, and tensor

A scalar is a physical quantity defined by its magnitude without direction. For example, in this book, the mass partial density and mixture density of the αth phase (denoted as ρ_i^α and ρ_α, respectively) are scalars.

A vector describes a physical quantity with both magnitude and direction. For example, the velocity of the αth phase $\mathbf{v}_\alpha$ is a vector.

A tensor is a matrix that can be used to describe the physical/chemical state or properties of a material. A mathematical matrix is an ordered rectangular array of numbers or symbols. Tensors are described using a matrix, with an associated physical meaning. For example, the Cauchy stress tensor $\boldsymbol{\sigma}$ is a matrix described as

$$\boldsymbol{\sigma} = [\sigma_{ij}] = \begin{bmatrix} \boldsymbol{\sigma}_1 \\ \boldsymbol{\sigma}_2 \\ \boldsymbol{\sigma}_3 \end{bmatrix} = \begin{bmatrix} \sigma_{11} & \sigma_{12} & \sigma_{13} \\ \sigma_{21} & \sigma_{22} & \sigma_{23} \\ \sigma_{31} & \sigma_{32} & \sigma_{33} \end{bmatrix} \quad (i, j = 1,\ 2,\ \text{and } 3) \tag{8.1}$$

where $\sigma_{11}$is a scalar and $\boldsymbol{\sigma}_1 = [\sigma_{11}, \sigma_{12}, \sigma_{13}]$ is a vector. An important function is that $\sigma_{ij} = \sigma_{ji}$, which indicates the Cauchy stress is symmetric.

The order (or rank) of a tensor determined by the number of subscripts (e.g., i, j in equation (8.1) indicates $\boldsymbol{\sigma}$ is a second-order tensor). Zero-order tensors are scalars (e.g., mass density ρ); first-order tensors are vectors (e.g., $\mathbf{v}_\alpha$).

The Kronecker delta δ_{ij} is the derivatives of the coordinate axis with respect to themselves. For example:

$$\delta_{11} = \frac{\partial x_1}{\partial x_1} = 1;\ \delta_{12} = \frac{\partial x_1}{\partial x_2} = 0;\ \delta_{13} = \frac{\partial x_1}{\partial x_3} = 0 \tag{8.2}$$

δ_{ij} can be defined as

$$\delta_{ij} = \begin{Bmatrix} 1\ (i = j) \\ 0\ (i \neq j) \end{Bmatrix} \tag{8.3}$$

where δ_{ij} is a scalar value that serves as an identity matrix $\mathbf{I}_1$as it equals 1 when $i = j$ and equals 0 when $i \neq j$. The matrix $\mathbf{I}_1$ is defined as

$$\mathbf{I}_1 = [\delta_{ij}] = \begin{bmatrix} 1 & 0 & 0 \\ 0 & 1 & 0 \\ 0 & 0 & 1 \end{bmatrix} \tag{8.4}$$

Vector and tensor: **A** and **B** are second-rank tensors. Two 3×3 matrices for the second-rank tensors A_{ij} and B_{jk}, where the indices i, j, k range from 1 to 3, are given to demonstrate some key calculation processes:

$$\mathbf{A} = \begin{bmatrix} 1 & 2 & 3 \\ 4 & 5 & 6 \\ 7 & 8 & 9 \end{bmatrix} \quad \text{and} \quad \mathbf{B} = \begin{bmatrix} 9 & 8 & 7 \\ 6 & 5 & 4 \\ 3 & 2 & 1 \end{bmatrix}$$

1. tr(**A**) denotes the trace of matrix **A**, and it is the sum of the elements (e.g. A_{ii}) on the main diagonal. For example, $\text{tr}(\mathbf{A}) = A_{11} + A_{22} + A_{33} = 1 + 5 + 9 = 15$.
2. The transpose of matrix **A**, denoted $\mathbf{A}^{\mathrm{T}}$, is obtained by swapping rows and columns:

$$\mathbf{A}^{\mathrm{T}} = \begin{bmatrix} 1 & 4 & 7 \\ 2 & 5 & 8 \\ 3 & 6 & 9 \end{bmatrix}$$

3. $\mathbf{C} = \mathbf{A}^{\mathrm{T}}\mathbf{B}$ is defined as the product of matrices **A** and **B**; it is an $i \times k$ matrix, described as

$$\mathbf{C} = \begin{bmatrix} c_{11} & c_{12} & \cdots & c_{1k} \\ c_{21} & c_{22} & \cdots & c_{2k} \\ \vdots & \vdots & \ddots & \vdots \\ c_{i1} & c_{i2} & \cdots & c_{ik} \end{bmatrix} \tag{8.5}$$

where

$$c_{ik} = \sum_{j=1}^{n} a_{ij} b_{jk} = a_{i1} b_{1k} + a_{i2} b_{2k} + \ldots + a_{in} b_{nk}$$

For example:

$$\mathbf{A}^{\mathrm{T}}\mathbf{B} = \begin{bmatrix} 1 & 4 & 7 \\ 2 & 5 & 8 \\ 3 & 6 & 9 \end{bmatrix} \begin{bmatrix} 9 & 8 & 7 \\ 6 & 5 & 4 \\ 3 & 2 & 1 \end{bmatrix}$$

The resulting matrix product $\mathbf{A}^{\mathrm{T}}\mathbf{B}$ can be calculated element by element:

$$\mathbf{A}^{\mathrm{T}}\mathbf{B} = \begin{bmatrix} (1*9+4*6+7*3) & (1*8+4*5+7*2) & (1*7+4*4+7*1) \\ (2*9+5*6+8*3) & (2*8+5*5+8*2) & (2*7+5*4+8*1) \\ (3*9+6*6+9*3) & (3*8+6*5+9*2) & (3*7+6*4+9*1) \end{bmatrix}$$

$$= \begin{bmatrix} 54 & 42 & 30 \\ 72 & 57 & 42 \\ 90 & 72 & 54 \end{bmatrix}$$

4. The double inner product (also known as the Frobenius inner product) of two second-rank tensors **A** and **B** is defined as the sum of the products of the corresponding components of the matrices **A** and **B**.

   The double inner product of two matrices is given by the formula:

$$\mathbf{A} : \mathbf{B} = \mathrm{tr}(\mathbf{A}^{\mathrm{T}}\mathbf{B}) = \sum_{i,j,k} A_{ij} B_{jk} \tag{8.6}$$

This represents a scalar quantity. For example,

$$\text{Since } \mathbf{A}^{\mathrm{T}}\mathbf{B} = \begin{bmatrix} 54 & 42 & 30 \\ 72 & 57 & 42 \\ 90 & 72 & 54 \end{bmatrix}, \text{ therefore}$$

$$\mathbf{A} : \mathbf{B} = \mathrm{tr}(\mathbf{A}^{\mathbf{T}}\mathbf{B}) = 54 + 57 + 54 = 165$$

APPENDIX 2: MATHEMATICAL PROOF OF EQUATION (3.15)

Since

$$\mathbf{T} = J\mathbf{F}^{-1}\boldsymbol{\sigma}\mathbf{F}^{-\mathbf{T}} \text{ and } \mathbf{E} = \frac{1}{2}(\mathbf{F}^{\mathbf{T}}\mathbf{F} - \mathbf{I}),$$

by using

$$\dot{\mathbf{E}} = \frac{1}{2}(\dot{\mathbf{F}}^{\mathbf{T}}\mathbf{F} + \mathbf{F}^{\mathbf{T}}\dot{\mathbf{F}}) \text{ and } \dot{\mathbf{F}} = \mathbf{F} \cdot \nabla \mathbf{v}^{s},$$

the following relationship can be established:

$$\begin{aligned}\mathbf{T}\dot{\mathbf{E}} &= J\mathbf{F}^{-1}\boldsymbol{\sigma}\mathbf{F}^{-\mathbf{T}}\frac{1}{2}(\dot{\mathbf{F}}^{\mathbf{T}}\mathbf{F} + \mathbf{F}^{\mathbf{T}}\dot{\mathbf{F}}) = \frac{J}{2}(\mathbf{F}^{-1}\boldsymbol{\sigma}\mathbf{F}^{-\mathbf{T}}\dot{\mathbf{F}}^{\mathbf{T}}\mathbf{F} + \mathbf{F}^{-1}\boldsymbol{\sigma}\mathbf{F}^{-\mathbf{T}}\mathbf{F}^{\mathbf{T}}\dot{\mathbf{F}}) \\ &= \frac{J}{2}(\boldsymbol{\sigma}\mathbf{F}^{-\mathbf{T}}\dot{\mathbf{F}}^{\mathbf{T}} + \mathbf{F}^{-1}\boldsymbol{\sigma}\dot{\mathbf{F}}) = \frac{J}{2}(\boldsymbol{\sigma}\mathbf{F}^{-\mathbf{T}}F^{T}\nabla\mathbf{v}_{s} + \mathbf{F}^{-1}\boldsymbol{\sigma}F\nabla\mathbf{v}_{s}) = J\boldsymbol{\sigma}^{\mathrm{T}}\nabla\mathbf{v}_{s}\end{aligned} \tag{8.7}$$

APPENDIX 3: MATHEMATICAL DERIVATION OF EQUATIONS (4.27) AND (4.28)

The derivation process for equation (4.28) is very similar to that followed in Chapter 3, except for replacing p_w with p_{pore}. To provide a complete chapter for readers, as well as a reference for later chapters in unsaturated conditions, some of the major derivation processes are listed as:

Since $T_{ij} = \left(\dfrac{\partial W}{\partial E_{ij}}\right)_{p_{pore},\mu_w}$, using differentiation by the chain rule leads to

$$\frac{\partial T_{ij}}{\partial t}=\frac{\partial}{\partial t}\left(\frac{\partial W}{\partial E_{ij}}\right)_{p_{pore},\mu_w}=\left(\frac{\partial}{\partial E_{ij}}(\frac{\partial W}{\partial t})\right)_{p_{pore},\mu_w}=\left(\frac{\partial}{\partial E_{ij}}(\dot{W})\right)_{p_{pore},\mu_w} \tag{8.8}$$

Substituting equation 4.23 in equation (8.8) leads to

$$\begin{aligned}\frac{\partial T_{ij}}{\partial t}=\left(\frac{\partial}{\partial E_{ij}}(\dot{W})\right)_{p_{pore},\mu_w}=\left(\frac{\partial T_{ij}}{\partial E_{ij}}\right)_{p_{pore},\mu_w}\dot{E}_{kl}-\left(\frac{\partial \upsilon}{\partial E_{ij}}\right)_{p_{pore},\mu_w}\\ \dot{p}_{pore}-\left(\frac{\partial \rho_{bound,ref}}{\partial E_{ij}}\right)_{p_{pore},\mu_w}\dot{\mu}_w\end{aligned} \tag{8.9}$$

Comparing equation (8.9) with equation (4.24) leads to

$$L_{ijkl}=\left(\frac{\partial T_{ij}}{\partial E_{ij}}\right)_{p_{pore},\mu_w},\ M_{ij}=\left(\frac{\partial \upsilon}{\partial E_{ij}}\right)_{p_{pore},\mu_w},\ S_{ij}=-\left(\frac{\partial \rho_{bound,ref}}{\partial E_{ij}}\right)_{p_{pore},\mu_w}$$

Note: Other derivations are as follows:

$\because \upsilon=-\left(\frac{\partial W}{\partial p_{pore}}\right)_{E_{ij},\mu_w}$, using differentiation by the chain rule leads to

$$\therefore \frac{\partial \upsilon}{\partial t}=-\frac{\partial}{\partial t}\left(\frac{\partial W}{\partial p_{pore}}\right)_{E_{ij},\mu_w}=-\left(\frac{\partial}{\partial p_{pore}}(\frac{\partial W}{\partial t})\right)_{E_{ij},\mu_w}=-\left(\frac{\partial \dot{W}}{\partial p_{pore}}\right)_{E_{ij},\mu_w}$$

$$\begin{aligned}\because\ \frac{\partial \upsilon}{\partial t}=-\left(\frac{\partial \dot{W}}{\partial p_{pore}}\right)_{E_{ij},\mu_w}=-\left(\frac{\partial T_{ij}}{\partial p_{pore}}\right)_{E_{ij},\mu_w}\dot{\mathbf{E}}+\left(\frac{\partial \upsilon}{\partial p_{pore}}\right)_{E_{ij},\mu_w}\\ \dot{p}_{pore}+\left(\frac{\partial \rho_{bound,ref}}{\partial p_{pore}}\right)_{E_{ij},\mu_w}\dot{\mu}_w\end{aligned}$$

$$\therefore M_{ij}=-\left(\frac{\partial T_{ij}}{\partial p_{pore}}\right)_{E_{ij},\mu_w},\ Q=\left(\frac{\partial \upsilon}{\partial p_{pore}}\right)_{E_{ij},\mu_w},\ B=\left(\frac{\partial \rho_{bound,ref}}{\partial p_{pore}}\right)_{E_{ij},\mu_w}$$

$\because \rho_{bound,ref} = -\left(\frac{\partial W}{\partial \mu_w}\right)_{E_{ij},p_{pore}}$, using differentiation by the chain rule leads to

$$\therefore \frac{\partial \rho_{bound,ref}}{\partial t} = -\frac{\partial}{\partial t}\left(\frac{\partial W}{\partial \mu_w}\right)_{E_{ij},p_{pore}} = -\left(\frac{\partial}{\partial \mu_w}\left(\frac{\partial W}{\partial t}\right)\right)_{E_{ij},p_{pore}} = -\left(\frac{\partial \dot{W}}{\partial \mu_w}\right)_{E_{ij},p_{pore}}$$

$$\frac{\partial \rho_{bound,ref}}{\partial t} = -\left(\frac{\partial \dot{W}}{\partial \mu_w}\right)_{T_{ij},p_{pore}} = -\left(\frac{\partial T_{kl}}{\partial \mu_w}\right)_{E_{ij},p_{pore}} \dot{\mathbf{E}} + \left(\frac{\partial \upsilon}{\partial \mu_w}\right)_{E_{ij},p_{pore}}$$

$$\dot{p}_{pore} + \left(\frac{\partial \rho_{bound,ref}}{\partial \mu_w}\right)_{E_{ij},p_{pore}} \dot{\mu}_w$$

$$\therefore S_{ij} = -\left(\frac{\partial T_{kl}}{\partial \mu_w}\right)_{E_{ij},p_{pore}}, B = \left(\frac{\partial \upsilon}{\partial \mu_w}\right)_{E_{ij},p_{pore}}, Z = \left(\frac{\partial \rho_{bound,ref}}{\partial \mu_w}\right)_{E_{ij},p_{pore}}$$

APPENDIX 4: MATHEMATICAL DERIVATION OF EQUATIONS (5.36)–(5.38)

Since $T_{ij} = \left(\frac{\partial W}{\partial E_{ij}}\right)_{p_{pore}}$, using differentiation by the chain rule leads to

$$\frac{\partial T_{ij}}{\partial t} = \frac{\partial}{\partial t}\left(\frac{\partial W}{\partial E_{ij}}\right)_{p_{pore}} = \left(\frac{\partial}{\partial E_{ij}}\left(\frac{\partial W}{\partial t}\right)\right)_{p_{pore}} = \left(\frac{\partial}{\partial E_{ij}}(\dot{W})\right)_{p_{pore}} \tag{8.10}$$

Substituting equation (5.33) in equation (8.10) leads to

$$\frac{\partial T_{ij}}{\partial t} = \left(\frac{\partial}{\partial E_{ij}}(\dot{W})\right)_{p_{pore}} = \left(\frac{\partial T_{ij}}{\partial E_{ij}}\right)_{p_{pore}} \dot{E}_{kl} - \left(\frac{\partial \upsilon}{\partial E_{ij}}\right)_{E_{ij}} \dot{p}_{pore} \tag{8.11}$$

Therefore,

$$\dot{T}_{ij} = L_{ijkl}\dot{E}_{kl} - M_{ij}\dot{p}_{pore} \tag{8.12}$$

where

$$L_{ijkl} = \left(\frac{\partial T_{ij}}{\partial E_{ij}} \right)_{p_{pore}}, M_{ij} = \left(\frac{\partial \upsilon}{\partial E_{ij}} \right)_{p_{pore}} \tag{8.13}$$

Since $\upsilon = -\left(\frac{\partial W}{\partial p_{pore}} \right)_{E_{ij}}$, using differentiation by the chain rule leads to

$$\frac{\partial \upsilon}{\partial t} = -\frac{\partial}{\partial t}\left(\frac{\partial W}{\partial p_{pore}} \right)_{E_{ij}} = -\left(\frac{\partial}{\partial p_{pore}} (\frac{\partial W}{\partial t}) \right)_{E_{ij}} = -\left(\frac{\partial \dot{W}}{\partial p_{pore}} \right)_{E_{ij}} \tag{8.14}$$

Substituting equation 5.33 into equation 8.14 leads to

$$\frac{\partial \upsilon}{\partial t} = -\left(\frac{\partial \dot{W}}{\partial p_{pore}} \right)_{E_{ij}} = -\left(\frac{\partial T_{ij}}{\partial p_{pore}} \right)_{E_{ij}} \dot{\mathbf{E}} + \left(\frac{\partial \upsilon}{\partial p_{pore}} \right)_{E_{ij}} \dot{p}_{pore} \tag{8.15}$$

$$\dot{\upsilon} = M_{ij}\dot{E}_{ij} + Q\dot{p}_{pore} \tag{8.16}$$

where

$$M_{ij} = -\left(\frac{\partial T_{ij}}{\partial p_{pore}} \right)_{E_{ij}}, Q = \left(\frac{\partial \upsilon}{\partial p_{pore}} \right)_{E_{ij}} \tag{8.17}$$

The proof of $M_{ij} = -\left(\frac{\partial T_{ij}}{\partial p_{pore}} \right)_{E_{ij}} = \left(\frac{\partial \upsilon}{\partial E_{ij}} \right)_{p_{pore}}$ in equations (8.13) and (8.17) can be described as follows:

$$M_{ij} = \left(\frac{\partial \upsilon}{\partial E_{ij}} \right)_{p_{pore}} = -\left(\frac{\partial}{\partial E_{ij}} \left(\frac{\partial W}{\partial p_{pore}} \right)_{E_{ij}} \right)_{p_{pore}} = -\left(\frac{\partial}{\partial E_{ij}} \left(\frac{\partial W}{\partial p_{pore}} \right)_{E_{ij}} \right)_{p_{pore}}$$

$$= -\frac{\partial^2 W}{\partial p_{pore} \partial E_{ij}}$$

$$M_{ij} = -\left(\frac{\partial T_{ij}}{\partial p_{pore}} \right)_{E_{ij}} = -\left(\frac{\partial}{\partial p_{pore}} \left(\frac{\partial W}{\partial E_{ij}} \right)_{p_{pore}} \right)_{E_{ij}} = -\frac{\partial^2 W}{\partial p_{pore} \partial E_{ij}}$$

APPENDIX 5: MATHEMATICAL DERIVATION FOR SECTIONS 6.4.3 AND 7.4.3

Following a similar process to that in Section 3.3.3 as follows, the constitutive relationship of equation (6.46) can be obtained (Note: As swelling is not considered in Chapters 6 and 7, the deformation potential equations are the same.):

Equation (6.39) is described as

$$\dot{W} = tr(\mathbf{T}\dot{\mathbf{E}}) - \dot{p}_{pore}\upsilon - \dot{T}\mathrm{H}_s$$

where W is a function of $\mathbf{E}$, p_{pore}, and T, and the following equations are obtained:

$$T_{ij} = \left(\frac{\partial W}{\partial E_{ij}}\right)_{p_{pore},T}, \upsilon = -\left(\frac{\partial W}{\partial p_{pore}}\right)_{E_{ij},T}, \mathrm{H}_s = -\left(\frac{\partial W}{\partial T}\right)_{E_{ij},p_{pore}} \tag{8.18}$$

Therefore, expressions of $\dot{W}$ for $\boldsymbol{\sigma}$, υ, and H_s may be obtained:

$$\dot{W}(\mathbf{E}, p_{pore}, T) = \left(\frac{\partial W}{\partial E_{ij}}\right)_{p_{pore},T}\dot{E}_{ij} + \left(\frac{\partial W}{\partial p_{pore}}\right)_{E_{ij},T}\dot{p}_{pore} + \left(\frac{\partial W}{\partial T}\right)_{E_{ij},p_{pore}}\dot{T} \tag{8.19}$$

or as

$$\dot{W} = \mathrm{tr}(\mathbf{T}\dot{\mathbf{E}}) - \dot{p}_{pore}\upsilon - \dot{T}\mathrm{H}_s \tag{8.20}$$

Equation (8.18) may be differentiated with respect to time to give

$$\dot{T}_{ij} = \frac{\partial T_{ij}}{\partial t} = \frac{\partial}{\partial t}\left(\frac{\partial W}{\partial E_{ij}}\right)_{p_{pore},T} = \left(\frac{\partial}{\partial E_{ij}}\left(\frac{\partial W}{\partial t}\right)\right)_{p_{pore},T} = \left(\frac{\partial}{\partial E_{ij}}(\dot{W})\right)_{p_{pore},T}$$

$$\dot{\upsilon} = \frac{\partial \upsilon}{\partial t} = -\frac{\partial}{\partial t}\left(\frac{\partial W}{\partial p_{pore}}\right)_{E_{ij},T} = -\left(\frac{\partial}{\partial p_{pore}}\left(\frac{\partial W}{\partial t}\right)\right)_{E_{ij},T} = -\left(\frac{\partial \dot{W}}{\partial p_{pore}}\right)_{E_{ij},T} \tag{8.21}$$

$$\dot{\mathrm{H}}_s = \frac{\partial \mathrm{H}_s}{\partial t} = -\frac{\partial}{\partial t}\left(\frac{\partial W}{\partial T}\right)_{E_{ij},p_{pore}} = -\left(\frac{\partial}{\partial T}\left(\frac{\partial W}{\partial t}\right)\right)_{E_{ij},p_{pore}} = -\left(\frac{\partial \dot{W}}{\partial T}\right)_{E_{ij},p_{pore}}$$

By substituting equation (8.19) into the equation group (8.21), the fundamental constitutive equations for the evolution of stress, pore volume fraction, and entropy density of the solid can be expressed as the group equations:

$$\begin{aligned}
&\frac{\partial T_{ij}}{\partial t} = \left(\frac{\partial}{\partial E_{ij}}(\dot{W})\right)_{p_{pore},T} = \left(\frac{\partial T_{ij}}{\partial E_{ij}}\right)_{p_{pore},T} \dot{E}_{kl} - \left(\frac{\partial \upsilon}{\partial E_{ij}}\right)_{p_{pore},T} \\
&\dot{p}^{pore} - \left(\frac{\partial \mathrm{H}_s}{\partial E_{ij}}\right)_{p_{pore},T} \dot{T} \\
&\frac{\partial \upsilon}{\partial t} = -\left(\frac{\partial \dot{W}}{\partial p_{pore}}\right)_{E_{ij},T} = -\left(\frac{\partial T_{ij}}{\partial p_{pore}}\right)_{E_{ij},T} \dot{\mathbf{E}} + \left(\frac{\partial \upsilon}{\partial p_{pore}}\right)_{E_{ij},T} \\
&\dot{p}_{pore} + \left(\frac{\partial \mathrm{H}_s}{\partial p_{pore}}\right)_{E_{ij},T} \dot{T} \\
&\frac{\partial \mathrm{H}_s}{\partial t} = -\left(\frac{\partial \dot{W}}{\partial T}\right)_{T_{ij},p_{pore}} = -\left(\frac{\partial T_{kl}}{\partial T}\right)_{E_{ij},p_{pore}} \dot{\mathbf{E}} + \left(\frac{\partial \upsilon}{\partial T}\right)_{E_{ij},p_{pore}} \\
&\dot{p}_{pore} + \left(\frac{\partial \mathrm{H}_s}{\partial T}\right)_{E_{ij},p_{pore}} \dot{T}
\end{aligned} \tag{8.22}$$

For convenience, Equation (8.22) can be written in matrix format as follows:

$$\begin{bmatrix} \dot{T}_{ij} \\ \dot{\upsilon} \\ \dot{\mathrm{H}}_s \end{bmatrix} = \begin{bmatrix} \left(\frac{\partial T_{ij}}{\partial E_{ij}}\right)_{p_{pore},T} & -\left(\frac{\partial \upsilon}{\partial E_{ij}}\right)_{p_{pore},T} & -\left(\frac{\partial \mathrm{H}_s}{\partial E_{ij}}\right)_{p_{pore},T} \\ -\left(\frac{\partial T_{ij}}{\partial p_{pore}}\right)_{E_{ij},T} & \left(\frac{\partial \upsilon}{\partial p_{pore}}\right)_{E_{ij},T} & \left(\frac{\partial \mathrm{H}_s}{\partial p_{pore}}\right)_{E_{ij},T} \\ -\left(\frac{\partial T_{kl}}{\partial T}\right)_{E_{ij},p_{pore}} & \left(\frac{\partial \upsilon}{\partial T}\right)_{E_{ij},p_{pore}} & \left(\frac{\partial \mathrm{H}_s}{\partial T}\right)_{E_{ij},p_{pore}} \end{bmatrix} \begin{bmatrix} \dot{E}_{kl} \\ \dot{p}_{pore} \\ \dot{T} \end{bmatrix} \tag{8.23}$$

The matrix function of equation (8.23) describes the relationship between variables $\dot{T}_{ij}, \dot{\upsilon}, \dot{\mathrm{H}}_s$ and $\dot{E}_{kl}, \dot{p}_{pore}, \dot{T}$. The matrix that links these two groups of variables is called the coupling matrix for the open thermodynamic system. There are nine parameters in this matrix, and the next step is to discuss the relationships defining these coefficients.

Substituting equation (8.18) into the coupling matrix leads to

$$\left(\frac{\partial T_{ij}}{\partial E_{kl}}\right)_{p_{pore},T} = \left(\frac{\partial}{\partial E_{kl}}\left(\left(\frac{\partial W}{\partial E_{ij}}\right)_{p_{pore},T}\right)\right)_{p_{pore},T} = \left(\frac{\partial^2 W}{\partial E_{kl}\,\partial E_{ij}}\right)_{p_{pore},T}$$

$$= \left(\frac{\partial T_{kl}}{\partial E_{ij}}\right)_{p_{pore},T} = L_{ijkl}$$

$$-\left(\frac{\partial \upsilon}{\partial E_{ij}}\right)_{p_{pore},\mu} = \left(\frac{\partial}{\partial E_{ij}}\left(\frac{\partial W}{\partial p_{pore}}\right)_{E_{ij},T}\right)_{p_{pore},T} = \left(\frac{\partial^2 W}{\partial p_{pore}\,\partial E_{ij}}\right)_{T} = -M_{ij}$$

$$-\left(\frac{\partial T_{ij}}{\partial p_{pore}}\right)_{E_{ij},T} = -\left(\frac{\partial}{\partial p_{pore}}\left(\frac{\partial W}{\partial E_{ij}}\right)_{p_{pore},T}\right)_{E_{ij},T} = -\left(\frac{\partial^2 W}{\partial p_{pore}\,\partial E_{ij}}\right)_{T} = M_{ij}$$

$$-\left(\frac{\partial \mathrm{H}_s}{\partial E_{ij}}\right)_{p_{pore},T} = \left(\frac{\partial}{\partial E_{ij}}\left(\left(\frac{\partial W}{\partial T}\right)_{E_{ij},p_{pore}}\right)\right)_{p_{pore},T} = \left(\frac{\partial^2 W}{\partial E_{ij}\,\partial T}\right)_{p_{pore}} = S_{ij}^{q}$$

$$\left(\frac{\partial T_{kl}}{\partial T}\right)_{E_{ij},p_{pore}} = -\left(\frac{\partial}{\partial T}\left(\left(\frac{\partial W}{\partial E_{ij}}\right)_{p_{pore},T}\right)\right)_{E_{ij},p_{pore}} = -\left(\frac{\partial^2 W}{\partial T\,\partial E_{ij}}\right)_{p_{pore}} = -S_{ij}^{q} \tag{8.24}$$

$$-\left(\frac{\partial \mathrm{H}_s}{\partial p_{pore}}\right)_{E_{ij},T} = -\left(\frac{\partial}{\partial p_{pore}}\left(-\left(\frac{\partial W}{\partial T}\right)_{E_{ij},p_{pore}}\right)\right)_{E_{ij},T} = \left(\frac{\partial^2 W}{\partial p_{pore}\,\partial T}\right)_{E_{ij}} = B_q$$

$$-\left(\frac{\partial \upsilon}{\partial T}\right)_{E_{ij},p_{pore}} = -\left(\frac{\partial}{\partial T}\left(-\left(\frac{\partial W}{\partial p_{pore}}\right)_{E_{ij},T}\right)\right)_{E_{ij},p_{pore}} = \left(\frac{\partial^2 W}{\partial T\,\partial p_{pore}}\right)_{E_{ij}} = B_q$$

$$-\left(\frac{\partial \upsilon}{\partial p_{pore}}\right)_{E_{ij},T} = -\left(\frac{\partial}{\partial p_{pore}}\left(-\left(\frac{\partial W}{\partial p_{pore}}\right)_{E_{ij},T}\right)\right)_{E_{ij},T} = \left(\frac{\partial^2 W}{\partial {p_{pore}}^2}\right)_{E_{ij},T} = Q$$

$$\left(\frac{\partial \mathrm{H}_s}{\partial T}\right)_{E_{ij},p_{pore}} = \left(\frac{\partial}{\partial T}\left(-\left(\frac{\partial W}{\partial T}\right)_{E_{ij},p_{pore}}\right)\right)_{E_{ij},p_{pore}} = -\left(\frac{\partial^2 W}{\partial T^2}\right)_{E_{ij},p_{pore}} = Z_q$$

Equation group (8.24) demonstrates the interrelationship between the coefficients and also concludes that some of these coefficients are equal in value. Note that the matrix reduces by almost one half the number of coefficients that need to be determined, thereby partly addressing the challenge of too many coefficients for coupled analysis. Incorporating equation (8.24) in equation (8.23) and using simple symbols to replace the complex coefficients lead to

$$\dot{T}_{ij} = L_{ijkl}\dot{E}_{kl} - M_{ij}\dot{p}_{pore} + S_{ij}^{q}\dot{T} \tag{8.25}$$

$$\dot{\upsilon} = M_{ij}\dot{E}_{ij} + Q\dot{p}_{pore} + B_q\dot{T} \tag{8.26}$$

$$\dot{\mathrm{H}}_s = -S_{ij}^{q}\dot{E}_{ij} + B_q\dot{p}_{pore} + Z_q\dot{T} \tag{8.27}$$